Doctoral theses at NTNU, 2022:54

Espen Flo Bødal

Hydrogen Production from Wind and Hydro Power in Constrained Transmission Grids

Doctoral thesis

NTNU
Norwegian University of Science and Technology
Thesis for the Degree of Philosophiae Doctor
Department of Electric Power Engineering

NTNU
Norwegian University of Science and Technology

Espen Flo Bødal

Hydrogen Production from Wind and Hydro Power in Constrained Transmission Grids

Thesis for the Degree of Philosophiae Doctor

Trondheim, February 2022

Norwegian University of Science and Technology
Department of Electric Power Engineering

NTNU

Norwegian University of
Science and Technology

NTNU
Norwegian University of Science and Technology

Thesis for the Degree of Philosophiae Doctor

Department of Electric Power Engineering

ISBN 978-82-326-5488-8 (printed ver.)
ISBN 978-82-326-5648-6 (electronic ver.)
ISSN 1503-8181 (printed ver.)
ISSN 2703-8084 (online ver.)

Doctoral theses at NTNU, 2022:54

Printed by NTNU Grafisk senter

Preface

This doctoral thesis was written at the Department of Electric Power Engineering at the Norwegian University of Science and Technology. The research presented in this thesis was carried out from 2016 to 2020 under the supervision of Professor Magnus Korpås. During this time a research stay was conducted in the Laboratory for Information & Decision Systems at Massachusetts Institute of Technology, working with Dr. Audun Botterud. The research stay included a scientific cooperation with Dr. Dharik Mallapragada at the MIT Energy Initiative.

The PhD was carried out as a part of the HYPER project - Liquefied hydrogen production from surplus wind/hydro power and fossil sources in Norway. The project was supported by Equinor, Shell, Kawasaki Heavy Industries, Linde Kryotechnik, Mitsubishi Corporation, Nel Hydrogen and the Research Council of Norway.

Espen Flo Bødal

Trondheim, April 2021

Acknowledgments

During my four years of PhD studies I have been fortunate to meet and work with many interesting and skilled people. I first and foremost want to thank Professor Magnus Korpås. He was my supervisor during both master and PhD studies, during which he was a great teacher and excellent motivator. Without him, I would never have started or finished the PhD studies. I would also like to thank the participants in the HYPER project, especially David Berstad, Petter Nekså and Øivind Wilhelmsen, for motivation and insight in hydrogen research and facilitating meetings and workshops.

From my research stay in the US, I would like to thank Dr. Audun Botterud for giving me that opportunity. Our discussions and research cooperation was important for both motivation and the final outcome of this thesis. I am also grateful for the cooperation with Dr. Dharik Mallapragada, he provided important contributions for one of the articles resulting from the research stay and I learned a lot from him. The people at the Visiting Students Association at MIT, both MIT students and other visiting students, deserves a big thanks for making my research stay memorable and fun. Also, thanks to Matias Vikse and Andreas Kleiven for making the year abroad in the US fun with bar quizzes, awesome biking trips and interesting conferences.

The best part of the PhD studies was, without a doubt, the friendships made along the way. Martin Hjelmeland was my co-supervisor during my master thesis, today I am grateful for that he and Martin Kristiansen motivated me to study for the PhD. I would like to thank them and the rest of the PhDs, postdocs and professors for creating a great group at the department, especially, Markus Löchenbrand, Erlend Engevik, Martin Håberg, Sigurd Jakobsen, Salman "Kaveh" Zaferanlouei, Hans Kristian Meyer, Emre Kantar, Venkat Lakshmanan, Hallvar Haugdal, Frank Mauseth, Erlend Sandø Kiel, Dimitri Pinel, Christian Øyn Naversen, Kasper Thorvaldsen, Sigurd Bjarghov, Fredrik Göthner and Linn Emelie Schäffer.

A special tanks to Sigurd Jakobsen, Kasper Thorvaldsen and Andreas Kleiven for

reviewing and providing feedback on this thesis. Finally, I would like to thank my family for moral support through four mostly fun, but sometimes also challenging years.

Abstract

Hydrogen (H_2) production from variable renewable energy (VRE) sources can be an important technology for reducing CO_2 emissions. Integrating electrolytic H_2 production into the electricity system can contribute to this objective on two fronts. Firstly, electrolytic H_2 production will be important to enable large shares of VRE integration into the electricity system as it can provide demand-side flexibility at scale. Secondly, H_2 can mitigate CO_2 emissions in end-use applications that is hard to decarbonize by other means, such as direct electrification. The scope of this thesis is limited to study the effects of large-scale H_2 production on the electricity system.

Mathematical models are developed and used to study how flexible H_2 production can enable cost efficient VRE integration and reduction of CO_2 emissions. The models include representations of H_2 production as flexible demand and sector-coupling between H_2 and electricity systems. The sector coupled model enables an integrated analysis of multiple H_2 production pathways, based on electricity and natural gas. A stochastic rolling horizon dispatch capacity expansion problem is formulated and modeled to investigate the impact of short-term uncertainty from VRE sources on investments in the electricity system. This approach also incorporates the modeling of long-term storage. The results shows that more installed capacity will be needed to handle short-term uncertainty compared to the results from deterministic models. This model can provide an important foundation for future models that studies the impacts of flexibility from H_2 production on electricity systems.

H_2 production is studied in two different case studies, based on the electricity systems of northern Norway and the state of Texas in the US. The two electricity systems have different sources of flexibility, where hydro power provides flexibility in northern Norway and natural gas in Texas. Flexibility from natural gas is a source of CO_2 emissions while the emissions from hydro power are negligible. Thus, flexibility from electrolytic H_2 production has more potential to reduce elec-

tricity system emissions in Texas, while it will be important for efficient integration of high shares of VRE in both systems.

In northern Norway, the results from the case studies show that it will be important to operate H_2 production in a flexible way to not reduce security of supply. This is especially important in regions where the transmission grid is constrained, such that flexible H_2 production can help reduce the amount of transmission grid expansion that is needed in relation to wind power integration. Competitive production of low-cost H_2 in northern Norway is dependent on sufficient hydro power flexibility and low wind power investment costs. This result in low and stable electricity prices, which represent 77-89% of the levelized cost of H_2 production. In the case studies for northern Norway with 24 hours of hydro power flexibility, the future H_2 production cost is estimated to be 1.89 €/kg.

In Texas, the results from the case study show that CO_2 emissions can be reduced by using flexible H_2 production to provide some of the balancing energy which is currently provided by natural gas turbines. H_2 can also be produced from natural gas in combination with carbon capture and storage (CCS) to utilize the natural gas resources with low CO_2 emissions. This is more cost-efficient than using CCS with natural gas turbines. Furthermore, the results show that higher CO_2 prices favor electrolytic H_2 production while more H_2 demand favors natural gas based H_2 production. Electrolytic H_2 production is competitive with natural gas based H_2 pathways for CO_2 prices of more than 60 $/tonne, supplying 40-80 % of the total H_2 demand. Emissions from H_2 production is less than 1.2 kg CO_2/kg H_2 with a CO_2 price of more than 90 $/tonne as H_2 is produced from electrolysis and natural gas with CCS.

Flexible H_2 production is necessary to enable high shares of VRE integration above 80-85% in the Texas case study. With high shares of VRE electricity generation the electricity price will be variable and electrolytic H_2 production will be concentrated to surplus hours when the electricity price is low. The results show that H_2 storage has a duration of 5-37 hours and provides flexibility which is complimentary to batteries (2-7 hours). The future H_2 production cost in Texas was estimated to around 1.30-1.66 $/kg when the CO_2 price is 60 $/tonne CO_2. This shows that electrolytic H_2 based on renewable electricity can be produced at lower costs than the current H_2 price which are around 2.8-3.3 €/kg in Europe and the US (late 2020).

Contents

Acronyms

ACER	Agency for the Cooperation of Energy Regulators. 21
AEL	alkaline electrolysis. 28–31
AMR	automatic meter reading. 23
ATB	annual technology baseline. 16
ATR	Auto Thermal Reforming. 24, 25, 41
CAPEX	capital expenditure. 29–32, 68, 76, 81
CCS	carbon capture and storage. vi, 4, 5, 24–27, 32, 40, 41, 49, 70–72, 74, 75, 81, 89–93
CEP	capacity expansion problem. 6, 7, 43–47, 49, 55, 62, 63, 83, 90–92
CHP	combined heat and power. 38
D-CEP	deterministic capacity expansion problem. 64, 65, 82–84, 86, 87, 91
DAM	day-ahead market. 19, 21, 22
DOE	U.S. Department of Energy. 81, 92
DP	Dynamic Programming. 55
EC	European Commission. 21, 57
EIA	U.S. Energy Information Administration. 71
ENTSO-E	European Network of Transmission System Operators. 21
FCR	Frequency Containment Reserves. 20, 21
FCR−D	Frequency Containment Reserves − Disturbance. 21

FCR−N	Normal Frequency Containment Reserves. 21
FRR−A	Automatic Frequency Restoration Reserves. 21
FRR−M	Manual Frequency Restoration Reserves. 21
GEP	generation expansion problem. 43, 44
IDM	intraday market. 19, 21, 22
IRENA	International Renewable Energy Agency. 2, 3
ISOs	Independent System Operators. 19, 20
LCOE	levelized cost of energy. 14–16, 18, 76
LCOH	levelized cost of hydrogen. 31
LHV	lower heating value. 30, 71, 72
LNG	Liquefied Natural Gas. 41, 65
LP	linear program. 46, 52
LQR	local quantile regression. 60
MILP	mixed-integer linear programming. 52, 88
NRAs	National Regulatory Authorities. 21
NREL	National Renewable Energy Laboratory. 16, 71
NVE	The Norwegian Water Resources and Energy Directorate. 18, 48
OPEX	operational expenditure. 31, 32
PEMEL	proton exchange membrane electrolysis. 27–31, 33, 49, 71, 75, 81, 87
PG&E	Pacific Gas and Electric Company. 38
PH	Progressive Hedging. 55
PV	photo-voltaic. 12–14
REZs	Renewable Energy Zones. 36
RPM	Regulating Reserves Market. 21
RPO	Regulating Reserves Options Market. 21
RSOs	Regional System Operators. 19
RTM	real-time market. 19, 21
S-CEP	stochastic capacity expansion problem. 55, 56
SCOPF	security-constrained optimal power flow. 19, 93
SDAC	Singel Day-Ahead Coupling. 21
SDDP	Stochastic Dual Dynamic Programming. 52, 55
SDP	Stochastic Dynamic Programming. 55
SIDC	Singel Intraday Coupling. 22
SMR	Steam Methane Reforming. 4, 5, 24, 25, 41, 49, 70–72, 74, 75, 81, 90–92

SoC	state-of-charge. 60
SOEL	solid oxide electrolysis. 28–30
SRHD	stochastic rolling horizon dispatch. 6, 58–60, 62–64, 77–79, 82–88, 90
SRHD-CEP	stochastic rolling horizon dispatch capacity expansion problem. v, 7, 64, 65, 81–88, 90–93
TEP	tranmission expansion problem. 43
TRG	techno-resource groups. 16
TSO	Transmission System Operator. 19–22, 77, 93
VRE	variable renewable energy. v, vi, viii, 2–7, 9, 14–16, 22–24, 27–29, 32, 33, 36–41, 44, 54, 55, 57, 58, 61–63, 65, 66, 70, 72, 74–77, 79, 87, 89–92

List of Symbols

Indices

i, j	Power plant or storage
k	Cut
n, m	Bus
s	Scenario
t	Time stage

Parameters

η_i^x	Energy storage efficiency for changing (in) or discharging(out).
ρ_s	Probability of renewable power scenario
A_i	Ancillary electricity consumption $[MW]$
B_{nm}	Susceptance between bus n and m $[p.u.]$
C^x	Investment cost for wind (w), storage energy (s) or power (p) $[€/MW]$
D_{tn}	Electricity demand $[MWh]$
E_i, S_i	Storage power and energy capacity $[MW]$
F_i	Electricity or hydrogen consumption rate of conversion technology $[MW/kg]$ or $[kg/MW]$
H_{tn}	Hydrogen demand $[kg]$

I_{ti} Inflow to hydro power reservoirs $[MWh]$

O^x Operational cost from fuel (f), regulation (r), load shedding (s) or exchange (ex) $[€/MWh]$

P_{ti}^{sch} Scheduled power production $[MW]$

P_i^x Max or min production capacity $[MW]$

P_{tis} Power profile $[MWh]$

R_i^x Ramping up or down capability $[MW/h]$

T_{nm} Transmission capacity from bus n to m $[MW]$

V_i^0, S_i^0 Initial reservoir or storage level $[MWh]$

V_T End-of-horizon storage value $[€/MWh]$

W_i^{Pot} VRE resource capacity $[MW]$

X_{in}^{init} Number of initially installed plants

Sets

$\mathcal{A}_n$ Plants consuming ancillary power at bus n

$\mathcal{B}$ All buses

$\mathcal{C}_n$ Buses connected to bus n by transmission line

$\mathcal{E}$ Energy storage

$\mathcal{F}_n$ Energy conversion plants representing a demand as bus n

$\mathcal{H}$ Hydro power plants

$\mathcal{H}_2$ Hydrogen plants

$\mathcal{K}$ Set of cuts

$\mathcal{L}$ Set of transmission lines

$\mathcal{N}, \mathcal{M}$ Normal/ market buses

$\mathcal{P}, \mathcal{R}$ Power plant/ renewable power plants

$\mathcal{S}$ Scenarios

$\mathcal{T}, \mathcal{T}_s$ All time steps/ time steps in scenario s

Variables

α, α^k Estimated/ actual operational cost [€]

$\beta_{tis}, \gamma_{tis}$ Dual values of storage energy and power constraints

δ_{tns} Voltage phase angle at bus

π_{tis} Dual values of production constraints

c_{tis} Curtailment of VRE $[MW]$

d^x_{tis} Negative (n) or positive (p) regulation $[MW]$

e^{max}_i, s^{max}_i Storage power/ energy capacity $[MW]$

e^x_{tis} Energy from (out) or to (in) the energy storage [MWh]

h^{max}_i Hydrogen storage capacity $[kg]$

h^x_{ti} Hydrogen directly from rlrctrolyzer (d), imported (i), to storage (p) or from storage (s) $[kg]$

h_{ti} Hydrogen storage level $[kg]$

p^{ex}_{tns} Power exchange with other buses $[MW]$

p^{sch}_{ti} Power production to be scheduled $[MW]$

p_{tis} Production $[MW]$

q_{ti} Energy produced from reservoir water discharge $[MWh]$

r_{tns} Curtailment of load $[MW]$

s_{ti} Energy lost to reservoir water spillage $[MWh]$

u_{tin} Number of plants in active operation

v^x_i Positive (+) and negative (-) deviation from target reservoir level $[MWh]$

v_{ti} Hydro power reservoir level $[MWh]$

w^{max}_i Generation capacity $[MW]$

x^{ret}_{tin} Number of retired plants

x_{tin} Number of new plants

Chapter 1

Introduction

1.1 Motivation and Scope of Thesis

Reducing world-wide CO_2 emissions to limit global warming is one of the most important challenges of modern society. Starting with the United Nations Framework Convention on Climate Change in 1994 and the Kyoto protocol in 1997, policies have been enforced in many parts of the world to reduce global CO_2-emissions. Limiting the global temperature rise to 1.5°C over pre-industrial levels is crucial for reducing damages on natural and human systems caused by sea-level rise and extreme weather. Central to this work is the IPPC report on global warming from 2018 [1], which states the following about the future energy system:

> In energy systems, modeled global pathways (considered in the literature) limiting global warming to 1.5°C with no or limited overshoot generally meet energy service demand with lower energy use, including through enhanced energy efficiency, and show faster electrification of energy end use compared to 2°C. In 1.5°C pathways with no or limited overshoot, low-emission energy sources are projected to have a higher share, compared with 2°C pathways, particularly before 2050. In 1.5°C pathways with no or limited overshoot, renewables are projected to supply 70–85% (interquartile range (IQR)) of electricity in 2050. In electricity generation, shares of nuclear and fossil fuels with carbon dioxide capture and storage (CCS) are modeled to increase in most 1.5°C pathways with no or limited overshoot. In modeled 1.5 °C pathways with limited or no overshoot, the use of CCS would allow the electricity generation share of gas to be approximately 8% (3–11% IQR) of global electricity in 2050, while the use of coal shows

> a steep reduction in all pathways and would be reduced to close to 0% (0–2% IQR) of electricity. While acknowledging the challenges, and differences between the options and national circumstances, political, economic, social and technical feasibility of solar energy, wind energy and electricity storage technologies have substantially improved over the past few years. These improvements signal a potential system transition in electricity generation.

Currently, the increase in variable renewable energy (VRE) integration is happening fast, facilitated by dropping prices for wind and solar power. In this regard, the International Renewable Energy Agency (IRENA) have made a road-map for 2050 [2], where they identify five pillars for the transition to a low carbon energy system:

1. Electrification
   - The electrification of end uses will drive increased power demand to be met with renewables

2. Increased power system flexibility
   - Flexibility in power systems is a key enabler for the integration of high shares of variable renewable electricity – the backbone of the electricity system of the future

3. Conventional renewable sources
   - Hydropower can bring important synergies to the energy system of the future
   - Bioenergy will become increasingly vital in end-use sectors

4. Green hydrogen
   - Hydrogen can offer a solution for types of energy demand that are hard to directly electrify
   - Hydrogen can be processed further into hydrocarbons or ammonia, which can then help reduce emissions in shipping and aviation

5. Fostering innovation to address challenging sectors
   - Half of energy demand could be supplied by electricity by 2050, but the remaining half must also be considered

Increasing shares of VRE sources introduces new challenges, central to these challenges are the need for power system flexibility as stated in the second pillar in the

IRENA road-map. Storage systems such as grid-scale batteries, hydro power reservoirs, heat-based storage and hydrogen storage will play an important role in the creating the cost effective and low carbon energy systems of the future. Flexible resources can also contribute to increase the capacity utilization on transmission lines and make distantly located renewable resources of high quality cost efficient.

Hydrogen (H_2) has the potential to play a significant role in the future low carbon energy system as it can be stored at low cost and used in end-use applications throughout many sectors of the economy. H_2 can be reconverted to electricity in fuel-cells or gas turbines and thus increase the security of electricity supply by providing stable power generation in VRE dominated systems. Due to high gravimetric energy density, H_2 can be more preferable than batteries to power emission-free long-distance transport by trucks, ships and airplanes. Furthermore, H_2 can be used to reduce emissions in industry as stated in the IPCC report:

> CO_2 emissions from industry in pathways limiting global warming to 1.5°C with no or limited overshoot are projected to be about 65–90% (IQR) lower in 2050 relative to 2010, as compared to 50–80% for global warming of 2°C. Such reductions can be achieved through combinations of new and existing technologies and practices, including electrification, hydrogen, sustainable bio-based feedstocks, product substitution, and carbon capture, utilization and storage (CCUS).

In 2020, the European Commission released a plan towards large scale H_2 production from electrolysis. The plan states targets of 6 GW and 40 GW of electrolysis capacity within 2024 and 2030 respectively, which can result in 1 and 10 million tonnes of renewable H_2 that enables emission reductions in hard-to-decarbonize sectors of the economy [3].

1.1.1 Role of Hydrogen in the Future Energy System

H_2 and O_2 is produced from water using electricity in the electrolysis process. H_2 produced by electrolysis is called "green H_2" if the electricity is produced from renewable sources with no significant CO_2 emissions [4, p.34]. H_2 production from electrolysis can become a flexible asset in the electricity system by adding H_2 storage, thus from a electricity system point-of-view the H_2 becomes a flexible load. Further flexibility can be obtained by adding a fuel cell or gas turbine, which reconvert H_2 back to electricity. However, the round-trip efficiency of these systems are quite low, typically 20-50 % in practical applications[5, 6]. Thus, using H_2 production as a flexible load and the resulting H_2 for further emission reduction in end use applications that are hard to electrify seems like a more attractive

option [7]. Regardless of flexibility from H_2 production or H_2 storage systems, it is increasingly interesting on a longer time-scale as the cost of adding storage energy capacity is much lower than for most flexible assets that is not bound to geographical constraints (such as hydro power) [8, 9].

Another method of producing H_2 is to use methane from fossil sources in a process called Steam Methane Reforming (SMR). H_2 produced from SMR with carbon capture and storage (CCS) is often called "blue H_2" [4, p.34] and result in low levels of CO_2 emissions. This represent a way of utilizing fossil resources with low emission rates which, combined with flexible electrolysis, results in a cost efficient and flexible system for H_2 production that will have positive synergies with the electricity system.

The physical properties of H_2 makes it a valuable energy carrier way beyond energy storage. H_2 can be transported on ships, trucks or pipelines, thus it offer an alternative to electric transmission lines for energy transport from remote VRE sources. The combination of transporting H_2 itself and flexible H_2 production in order to increase electric transmission line capacity can reduce the costs of developing remote renewable energy sources [10, p.67-93]. Utilizing remote energy resources will only become more important as the demand for renewable energy increase and the best resources closest to the energy demand are fully utilized. Remote energy resources that remain undeveloped due to the cost of energy transport are often characterized as "trapped" or "stranded", examples of this are found in several regions all over the world. In Norway, the best wind power resources are located in the northern part of the country [11], while the load is mainly in the south. Germany also has good wind power resources in the northern part of the country around the north sea while the load is in the south, which has led to significant grid congestion and costly generation re-scheduling [12, p.27]. Large amounts of wind power resources have been developed in north-western Texas, also called Texas pan handle, over the last decade. The integration of wind power in the Texas pan handle required significant transmission investments to the electric demand in the east [12, p.24].

This thesis is connected to the HYPER project [13], which looks at the possibility of transporting energy as liquid H_2 from the remote areas where renewable resources are underdeveloped due to the distances to the energy demand. In one scenario, H_2 is produced from a combination of natural gas and renewable electricity in northern Norway, liquefied and transported aboard ships to locations far away such as central-Europe or Japan.

1.1.2 Scope of Thesis

In light of the potential of H_2 to enable reductions in CO_2-emission, the benefits and costs of flexible H_2 production in the electricity system needs to be studied. The scope of this thesis is to study the benefits obtained by the electricity system from flexible H_2 production, especially in the context of variable renewable energy (VRE) and restricted transmission capacity.

To make H_2 production in the electricity system viable it has to be cost effective compared to other ways of producing H_2 with a low CO_2 footprint, mainly from natural gas using SMR with CCS. Thus, this thesis evaluates the cost components of electrolytic H_2 production and how they can be reduced.

Different model approaches are developed and used in the analysis. First, a model for capacity expansion in the electricity system was created in order to determine the optimal sizing of the comprising the electrolysis system, namely the electrolyzer and H_2 storage capacity. The expansion of wind power capacity are also included in order to analyze the synergies with flexibility from H_2 production. secondly, investments energy transport, storage and production is investigated for a sector coupled system energy system with interconnected electricity and H_2 systems. Thirdly, a stochastic model is developed for power system operation in order to fully assess the value of flexibility from H_2 production and hydro power. This model includes a realistic representation of electricity system operations considering uncertainty from wind power and electricity market structure. Finally, the stochastic operation model is integrated as the sub-problem in a decomposed capacity expansion model to capture any effects of short-term uncertainty on investments, typically ignored or simplified by traditional capacity expansion models.

To limit the scope of work, the thesis focus on regions of electricity systems (northern Norway) or large and self-supplied systems (Texas). When analyzing a region of the electricity system, the rest of the system is simply represented by the electricity market as a price series. The scope of the capacity expansion models are limited to using one target year and annualized investment costs. We focus on the production side of the H_2 supply chain and do not represent the demand side beyond a fixed constant H_2 demand. In the case of northern Norway it is assumed that there is a H_2 demand for energy export to other parts of the world. Estimates of future H_2 demand is obtained from literature references for the case study of H_2 production in Texas, were the analysis include a order-of-magnitude analysis of the H_2 demand. For simplicity, the temporal profile of the hydrogen demand is assumed to be constant in all cases.

1.1.3 Research Objectives

Following from the scope of this thesis the research objectives are formulated as follows:

- Investigate how flexible H_2 production influence the electricity system, analyze which benefits it provides.
- Determine how the synergies between the electricity system and H_2 production affect the sizing of the components comprising the electrolysis plant, transmission grid and wind power.
- Estimate the price of H_2 from electricity and determine the optimal operation strategies for minimizing production costs in the future when H_2 is produced on a large scale from variable renewable energy (VRE).
- Analyze the potential contribution of flexible H_2 production to reduce CO_2-emissions in the electricity system.
- Evaluate the two main pathways of H_2 production, electrolysis or natural gas reformation, in a interconnected electricity and H_2 energy system.
- Investigate whether short-term uncertainty have a significant effect on the optimal capacity of flexible resources, such as H_2 production.

1.2 Contributions

In this thesis, we investigate the benefits and costs of H_2 production from electricity and natural gas. We develop several capacity expansion problems in order to analyze the role H_2 production can have in systems that are traditionally dominated by VRE and fossil energy sources. The contributions from this thesis are published in five articles, where the main contributions are summarized below:

- The power systems of northern Norway is studies in order to show how H_2 production can provide flexibility to the power system in order to integrate VRE electricity production and provide security of supply in areas with constrained transmission grids.
- A stochastic rolling horizon dispatch (SRHD) is developed for simulating power system operation within a market setting with uncertain VRE generation and storage. Long-term storage strategies are used to analyze the importance of hydro power flexibility for cost efficient H_2 production from wind power with uncertain electricity generation in northern Norway.

- A capacity expansion problem (CEP) is developed for capturing the synergies between detailed electricity and H_2 systems including production, storage and transport of both energy carriers. The model is used to show the potential synergies between electricity and hydrogen production in Texas based on a cost scenario for 2050.

- The impact of short-term uncertainty on investments in the power system is analyzed. This shows that deterministic models significantly underestimate the optimal capacities and operational costs, especially in constrained transmission grids.

- A stochastic rolling horizon dispatch capacity expansion problem (SRHD-CEP) is developed which allows for realistic simulation of operation (considering short-term uncertainty and markets) within CEPs and requires relatively low computational resources. This model is shown well suited for future systems where uncertainty from VRE generation and storage play an increasingly important role.

1.3 List of Publications

The main work of this thesis is represented by the following publications.

Article 1 E. F. Bødal and M. Korpås, "Regional Effects of hydrogen Production in Congested Transmission Grids with Wind and Hydro Power," in 14th International Conference on the European Energy Market - EEM, 2017, pp. 1–6.

Article 2 E. F. Bødal, D. Mallapragada, A. Botterud, and M. Korpås, "Decarbonization synergies from joint planning of electricity and hydrogen production: A Texas case study," Int. J. Hydrogen Energy, vol. 45, no. 58, pp. 32899–32915, Nov. 2020.

Article 3 E. F. Bødal and M. Korpås, "Production of hydrogen from Wind and Hydro Power in Constrained Transmission grids, Considering the Stochasticity of Wind Power," J. Phys. Conf. Ser., vol. 1104, no. 1, p. 012027, Oct. 2018.

Article 4 E. F. Bødal and M. Korpås, "Value of hydro power flexibility for hydrogen production in constrained transmission grids," Int. J. Hydrogen Energy, vol. 45, no. 2, pp. 1255–1266, 2020.

Article 5 E. F. Bødal, A. Botterud and M. Korpås, "Capacity Expansion Planning with Stochastic Rolling Horizon Dispatch," Submitted to Journal for review.

As a part of the PhD work, I have assisted with guidance and optimization models for the following master thesis on H_2 production:

- D. Q. A. Pinel, “Hydrogen Production from Wind and Solar Power in Weak Grids in Norway,” Norwegian University of Science and Technology, 2017. [14]
- M. Moldestad, “Evaluating pathways for hydrogen produced from low-carbon energy sources,” Norwegian University of Science and Technology, 2020. [15]

1.4 Thesis Structure

The main results of this thesis are the articles attached in Appendix A. In the following chapters, a summary of the work presented in the articles is given with the following structure. In Chapter 2 the context of H_2 production in the electricity system is laid out in the form of technology, costs and the electricity system aspects considered in this thesis. Chapter 3 gives an overview of the methodologies used to analyze H_2 production by explaining the different types of optimization problems utilized. The main results from the publications are presented and discussed in Chapter 4. Conclusions from the work are given in Chapter 5, along with recommendations for future research on the topic of this thesis.

Chapter 2

Research Context

Transforming the energy system to reduce the CO_2 footprint of power generation is a important part of reducing global emissions. Central to this transformation is the development and cost reduction of VRE. These technologies, mainly wind and solar power on a global scale, also lead to significant challenges for system planning and operation. Flexible H_2 production has the potential to mitigate some of the challenges with integrating high shares of renewable energy in the electricity system by providing demand-side flexibility. Furthermore, H_2 can reduce emissions in hard-to-decarbonize end-use applications.

2.1 Integration of Variable Renewable Energy

Renewable energy can be generated by a wide range of technologies based on energy sources such as wind, solar, biomass, hydro geothermal, tidal and others. Wind and solar power have the greatest potential world-wide, thus the most important principals behind these technologies are descried briefly in this section.

2.1.1 Wind Power

A wind power turbine generates electricity by harvesting the kinetic energy of the wind. The energy in the wind flowing across the area swept by the wind turbine blades is proportional to the density of the wind (ρ), area swept by the blades (A) and the speed of the wind ($\bar{u}$) as shown in Equation (2.1).

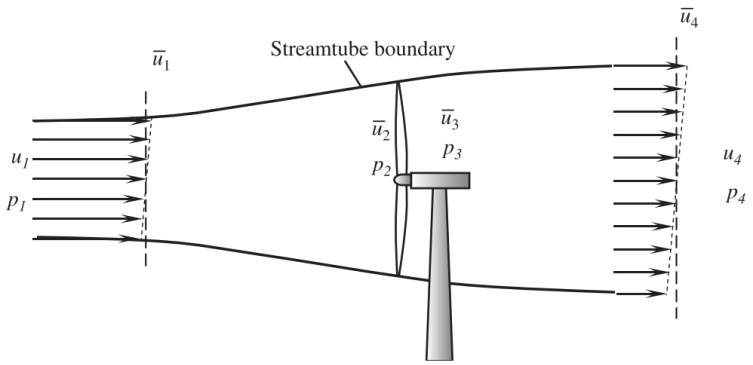

Figure 2.1: Cross section of airflow trough a wind power turbine [16].

$$P_w = \frac{1}{2} m \bar{u}^2 = \frac{1}{2} \rho A \bar{u}^3 \tag{2.1}$$

where

$$m = \rho u \tag{2.2}$$

All the wind energy cannot be converted into mechanical power. The mechanical energy captured by the wind turbine is given by the pressure (p) differential over the wind power blades and the swept area of the blades as illustrated in Figure 2.1. The mechanical energy is given by Equation (2.4), derived from Equation (2.3).

$$p_1 - p_2 = \frac{1}{2} \rho \bar{u}_2 (\bar{u}_1^2 - \bar{u}_4^2) \tag{2.3}$$

$$\begin{aligned} P_{me,out} &= (p_1 - p_2) A \\ &= \frac{1}{2} \rho A \bar{u}_2 (\bar{u}_1^2 - \bar{u}_4^2) \\ &= \frac{1}{2} \rho A \bar{u}_1^3 4a(1-a)^2 \end{aligned} \tag{2.4}$$

where

$$a = \frac{\bar{u}_1 - \bar{u}_2}{\bar{u}_1} \tag{2.5}$$

The power factor of a wind power turbine is defined as the share of mechanical power that can be extracted from the wind energy and is given by Equation (2.6).

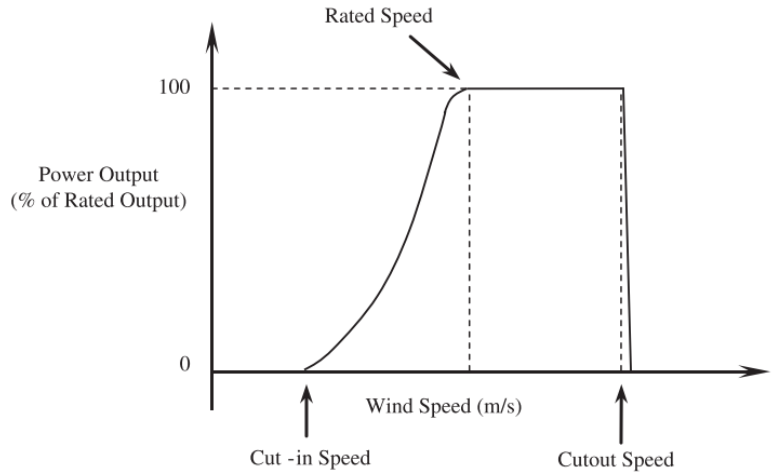

Figure 2.2: Typical wind turbine power output as a function of wind speed [16].

$$C_p = \frac{P_{me,out}}{P_w} = 4a(1-a)^2 \tag{2.6}$$

The technical limit of the power factor that can be achieved is given by the Landchester-Benz limit at 59.26 %, however modern wind power turbines typically has a power coefficient of 30 to 45 %[16].

The wind speed is determined by the location of the plant and is the most important factor for a wind power plant as the power output is proportional to the wind speed cubed as shown in Equation (2.4). The effective electric power output of a wind power turbine is given by the mechanical power and losses in the gears, generator and electric power converters. The electric power output is plotted as a function of the wind speed in Figure 2.2 and characterized by the cut-in, rated and cutout speed. Electricity generation begin at the cut-in speed and reaches its maximum value at the rated speed. Higher wind speed than the rated speed does not give higher power output but is kept at the maximum value by the power control. The turbine is shut down at the cutout speed when the wind speed is too strong, preventing potential damage to the turbine.

The rotor diameter is the second most important factor of a wind power turbine. The area swept by the blades is proportional to the rotor diameter squared, A $= \pi r^2$, and directly proportional to the power output of the turbine as shown in Equation 2.4. Thus, the development in wind power turbine and plant design is

Table 2.1: Trends in wind power turbine and plant design is expected to lead to larger turbines and fewer turbines for each wind power plant [17].

		Base (2018)	Conservative (2030)	Moderate (2030)	Advanced (2030)
Hub height	m	88.0	110.0	120.0	135.0
Number of turbines		84.0	50.0	37.0	29.0
Turbine rating	MW	2.4	4.0	5.5	7.0
Rotor diameter	m	116.0	150.0	175.0	200.0
Specific power	W/m^2	227.0	226.0	229.0	223.0
Wind plant rating	MW	200.0	200.0	200.0	200.0
Wind speed at hub	m/s	7.9			

heading towards plants with fewer but larger wind power turbines as shown in Table 2.1.

2.1.2 Solar Power

Photo-voltaic (PV) solar power is the most widely deployed solar power technology. The most fundamental component of a PV solar power plant is the PV cell as shown by the plant breakdown in Figure 2.3. The PV cell is a pn-junction diode which consist of two semiconductors, one doped with electron-donating impurities (n-doped) and the other with hole-donating impurities (p-doped). When the two doped semiconductors are put in contact the excess electrons in the n-doped semiconductor fills the holes in the p-doped semiconductor and creates a electric field (bandgap[1]) at the interface between the conductor[2] and valance[3] bands. Photons (light) that strikes the PV cell with higher energy content (i.e. high frequency photons) than the bandgap are absorbed by the cell as illustrated in Figure 2.3.c. These photons generate a hole on the positive side as it enables a electron to cross the valance band over to the negative charged side of the cell. Excess energy is dissipated if a photon have more energy than what is required to cross the bandgap. Photons with lower energy than the band gap (i.e. low frequency photons) does not transfer a electron to the negative charged side and does not contribute to the electricity generation.

The efficiency of a cell is calculated according to Equation (2.7), where the power output of the cell is given by the form factor (FF), open-circuit voltage (U_{oc}) and the short-circut current (I_{sc}) [19].

[1]Bandgap refers to the energy needed for an electron to cross from the valance to the conductor band.

[2]The conductor band is the area of the n-doped semiconductor with free electrons.

[3]The valence band is the area of the p-doped semiconductor with free holes.

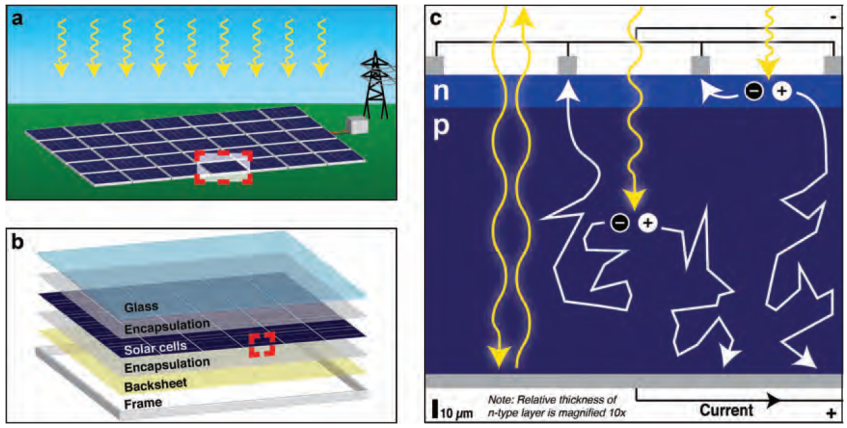

(a) Illustration of grid-connected PV system

(b) Breakout view of PV module

(c) Cross section of silicon solar cell showing PV mechanism

Figure 2.3: Breakdown of a PV solar power plant (a) on the module (b) and cell level (c) [18].

$$\eta_{em} = (\frac{FF \cdot U_{oc} \cdot I_{sc}}{A_m \cdot I_p}) \cdot 100 \tag{2.7}$$

The choice of semiconductor material determines the band gap, open-circuit voltage and short-circuit current. The efficiency is limited as reducing the band gap increases the short-circuit current because the cell absorbs more photons, however the open-circuit voltage is reduced as excess energy is dissipated [18]. The maximum efficiency of a single-junction (one material) solar cell with unconcentrated irradiation is around 33%, known as the Shockley-Queisser Limit. This can be increased to a theoretical maximum of 68% by combining layers of semiconductors with different bandgaps, known as multi-junction cells. Silicone is the most common semiconductor material in commercial solar cells as it is non-toxic and results in efficient and extremely reliable PV cells.

Improvements in solar cell technology focuses on increasing efficiency, improving manufacturing (techniques and costs) and reducing material usage of silver and silicone. PV cells can be classified in two main categories based on the manufacturing technique used, wafer-based and thin film solar cells [18]. While wafer-based cells remain the leading technology thin film cells can provide the answer to some of the main challenges faced by wafer-based cell. Thin film solar cells do not require the same high level of purity and quantity (10-50 % less) of silic-

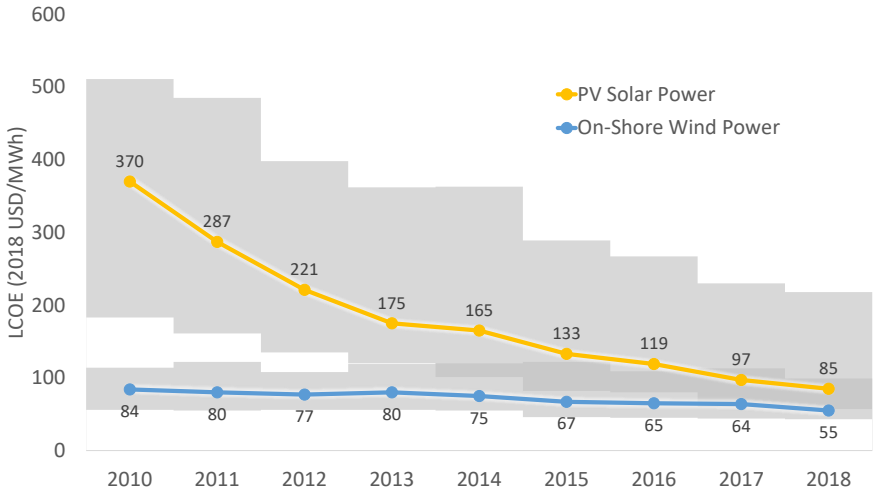

Figure 2.4: Levelized cost of energy for solar power and on-shore wind power projects for the period 2010-2018, represented by the weighted mean values (lines) and 5 to 95 percentile range. The figure is reproduced from [20].

one as wafer-based cells. They are also flexible and could potentially enable high throughput manufacturing [18].

Large-scale PV solar power plants consist of many PV arrays as illustrated in Figure 2.3.a. In a PV array, PV modules are connected in series to get the desired voltage, several of these series of modules are connected in parallel to increase the current and power output. Power converters are needed to convert the DC power output of the PV modules to AC power which is fed into the electricity grid. The main component of the PV modules are the PV cells, while other components as glass, encapsulation, back-sheet, frame and electric conductors (see Figure 2.3 b) are needed to protect the PV cells, provide structural integrity and transport the electricity throughout the module.

2.1.3 Historical Development of VRE Costs

The cost of electricity from VRE is reduced significantly the last decade as shown in Figure 2.4 [20]. In the period from 2010 to 2018, the average levelized cost of energy (LCOE)[4] from solar power has been reduced from 370 to 85 $/MWh, which is a reduction of almost 80 %. During the same period, the average LCOE from wind power is reduced from 84 to 55 $/MWh, a 35 % reduction. The main reason for this cost reduction is years of subsidies for VRE which has contrib-

[4]Total cost per MWh produced.

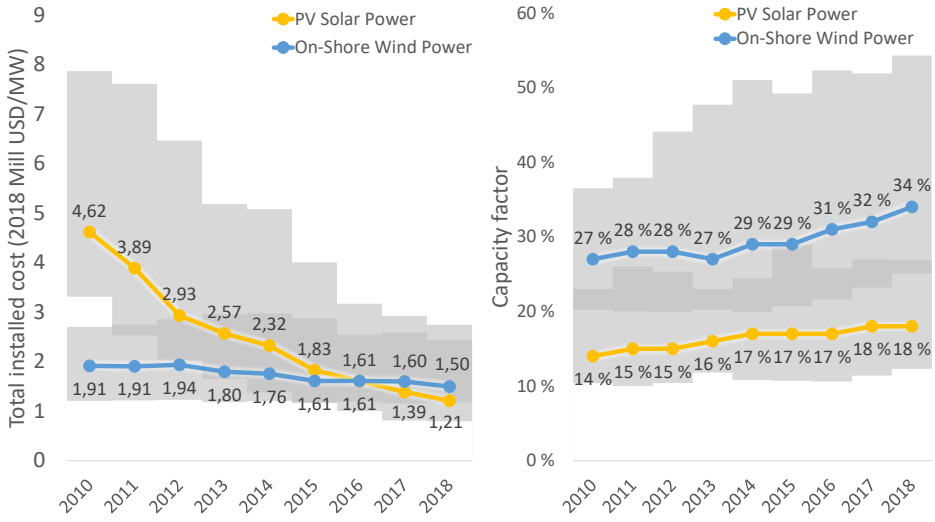

Figure 2.5: Development in total installed cost and capacity factor from 2010-2018, represented by the weighted mean values (lines) and 5 to 95 percentile range. The figure is reproduced from [20].

uted to lowering costs and improve technology. VRE electricity generation is now competitive with traditional electricity generation based on fossil energy sources, without the need for subsidies. The least-cost electricity generation technology is dependent on local variations in resource conditions for VRE, fuel and CO_2 prices. In comparison, thermal electricity generation have LCOEs of around: 33-39 $/MWh for base-load natural gas, 64-149 $/MWh for peak-load natural gas, 67 $/MWh for nuclear and 78-108 $/MWh for coal.

Reduced total installed cost and increased capacity utilization are two of the main contributing factors for lowering the LCOE of VRE electricity generation in recent years as shown in Figure 2.5. The total installed cost for solar power was reduced from 4.62 to 1.21 Mill $/MW from 2010 to 2018, and is now less than the installed cost for wind power at 1.5 Mill $/MW. The total installed cost of wind power was reduced from 1.91 to 1.5 $/MW in the same period, largely driven by larger rotor-diameters and higher rated capacity per turbine. The higher turbine capacity enables wind power plants to produce more energy at lower wind speeds, thus increasing the average capacity factor from 27 % to 34 % as shown in Figure 2.5 [21]. Higher turbine capacity also reduces the the total number of turbines in a wind farm and thus the operation and maintenance costs. Wind power turbines have a significantly higher capacity factor than for solar at 18 %, resulting in a lower LCOE for wind power despite higher installation costs than for solar power.

Table 2.2: Techno-Resource Groups for wind power and potential available capacity in the US [17].

Techno-Resource Group (TRG)	Wind Speed Range (m/s)	Weighted Average Wind Speed (m/s)	Potential Wind Plant Capacity (GW)
1	8.2 - 13.5	8,7	100
2	8.0 - 10.9	8,4	200
3	7.7 - 11.1	8,2	400
4	7.5 - 13.1	7,9	800
5	6.9 - 11.1	7,5	1600
6	6.1 - 9.4	6,9	1600
7	5.4 - 8.3	6,2	1600
8	4.7 - 6.9	5,5	1600
9	4.0 - 6.0	4,8	1600
10	1.0 - 5.3	4,0	1148
Total			10 648

2.1.4 Expected Future Reductions in VRE Costs

The LCOE of VRE technologies are dependent on location and resource quality. Currently, the LCOE of the best 50 % of US onshore wind resources range between 30-50 $/MWh. Solar power has a LCOE in the range of 33-59 $/MWh depending on the latitude from south to north in the US [17].

It is expected that the cost of investing in VRE will be further reduced. Technology cost projections for VRE electricity generation in the US are shown for wind in Figure 2.6 and solar power in Figure 2.7. The cost projections are obtained from the annual technology baseline (ATB) from the National Renewable Energy Laboratory (NREL) and are differentiated based on the wind speed and location for wind and solar resources respectively. Wind power resources are divided by techno-resource groups (TRG) which are shown in Table 2.2. The cost projections expect most of the cost reductions for wind power before 2030, as seen from the NREL ATB in Figure 2.6, where the LCOE for 70% of wind power resources are in the range of 20-40 $/MWh.

The solar power cost predictions are differentiated by latitude represented by five different cities in the US as shown in Figure 2.7, from Seattle (N 48°) in the north to Los Angeles and Daggett (N 34°) in southern California. The cost projections for solar power in this region is on the same level as TRG 1-8 for wind power. In the European context, the latitude of Seattle is equivalent to northern France or southern Germany. The LCOE of solar and wind is projected to be similar in this region in 2050 (both around 18-30 $/MWh), while further north wind power

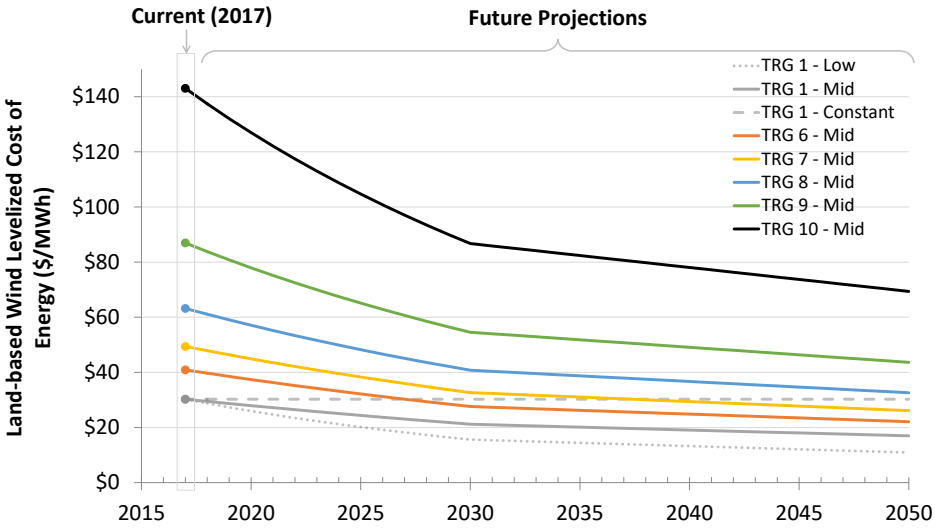

Figure 2.6: 2017 values for levelized cost of energy from wind power with future projections until 2050 [17]. To simplify the figure, TRG 2-5 are excluded as they are all tightly located between TRG 1 and 6.

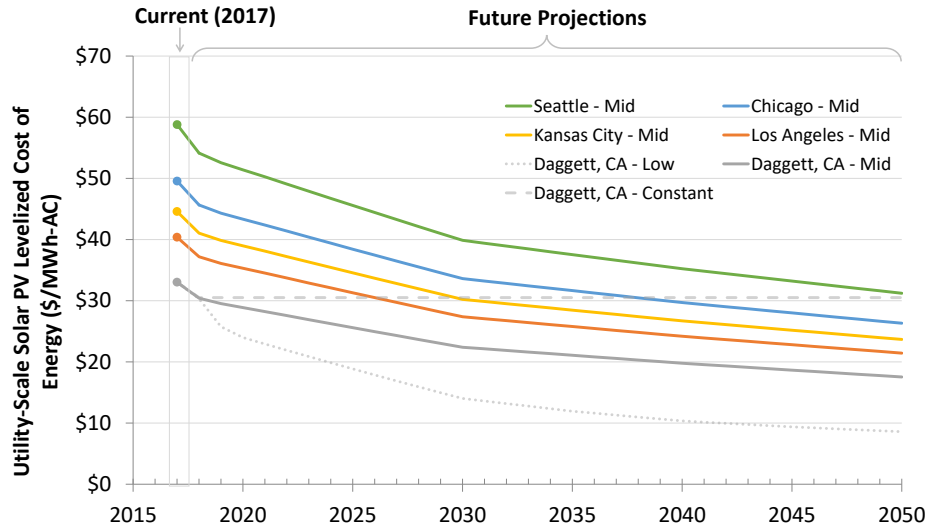

Figure 2.7: 2017 values for levelized cost of energy from photo-voltaic solar power with future projections until 2050 [17]

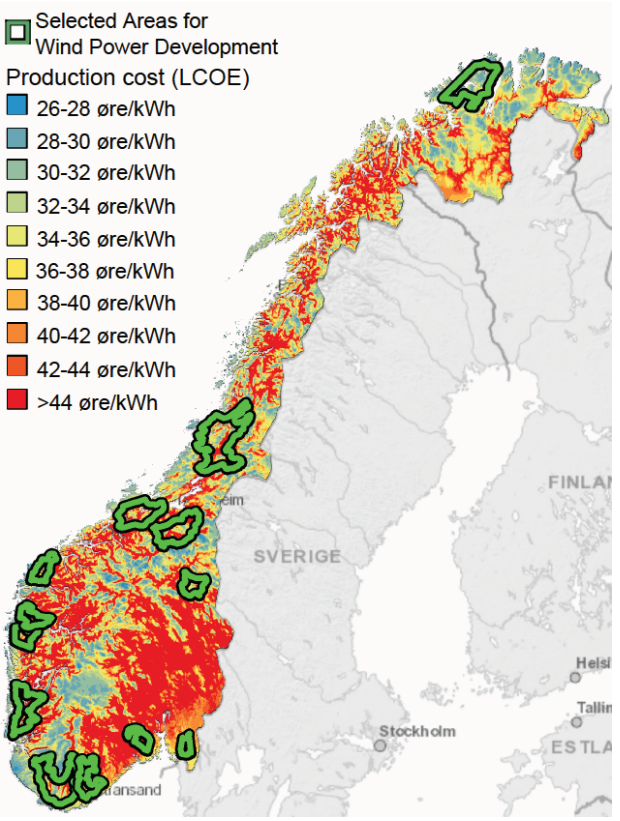

Figure 2.8: LCOE for wind power and the areas identified as the best suited for wind power development in Norway [22].

is likely to have a lower LCOE for large-scale electricity generation.

In Europe, Norway have some of the best wind resources alongside Ireland, Denmark and northern Germany. The average LCOE for wind power in Norway has seen a steep decrease since 2008 from 62 to 35 $/MWh in 2016, while projections for 2020 show a further decease to 29 $/MWh [23]. The Norwegian Water Resources and Energy Directorate (NVE) has created a national framework for wind power based on thorough interdisciplinary analysis where they point out several regions suited for wind power development [22]. These regions are marked with green lines in Figure 2.8. The best wind resources for further development of wind power in Norway are located in the northern part of the country as shown in Figure 2.8, where significant wind resources are available at LCOE of 26-32 øre/kWh (27-34 $/MWh).

2.2 Electricity markets

The operation of many power systems throughout world have been organized through energy markets since wide-spread deregulation in the 1990's [24, 25]. Most power systems was traditionally organized in vertically integrated monopolies, deregulation resulted in a separation between electricity generation and transmission. This led to a wide variety of competitive market systems for electricity generation. In Europe, the Transmission System Operator (TSO) remains natural monopolies. While in the US, there are Independent System Operators (ISOs) or Regional System Operators (RSOs), which perform a similar function. Many market products are needed to incentivise close to optimal socio-economic operation of such a complex system. The operational markets can be grouped into three main categories, the financial futures market, energy markets and ancillary services markets. The futures market is a financial instrument were electricity can be traded years ahead of production and is used for risk management by participants in the electricity markets. The futures market for the Nordic electricity system is organized on the NASDAQ stock exchange [26].

2.2.1 Day-ahead, real-time and intraday markets

Most of the electricity markets in the US and Europe are organized according to the two-settlement system, with a day-ahead market (DAM) and one or more markets which clears closer to the time of operation [27]. In the DAM, operation is cleared one day prior to real-time in order to provide sufficient time for slow ramping generators to adjust production, provide a hedging against price volatility and secure reliable operation of the electricity system.

Different approaches are found in terms of market structures close to the time of operation, in the US the real-time market (RTM) clears continuously every 5 minutes before operation through a centralized security-constrained optimal power flow (SCOPF). While balancing markets are used in Norway and most of Europe. The balancing market close 45 minutes prior to the operational hour and bids are activated continuously when needed by the TSO according to the lowest price. In addition, the electricity systems in Europe typically have a intraday market (IDM) that enables market participants to correct their market bids prior to the balancing market. The IDM is based on continuous bilateral trading until one hour before the operational hour. The prices in the IDM are typically lower than prices in markets closer to the operational time. This is due to the "cost-of-readiness", which represents cost premium as generators that are able to change their power output fast typically are more expensive to operate such as natural-gas power plants [28].

Even though most deregulated electricity markets share many of the same traits,

Market	Period	Res.	Comm.	October	Thursday - 10:00	Thursday - 12:00	Friday - 12:00	Day-1 - 12:00	Day-1 - 18:00	Hour-1	Hour - 0:45
RKOM	Winter	Season	Capacity	✓							
FFR-M	Week	N/D/E	Capacity		✓						
FCR-N	Weekend	N/D/E	Capacity			✓					
RKOM	Week	N/D	Capacity				✓				
FCR-N	Weekday	N/D/E	Capacity				✓				
Elspot	Day	Hour	Energy					✓			
FCR-N/D	Day	Hour	Capacity						✓		
Elbas	Cont.	Hour	Energy							✓	
FRR-M	Hour	Hour	Energy								✓

Figure 2.9: Period, resolution and commodity of market products in the Nordic electricity market, copied from [29], originally reproduced from [30]. Capacity procurement markets for ancillary services are divided into night (N), day (D) and evening (E).

there are some general differences between the US and European electricity markets [27]. In the US, electricity markets have a higher degree of centralized dispatch than in most European electricity markets where generation scheduling is mostly based on self-dispatch. In self-dispatched electricity markets the producers send bids to the market in the form of price and quantity pairs which is used to clear the market in a exchange similar to the stock market. In systems with a higher degree of centralized dispatch, more information is provided by the producers to the system operator such as the cost of incremental energy supplied, start-up of generators and no-load costs in addition to physical constraints on ramping, minimum up-time and more.

2.2.2 Ancillary services and reserves markets

The TSO (or ISOs) operates the transmission grid and is responsible of balancing electricity generation and consumption in order to keep the frequency at 50 Hz (60 Hz in the US). The TSO use markets for capacity procurement for reserves in order to operate the system efficiently and reliably.

Reserves are divided into three different segments based on purpose and time of response. Frequency Containment Reserves (FCR) is the primary frequency control and fastest type of frequency control where 50% of the response have to be delivered within 5 seconds of frequency deviation outside $\pm$ 0.1 Hz of nominal

frequency and 100% within 30 seconds. In addition to Normal Frequency Containment Reserves (FCR−N), there is an additional product for upwards reserves (FCR−D) to keep the frequency from falling too much when there is disturbances in the system which is activated between from 49.9 to 49.5 Hz. The FCR is activated automatically as generator regulators change the power output automatically based on the electric frequency in the system. Capacity procurement markets are required in order to ensure that some generators operate with a sufficient margin to their maximum capacity limits in order to provide enough FCR control to the system. The need for FCR is dependent on the state of the system, thus there are three market products for FCR−N (daily, weekdays and weekend) and one for FCR−D (daily) as shown in Figure 2.9.

Secondary frequency control is provided by Automatic Frequency Restoration Reserves (FRR−A), these reserves are activated automatically with a maximum start dealy of 30 seconds and are fully activated within 120-210 seconds. The purpose of secondary frequency control is to bring the frequency back to nominal values and relieve FCR. Manual Frequency Restoration Reserves (FRR−M) needs to be activated within 15 minutes to provide tertiary frequency control in order to relieve FRR−A and bottlenecks in the transmission system. Both FRR−A and FRR−M are re-numerated by marginal pricing in the Regulating Reserves Market (RPM) (RTM). Each TSO is responsible for providing enough reserve capacity according to the dimensioning fault in their part of the synchronous system, sufficient reserves can be acquired in the Regulating Reserves Options Market (RPO). An overview of the different markets by market period, resolution, commodity type and time of market closure in the nordic electricity market is given in Figure 2.9, where the DAM is called Elspot, the IDM is Elbas, the RPM is the FRR−M market with "regulerkraft opsjonsmarkedet" (RKOM) as the RPO market.

2.2.3 European market integration

Electricity market design and cooperation between countries is crucial to get the maximum socio-economic utility form the electricity system by efficiently utilizing transmission capacity and thus also generation and storage capacity. The EU Target Model for electricity markets is developed in cooperation between the European Commission (EC), the Agency for the Cooperation of Energy Regulators (ACER), the National Regulatory Authorities (NRAs), and ENTSO-E an aim to make institutional arraignments and provide conceptual market definitions for the harmonization of European energy markets with the goal of efficient cross border exchange [31].

In 2014 the Singel Day-Ahead Coupling (SDAC) was launched in Europe based on the PCR EUPHEMIA algorithm which was in 2019 simultaneously clearing

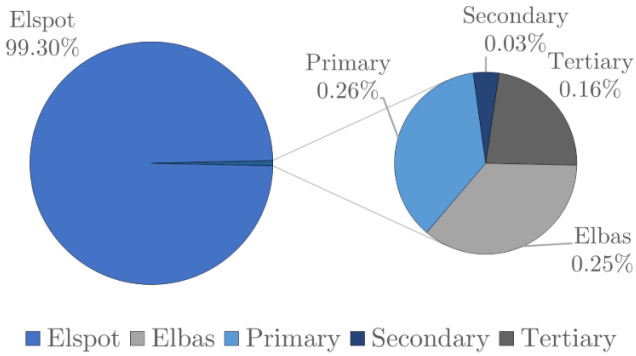

Figure 2.10: Economic turnover in the different energy markets in Norway for 2017 [29]. Elspot refers to the DAM, Elbas to the IDM and the rest to the primary, secondary and tertiary markets for capacity reserves.

the DAM for 27 European countries accounting for 95 % of the electricity consumption. Clearing all the DAM in one algorithm results in more efficient use of transmission capacity an is estimated to have resulted in annual welfare gains of more than 1 B€ [32]. The cooperation between European countries was from 2018 extended to also include IDMs by Singel Intraday Coupling (SIDC) through the XBID algorithm [32] which currently based on continuous trading and allocation of transmission capacity on a first-come first-served basis. Future development of the SIDC is currently discussed in order to allocate the intraday transmission capacity more efficiently by introducing intraday auctions, however the timing and amount of intraday auctions are not decided [33].

Real-time imbalances in the power system is expected to increase as a result of higher shares of VRE generation [34] as the output of these energy sources are hard to predict. Similar to the DAM and IDM there are ongoing processes to harmonize the balancing markets operated by TSOs across Europe with the end goal of increasing the efficiency, competition and security of supply of these markets [35]. Integrating balancing markets are challenging as the available cross-border capacity of balancing is dependent on DAM and IDMs. Increased cooperation between TSOs would reduce the amount of operational reserves needed by netting up and down regulation in the respective areas thus reducing the operational cost of VRE dominated electricity systems [31].

2.2.4 Multi-market operation

The DAM has traditionally been the main short-term energy market and represent the main share of the revenue of power procures as shown in Figure 2.10 [29].

Good design of all the short-term markets are essential to incentivize the flexible operation of generators and loads in the power system which is needed for VRE integration. It is expected to become increasingly important for market participants to participate in multiple markets as much of the future income will be based on providing flexibility in addition to energy [36]. This represent an opportunity for hydro power producers [29], but alto other market participants with flexible assets such as batteries, gas turbines, H_2 producers and other flexible consumers.

2.2.5 Market issues in electricity systems with high shares of renewables

Electricity markets have been affected by typical market failures that are common for many types of markets, these include externalities (not pricing CO_2 emissions etc.), public good attributes (the transmission grid), market price caps and market power [24]. There are also challenges for electricity markets that is more specific to the electricity sector such as the lack of proper demand response and the lack of large-scale electricity storage [37]. In the last decade, significant resources have been invested to amend these problems. The importance of an efficient electricity sector is increasing as the sector is growing because electrification of end-use energy demand is one of the main strategies for reducing CO_2 emissions.

Increasing shares of VRE sources for electricity generation have put an emphasis on the lack of demand-side response which is arguably the most impactful electricity market failure historically [37]. To mitigate this market failure there have been a roll-out of automatic meter reading (AMR) in Norway and many other countries. Traditionally, electricity consumption was measured and billed on a monthly basis. Thus, retailers used to calculate the costumers bill based on the demand profile of a typical consumer. AMR systems enables the end-users to pay the actual spot price of the electricity they are using, which gives them a better incentive to react to the changing electricity prices. As end-users are charged the cost of electricity in the hours they actually use the electricity they are incetivized to invest in home automation systems that can shift the electricity demand of household appliances, electric vehicle charging, water heaters or space heating according to the electricity price.

Aggregators can provide useful demand-side flexibility to the system through the electricity markets by controlling (price signals or direct control) a large amount of end-use demand [38]. Demand-side flexibility can also be provided on a larger scale through sector-coupling with heating or H_2 systems as discussed extensively in this thesis.

2.3 H_2 production

In 2019, 76 % of the global H_2 demand was produced from natural gas, 23 % from coal and only 2 % from electrolysis. Current H_2 production is associated with 830 $MtCO_2$/yr emissions, equal to the annual emissions for Indonesia and the United Kingdom combined [4]. For H_2 to be an energy carrier that efficiently reduce global CO_2 emissions it has to be produced from low emission energy sources or fossil sources combined with CCS. Electrolytic H_2 is expected to become competitive with fossil based H_2 for three main reasons: 1) reducing electrolyzer capital costs, 2) development of VRE leading to periods with low electricity prices and 3) higher CO_2 prices favors H_2 from low emission electricity.

In the following sections, an overview and comparison in terms of technology and costs is made for the two hydrogen production pathways that are likely to be dominant in the near future, natural gas reforming and electrolysis.

2.3.1 H_2 from Natural Gas Reforming with CCS

There are two main processes for producing H_2 from natural gas: Steam Methane Reforming (SMR) and Auto Thermal Reforming (ATR). SMR, which is currently the most common process, mixes steam and natural gas, resulting in H_2 and CO_2 as the products. Typically 30-40 % of the natural gas is combusted to heat the gas mixture to about 900 °C in the reaction shown in Equation (2.8).

$$CH_4(g) + 2H_2O(l) \rightarrow 4H_2(g) + CO_2(g) \qquad \Delta H = 207 \text{ kJ/mol} \tag{2.8}$$

The most important cost component in SMR is the feedstock cost of the natural gas, accounting for around 72% of the total costs of \$1.15-1.32/kg H_2 [39].

The other main process for producing H_2 from natural gas is Auto Thermal Reforming (ATR). In ATR, O_2 is added to the natural gas feed to enable combustion within the reactor as shown in Equation (2.9)

$$CH_4(g) + H_2O(l) + \frac{1}{2}O_2(g) \rightarrow 3H_2(g) + CO_2(g) \quad \Delta H = -22.8 \text{ kJ/mol} \tag{2.9}$$

ATR results in less hydrogen per molecule of methane than SMR (see Equation (2.8) and (2.9)) and is thus less common in current natural gas based H_2 production. On the other hand, ATR is a net positive energy process while SMR require

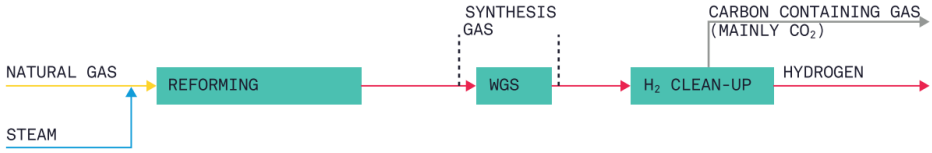

Figure 2.11: Flow chart of the production process for H_2 from natural gas [40].

additional energy input. Furthermore, ATR has potential for higher shares of CO_2 capture (above 90%) at lower cost than SMR. This is achieved as heat is generated by combustion of the natural gas inside the reactor itself, resulting in higher CO_2 concentration in the resulting synthesis gas [4], while in SMR heat is produced before the reactor which result in a flue gas stream that is released to the atmosphere.

The synthesis gas after the reformation stage contains significant amounts of Carbon Monoxide (CO) regardless of the reforming method. In both natural gas reformation processes the CO is used to extract additional hydrogen in a Water Shift Gas (WGS) reactor as shown in Figure 2.11. The gas exiting the WGS reactor contains about 78% H_2, 20 % CO_2 and some small amounts of CH_4 and CO [40].

The total CO_2 emissions of natural gas reforming are about 10-16 kg CO_2/kg H_2 [41, 42, 43], of which reformation process related emissions are around 9 kg CO_2/kg H_2. Emissions from SMR can be reduced by about 90%, to 0.93 kg CO_2/kg H_2, by utilizing carbon capture and storage (CCS). The cost of CO_2 sequestration in the SMR process is estimated to range from \$47-110/kg CO_2 for a capture ratio from 60% to 90% respectively (\$0.3-2.1/kg H_2 [43]). For a CO_2 capture ratio of 60 %, CO_2 is captured from the synthesis gas at high pressure. To obtain a capture ratio of 90 %, CO_2 also has to be captured from the low-pressure flue gas. In comparison to the synthesis gas, sequestrating CO_2 from the flue gas is significantly more expensive.

In ATR it is more efficient to obtain high capture rates of more than 90 %, as most of the CO_2 is remains with high concentration and pressure in the synthesis gas. H_2 production from the two natural gas reformation processes with high capture rates are compared in the H21 North of England project [40], where they concluded that ATR is the best method when targeting CCS capture rates of 95 % as shown in Figure 2.12.

Costs for CO_2 transport and storage is hard to predict as there exist few of these systems at scale. In addition, the costs are dependent location, for some locations in the US the costs for CO_2 transport and storage are estimated to be around \$10-

1.5 GW H_2 PRODUCTION	ATR OPTION 2	SMR OPTION 2
Carbon capture rate (%)	94.1	91.2
CO_2 footprint (g CO_2/kwh)	13.1	20.5
Efficiency % (HHV)	79.9	79.5
CAPEX (£m) – Total	947	1,082
Electric Power Import (MW)	72.6	35.6
CAPEX £/kW$H_{2\ HHV}$)	631	721
Area (ha)	15-20	35-40
Configuration	1 ATR train + ASU	2 SMR trains

Figure 2.12: Key parameters from comparing the different processes for H_2 production from natural gas reformation in the H21 North of England project [40].

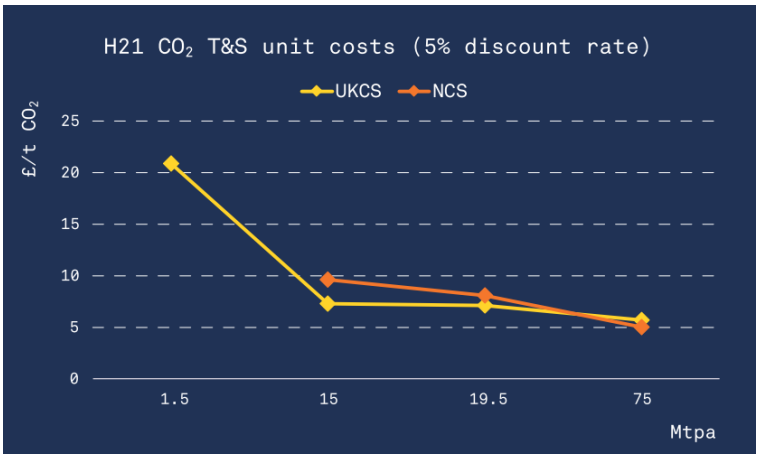

Figure 2.13: Estimated CO_2 transport and storage cost from the UK mainland to reservoirs on the United Kingdom (UKCS) and Norwegian continental shelf (NCS) [40]. The CCS costs are shown as a function of million tonnes CO_2 stored per year (Mtpa).

22/tonne CO_2 at injection rates of 4.3 Million tonnes per annum (Mtpa) [44]. In Europe, CO_2 transport and storage costs from large-scale natural-gas based hydrogen production scenarios in the UK in the H21 North of England project are estimated to 5-21 £/tonne (7-28 $/tonne) as shown in Figure 2.13 [40]. The Northern Lights project is piloting large-scale CO_2 storage in Norway from a cement plant and a waste-heat plant where 0.8 Mtpa CO_2 are liquefied, transported by ship and stored in reservoirs beneath the North-Sea [45]. For the Northern Lights project the expected costs for CO_2 transport and storage are 436 or 1138 NOK/tonne (equivalent to 50 or 130 $/tonne), this is dependent on taking the perspective of the government or an investor respectively (different discount rates and CO_2 cost considerations). This is higher than for the larger gas reformation projects where CO_2 are transported by pipelines and illustrates the variation in CCS costs based on location, quantity and type of CO_2 source. Increasing the volume of CO_2 stored to 5-10 Mtpa can reduce the overall CO_2 capture cost (cost of capture, transport and storage) by around 50%, while a volume of 320 Mtpa is estimated to reduce the cost by around 75% [45].

2.3.2 Water electrolysis

Electrolytic H_2 production is currently only in operation on smaller scales. However, electrolytic H_2 was previously produced in significant quantities at large-scale electrolysis plants from the 1920s to the 1970s [46, 4]. An example of such a facility is the H_2 production plant at Rjukan with a capacity of 60 tonnes/day, representing 130 MW of electric demand. This facility was used by Norsk Hydro to produce ammonia for fertilizers. In recent years the momentum has turned for electrolytic H_2 production and tangible plans for construction of larger electrolysis plants are emerging. One example is the REFHYNE project in connection to Rhineland Refinery in Germany [47], where the worlds largest PEMEL electrolysis plant is under construction with a 3.6 tonnes/day (10 MW) production capacity. This development is enabled by surplus energy from large amount of regional VRE production, new electrolysis technology and cost reductions for electrolyzers.

In water electrolysis, water (H_20) is split into hydrogen (H_2) and oxygen (O_2) by applying electric current as shown in Equation 2.10.

$$H_2O \rightarrow H_2 + \frac{1}{2}O_2 \qquad \Delta H = 285 \text{ kJ/mol}(39.5kWh/kg) \tag{2.10}$$

This reaction occurs in a electrolytic cell, which consist of two electrodes, a diaphragm and an electrolyte. O_2 gas is generated at the positive electrode (anode), while H_2 gas is generated at the negative electrode (cathode). The diaphragm sep-

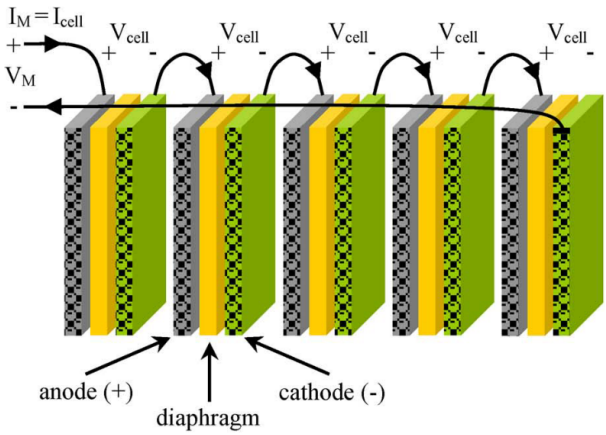

Figure 2.14: Electrolysis cells connected in series forming a cell stack [48].

arates the anode and cathode in order to keep the resulting gases from recombining and prevents the electrodes from short-circuiting. Another important property of the diaphragm is to enable ionic transport within the electrolytic cell. In electrolyzers, several electrolytic cells are connected as illustrated in Figure 2.14. It is most common to connect the electrolytic cells in series as shown in the Figure 2.14. This collection of cells is typically referred to as a cell stack.

2.3.3 Electrolysis Technologies

Three main technologies are usually referenced when discussing electrolysis; alkaline electrolysis (AEL), proton exchange membrane electrolysis (PEMEL) and solid oxide electrolysis (SOEL) [48]. A summary of the technical system characteristics comprising the main differences between the different electrolysis technologies are given in Table 2.3.

AEL is the most mature technology, since it has the lowest capital costs, long stack lifetime and is broadly available. This is the traditional kind of electrolyzer used in the large electrolysis plants for ammonia production. Traditional AEL required stable operation conditions and was not designed for a power system with a lot of VRE sources. Modern AEL have improved dynamic performence compared to the traditional designs, but they perform best under somewhat stable conditions. AEL use a liquid electrolyte, where a solution of 25-30 wt.% KOH is most common [48]. OH^--anions moves across the diaphragm from the cathode to the anode. A drawback with using this type of electrolyzers is the corrosive nature of the alkaline electrolyte, which affects the choice of materials for the electrodes.

PEMEL use a solid polymer electrolyte to conduct H^+-ions from the anode to the

Table 2.3: System characteristics for the different electrolysis technologies, adapted from Table 1 in [46]

		AEL	PEMEL	SOEL
Operating Temp.	°C	60-80	50-80	650-1000
Operating Pressure	bar	<30	<200	<25
System energy	kWh_{el}/m^3	4.5-6.6	4.2-6.6	>3.7 (>4.7)
Lower dynamic range	%	10-40	0-10	>30
System Response		Seconds	Milliseconds	Seconds
Cold-start time	min.	<60	<20	<60
Stack Lifetime	h	60,000-90,000	20,000-60,000	<10,000
Maturity		Mature	Commercial	Demo

cathode. A solid polymer electrolyte results in lower inertia for the ionic transport in the electrolytic cell compared to liquid alkaline electrolytes [48]. Thus, PEMEL are better than AEL under dynamic operation and can utilize their entire nominal operating range. PEMEL is still more expensive than alkaline electrolysis as the electrodes requires expensive noble metals and more structural complexity due to high operating pressure. However, the costs of PEMEL have been reduced significantly in the last years to become competitive with AEL. PEMEL are often preferred for applications where dynamic operation is required such as in connection with VRE sources [46]. For this reason, PEMEL is expected to become the most important electrolysis technology by 2030.

SOEL is different from the two other type as it use steam in the reaction instead of water. The major advantage of this kind of electrolysis is that the electric efficiency can become very high as some of the electric energy can be substituted with high temperature heat. The solid oxide electrolyte is gas-tight and transport O^{2-}-anions from the anode to the cathode [48]. In a commercial setting, the solid oxide technology is more established for high temperature fuel cells, while SOEL is still in the R&D-phase. The main challenge that have to be overcome to commercialize SOEL is the high material degradation of the electrodes and the solid oxide electrolyte, which results in a short lifetime for the electrolytic cells.

2.3.4 Future Electrolysis Cost Reduction

Reducing cell stack cost is the main driver for electrolysis capital expenditure (CAPEX). Research has focused on stack design and electrode materials, this has lead to a reduction in the CAPEX of electrolysis cells. AEL have been the leading technology and cheapest solution for decades, but PEMEL is closing the gap and is expected to reach cost parity with alkaline systems within 2030 as shown in Figure 2.15 [49]. Electrolyzers production is still highly based on manual labor and signi-

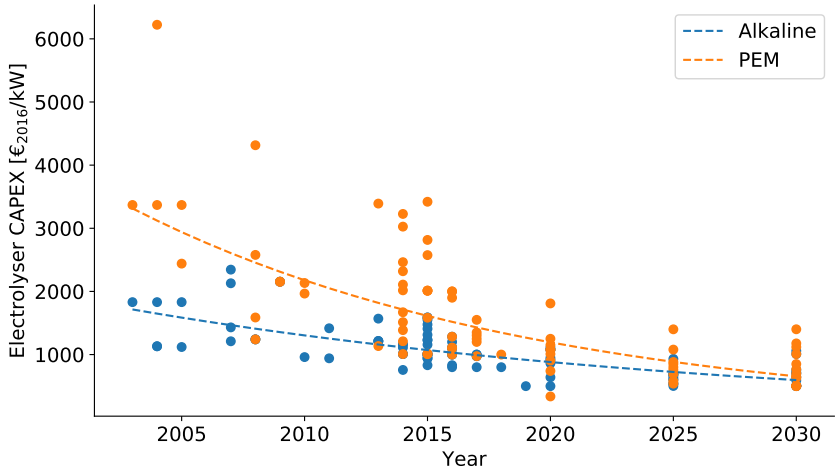

Figure 2.15: Historic reduction in electrolyzer cost until 2016, and estimation of future costs. Data collected from academic publications and industry experts in [49].

Table 2.4: Current, 2030 and future range of efficiency and cost of electrolyzer types, adopted from [4].

		AEL			PEMEL			SOEL		
		Today	2030	Future	Today	2030	Future	Today	2030	Future
Electrical efficiency (% LHV)	Low	63	65	70	56	63	67	74	77	77
	High	70	71	80	60	68	74	81	84	90
CAPEX (USD/kW$_e$)	Low	500	400	200	1100	650	200	2800	800	500
	High	1400	850	700	1800	1500	900	5600	2800	1000

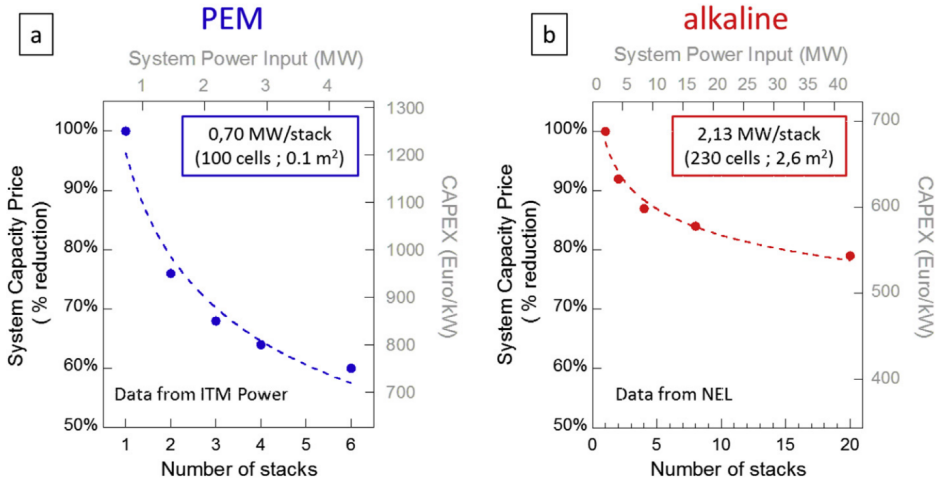

Figure 2.16: Reductions in CAPEX due to increasing number of electrolysis cell-stacks. For PEM in part (a) and alkaline in part (b) [51].

ficant capital cost reductions can still be gained for both electrolyzer technologies through automation and scaling up the production volumes [50]. Expected future improvements in efficiency and CAPEX is shown in Table 2.4.

Larger electrolysis systems drives down the CAPEX further as it allows for sharing of ancillary equipment through smart design of the electrolysis plants. The benefits of multi-stack systems for PEMEL and AEL is shown in Figure 2.16, with data provided by two of the leading manufacturers of electrolyzers. PEMEL draws more advantages per added cell stack compared to alkaline systems, where 6 stacks reduces the CAPEX to 60 % per kW compared to the cost of a single stack. For alkaline electrolysis systems, 20 stacks reduces the CAPEX per kW to 80 % of a single stack system. The market leading CAPEX of large-scale AEL and PEMEL plants is estimated to be as low as 550 €/kW (40 MW) and 750 €/kW (4 MW) respectively.

The traditional operation pattern of electrolyzers have been to produce H_2 at a constant rate in order to achieve full capacity utilization. This operational strategy focuses mainly on minimizing the impact of the CAPEX on the levelized cost of hydrogen (LCOH). However, the cost of H_2 produced from electrolysis is mainly driven by the operational expenditure (OPEX), which is essentially the cost of electricity. The cost of electricity consumption is currently 77.2 % of the levelized cost of hydrogen (LCOH), based on case studies of large PEMEL plants with a stack CAPEX of 900 $/kW and full capacity utilization ($\sim$ 97 %) [52]. Assuming the fu-

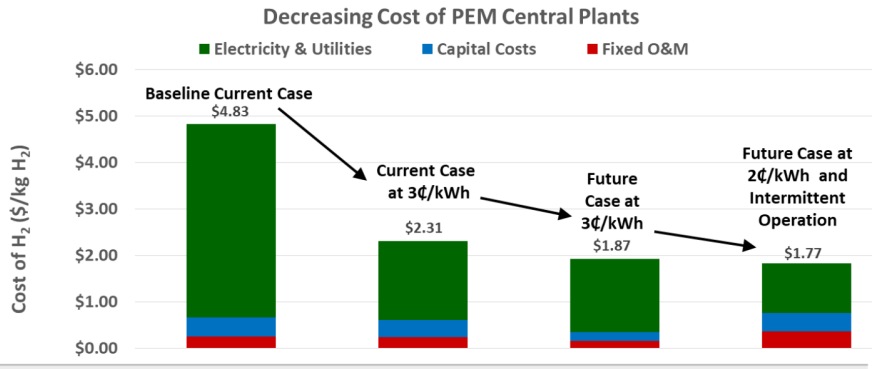

Capacity Factor	97%	97%	97%	40%
Stack Electrical Efficiency	66.1%	66.1%	69.8%	69.8%
System Cap Cost	$460/kW	$460/kW	$233/kW	$233/kW
Effective Electricity Cost	7.4¢/kWh	3.0¢/kWh	3.0¢/kWh	2.0¢/kWh
Degradation Rate	1.5 mV/khrs	1.5 mV/khrs	1 mV/khrs	1 mV/khrs
Stack Lifetime	7 yrs	7 yrs	10 yrs	10 yrs

Figure 2.17: Pathway towards large-scale H_2 production from electrolysis [53]

ture electrolyzer cost is reduced to 400 $/kW and full capacity utilization, the cost of electricity represent a larger share of the H_2 production costs at about 88.5 %. Thus, reducing the OPEX becomes even more important for making electrolytic H_2 competitive.

In the future, electricity price volatility and number of longer periods of low and zero electricity prices will be dependent on the level of flexible resources and VRE integrated into the electricity system. Such that, minimizing the electrolyzer OPEX is not consistent full capacity utilization. A pathway towards large-scale low cost H_2 production from electrolysis is shown in Figure 2.17. This includes technical development of electrolyzer with higher stack efficiency and longer lifetime and manufacturing improvements to lower CAPEX. However, a low electricity price (2-3 cent/kWh) is the key element to make electrolytic H_2 competitive with H_2 from natural gas with CCS (3-4 $/kg) or without CCS (2.5-2.8 $/kg) [54, 49]. The capacity factor of electrolyzers are typically above 80% [54, 55] with current electricity prices. To achieve low electricity costs in the future, the operators of the electrolyzer plants have to consume electricity in periods with electricity surplus and low electricity prices. This results in lower capacity factors for the electrolyzers, often between 40-80%, in studies of future electrolytic H_2 production in systems with high VRE shares [7, 10, 56, 57, 55]. However, the optimal capacity

factor of electrolyzers are very case specific and also depends on factors such as transmission grid connectivity, types of renewable generation, demand profiles etc.

H_2 production can provide important ancillary services such as real-time balancing that will be of increasing importance as more VRE is integrated into the electricity system. PEMEL has a system response time in the range of milliseconds and can be used even for fast reserves [58]. Balancing reserves provision can become a important source of revenue for electrolysis operators and contribute to further lowering the H_2 cost [10]. Electrolytic H_2 production is considered in California to limit the mismatch between solar power production and demand related to the "duck curve" [59]. Thus, it can be beneficial for the cost of H_2 to operate the electrolyzer in close integration to several electricity markets (whole-sale and ancillary markets) in order to extract the economic revenues that can be gained from flexible operation.

2.4 H_2 Storage

H_2 storage is needed for electrolysis plants to produce flexibly from renewable sources and at the same time deliver H_2 reliably to the H_2 loads. The most common way of storing H_2 is as pressurized gas in steel tanks [60]. Steel tanks are readily available and can be installed at most locations. One issue that H_2 storage technologies have to consider is the low volumetric density of H_2. Pressurizing the gas requires extra energy that is dependent on the pressure, the most common output pressures are less than 30 bar from the electrolyzer or 200-700 bar after compression. The higher pressure level is common in application such as transportation, but can also be preferable in stationary application as it requires smaller but thicker steel tanks. In the end the optimal pressure is dependent on the relationship between steel and electricity costs.

To store large amounts of H_2 two technologies are usually considered; liquid H_2 storage or storage in geological formations (aquifers, salt caverns or lined rock caverns). In liquid H_2 storage, H_2 is cooled to -253 °C. With current technology this requires large amount of energy, up to 40 % of the energy content of the H_2, which is high compared to pressurization that requires around 10 % of the energy content dependent on the pressure [60]. The liquid H_2 storage system requires constant energy for cooling as H_2 evaporates at these temperatures, thus this kind of H_2 storage is mostly considered for applications with limited duration, such as transport of large quantities of H_2 on trucks, train or ship.

Geological H_2 storage is considered for storing large quantities of H_2 over longer periods of time, such as seasonal H_2 storage in depleted oil and gas reservoirs, aquifers salt caverns and lined rock caverns. Salt caverns are ideal for H_2 stor-

Table 2.5: Cost of stationary H_2 storage from the literature, reproduced from [62].

Literature source	Pub. Year	Pressure (bar)	Storage size (m^3)	Costs (€/m^3)
Carr et al. [66]	2014	200	Different sizes	45-22-11-4
Darras et al. [67]	2015	-	-	70
Gammon et al.[68]	2006	137	2856	50
Grond et al.	2013	-	-	81
Karellas and Tzouganatos [69]	2014	-	11,123	38
Katikaneni et al [70].	2014	173	3337	102
Katikaneni et al.	2014	432	1557	98
Linnemann and Steinberger-Wilckens [71]	2007	500	5000	40
Ozaki et al. [72]	2014	350	204	41
Pääkkönen et al. [73]	2018	1	85	490
Prince-Richard et al. [74]	2005	414	Different sizes	17 (4 – 43)
Ulleberg et al. [5]	2010	200	2400	23
Weinert [75]	2005	141–552	556 – 13,793	23 – 182
X. Xu et al. [76]	2017	350	3337 – 156	110 – 195
Zoulias et al. [77]	2006	30	5 – 10,000	38 $\rightarrow$ 25

age as salt is chemically inert to H_2 and rock salt provides an extremely gas tight seal and has been used for storing H_2 since the 1970s [61, 62, 63]. H_2 stored in aquifers and depleted oil and gas reservoirs have to be purified after the fact as it can be contaminated with residual hydrocarbons or sulfates [64]. Furthermore, salt caverns requires low amounts of cushion gas compared to the other alternatives, i.e. gas that is initially injected into the storage but not extracted in normal operation. For depleted oil and gas reservoirs this can be as much as 50 % of the storage capacity, for aquifers this might be even higher in addition to a large risk of leaks. These methods of H_2 storage requires the proper geological conditions and is not suitable for every location. However, wast amounts of salt cavern storage is available across Europe amounting to a total technical potential of 84.8 PWh_{H2} [63]. Most of the salt caverns are located around the north sea, an area with major potential and ongoing development of both on-shore and off-shore wind power.

Indirect methods for storing H_2 is to convert it into ammonia [65] or petrochemicals. These substances have higher volumetric densities and are liquids under standard conditions. They are also considered to be easier to handle as they are less flammable and has a distinct smell compared to H_2 which is odorless. Further processing H_2 to ammonia or petrochemicals requires extra steps which lead to higher production costs which has to be weighed against these benefits.

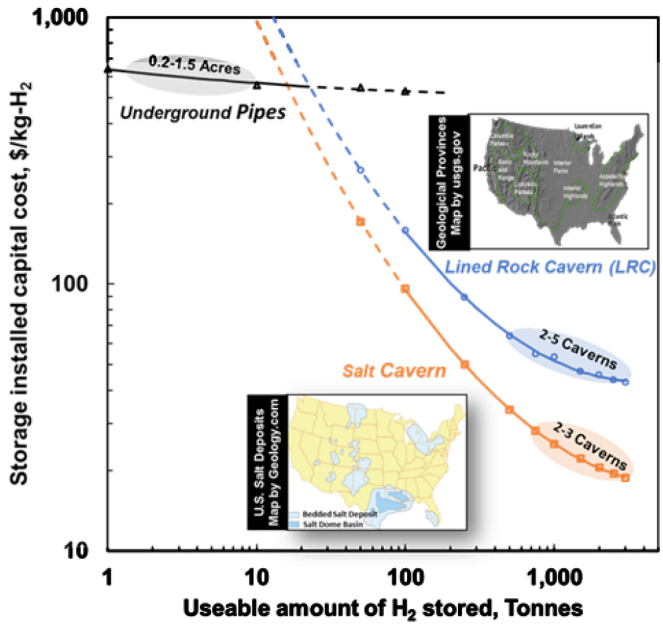

Figure 2.18: Cost of large-scale H_2 storage options as a function of storage capacity [78, 79]

Table 2.5 summarize the cost for gaseous H_2 storage used in the literature [62]. The cost of H_2 storage vary significantly between studies, but is mostly between 23-195 €/m^3 (255-2170 $/kg). In a recent analysis of large-scale H_2 storage with 500 ton (5.56 Mill Nm^3) capacity the cost of gaseous H_2 storage is calculated to 516 $/kg (46.4 $/$Nm^3$) [78, 79]. Coated steel pipes buried underground with a pipe outside diameter of 24 inches and a wall thickness of 0.968 inches (schedule 60) was determined to be the most cost efficient design of tank-based storage. This storage design allows for working pressures between 8-100 bars.

Lined rock caverns and salt caverns is also considered in the report at costs of 56 $/kg (5 $/$Nm^3$) and 35 $/kg (3.1 $/$Nm^3$) respectively. The cost of the three different options for gaseous H_2 storage as a function of storage capacity is depicted in Figure 2.18. Underground pipes are the cheapest option for H_2 storage of 20 tonnes or less, while salt caverns are cheapest for H_2 quantities larger than 20 tonnes. Lined rock caverns are more expensive than salt caverns, but cheaper than underground pipes for quantities above 30 tonnes of H_2. Both salt caverns and lined rock caverns are dependent on the geological conditions but significant capacity exist in several locations both in Europe and the US [63, 79]. H_2 storage can potentially be combined with pipeline transport by increasing the pressure of

the pipeline also called "line-packing", thus using the full economic potential that arise from pipeline H_2 transport.

2.5 Electricity System Challenges

Competitive VRE resources facilitate increasing shares of electricity generation from VRE in the power system and reduced CO_2 emissions. On the other hand, it also result in new challenges that have to be resolved to ensure cost-efficient VRE integration. Some of the main challenges for integrating VRE are listed below [80, 81].

- Building long and expensive transmission lines
- Balancing production and consumption as VRE is variable and the production is uncertain
- Reduced power system frequency and voltage stability, since VRE does not contribute with inertia
- New market structures combined with reliable forecasting is needed to accommodate variation and uncertainty of VRE production.

VRE technologies require larger land areas compared to most other sources of electricity generation. Thus, VRE are more restricted by geographical location compared to thermal generation which can be constructed close to the demand. Transmission congestion is already occurring in many regions where significant integration of renewables are taking place. This is expected to increase with increasing VRE development [82, 83].

Transmission projects has to be planned in advance of VRE development as construction of transmission lines takes longer time. Transmission projects typically take 5-10 years versus 1-3 years for VRE projects [85]. In this regard, frameworks are established in order to ensure efficient planning of transmission capacity from Renewable Energy Zones (REZs), areas that enables development cost-efficient renewable energy. An example is found in Texas, where large amounts of wind power development in the west triggered the CREZ transmission line project. The CREZ project enabled western Texas to accommodate 18 GW of additional wind power capacity. An overview of the CREZ project is shown in Figure 2.19. Another example is the Sunrise Powerlink in California, which was significantly more expensive at $16,000/MW·mile than CREZ at $2,500/MW·mile and exemplifies the large range in transmission expansion costs [86]. The wind power resources in northern Norway are located far from the major load centers in the south and are

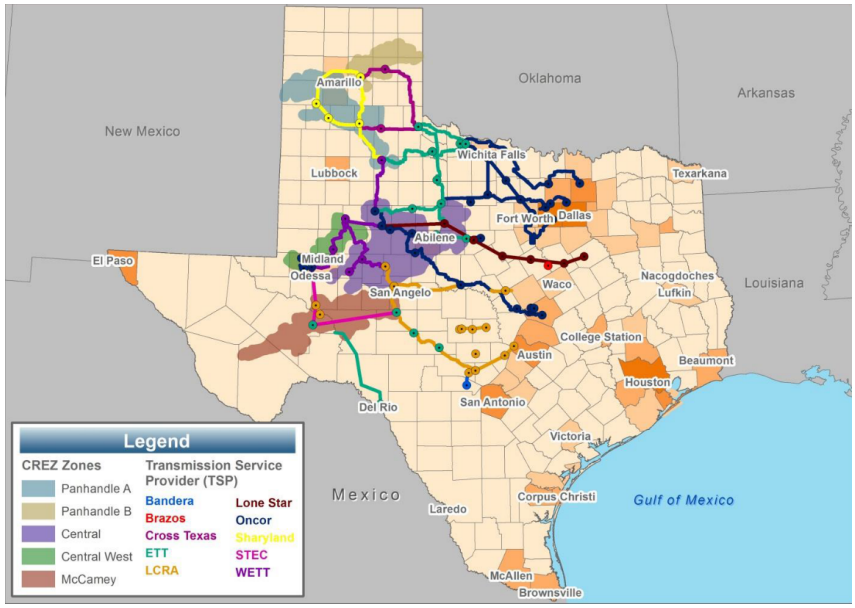

Figure 2.19: The CREZ transmission expansion project in Texas was constructed in order to accommodate more wind power in the west and north-west and transport the energy to the demand located in the east and south [84]

example of VRE resources that remains undeveloped due to the lack of transmission capacity. The lack of transmission capacity is one of the main reasons for not including more of northern Norway among the areas best suited for wind power development, shown in Figure 2.8 [22].

Denmark and Ireland have successfully integrated large shares of electricity generation from VRE, mostly wind power, which reached 53% and 29.7% in 2017 respectively [12]. Strong transmission grid connection to neighboring countries have been crucial to realize the high levels of wind power integration in Denmark. Hydro power flexibility in Norway and Sweden is used to balance wind power in Denmark by exchanging electricity over HVDC transmission lines. Cross border transmission capacity also increase the diversity of the energy mix in all three countries which improves the security-of-supply. In Northern Ireland and Ireland, more transmission capacity is constructed to Wales and Scotland to enable higher VRE shares without increasing curtailment. Further transmission connections the UK are planned [87].

Regions with high VRE shares face challenges with balancing electricity production and consumption. A well know example is the phenomenon caused by large

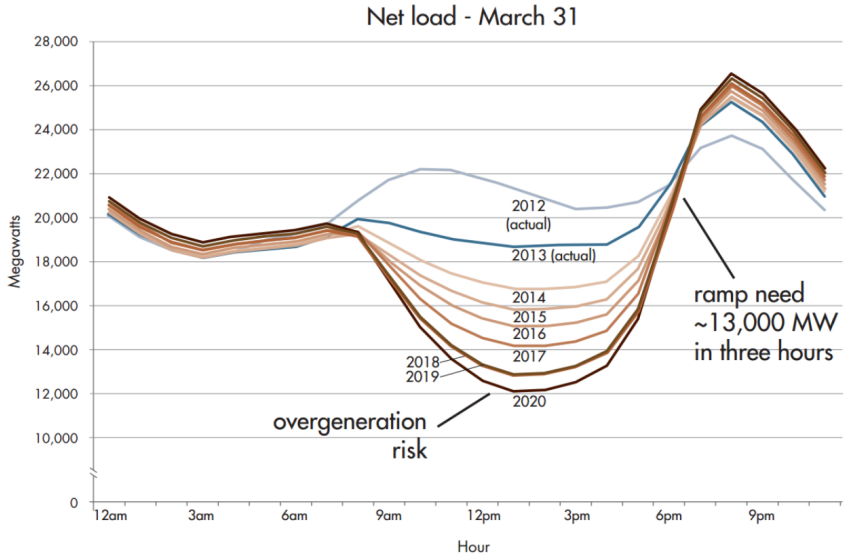

Figure 2.20: The "duck-curve" caused by large-shares of solar power in the electricity system, causing over-generation in the middle of the day and steep ramping in the evening [88]

amounts of solar power in California, known as the "duck curve" [88]. The "duck curve" refer to the shape of the net load profile when solar generation is subtracted from the electric load profile, as shown in Figure 2.20. This net load profile requires fast ramping of power generation in the morning and afternoon. Fast ramping makes balancing difficult and requires changes in operational practices of conventional generators. New market products was implemented to give incentives for flexible ramping and enable 20% of total electricity generation from VRE without significant curtailment. The target of 20% electricity generation from VRE was reached in 2017 [12]. More system flexibility is needed to reach the new target of 50% VRE generation by 2026 [89]. To facilitate further renewable energy integration in California, Pacific Gas and Electric Company (PG&E) are constructing five grid-scale lithium-ion battery storage systems which are expected to be on-line in August 2021. In total, these systems will be capable of 4 hours with 423 MW of discharge. This is the first of two stages in order to provide 716.9 MW of system reliability resources [90]. While battery storage is well suited for solar power integration, wind power requires storage on a longer time-scale where batteries become too expensive [91].

In Denmark, many of the CHP plants have been upgraded to allow for lower minimum operation and faster ramping. This enables the CHP plants to contribute

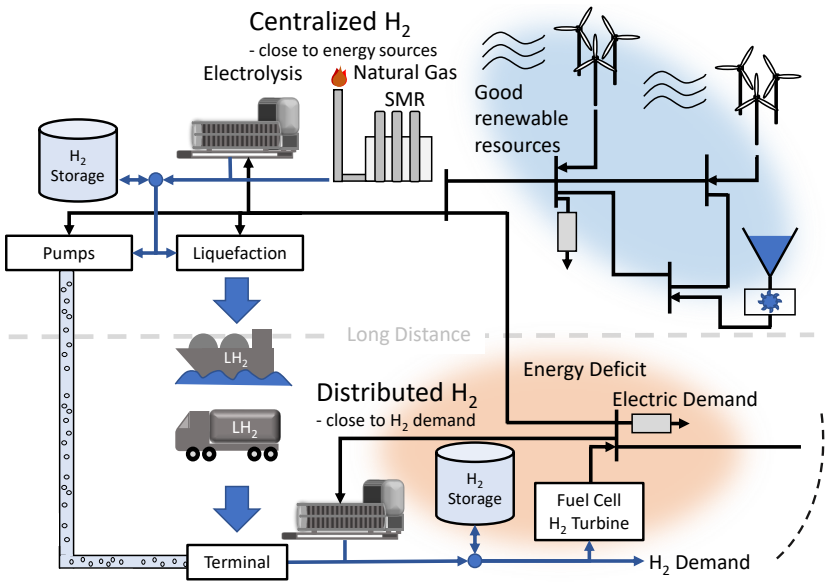

Figure 2.21: Illustration of a integrated hydrogen and electricity systems producing hydrogen and electricity in areas with good resources and exporting it to a deficit region. Alternatively, hydrogen can be produced by distributed electrolysis close to the demand.

in balancing the increasing share of wind power in the power system. Research and demonstration project for power-to-x solutions are key drivers in Denmark in order to reach the target of 100 % renewables by 2050 [12]. Two of the main power-to-x options are power-to-heat and power-to-hydrogen [92, 93]. The ability of hydrogen and heat generation to balance excess wind power is demonstrated on the pilot stage. For example, the HyBalance project [94] and a case study for a CHP plant in Aarhus where a 80 MW electric boiler/ 2MW heat pump system is installed [95] to balance wind power fluctuations. Similarly, H_2 and pumped-hydro systems are considered in Ireland for balancing wind power [96]. Flow batteries and compressed air storage is also often considered as storage options, alongside H_2 storage and pumped-hydro, for wind power dominated systems. All of these technologies are well suited for large-scale storage of energy over longer periods of time [97].

2.5.1 H_2 for supporting VRE integration

The German government initiated the 1.4 Billion € National Innovation Program on Hydrogen and Fuel Cell Technology (NIP) in 2006, to support development of H_2 technology and demonstration projects [98]. This is a part of the German energy transition strategy currently targeting 65% renewables in electricity by 2030

[12]. Worldwide, the potential for power-to-hydrogen systems is shown in more than 192 demonstration projects carried out in 32 countries. The scope of these projects have been expanded over the years to also include industry applications [99]. Sector coupling through power-to-H_2 systems has some benefits compared to other utility-scale flexibility sources in terms of energy transmission and end-use decarbonization, as illustrated by Figure 2.21.

H_2 based energy carriers, whether it is H_2, methane, ammonia or other synthetic fuels, can be transported on trucks, ships and pipelines. H_2 transmission is envisioned in Germany by pipelines [100, 101] and compressed gas on trucks [102]. Recent research literature investigates pipeline transport is in Great Britain [103, 104] and France [105]. In general, the most cost efficient method for H_2 transport is determined by quantity and distance. Gaseous H_2 is preferred for low quantities and short distances, lager quantities favor pipelines and long distances favor liquid H_2 (LH_2) [106]. LH_2 technology has historically been expensive due to low production quantities of LH_2 and significant cost reductions can be made related to economy-of-scale in order make it more cost competitive with other H_2 transport options [107]. Blending H_2 into natural gas distribution system (5-15% without modifications) [108, 109] or further refining H_2 to petrochemicals/ammonia [62, 110] allows utilization of existing infrastructure.

Flexibility from H_2 systems are expected to be especially important for deeper decarbonization of the energy system with a VRE share of more than 50% [57]. Many studies on the future low and zero emission power systems show that a tight coupling between the electricity, heating and H_2 is crucial for providing emission-free flexibility as the share of variable renewable energy (VRE) in the electricity system increases [8, 111, 112, 113]. H_2 can both reduce emission in the electricity system by providing flexibility needed for renewable integration and reduce CO_2 emissions in sectors that is hard to decarbonize, such as heavy-duty transport (long distance trucks, ships, air-planes and trains) [114, 115] and some industry applications. A comprehensive H_2 system will likely leverage production through multiple pathways, using both natural gas, which is currently the main source of H_2, and electricity to enable maximum flexibility and low cost. Furthermore, H_2 production from natural gas can have positive impact on the development of CCS infrastructure and technology [116].

2.6 The HYPER project - Liquid H_2 export from natural gas and wind power

The path towards future low emission H_2 production is uncertain and depend on the demand for H_2 and desire to reduce CO_2 emissions that is reflected by the

CO_2 price. Electricity from VRE sources can be more efficiently used to reduce emission by direct electrification of polluting end-use energy demand as long as the share of VRE electricity generation are low or moderate. Natural gas based H_2 with CCS can be an efficient and fast solution to reducing CO_2 in the short to medium-term. The infrastructure developed for natural gas based H_2 such as liquefaction plants and supply chains can also be leveraged by electrolytic H_2 as VRE shares in the electricity system becomes high and large amounts of energy storage in the form of hydrogen storage is needed to support the fluctuating energy output from the VRE generation.

This form the background of the HYPER project [13], which studied the large-scale production of low emission H_2 from natural gas and electricity using stranded resources with subsequent liquefaction and transport to energy deficit areas. Here the term "stranded resources" means energy resources, such as natural gas and wind power, which are not developed due to the costs of transporting the energy to end-use costumers. The base case H_2 production system investigated was designed to produce 450 tonnes H_2 from natural gas and 50 tonnes H_2 from electrolysis [117]. HYPER investigated both state-of-the art SMR and advanced ATR plant designs where potential synergies with electrolysis can be gained by utilizing O_2, which is typically considered a byproduct of electrolysis, in the ATR process.

Large parts of the HYPER project was focused towards liquefaction of H_2 for transport on ships similar to the current practice for LNG. The liquefaction and loading of liquid hydrogen aboard LH_2 carrier ships represent challenges where research can lead to significant advances in liquefaction plant design [118, 119] and technology [120, 121, 122] that reduce energy consumption and cost of H_2 liquefaction processes.

As part of the HYPER project, this thesis studies the impact of hydrogen production on the electricity system in northern Norway and electricity systems in general as explained in detail in the subsequent chapters. Furthermore, a detailed value chain analysis is performed for energy transport by LH_2 and ammonia (NH_3) by ship from Hammerfest in northern Norway [123]. The value chain analysis shows that energy transport by LH_2 is less energy intensive and results in lower total emissions while the costs are similar to the NH_3. However, there is potential to reduce the relatively high capital costs of liquefaction and LH_2 shipping, which highlights the need for further R&D and innovation activities building on the research in the HYPER project.

Chapter 3

Electricity System Modeling

Previous studies of energy storage and flexible demand have shown that most of the benefits from technologies that provides flexibility arise from avoiding investments in new transmission and generation capacity [124, 125]. For this reason, models that aim to analyze the potential synergies between electrolytic H_2 production and the electricity system have to take investments into account.

3.1 The Capacity Expansion Problem

3.1.1 Development in Capacity Expansion Studies

One of the fundamental problems in power system planning is the capacity expansion problem (CEP). Models for solving the CEP date back to the 1960s, when the emergence of computers allowed for detailed investment analysis in the electricity system [126]. The objective of CEP is to find the generation portfolio that maximize the social-welfare of the power system. If the electricity demand is considered inflexible (no price elasticity) this is equivalent to finding the least-cost generation portfolio. All CEPs include two types of decisions, investments and operations, and should ideally include dynamic investment decisions with detailed descriptions of the physical system and how it is operated. In practice however, the CEP has to be limited in the detail of the technology description, spatial or temporal dimension in order to reduce the computational complexity and make the problem tractable [126, 127].

The CEP was traditionally in the interest of centralized utilities in charge of the development of generation and transmission infrastructure. After the liberalization of the power system in the 1990's, the tranmission expansion problem (TEP) was the domain of the System Operator while the generation expansion problem

(GEP) was resolved by the electricity markets governed by the regulators. In recent years, climate policies have been an important incentive for new technological developments for VRE electricity generation and energy storage. Technological developments combined with more computational resources have shifted the state-of-the-art CEPs to focus on other topics such as: sector coupling (synergies with heating and gas), short-term uncertainty from VRE, demand management, decentralized market structures, electric vehicle integration [128]. This thesis considers two of these topics in detail, namely sector coupling with H_2 systems and short-term uncertainty from VRE.

3.1.2 Classification of the Capacity Expansion Problem

The CEP can be separated into two main types based on the representation of investment decisions, namely dynamic and static investment problems [129]. The electricity system is changing over time with changing demand, technology costs, interest rates and more. A CEPs with dynamic investments include the temporal sequence of investment decisions. A representation of the temporal sequence of investments is important when investment conditions are changing, which is typically caused by uncertain factors such as economic policies, investment costs, interest rates, demand growth, etc. These CEPs often have less spatial resolution, typically aggregated on a country level. They are designed to give realistic high-level insight in how the electricity system will develop over time, typically for key factors such as the aggregated generation portfolio or the total emissions.

The JRC-EU-TIMES model is an example of a capacity expansion model with many technologies which is often used to cover a large geographical area. The TIMES model is often used in studies for investigating the impact of technologies and economic policies on energy production and emission reduction [130]. In the context of H_2 production, the TIMES model is recently used to study power-to-liquid [131] and the potential role of H_2 in a scenario for the future decarbonized European power systems in 2050 [57]. In [57] the TIMES model is combined with a more detailed model for power and gas system operations in the METIS model [132]. Another example is the EMPIRE model which considers long-term operational uncertainty using a multi-horizon stochastic model [133]. The EMPIRE model is used to study the role of demand response [134] and flexibility from heating systems and electric vehicles on the power system [135] on the development of power systems in Europe and Norway respectively. Some models that are developed for design of local (smaller) multi-energy systems such as the dynamic-programming based eTransport model (renamed to INTEGRATE) [136] have higher detailed representation of technologies and spatial and temporal resolution.

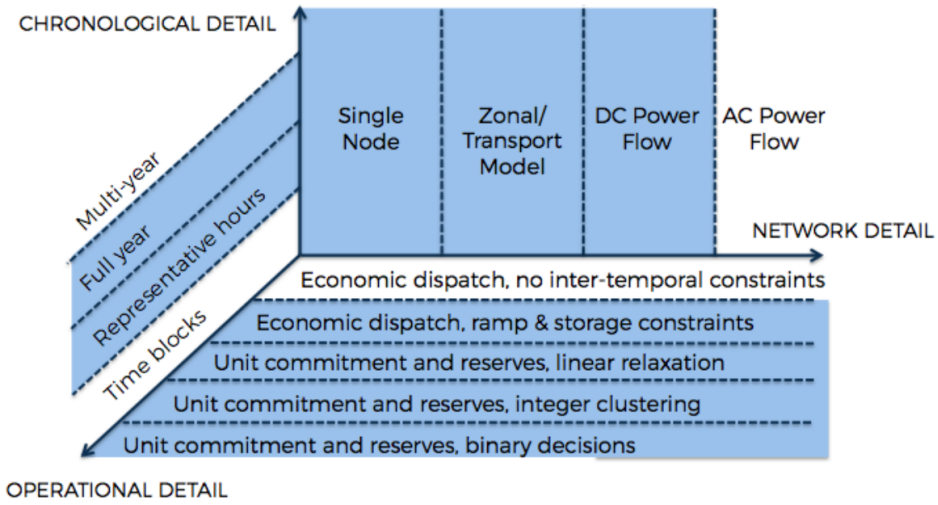

Figure 3.1: Modeling complexity of CEP models along three different dimensions, the blue sections are currently available model configurations for the GenX model [137].

Static CEPs assume that the timing of the investment is known which reduce the number of investment variables. Static CEPs can be grouped into two subcategories with respect to the representation of the temporal dimension of operations, marginal or integral CEPs. Longer periods of several years are usually modeled in integral models to account for changing operational conditions. In marginal CEPs, the operational conditions are assumed to be constant and operations are typically represented by a representative year with annualized investment the costs. As a result, the size of marginal models are significantly smaller and allows for inclusion of more technical and operational details. Thus, marginal CEPs are often used for analysis of cases where these features are important.

An example of a model with static investment decisions is the GenX model [137] where the modeling detail can be configured according to the users needs as shown in Figure 3.1. The GenX model is recently used for studying integration of renewables and batteries for power system decrabonization [91]. The development of investments over time can also be simulated by running models with static investment decisions sequentially such as in the ReEDS model [138] and allows for high spatial resolution and detailed modeling of electricity generation, consumption and renewable energy resources.

The analysis in this thesis do not seek to provide pathways to large-scale electrolytic H_2 production. Only marginal CEPs are studied in this thesis, as the objective is to analyze the potential impact of H_2 production on the electricity system.

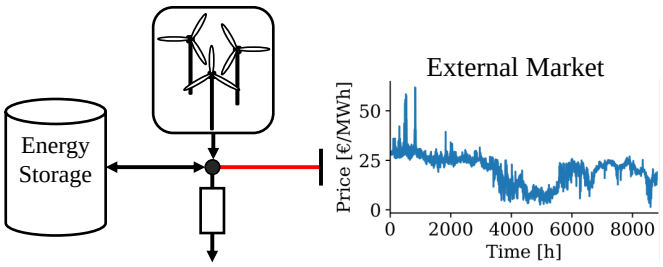

Figure 3.2: Example of a subsystem in the electricity system, consisting of a wind farm, energy storage, electric load and transmission lines connected to an external market.

3.1.3 Deterministic Capacity Expansion Model

An example of a CEP is shown in Equation (3.1) to (3.10) where the model optimizes investments in wind power and energy storage as illustrated in Figure 3.2. This is the extensive form of the CEP, meaning it is modeled as one big linear program (LP). This model is simpler than the models in Article 1 and Article 2 that include more technologies, but the modeling principles are the same.

$$\min \sum_{i\in\mathcal{R}} C_i^w w_i^{max} + \sum_{i\in\mathcal{E}} (C_i^s s_i^{max} + C_i^e e_i^{max}) + \sum_{t\in\mathcal{T}} \Big[\sum_{i\in\mathcal{P}} O_i^f p_{ti} + \sum_{n\in\mathcal{B}} O^s r_{tn} + \sum_{n\in\mathcal{M}} O_{tn}^{ex} p_{tn}^{ex} \Big] \tag{3.1}$$

$$w_i^{max} \leq W_i^{Pot} \qquad \forall i \in \mathcal{R} \tag{3.2}$$

$$s_i^{max} \leq S_i^{Pot}, e_i^{max} \leq E_i^{Pot} \qquad \forall i \in \mathcal{S} \tag{3.3}$$

$$p_{ti} + c_{ti} = P_{ti} w_i^{max} \qquad \forall t \in \mathcal{T}, \forall i \in \mathcal{P} \tag{3.4}$$

$$s_{ti} = s_{(t\text{-}1)i} + \eta_i^{in} e_{ti}^{in} - \frac{1}{\eta_i^{out}} e_{ti}^{out} \qquad \forall t \in \mathcal{T}, \forall i \in \mathcal{E} \tag{3.5}$$

$$s_{ti} \leq s_i^{max} \qquad \forall t \in \mathcal{T}, \forall i \in \mathcal{E} \tag{3.6}$$

$$e_{ti}^{in} + e_{ti}^{out} \leq e_i^{max} \qquad \forall t \in \mathcal{T}, \forall i \in \mathcal{E} \tag{3.7}$$

$$\sum_{j\in\mathcal{P}_n} p_{tj} - p_{tn}^{ex} + r_{ti} + \sum_{j\in\mathcal{E}_n} (e_{tj}^{out} - e_{tj}^{in}) = D_{tn} \qquad \forall t \in \mathcal{T}, \forall n \in \mathcal{N} \tag{3.8}$$

$$p_{tns}^{ex} = \sum_{m\in\mathcal{C}_n} B_{nm}(\delta_n - \delta_m) \qquad \forall t \in \mathcal{T}, \forall n \in \mathcal{B} \tag{3.9}$$

$$-T_{nm} \leq B_{nm}(\delta_n - \delta_m) \leq T_{nm} \qquad \forall t \in \mathcal{T}, \forall n \in \mathcal{B}, \forall m \in \mathcal{C}_n \tag{3.10}$$

The CEP has an objective function where investments and operational costs are minimized as in (3.1), subject to investment constraints exemplified by Equation (3.2) to (3.3) and operational constraints in Equation (3.4) to (3.10). The operational constraints include balances for storage (3.5), energy (3.8) and power flow (3.9). Moreover, the constraints include upper limits on production (3.4), storage energy (3.6), storage power (3.7) and power flows (3.10). The upper limit constraints on operations connects the investment problem with the operational problem and are subject to special treatment when the two parts are split into separate models in decomposition schemes.

3.1.4 Modeling of Hydro Power

The electricity system modeled in Article 1 is illustrated in Figure 3.3. The model is inspired by the work on H_2 production in constrained grids in the PhD thesis of J.C. Greiner (2010) [10, p. 67-93]. Article 1 extend the previous work by including a representation of hydrogen delivered directly to the hydrogen load without storage, the DC power flow equations and hydro power operation.

The Norwegian power system is dominated by hydro power, which is modeled by a special case of the storage balance in Equation (3.5). The hydro power model differs from the generic storage balance as input is determined by inflow instead of charging as shown in Equation (3.11). Inflow is modeled as a parameter, I_{ti}, instead of a variable as it would be for charging and can not be controlled as it is dependent on naturally occurring precipitation and snow melting. As a result, spillage of water might occur if there is not sufficient capacity available in the reservoir at any given moment in time. Spillage is modeled by a separate variable, s_{ti}.

$$v_{ti} = v_{(t-1)i} - q_{ti} - s_{ti} + I_{ti} \qquad \forall i \in \mathcal{H}, \forall t \in \mathcal{T} \tag{3.11}$$

$$v_{0i} = V_i^0 \qquad \forall i \in \mathcal{H} \tag{3.12}$$

$$v_{Ti} - v_i^+ + v_i^- = V_i^0 \qquad \forall i \in \mathcal{H} \tag{3.13}$$

Water can be stored for many years in hydro power reservoirs, dependent on the inflow and size of the reservoirs. A marginal CEP that represents operation with a single year requires assumptions for the start and end reservoir levels. The start and end reservoir levels are specified in Equation (3.12) and (3.13) respectively.

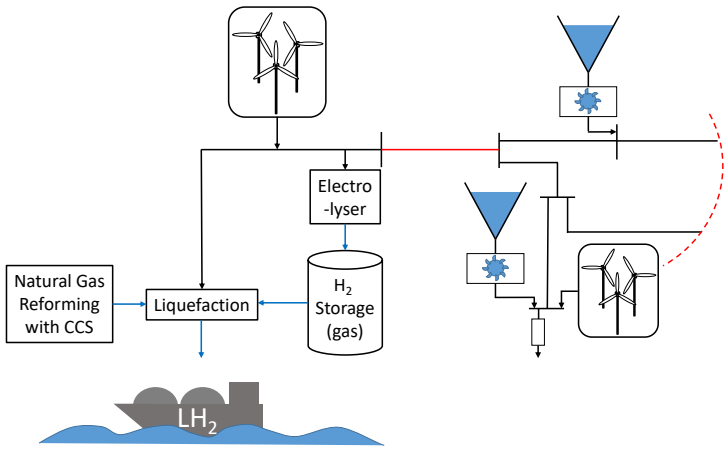

Figure 3.3: Illustration of the electricity system modeled in Article 1, H_2 is represented as a flexible load.

Deviations from the end reservoir levels are allowed to ensure feasibility of the solution. These deviations are accounted for by the slack variables v_i^+ and v_i^- in Equation (3.13) and penalized in the objective function. The end reservoir level represent the long-term strategy beyond the single year represented by this model, such that deviations from this level represents unfavorable behavior in the long-term. End reservoir level deviations are penalized by adding the costs $O^{v+}v_i^+ + O^{v-}v_i^-$ for each reservoir.

In this thesis, it is assumed that there is no new investments in hydro power capacity. Modeling hydro power capacity expansion is challenging as it is very dependent on the natural conditions of the region and is typically restricted by regulations. Most of the big hydro power resources in Norway are already developed. According to NVE around 23 TWh/year remains of the total techno-economically viable hydro power resources which is estimated to be around 216 TWh/year, of which 15.1 TWh/year is from new plants and 7.6 TWh/year from upgrades and extensions of existing plants [139]. Ignoring new hydro power development is assumed to be a reasonable assumption for our purpose in light of the relatively limited potential for new hydro power plants.

3.1.5 H_2 Production as Flexible Demand

In Article 1, H_2 demand is modeled as a firm demand connected to electrolysis with H_2 storage. The H_2 demand is served directly from the electrolysis, via storage or imported from other sources as shown in Equation (3.15). This is a special instance of the energy balance in Equation (3.8). The H_2 storage is governed by a storage

balance in Equation (3.14), equivalent to Equation (3.5), where h^p_{ti} is H_2 from the electrolyzer to the H_2 storage while h^s_{ti} is H_2 discharged from the H_2 storage to the load. H_2 can also be delivered directly from the electrolyzer, h^d_{ti}, to the H_2 load or imported from other sources, h^i_{ti}, at a cost.

$$h_{ti} = h_{(t-1)i} + h^p_{ti} - h^s_{ti} \qquad \forall i \in \mathcal{H}_2, \forall t \in \mathcal{T} \tag{3.14}$$

$$h^d_{ti} + h^s_{ti} + h^i_{ti} = H^D_{ti} \qquad \forall i \in \mathcal{H}_2, \forall t \in \mathcal{T} \tag{3.15}$$

The electrolysis represents an additional electric load given by the amount of hydrogen produced and the electricity requirement for electrolysis. The electricity requirement is higher for the hydrogen that is stored as it requires additional electricity from compression to higher pressures. The H_2 demand can be considered flexible from the perspective of the electricity system when H_2 storage is included with the electrolyzer, while from the external hydrogen system it is considered to be constant.

Upper limits for electrolysis and H_2 storage is given in Equations (3.16) and (3.17) respectively. The total H_2 produced by electrolysis, the sum of H_2 going directly to the load and storage, is bounded by the electrolysis capacity.

$$\eta^d h^d_{ti} + \eta^s h^p_{ti} \leq e^{max}_i \leq E^{pot}_i \qquad \forall i \in \mathcal{H}_2, \forall t \in \mathcal{T} \tag{3.16}$$

$$h_{ti} \leq h^{max}_i \leq H^{pot}_i \qquad \forall i \in \mathcal{H}_2, \forall t \in \mathcal{T} \tag{3.17}$$

3.1.6 Sector Coupling of Electricity and H_2 Systems

In Article 2 the H_2 system is modeled more comprehensively as a mirror image of the electricity system, illustrated in Figure 3.4, where the same constraints are used to model both systems. The CEP invest in generation, storage and transport for both the electricity and H_2 system. H_2 is produced from both electricity and natural gas using two of the major technology options, PEMEL and SMR w/wo CCS. The H_2 and electricity systems are coupled by technologies for converting electricity to H_2 (PEMEL) and H_2 to electricity (H_2 turbines and fuel cells).

Two new terms are added to the right-hand-side of the energy balance which represent the sector-coupling as shown in Equation (3.18). The same formulation is used for the electricity and H_2 balance in the respective nodes. $F_i p_{tin}$ is the load represented by the electrolysis at an electric bus or electricity produced from reconversion of H_2 in PEMEL fuel cells and H_2 turbines at H_2 nodes. The second

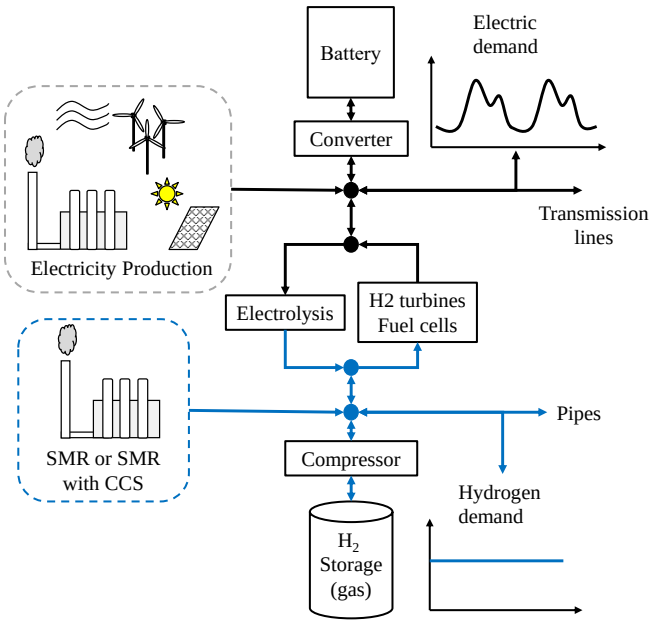

Figure 3.4: Illustration of a set of electricity bus and H_2 node in the sector-coupled electricity and H_2 system modelled in Article 2.

term, $A_i e^{in}_{tin}$, represents the auxiliary power used for example in H_2 compressors. For a detailed description on this notation see Appendix A. in Article 2.

$$\sum_{i \in \mathcal{P}_n} p_{tin} - p^{exp}_{tn} + p^{imp}_{tn} + \sum_{i \in \mathcal{S}} (e^{out}_{tin} - e^{in}_{tin}) + r_{tn} = D_{tn} + \sum_{i \in \mathcal{F}_n} F_i p_{tin} + \sum_{i \in \mathcal{A}_n} A_i e^{in}_{tin} \tag{3.18}$$

The model in Article 2 includes more generation technologies such as steam methane reforming, natural gas, coal and nuclear power plants. Thermal generation technologies have lower power limits and ramping constraints that limit how fast they can ramp up and down. To model this behavior the commitment state of each plant, i.e. the on/off state of the plant, has to be included in a separate variable, u_{tin}. The number of committed units is bounded by the number of already existing plants, X^{init}_{in}, plus the new installations, x_{in}, minus the retired plants, x^{ret}_{in}, as stated in Equation (3.19). Plant retirement has a small cost at about 10-15% of installing a new plant, but can be profitable in some cases where the capacity of some plant types are not utilized as retiring plants removes the fixed O&M costs. Up-

per and lower production in Equation (3.20) and ramping constraints in Equation (3.21) restrict the operation range and flexibility based on the plant type.

$$u_{tin} \leq X_{in}^{init} + x_{in} - x_{in}^{ret} \qquad \forall i \in \mathcal{P} \qquad (3.19)$$

$$P_i^{min} u_{tin} \leq p_{tin} \leq P_i^{max} u_{tin} \qquad \forall i \in \mathcal{P} \qquad (3.20)$$

$$-R_i^{down} u_{tin} \leq p_{tin} - p_{(t-1)in} \leq R_i^{up} u_{tin} \qquad \forall i \in \mathcal{P} \qquad (3.21)$$

Power and H_2 plants are grouped by technology type and location to reduce the number of binary or integer variables as these typically complicates the problem which leads to increased solution times. Grouping the plants allows the commitments variable to be a integer variable for each plant group instead of binary variables for each plant. The grouped representation of the commitment state is shown to drastically reduce the computational time with low approximation errors [140]. Thus, the problem can be solved for larger systems with a more detailed technology representation with limited computational resources. In Article 2, the integer commitments are further relaxed to continuous variables which is a reasonable approximation [141, p. 162-174], especially when the number of plants are high or the size of each plant is small.

3.1.7 Power and H_2 Transmission

Transmission of electricity on overhead lines is modeled by DC power flow equations as shown in Equation (3.22) which states that the power flow on a line that connects two electrical buses are proportional with the susceptance, B_{nm}, and the difference of the voltage angle of the buses.

$$f_{nm} = B_{nm}(\delta_n - \delta_m) \qquad (3.22)$$

Modeling transmission expansion with DC power flow results in quadratic constraints as the susceptance on the transmission lines is a function of the transmission line capacity. In Article 1, predefined deterministic transmission expansion scenarios are used to keep the model linear while studying the impact of different transmission grid investments. The model is solved independently for each transmission grid scenario.

In Article 2, simplified transportation model is used to represent the energy transport for both energy carriers. This is different than the DC power flow in Article 1 as it heavily simplifies the physical transport of energy, but is solely accounting the transport between nodes described in Equation (3.23). The energy flow between

the nodes, f_{tnm}, is limited by the existing and new transmission capacity in both directions as stated in Equation (3.24) and (3.24).

$$p_{tn}^{exp} - p_{tn}^{imp} = \sum_{m \in \mathcal{B}_n} f_{tnm} \qquad \forall n \in \mathcal{N} \qquad (3.23)$$

$$f_{tnm} \leq T_{nm}^{init} + T_{nm}^{max} x_{nm}^{trans} \qquad \forall n, m \in \mathcal{L} \qquad (3.24)$$

$$f_{tnm} \geq -(T_{nm}^{init} + T_{nm}^{max} x_{nm}^{trans}) \qquad \forall n, m \in \mathcal{L} \qquad (3.25)$$

This simplified grid representation makes it easier to include grid capacity as a variable in the optimization problem. The simplified energy transportation model is often used in models with coarse spatial resolution. Without sufficient spatial resolution the transmission lines are represented on a aggregated level, such that a physically detailed representation of the power flows with DC power flow equations is less meaningful. Another reason for using a simplified representation is the limited availability of detailed transmission system data. Furthermore, the DC power flow equations would introduce bi-linear terms in a transmission expansion model as the susceptance is a function of the transmission capacity.

3.1.8 Decomposing the Capacity Expansion Problem

The capacity expansion problem can be decomposed into two parts, investments and operations, by estimating the operational costs in the investment model with Benders cuts [142]. This leads to several advantages as the two parts can be modeled differently and solved by specialized methods [143]. The investment problem is much smaller than the operational problem and can be modeled as a mixed-integer linear programming (MILP) without considerably increasing the solution time. Modeling the investment decisions using integers is particularly useful for representing investments which naturally comes in large bulks, such as nuclear plants. Integers are also needed if the investment model has a high resolution such that power plants or transmission lines are modeled individually or by small groups. In the original Benders decomposition, the larger operational problem has to be modeled as a linear program (LP) as dual variables from the operational problem are used to create the Benders cuts. There is also a generalized version where the sub problem do not have to be linear [144]. While Benders decomposition was originally intended for solving MILPs [145], it is widely used in the L-Shaped method for decomposing two-stage stochastic problems and in Stochastic Dual Dynamic Programming (SDDP) for multi-stage stochastic problems [146].

At a high level, Benders decomposition is an iterative cutting-plane method which

iterates between solving the master (investment) and sub (operational) problem until convergence of the upper and lower bounds [147, 145]. An example of the decomposed capacity expansion problem with wind power and energy storage from Figure 3.2 is shown in Equation (3.26) to (3.31). The investment problem is represented by the objective function in Equation (3.26), the cuts in Equation (3.27) and the maximum limits on investments in (3.2) and (3.3). The operational cost, α, is constrained by the cuts and represents an optimistic estimation (lower bound) of the real operational costs at any moment in the algorithm. For a solution of the master problem the optimal capacities for wind power, w_i^{max*}, storage energy s_i^{max*} and storage power e_i^{max*} is sent to the sub problem (i.e. the operational problem).

$$\min \sum_{i \in \mathcal{R}} C_i^w w_i^{max} + \sum_{i \in \mathcal{E}} (C_i^s s_i^{max} + C_i^e e_i^{max}) + \alpha \tag{3.26}$$

$$\begin{aligned} \alpha \geq \alpha^k &+ \sum_{i \in \mathcal{P}} \pi_i^k P_i (w_i^{max} - W_i^k) \\ &+ \sum_{i \in \mathcal{E}} \beta_i^k (s_i^{max} - S_i^k) + \gamma_i^k (e_i^{max} - E_i^k) \qquad \forall k \in \mathcal{K} \end{aligned} \tag{3.27}$$

s.t. Equations (3.2) and (3.3)

The sub problem is represented by the objective in (3.28) the constraints defined by the capacities from the investment problem in Equation (3.29), (3.30) and (3.31), in addition to the other operational constraints in Equations (3.5), (3.8)-(3.24) as before.

$$\alpha^k = \min \sum_{t \in \mathcal{T}} \Big[\sum_{i \in \mathcal{P}} O^f p_{ti} + \sum_{n \in \mathcal{B}} O^s r_{tn} + \sum_{n \in \mathcal{M}} O_{tn}^{ex} p_{tn}^{ex} \Big] \tag{3.28}$$

$$p_{ti} + c_{ti} = P_{ti} W_i^k \qquad \pi_{ti} \qquad \forall t \in \mathcal{T}, \forall i \in \mathcal{P} \tag{3.29}$$

$$s_{ti} \leq S_i^k \qquad \beta_{ti} \qquad \forall t \in \mathcal{T}, \forall i \in \mathcal{E} \tag{3.30}$$

$$e_{ti}^i + e_{ti}^o \leq E_i^k \qquad \gamma_{ti} \qquad \forall t \in \mathcal{T}, \forall i \in \mathcal{E} \tag{3.31}$$

s.t. Equations (3.5), (3.8)-(3.24)

After solving the operational problem, difference between the upper (UB) and lower (LB) bounds are checked in Equation (3.32) and (3.33) to determine if the

algorithm has converged. The lower bound is equal to the objective function of the master problem. This gives a bound for how low the cost in the final solution possibly can be. The lower bound should be monotonically increasing as cuts are added and the representation of the sub problem costs in the master problem, α, is improved. The upper bound represents the solution found in the current iteration of the algorithm. The upper bound is calculated by adding the investment cost from the master problem to the operational costs (objective value) of the sub problem. This bound is generally decreasing over several iterations. If the difference between the upper and lower bound is less than a predefined convergence threshold, $|LB - UB| \leq \epsilon$, the optimal solution is obtained and the algorithm is terminated.

$$LB = \sum_{i \in \mathcal{R}} C_i^w w_i^{max} + \sum_{i \in \mathcal{E}} (C_i^s s_i^{max} + C_i^e e_i^{max}) + \alpha \tag{3.32}$$

$$UB = \sum_{i \in \mathcal{R}} C_i^w w_i^{max} + \sum_{i \in \mathcal{E}} (C_i^s s_i^{max} + C_i^e e_i^{max}) + \sum_{t \in \mathcal{T}} \Big[\sum_{i \in \mathcal{P}} O^f p_{ti} + \sum_{n \in \mathcal{B}} O^s r_{tn} + \sum_{i \in \mathcal{M}} O_{tn}^{ex} p_{tn}^{ex} \Big] \tag{3.33}$$

If the convergence criterion is not fulfilled, a new cut is added to the investment problem. The new cut improves the estimation of the operational costs. The cut is created according to Equation (3.27) using the duals from Equations (3.29), (3.30) and (3.31), the objective value of the operational problem and the capacities from this iteration of the algorithm. This cut represents the true operational costs for the capacities used in the operational problem in this iteration, for other capacities it is a linear approximation. The investment problem is solved again with a updated description of the operational costs, and the loop is repeated until the convergence criterion is fulfilled or a maximum number of iterations is reached.

3.2 Power System Operation with Storage and Short-Term Uncertainty

3.2.1 Storage Scheduling in Power Systems

Representing the uncertainty of VRE in the electricity system operations is challenging, especially in coordination with energy storage. Hydro power dominated systems such as Norway, Brazil, Switzerland and Canada have decades of experience and advanced modeling toolboxes for handling energy storage in water reservoir combined with uncertainty in precipitation, inflow and demand [148]. Combining scenarios for VRE production in a model with energy storage result in a

scenario-tree as the state (storage level) is dependent on the previous realizations of the uncertainty.The size of the scenario tree increases exponentially with the number of time stages.

The traditional way to solve this problem is by dividing the problem into smaller recursive sub-problems by stage-wise decomposition described by the Bellman equation [149]. This is the principal behind methods such as Dynamic Programming (DP) and Stochastic Dynamic Programming (SDP), which have been used in hydro power scheduling since the 1960s [150]. However, DP puts significant limitations on modeling detail as it requires discretization on the state variables (such as storage level) and solves a optimization problem for each state that lead to exponential growth in number of sub-problems.

More recent methods such as SDDP [146] use Benders-cuts and allows continuous state variables. Another important element of SDDP is the use of sample-average approximation in order to reduce the number of problem solved and thus reduce the computational time. Examples of other decomposition based methods for solving multistage stochastic programming problems are Progressive Hedging (PH) which is based on Lagrangian relaxation [151, 152] and stochastic decomposition [153]. These types of operational models are sometimes combined with the CEP to assess the impact of medium-term (weekly) uncertainty from VRE on investments [154, 155]. However, representing the full scenario tree for short-term operational uncertainties within the year in CEP requires significant resources such as computer clusters or heavy-duty workstations.

In CEPs where VRE is expected to represent significant amounts of the generation capacity the operational uncertainty within the year is typically neglected as year-to-year energy adequacy is more important for finding the optimal investments. Yearly uncertainty can be modeled as operational scenarios as for example in the EMPIRE model [156]. In EMPIRE, a multi-horizon approach is also utilized in order to simplify the problem as illustrated in Figure 3.5. In the multi-horizon formulation it is assumed that the operation of the system before and after a strategic decision (e.g. investment decision) are independent of each other. This might not be the case for hydro power systems with large reservoirs but is a reasonable assumption for a stochastic capacity expansion problem (S-CEP). With uncertainty in environmental policies, technology costs and long-term fuel costs the multi-horizon version becomes a simpler scenario tree with fewer strategic nodes and thus also operational years that have to be simulated as shown in Figure 3.5.b. If the investment related parameters are assumed to be known, the S-CEP is reduced to a two-stage problem with investments in the first-stage and operational scenarios in the second-stage as shown in Figure 3.5.d.

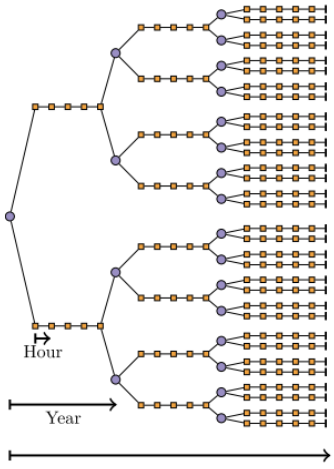

(a) Multi-stage stochastic program with strategic and operational uncertainty.

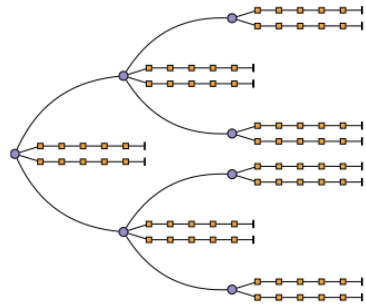

(b) Multi-horizon equivalent of (a).

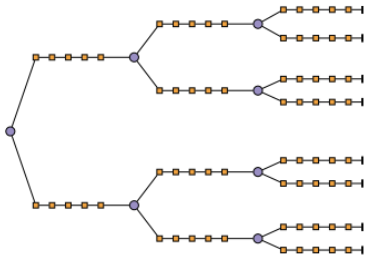

(c) Multi-stage stochastic program without strategic uncertainty.

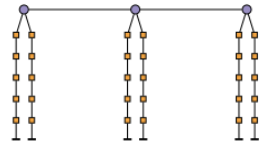

(d) Multi-horizon equivalent of (c).

Figure 3.5: Problem structure for the multi-stage and multi-horizon stochastic capacity expansion problem (S-CEP), with (a and b) and without (c and d) strategic uncertainty (investment level). Operational uncertainty is represented by yearly scenarios [133].

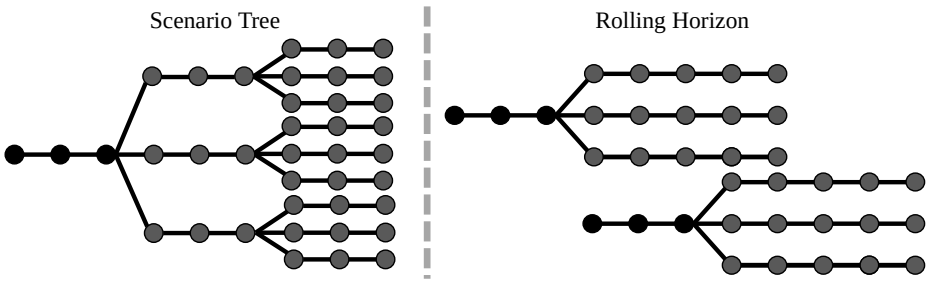

Figure 3.6: Example of the structure and size of the scenario tree (ST) and rolling horizon (RH) models. The model structure is illustrated by 3 periods of 3 nodes (dots) each, the problem use 3 scenarios to representing VRE uncertainty.

3.2.2 Stochastic Rolling Horizon Dispatch

The rolling horizon approach is well suited for detailed simulation of power system operation and representation of multiple electricity markets for real-time and day-ahead. When using this approach, a model is solved recursively and updated with new information as it becomes available. The model, for example a two-stage stochastic model, has a limited horizon of a fixed number of time steps into the future which is pushed forward as each model instance is solved.

A rolling horizon approach is often used to allow for more detailed operational modeling, such as representing short-term (daily) uncertainty in operational problems which includes VRE and flexibility sources. It is used for studies of wind power integration in Ireland [157], grid-scale battery operation [158] and wind-hydrogen storage systems [159], among others. A rolling horizon approach is also used by the Directorate-General for Energy of the European Commission (EC) in the METIS model for detailed simulation of the power system in the context of electricity markets, VRE integration and sector-coupling [132].

The rolling horizon approach offer an alternative for representing uncertainty as opposed to the scenario tree based models. The rolling horizon approach incorporates the fact that forecasting can be expensive and increasingly unreliable for long forecast horizons [160]. This representation of uncertainty is compared to the scenario tree formulation in Figure 3.6. The rolling horizon approach result in linear growth in problem size as the number of periods increase. This result in a much smaller overall problem compared to the full scenario tree representation as shown in Figure 3.7. The rate of growth for the rolling horizon approach is dependent on the horizon, where a horizon of 60 time periods results in a significantly larger model than 5 nodes as exemplified in 3.7.

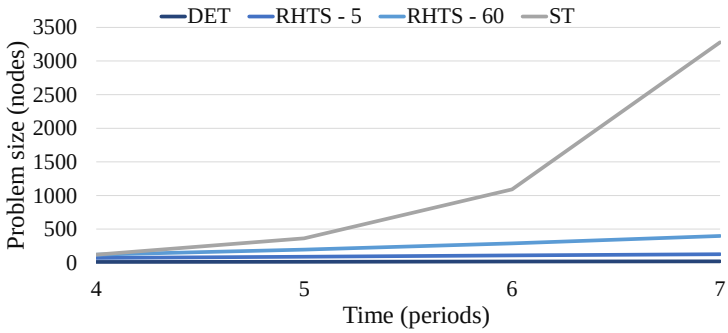

Figure 3.7: Model size for deterministic (DET), scenario tree (ST) and rolling horizon two-stage (RH) models. The RH is shown for horizons of 5 and 60 time periods.

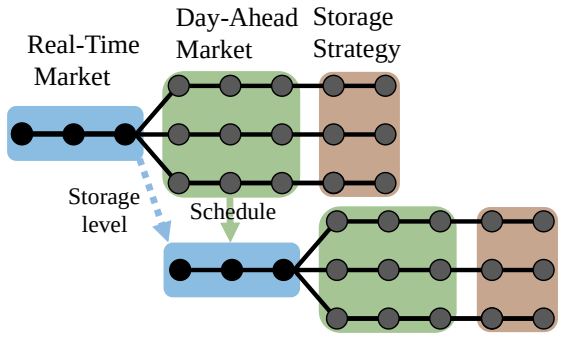

Figure 3.8: The market representation in the stochastic rolling horizon dispatch.

The reduced problem size and computational complexity is the primary advantage of the rolling horizon approach over a scenario tree representation. Reduced computational complexity enables the models to include more detailed representations of technologies, larger systems, higher temporal granularity or more detailed uncertainty representations. On the other hand, the rolling horizon approach incorporates a temporal decoupling. Hence, the impact of decisions made here-and-now on future costs are more approximate in models taking a rolling horizon approach compared to scenario tree representations.

Another benefit with the rolling horizon approach is that power system operation can be modeled similar to how the system is operated in reality. In this thesis, a rolling horizon approach is used to model power system operation in the two main short-term energy markets, namely the day-ahead and real-time markets, with hourly resolution and daily VRE generation uncertainty. The models in Article 3 and Article 5 represent power system operation with a rolling horizon approach and a two-stage stochastic economic dispatch model. This results in the stochastic

rolling horizon dispatch (SRHD) as illustrated in Figure 3.8. Generation schedules are submitted to the day-ahead market based on predicted key parameters such as load, inflow, wind and solar production.

3.2.3 Stochastic Economic Dispatch as a Two-Stage Problem

The mathematical formulation of the two-stage problem with stochastic wind power production from Article 5 is shown in Equation (3.34) to (3.44). The scenario index, s, is added to define the two-stage structure (Figure 3.8) where $\mathcal{S}_1$ is the realized first-stage "scenario" and $\mathcal{S}_2$ is the set of future scenarios for the second-stage based on wind power forecasts.

$$\min \sum_{s\in\mathcal{S}}\sum_{t\in\mathcal{T}_s}\Big[\sum_{i\in\mathcal{P}} O_i^f p_{tis} + \sum_{n\in\mathcal{B}} O^s r_{tns} + \sum_{n\in\mathcal{M}} O_{tn}^{ex} p_{tns}^{ex} + \sum_{i\in\mathcal{P},\mathcal{E}} O_{ti}^r (d_{tis}^n + d_{tis}^p)\Big] - \sum_{i\in\mathcal{E}} V_T s_{Tis} \tag{3.34}$$

$$p_{tis} + c_{tis} = P_{tis} W_i^* \qquad \forall t\in\mathcal{T}_s, \forall i\in\mathcal{P}, \forall s\in\mathcal{S} \tag{3.35}$$

$$p_{tis} - d_{tis}^n + d_{tis}^p = P_{ti}^{sch} \qquad \forall t\in\mathcal{T}_s, \forall i\in\mathcal{P}, \forall s\in\mathcal{S}_1 \tag{3.36}$$

$$p_{tis} - d_{tis}^n + d_{tis}^p = p_{ti}^{sch} \qquad \forall t\in\mathcal{T}_s, \forall i\in\mathcal{P}, \forall s\in\mathcal{S}_2 \tag{3.37}$$

$$s_{0is} = S^{prev} \qquad \forall i\in\mathcal{E}, \forall s\in\mathcal{S} \tag{3.38}$$

$$s_{tis} \le S_i^* \qquad \forall t\in\mathcal{T}_s, \forall i\in\mathcal{E}, \forall s\in\mathcal{S} \tag{3.39}$$

$$s_{tis} = s_{(t\text{-}1)is} + e_{tis}^i - e_{tis}^o \qquad \forall t\in\mathcal{T}_s, \forall i\in\mathcal{E}, \forall s\in\mathcal{S} \tag{3.40}$$

$$e_{tis}^i + e_{tis}^o \le E_i^* \qquad \forall t\in\mathcal{T}_s, \forall i\in\mathcal{E}, \forall s\in\mathcal{S} \tag{3.41}$$

$$\sum_{i\in\mathcal{P}_n} p_{tis} - p_{tns}^{ex} + r_{tns} + \sum_{i\in\mathcal{E}_n}(e_{tis}^o - e_{tis}^i) = D_{tn} \qquad \forall t\in\mathcal{T}_s, \forall n\in\mathcal{N}, \forall s\in\mathcal{S} \tag{3.42}$$

$$p_{tns}^{ex} = \sum_{m\in\mathcal{C}_n} B_{nm}(\delta_{tns} - \delta_{tms}) \qquad \forall t\in\mathcal{T}_s, \forall n\in\mathcal{B}, \forall s\in\mathcal{S} \tag{3.43}$$

$$-T_{nm} \le B_{nm}(\delta_{tns} - \delta_{tms}) \le T_{nm} \qquad \forall t\in\mathcal{T}_s, \forall n\in\mathcal{B}, \forall m\in\mathcal{C}_n, \forall s\in\mathcal{S} \tag{3.44}$$

The new features compared to the deterministic model is the generation schedules enforced by Equation (3.36) and (3.37), where positive and negative deviations

represent equal costs in both directions in the objective. Initial storage and generation schedules are obtained from the previous instance of the two-stage model and represented as parameters in this instance as shown in Equation (3.36) and (3.40). Likewise, the generations schedules are determined in Equation (3.37) and passed on to the following two-stage model in the SRHD along with the final storage level of the first-stage.

The forecast horizon is important in rolling horizon, even though only the first-stage decisions represent actual system operation. The first-stage decisions are affected by the future scenarios though temporal coupling by variables such as the storage levels. The first-stage is also affected by decisions made in the past through storage or commitments made in the day-ahead energy markets which determines regulating costs in the real-time market. Temporal dynamics are largely dependent on the typical charge and discharge time of the energy storage and determines the horizon needed for the two-stage model to give a realistic representation of system operation under uncertainty.

The typical charge and discharge rate of energy storage is dependent on the renewable energy resources and energy storage technologies available. Batteries typically have an daily state-of-charge (SoC) cycle such that the battery SoC in two weeks should not affect storage operations today and the two-stage model horizon can be limited to a few days. For H_2 storage the storage duration is usually longer, from days to months. To incorporate longer storage dynamics additional measures have to be taken with respect to storage strategy such as using storage values or guiding curves from external models. The alternative is longer forecast horizons and coarser temporal resolution in order to capture seasonal or yearly dynamics in long-term storage management such as hydro power scheduling problems would require a as in the SOVN/FANSI model [161].

3.2.4 Wind Power Scenario Generation

In this work, uncertain wind power production is forecasted by using historical meteorological forecasts of wind speeds combined with historical production records in a local quantile regression (LQR) model [162]. The LQR is used to generate non-parametric distributions for each future time step (lead times), resulting in a quantile forecast as shown in Figure 3.9. A co-variance matrix is calculated based on the correlation of wind power production. The co-variance matrix is used in order to capture correlations of wind power production in the temporal dimension for a single wind power farm and in the spatial dimension between different wind power farms. The co-variance matrix is used to sample random scenarios from a multi-variate normal distribution which is transformed into values between 0 and 1 by using the cumulative normal distribution. Matching these values with

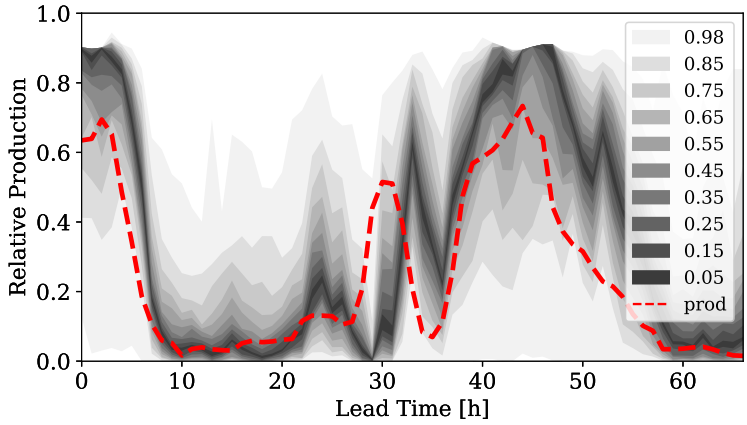

Figure 3.9: Quantile forecast generated from historical wind speed forecasts and wind power production, which are used for generating wind power production scenarios. The gray areas represent the day-ahead forecast intervals for wind power production, while the red line is the realized wind power production.

the quantile forecasts results in wind power production scenarios [163].

These wind power production scenarios are used in the second stage of the two-stage model which serves two main purposes 1) make a optimal generation schedule for the day-ahead market and 2) optimal real-time storage dispatch. One generation schedule is made in day 1 for each generator considering all the scenarios for VRE production. This schedule is passed on to the next two-stage model representing day 2. In day 2 the day-ahead generation schedule from day 1 represents commitments in the real time market (first-stage) and has to be followed. Deviations from the generation schedules have a cost which represents the "premium-of-readiness" for changing production close to real-time [28], this premium plus the generation cost gives the generation costs in the real-time market.

3.2.5 Long-Term Storage Strategy using a Rolling Horizon Approach

Long-term storage dynamics goes beyond the horizon of the two-stage model when using the rolling horizon approach and the second stage is based on wind power forecasts. This is the case for many types of energy storage. Here the focus will be on hydro power reservoirs, but the concepts for handling the long-term dynamics can be applied for many storage technologies. Long-term hydro power reservoir management has to be handled externally in other models with longer horizons. The division of the operational problem into several problems over different time-periods are common in systems dominated by hydro power such as Norway, where the problem is usually divided into three parts. The main purpose of the three op-

erational problems are; the long-term models project power prices and aggregated reservoir strategies, the medium-term problem finds detailed reservoir strategies with power prices as input parameters, while the short-term problems gives the detailed production schedules and bids to the day-ahead and balancing markets [148].

The water reservoir problem in a similar way in Article 3 and Article 5. Reservoir strategies are generated in a operational model with a yearly horizon similar to the long-term hydro-thermal models. To limit the complexity of the model, some simplifications are made compared to realistic hydro power scheduling by neglecting long-term uncertainties. Furthermore, the case studies are limited in size such that it is not necessary to include medium-term hydro power scheduling. The reservoir curve is used as input to a SRHD where daily operation of the electricity system is simulated in a market setting with short-term uncertainty and storage handling. The reservoir level has to be equal to the reservoir curve at predefined times T as shown in Equation (3.45), any deviations are penalized in the objective function by $C^{v+}v_{is}^{+} + C^{v-}v_{is}^{-}$.

$$v_{Tis} - v_{is}^{+} + v_{is}^{-} = V_{T,i}^{curve} \qquad \forall i \in \mathcal{H}, \forall s \in \mathcal{S} \tag{3.45}$$

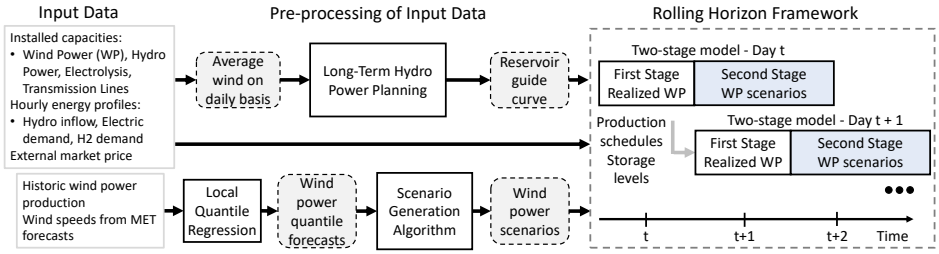

Figure 3.10: Flow chart for the rolling horizon approach with pre-processing of hydro power reservoir strategies and wind power forecasts.

3.2.6 Capacity Expansion Problem with Stochastic Rolling Horizon Dispatch

Modeling power system operation with SRHD in the decomposed CEP is a new way to represent short-term uncertainty from VRE that requires relatively low computational resources compared to other methods. Modern CEPs with short-term uncertainty and storage often use representative hours or periods to reduce the computational requirements. This reduces the temporal resolution and thus also the model size. However, the temporal resolution and chronology is shown to be crucial to the investments in flexibility in systems with large amounts of VRE

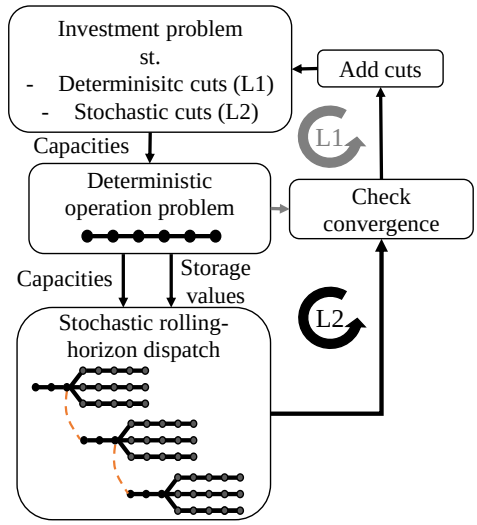

Figure 3.11: Flow chart of the algorithm for solving the investment problem with stochastic rolling horizon dispatch.

[164]. Accurate modeling of energy storage in a CEP based on representative hours is challenging and special considerations have to be taken in clustering algorithms for selecting the representative periods. For example have ramping events shown to favor storage over convectional generation and should be considered when selecting the representative periods [165].

The literature on simulating operation by SRHD in investment models is limited, where some recent examples include assessing the effect of VRE on different CO_2-emission policies [166], VRE and storage investments in micro-grids [167, 168] and placement of batteries in the distribution grid in a model with a detailed representation of battery degradation and power flow [169].

The Benders decomposed CEP is a good starting point for integrating the SRHD into a CEP which considers short-term uncertainty and market structures when optimizing investments. However, generating cuts for the investment master problem is not straight forward as the structure of the SRHD is different from the deterministic operational problem. This lead to different ways of creating the cuts to represent the stochastic operational costs which is investigated in Article 5. The work presented in Article 5 shows that cuts generated from the day-ahead values (first 24 hours of the second-stage scenarios) give the most correct investment signal for the master problem.

A challenge with Benders decomposition is that it requires many iterations to con-

verge [145]. This is not a big problem if the operational problem is deterministic and relatively small as it solves fast. However, as the size of the operational problem increase due to modeling a larger area, more detailed operation or including uncertainty the solution time increase drastically. Providing a good lower bound is critical to avoid unnecessary iterations in the SRHD-CEP. However, it is reasonable to assume that the deterministic operation part of the deterministic capacity expansion problem (D-CEP) is a relaxation of the SRHD as the only difference is that the SRHD includes the regulating market (Equation (3.36) and (3.37)) and the short-term uncertainty which lead to increased system operation costs. Solving the deterministic operational problem is much faster than solving the SRHD and results in a good lower bound for the stochastic operational costs. This is exploited by the algorithm in Article 5, which is illustrated by the high-level flow chart in Figure 3.11. The algorithm consists of two loops, first L1) solve the D-CEP to convergence followed by L2) where the deterministic cuts (created in L1) are kept in the master problem. In L2, the SRHD is used to calculate operational costs in the sub problem of the Benders decomposition algorithm which generates additional cuts that includes the cost of regulation arising from short-term uncertainty.

In L2, the deterministic operational model with a yearly horizon (see Figure 3.11) is no longer used to generate cuts as in the L1 iterations. The deterministic operational model is still included in the L2 loops in order to generate long-term storage strategies that are integrated into the SRHD as end-of-horizon storage values (V_t). This is similar to the long-term storage strategy generation in the deterministic model illustrated in Figure 3.10. However, with changing investments the long-term storage strategy has to change accordingly, thus the strategies are re-evaluated for each iteration. Essentially, the storage strategies are generated by two sub models in the L2 iterations, where the long-term strategies are generated by the deterministic sub model and the short-term storage operation is determined by the SRHD. The storage values obtained from the dual values of Equation (3.5) and included at the end of the objective function in Equation (3.34) to represent the value of the remaining energy in the storage at the end of each two-stage model on the SRHD, $V_T s_{Tis}$. This is an good alternative to the guiding curve method presented in 3.2.5 and Article 4, as the value of stored energy at the end of the two-stage model horizon is set to be the marginal value of stored energy (water value) which represent a real strategic value of using stored energy now or later. Another alternative could be to use a combination of the two methods, which would allow us to capture the dependency between the dual value of the storage balance and the corresponding storage level, where $V_t = f(s_t)$.

More details on the SRHD-CEP are given in Chapter 4.2.2 and Article 5.

Chapter 4

Results and Discussion

The results from this thesis is published in 5 articles as listed in Chapter 1.3. The articles can be grouped into to categories as shown in Figure 4.1.The first part deals with case studies of hydrogen in Norway and Texas using deterministic capacity expansion problem (D-CEP) and selected technologies for electricity production, transmission and storage. The second part attend to the need for short-term uncertainty and flexibility in the power system, where flexibility from hydro power is especially considered in Article 4. The modeling in the second part is firstly directed towards the operational aspects of short-term uncertainty which are later integrated in a stochastic rolling horizon dispatch capacity expansion problem (SRHD-CEP) as explained in Chapter 3.2.6.

4.1 Flexible H_2 Production in Electricity Systems

4.1.1 Optimal Capacities in Constrained Transmission Grids

The northern part of Norway is the region in Norway with the best wind power resources. The natural gas processing plant in Hammerfest is also located in this region, from which significant amounts of natural gas is exported to other parts of the world in the form of Liquefied Natural Gas (LNG). Liquefaction is the preferred method due to the long distance to any major gas user. For the same reason, it is expensive to take advantage of the good wind conditions to generate electricity as it will have to be transported to electricity load centers over long distances by transmission lines. A solution for the issue of stranded VRE potential can be to produce H_2 from both natural gas and electricity with subsequent liquefaction and transportation on ships similar to LNG carriers. This will also reduce the environmental impact of natural gas resources as the CO_2 from natural gas based H_2

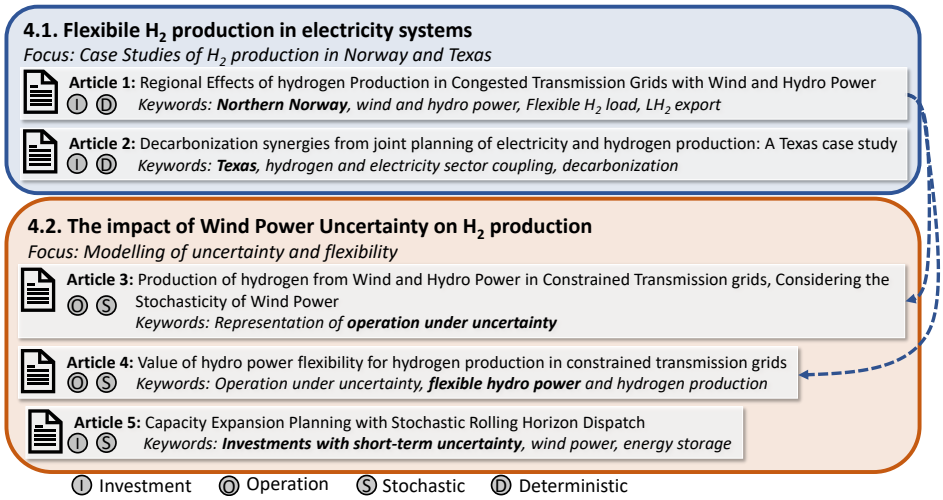

Figure 4.1: Overview of the organization of Chapter 4 and how it relates to the published articles from this thesis.

production can be injected back into the sub-sea reservoirs. Thus, with present technology, reducing the carbon footprint of the natural gas by 90 %. This is the motivation for the study in Article 1 which analyze future scenarios for H_2 production and LH_2 export from northern Norway.

The Norwegian electricity system is characterized by large amounts of hydro power with the possibility of storing energy in water reservoirs. The flexibility from hydro power enables the system to integrate large quantities of VRE in an efficient way, without excessive curtailment of the VRE production. However, this is dependent on sufficient transmission capacity between wind and hydro power plants. A scenario for the future electricity system in northern Norway (Finnmark) is illustrated in Figure 4.2, represented by hydro power plants, wind farms, transmission lines and H_2 production from electrolysis and natural gas.

In Article 1 the deterministic capacity expansion model outlined in Equations (3.1) to (3.10) is used to investigate the effects of H_2 production in Hammerfest (bus 6 in Figure 4.2), where hydro power is modeled as in Section 3.1.4 and H_2 is considered a flexible load as explained in Section 3.1.5. A total of 500 tonnes H_2/day is assumed to be produced from natural gas and electricity where electrolysis represent 10 % (50 tonnes) of the total H_2 production. Liquefaction of H_2 is an energy demanding process where liquefaction of 500 tonnes/day results in an electricity demand of 1436 GWh/year. As the process operate at a constant rate this is the same as a 164 MW electric load with a flat profile. In these scenarios the electricity demand at bus 6, where the H_2 production is located, accounts for around 60

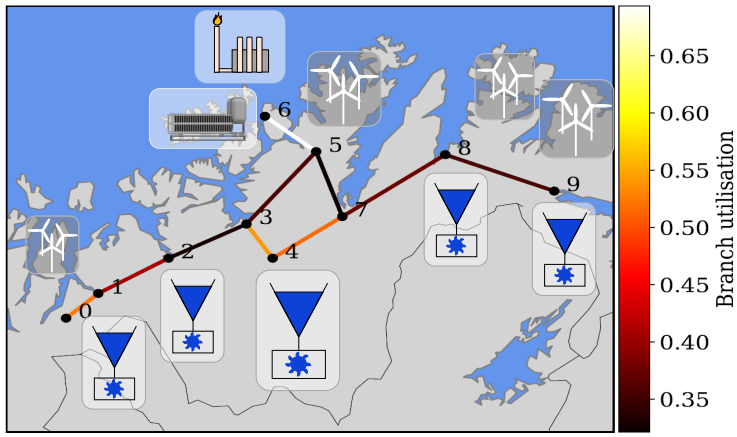

Figure 4.2: Illustration of a scenario for the future power system in Finnmark with H_2 production.

% of the total electricity demand of the region shown in Figure 4.2.

To accommodate the large amounts of new electricity demand the system will require a combination of new electricity generation and more transmission capacity. Three different transmission line scenarios are considered in order to evaluate the impact of transmission constraints. The three transmission line expansion scenarios are defined based on doubling the capacity of existing lines:

L - Local transmission expansion from the H_2 node (bus 5-6)

R - Regional transmission expansion from the H_2 node to the main wind power resources in the east (bus 5-6-7-8)

N - National transmission expansion to bus 0 which represents the rest of the power system (bus 0-1-2-3-5-6)

The transmission expansion scenarios are combined with four different designs for the electrolyzer facilities:

B - Base case with no H_2 load

D - Demand from H_2 liquefaction only, assuming H_2 is produced solely from natural gas

E - Electrolytic H_2 production with constant operation

ES - Electrolysis with storage which enables variable H_2 production

Table 4.1: The resulting capacities for electrolysis and H_2 storage and rationed energy from the case study of H_2 production in northern Norway. H_2 storage is represented by volume and hours of H_2 demand. H_2 storage is profitable in the National transmission expansion scenario such that the E and ES electrolyzer plant designs results in the same solution.

	Local		Regional		National
Capacities	E	ES	E	ES	
Elec [MW]	107.99	128.87	107.99	110.97	107.99
Storage [Nm^3]	-	231003.8	-	101550.8	0.0
Storage [h]	-	9.97	-	4.38	0.0
Rat [MWh]	199.47	0.0	354.63	0.0	0.0

The electrolysis plant design E is consistent with the traditional electrolysis operation, where electrolysis has been operated at a constant rate in order to maximize capacity utilization. With high shares of renewable, transmission constraints and lower CAPEX in the near future, electrolysis operation is expected to be more dynamic, this is enabled by plant design ES where H_2 allows for variable H_2 production while delivering H_2 when it is needed by the end-users.

The results shows that a better grid connection to the electricity market at node number 0 (which represents the rest of the power system) results in less H_2 storage as shown in Table 4.1. No storage is needed for the scenario with the best connection to the national transmission grid (N). This shows that storage is mainly used for alleviating internal grid constraints rather than reducing the electricity cost by moving H_2 production to hours with lower electricity prices. H_2 storage in constrained transmission grids serves to reduce rationing of load and curtailment of wind power production (Figure 4.3) by shifting the load represented by H_2 production, thus acting like a flexible load. This is shown for scenario L and R as the inclusion of H_2 storage in ES eliminates load curtailment from 199 and 355 MWh in the configuration without storage (E). Less transmission capacity in grid scenario L requires the electrolyzer plant to have twice as much storage as in grid scenario R.

Restricting transmission capacity to the market node represented by transmission scenario L and R leads to significant development of local wind power production to supply the new H_2 load as shown in Figure 4.3. The flexible electrolysis option requires less wind power capacity compared to the firm electrolysis option as curtailment of production is reduced as shown by the dotted lines in Figure 4.3. When the connection to the rest of the electricity system is strong in grid scenario

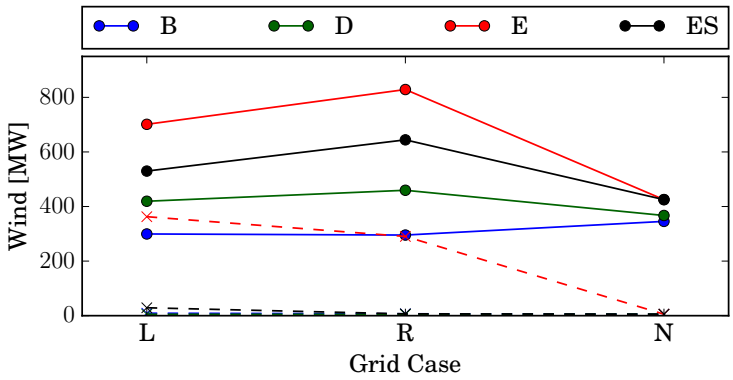

Figure 4.3: Total wind power capacity in the region (solid lines) and wind power curtailment (dotted lines) as resulting from the model for the different electrolyzer plant designs and transmission grid scenarios. Each line represent a electolyzer plant design as a function of the transmission grid scenarios.

N there is little difference in wind power development between the different load cases as more electricity is imported from the market.

Wind power development in combination with transmission constraints has a negative impact on the profitability of the local hydro power plants as seen in Figure 4.4 because they have to shift production to accommodate the less controllable wind power [11]. Less wind power development and stronger grid connections also lead to higher profits[1] for the hydro power plants as they can produce more electricity when prices are high.

These results show that an electricity system that is mainly based on hydro power has great potential for integration of wind power. However, it comes at the expense of hydro power plant profitability if the transmission capacity is limited. In such a system the role of flexible H_2 production is mainly to increase the security of supply by alleviating local transmission congestion and reduce wind power curtailment. The low variation in electricity prices are characteristic of power systems with high shares of hydro power, thus price variations are not high enough to make H_2 storage profitable and the electrolyzers will be operated to maximize capacity utilization in the traditional way. If the transmission grid is not upgraded significantly there will be significant transmission congestion in the scenarios analyzed in Article 1, in such a case it would be beneficial for the system to have incentives for investment in H_2 storage and flexible electrolysis operation. The socio-economic optimal transmission grid development in the region is not concluded in this ana-

[1] Calculated by the electricity market (node 0) prices and hydro power production

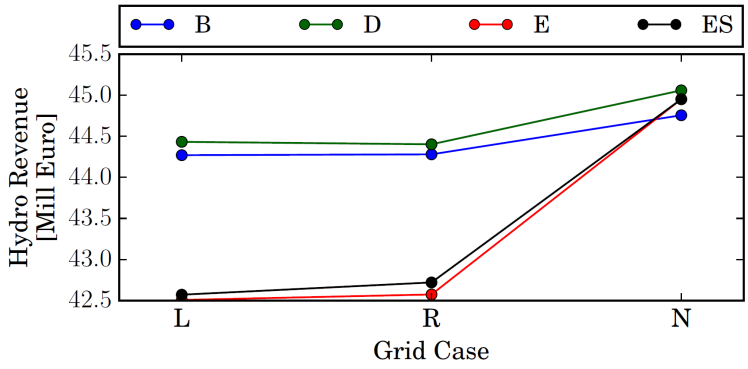

Figure 4.4: Total revenue for all hydro power plants in the region, calculated from the model results. Each line represent a electolyzer plant design as a function of the transmission grid scenarios.

lysis as it depends on the investment costs of the transmission expansion scenarios and total future electricity demand in the region.

4.1.2 H_2 Production for Power System Decarbonization

The state of Texas is known for having large oil and gas resources. Most of the electricity in Texas is currently produced from natural gas and coal due to the low fossil fuel prices. There are also significant amounts of wind and solar resources in the western/northern regions of the state, making it the state with the best potential for H_2 production from VRE sources in the US [170]. After a decade of major wind power development Texas is currently the U.S. state with the most installed wind power capacity at 28.1 GW, producing 84.4 TWh in 2019. Wind power accounts for 18% of the states total electricity generation which is a significant increase from 6% in 2010 [171].

Transitioning from natural gas to H_2 production can be a way for Texas to take advantage of both natural gas and VRE resources in a climate-friendly way. Some H_2 production from SMR are already in place in relation to the natural gas refineries and H_2 has been stored in salt caverns there since the 1970s. CO_2 captured by combining H_2 production from natural gas with CCS can be stored in underground geological structures such as saline aquifers reducing the storage costs compared to other options [44]. There is a significant distance between the best VRE resources in the west/north and the major load centers in the east/south and energy can be transported by overhead lines or as H_2 in pipelines.

In Article 2 the best mode of H_2 production in Texas is found while considering different scenarios for H_2 demand and CO_2 prices in 2050. A baseline H_2 demand for 2050 is estimated based on a scenario for H_2 adoption in the transport sector

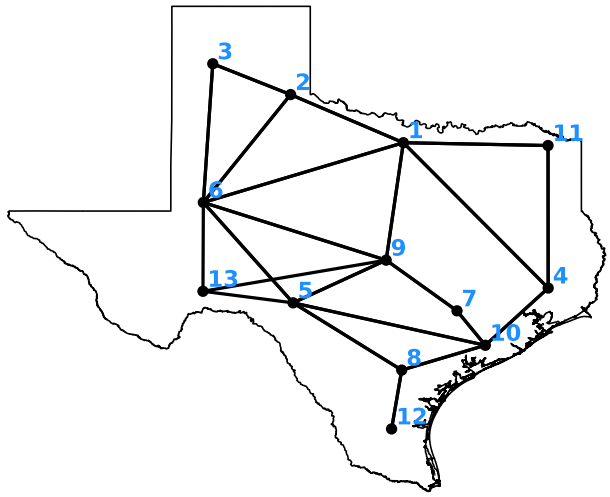

Figure 4.5: The spacial representation and distribution of nodes and the pathways considered for the overhead lines/pipelines in the Texas case study.

of 0.68 mmt/year (4.6 % of electricity demand by LHV of H_2) [172]. To put this in context the current total H_2 demand in the US is around 10 mmt/year [173] and expected to increase more than 9 times by 2050 [174]. The impact of scale for H_2 demand is investigated by increasing the baseline demand by 10 and 50 times. Both major technology options for H_2 production, natural gas (SMR) and electrolysis (PEMEL) are considered, along with H_2 storage and transport. Utility-scale batteries are also included as an energy storage investment option. This study utilize a capacity expansion model that consider the coupling between the electricity and H_2 sectors as illustrated in Figure 3.4.

The representation of the electricity system in Texas used for the case study is illustrated in Figure 4.5 [175]. The electricity load is assumed to increase from 347 TWh in 2015 to 492 TWh in 2050 based on an annual growth of 1% as estimated by the EIA in the Annual Energy Outlook from 2019 [176]. Existing generation capacity is obtained from the National Electric Energy Data System (NEEDS) v6 [177] and fitted to the case study system, new generation and battery storage capacity costs in 2050 are based on NRELs annual technology baseline (ATB) [17]. SMR plant design is based on a study of merchant plants by the EIA, where CCS can reduce the emissions from 9 to 0.93 CO_2/kg H_2 at a cost of \$83/tonne CO_2 [43]. Electrolyzer costs are estimated to be $\sim$ \$530/kW with a efficiency of 65%[2] [39].

[2]based on LHV

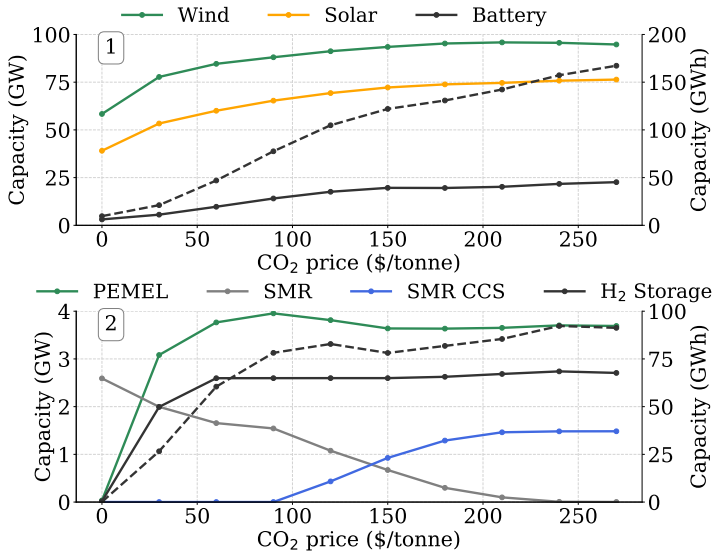

Figure 4.6: Resulting capacities from the model with baseline H_2 demand, grouped by 1) VRE and battery capacity and 2) H_2 production and storage capacity. H_2 capacities are converted to power by the LHV of H_2. Storage energy capacity is represented by the dotted lines and secondary y-axis (right).

Electricity production from renewables and battery storage for the case with baseline H_2 demand are shown in Figure 4.6.1 for different CO_2 prices between \$0-270/tonne. Introducing a CO_2 price of \$30/tonne results in a increased wind power capacity from 58 to 78 GW and solar power capacity from 39 to 53 GW as coal is completely phased-out. Further growth in the share of renewable energy require a significantly higher relative increase in CO_2 prices as it substitutes natural gas which has lower relative emissions. Natural gas is a important source of flexibility in the electricity system, thus replacing natural gas with electricity from VRE sources also requires significant amounts of batteries as shown in Figure 4.6.1.

In the absence of a CO_2 price there is no installed capacity for electrolysis or SMR with CCS. Some of the H_2 production from SMR is replaced by electrolysis which is gradually constructed as the CO_2 price increases from \$30-90/tonne. For CO_2 prices higher than \$120/tonne SMR with CCS is phased in to reduce the emissions from H_2 production.

The resulting deployment of electricity network, batteries and solar power is shown in Figure 4.7(a), while H_2 pipelines, H_2 storage and wind power is shown in Figure 4.7(b). Pipelines are used to transport H_2 from west to east while H_2 is co-located with wind power plants to smooth the variation in wind power production. Bat-

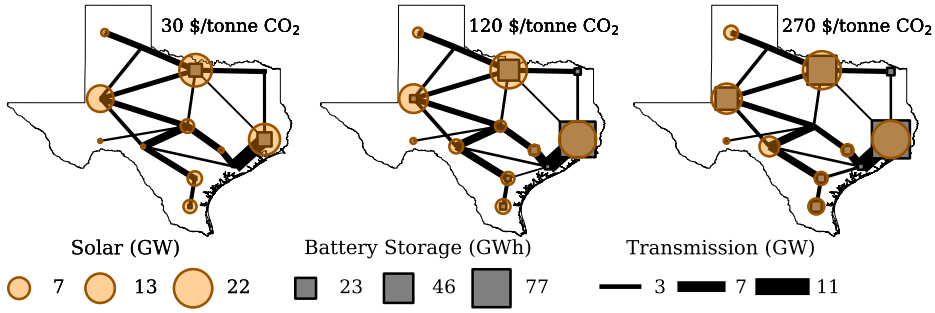

(a) Solar power, battery energy and overhead transmission line capacity.

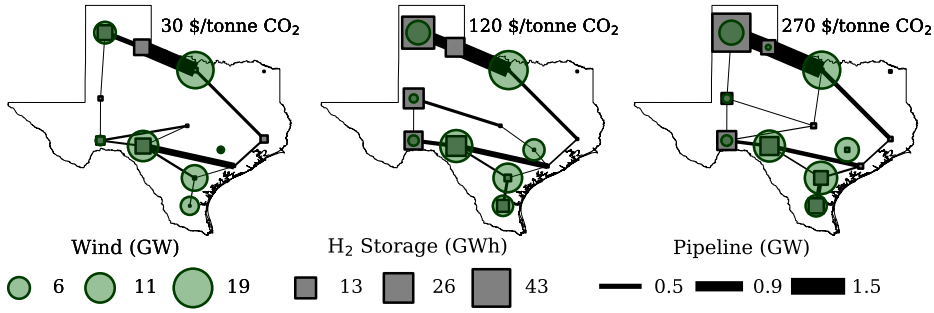

(b) Wind power, H_2 storage and pipeline capacity.

Figure 4.7: Development in a) solar power, battery energy and overhead transmission line capacity and b) wind power, H_2 storage and pipeline capacity.

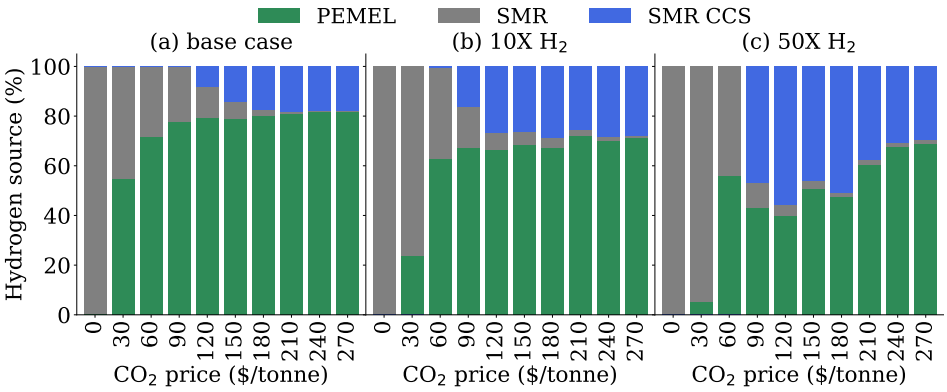

Figure 4.8: Share of H_2 demand by production technology for the different H_2 demand scenarios.

teries are largely co-located with solar power close to the electricity demand, but some solar power is developed in the west where the solar irradiation is strong. The capacity for batteries, H_2 storage and H_2 pipelines are increasing strongly with the CO_2 price compared to the increase in wind and solar power generation.

Flexible H_2 production enables large shares of renewable energy integration with less batteries, for the highest H_2 demand scenario (50X) the VRE share is 94 % with 1.3 GW of batteries compared to 78 % with 9.7 GW of batteries for the scenario with the lowest H_2 demand. H_2 is produced solely from SMR in the absence of emissions costs as shown in Figure 4.8, increasing the emissions cost strongly favors H_2 produced from electrolysis which represent around half the H_2 produced at CO_2 prices of 30-60 $/tonne (see Figure 4.8). Increasing H_2 demand favors SMR and makes CCS cost efficient at lower CO_2 prices, thus CCS is deployed for H_2 production at $90/tonne in the 10X H_2 and 50X H_2 H_2 demand scenarios compared to $120/tonne in the base case.

Flexible H_2 production reduces the need for electricity production from natural gas power plants compared to a system with no H_2 production by up to 5 %, 27 % and 53 % for the base, 10X H_2 and 50X H_2 case respectively. Thus, significant demand-side flexibility from H_2 production reduces the utilization factor for natural gas turbines and the emissions in the electricity sector. Lower utilization factors favors less capital intensive technologies such that significantly higher CO_2 prices ($180/tonne) are required to make CCS with natural gas power plants viable. As a result, CCS is more favorable in combination with H_2 production from SMR ($90/tonne) compared to capturing CO_2 from the exhaust gas of natural gas power plants.

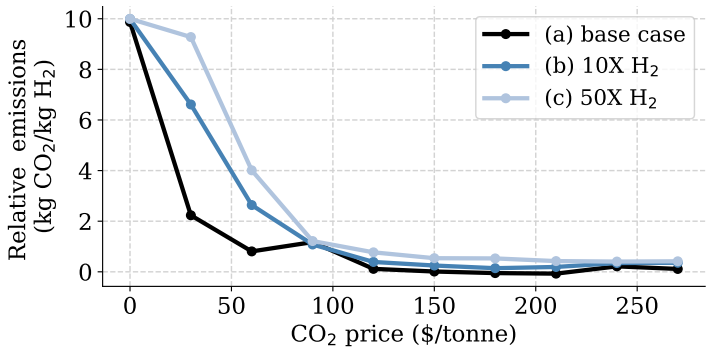

Figure 4.9: Relative CO_2 emissions from producing H_2.

The relative emissions from H_2 production increase with the H_2 demand as shown in Figure 4.9, but are relatively small (less than 1.2 kg CO_2/kg H_2) for all H_2 demands when CO_2 prices are more than \$90/tonne. This is because hydrogen is mainly produced from PEMEL or SMR with CCS which has low emissions ($\leq$ 0.99 kg CO_2/kg H_2) compared to standalone SMR (10 kg CO_2/kg H_2).

H_2 production has a low impact on the average electricity price for CO_2 prices less than \$180/tonne. The average electricity price is reduced for CO_2 prices of more than \$180/tonne as flexible electricity production from natural gas turbines with CCS in the electricity sector is avoided and replaced by flexibility from electrolysis and H_2 storage. Flexible H_2 production contributes to significantly reduce the variations in electricity prices typically associated with high VRE shares. The H_2 price varies between 1.30-1.66 \$/kg for a CO_2 of \$60/tonne dependent on the H_2 demand. Further increases in CO_2 prices only have a marginal impact on the H_2 price as the H_2 production is associated with low levels of CO_2 emissions. The H_2 price in the scenario with the highest H_2 demand is more impacted by increased CO_2 prices as more of the H_2 is from SMR with CCS, compared to the lower H_2 demand cases, which still has some CO_2 emissions.

4.1.3 Comparing the Role of Flexible H_2 Production in Electricity Systems

The results from Texas in Article 2 show how H_2 can provide significant flexibility and enables VRE integration and CO_2 emission reduction. Flexible H_2 production in Texas compliment other resources by providing flexibility on a longer time-scale (5-36 hours) as compared to for example batteries (2-7 hours). On the other hand, the development of H_2 flexibility in the electricity system in northern Norway is largely driven by local transmission constraints. Electricity system infrastructure investments in Texas are sensitive to changing CO_2 prices and H_2 demands due to the lack of zero emission options for flexibility on this time-scale. In Norway, H_2

production is likely to be less sensitive to changing CO_2 prices as hydro power can provide flexibility with zero marginal emissions on the same time-scales as H_2 and facilitate VRE integration in a similar fashion as shown in Article 1.

Both cases investigated in this thesis assumes a demand for H_2. The H_2 demand in Texas is based on local end-users in the transport sector and subject to sensitivity analysis by increasing the H_2 demand which would likely require H_2 export. The Norwegian case is purely based on H_2 export to regions with energy deficits. The level of the H_2 demands are subject to significant uncertainty but it is likely that the H_2 demand is also positively correlated with the CO_2 price as the H_2 would be used to reduce emissions for end-users, a effect that is not accounted for in the analyses in this thesis. Thus, the CO_2 price can provide incentives for electrolytic H_2 production on two sides, both for providing flexibility for VRE electricity production and through the H_2 demand for reducing emissions for end-users.

The future cost of H_2 production is potentially low for both systems, but for different reasons. In Texas, H_2 is produced in periods with low prices and surplus VRE generation for a fraction of the average electricity price (20-60 % dependent on H_2 demand). To enable this type of electrolysis operation while serving a stable H_2 demand it requires significant amounts of H_2 storage. The H_2 cost can potentially be further reduced by operating the electrolyzers according to the balancing market which can provide further revenues at low additional cost, this goes beyond our analysis in Article 2. Norway, on the other hand, has large shares of hydro power resulting in stable electricity prices. Electricity prices are likely be stable even if large amounts of wind power were to be integrated into the electricity system. Thus, the investment cost of wind power turbines and the quality of the local wind resource are key cost parameters in order to reduce the LCOE and drive down the average electricity price. In the absence of local transmission constraints, H_2 production is likely to be relatively constant to utilize the full electrolysis capacity and minimize the impact of the CAPEX on the levelized cost of H_2.

In the Norwegian electricity system, there are incentives for large-scale demand to be located close to renewable energy production through reduced grid tariffs. These incentives are largely evaluated on a case-to-case basis. For the electricity system to benefit from the relatively low-cost option of including H_2 storage with the electrolysis, it could be a good policy to reduce grid tariffs further for large-scale flexible H_2 production in relation to VRE electricity production. This might reduce or delay the need for new transmission lines, but would require active control of the H_2 production to avoid line overloading at specific times. Similar direct control of production currently exists in order to activate automatic frequency reserves and restore the frequency of the electricity system after generator or line faults. Direct control of end-use electricity load is widely considered in the dis-

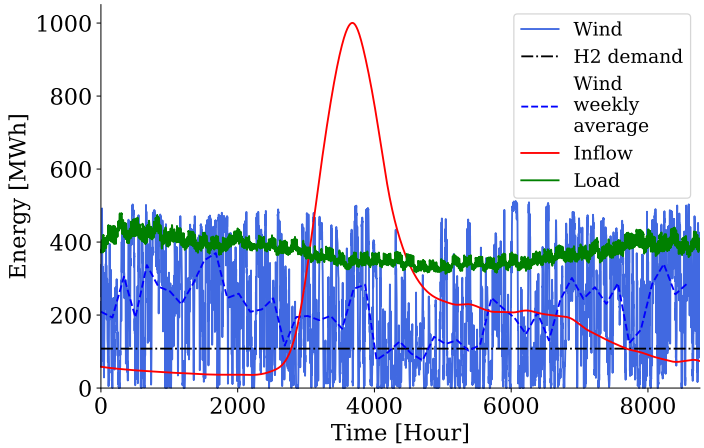

Figure 4.10: Energy profiles from 2015 for the Finnmark case study, these are used as input data in Article 4.

tribution gird and flexible H_2 production could offer the same service on a larger scale. This would be more favorable than other types of large-scale load management such as disconnecting traditional energy-intensive industries from the electricity system which often has relatively low tariffs for energy not served. Furthermore, for H_2 production to be considered an flexible alternative to transmission expansion it would require long-term contracts with the owner of the electrolysis plant to ensure sufficient electrolysis and storage capacity. These contracts should be designed to have a duration such that the TSO has a real option to build a transmission line.

4.2 The Impact of Wind Power Uncertainty on H_2 Production

Short-term uncertainty in power generation is an increasingly important aspect in power system operation as systems are moving towards higher shares of VRE. This is exemplified by the energy profiles in the Finnmark case study as shown in Figure 4.10 where the wind power resource is highly variable compared to the electric load. However, the seasonal profile of the wind power resources and electricity demand are generally positively correlated, with more wind power production and electricity demand in the winter and less in the summer. This is exemplified by the electric load and the weekly average wind energy availability in Figure 4.10.

In Article 3, the stochastic rolling horizon dispatch (SRHD) outlined in Section 3.2.2 is developed. The stochastic rolling horizon dispatch (SRHD) is used to show the impact of wind power uncertainty on power system operation. The impact of stochastic operation on the power system of northern Norway is analyzed

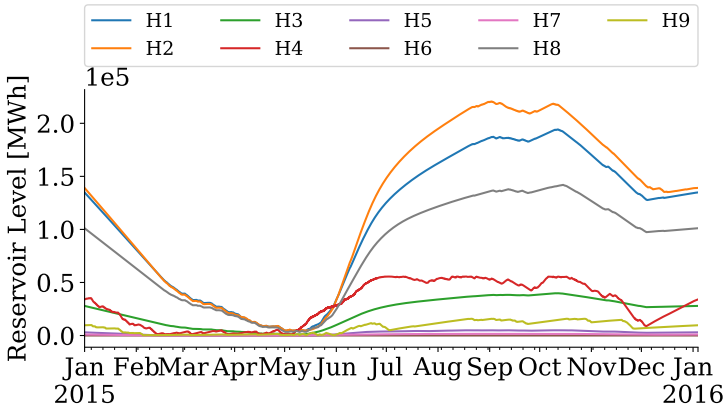

Figure 4.11: Long-term hydro power reservoir strategies for the eight reservoirs in the Finnmark case study which serves as input for the SRHD.

over a period of 10 days to assess the model performance. Using scenarios for wind power generation to plan short-term electricity system operation reduces the total operational costs by 5.6 % compared to an operational model which use expected wind power production. Modeling the system operation using a deterministic model with perfect information significantly underestimates the costs compared to the stochastic model, resulting in 37.6 % lower operational costs. This difference is dependent on the scenarios simulated and can be reduced by improving wind power forecasts. However a deterministic operation model is always going to underestimate operational costs compared to what is achievable during real operation. Operation with short-term uncertainty is further compared with deterministic operation in Article 5 which show that including short-term uncertainty in the operational model also have implications on investment decisions.

4.2.1 Hydro Power Flexibility and H_2 Production

The model framework from Article 3 is expanded in Article 4 to enable long-term storage strategies in the form of reservoir curves for hydro power reservoirs as explained in Section 3.2.5. The reservoir curves for the eight hydro power reservoirs in the Finnmark case study are obtained from running a deterministic operational model with a yearly horizon and hourly resolution and are shown in Figure 4.11. As the levels of wind power production are not accurately know when planning the hydro power strategy, the wind power resources are represented by wind power profiles with daily resolution. The resulting reservoir level from the one-year model serves as the long-term reservoir strategy and is an input to the two-stage model in the SRHD. This gives a long-term strategic perspective to the two-stage model which has a horizon of only three days due to the length of wind

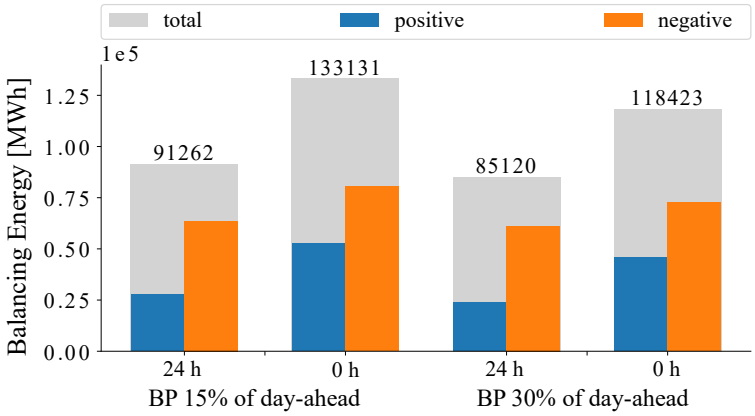

Figure 4.12: Balancing by the H_2 plant for different levels of hydro power flexibility and balancing price (BP).

power forecasts. These reservoir curves are sometimes referred to as "steering curves" and used in detailed models which combine seasonal storage and short-term uncertainty such as METIS, SiSTEM and Antares [36].

In Article 4, the SRHD is used to evaluate the impact of hydro power flexibility on H_2 production in northern Norway. The level of power system flexibility is important for integration of VRE and can significantly impact the benefits and costs of flexible H_2 production as seen in Article 1. However, it is difficult to quantify the levels of flexibility that can realistically be obtained from hydro power plants as they include complex operational constraints due to for example cascaded river systems, environmental regulations and other complexities related to plant design. Thus, the short-term flexibility of hydro power plants is restricted in the model to evaluate the impact of different levels of hydro power flexibility on system operation. Hydro power flexibility is restricted to time intervals of 0, 6 or 24 hours in which short-term deviations from the long-term reservoir curve is available. When the reservoir curve in the SRHD does not equal the long-term strategy at the end of the given intervals it results in penalties in the objective function.

The case study in Article 4 is based on the resulting wind power and electrolysis capacities from the regional grid scenario with H_2 storage in Article 1. Transmission grid capacities are increased (up to 2X of the regional grid scenario values) in order to avoid excessive curtailment and rationing due to the uncertain wind power production. This exemplifies the underestimation of the required system flexibility when a deterministic investment model is used to assess investments in VRE production, especially in the context of constrained transmission grids. The case study

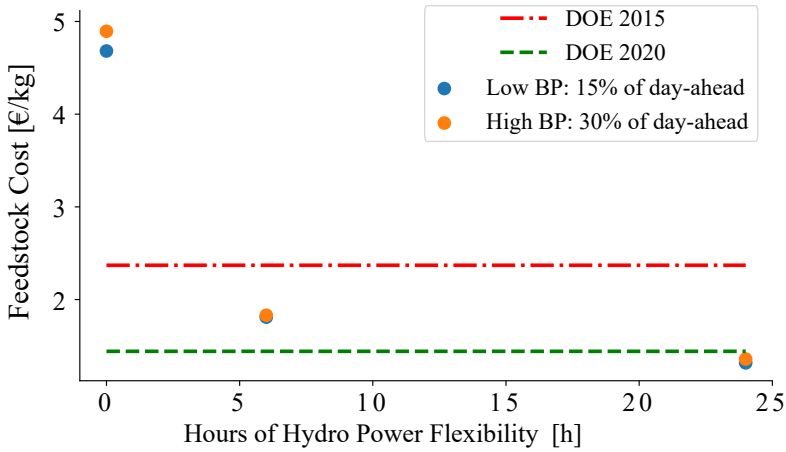

Figure 4.13: Cost of producing H_2 compared to the DOE targets for 2015 and 2020, the targets are converted from 2007 to 2015 values to adjust for inflation.

remain realistic as Statnett are currently building new transmission capacity to improve security of supply, facilitate new electricity generation and consumption in Finnmark. Briefly explained, a new 420 kV transmission line is under construction on segment 0-1-2 (Balsfjord - Alta, expected completion in 2021) and 2-3-5 (Alta-Skaidi, expected completion in 2023) from Figure 4.2 [178].

Demand-side flexibility from H_2 production becomes more important to balance electricity generation and consumption in the absence of short-term flexibility from hydro power. This results in up to 39-46 % more balancing by the electrolyzer as shown in Figure 4.12 and more active use of H_2 storage and electrolysis capacities. In comparison, doubling the balancing price results in a 7-11% decrease of balancing energy delivered by the electrolyzers. To put the levels of balancing energy from the electrolyzers in perspective it amounts to 9-14 % of the total electrolyzer energy consumption. Without flexibility from hydro power, the demand-side flexibility from H_2 production is insufficient to avoid rationing of demand. Thus, penalties for breaking the hydro power limitations are activated according to Equation (3.45).

The results from Article 4, indicate that the electricity system is dependent on at least 6 hours of short-term flexibility from hydro power together with the transmission investments to support the local H_2 production, H_2 liquefaction and for balancing wind power production. The H_2 production represents a significant increase in electricity consumption in the region with a doubling of the annual electricity demand. However, with sufficient flexibility from the hydro power plants (6 hours

Table 4.2: Cost of hydrogen production with high levels of hydro power flexibility from Article 4, using current and future estimates of capital and fixed O&M costs.

	Current	Future	DOE - 2020
Capital [€/kg]	0.72	0.31	0.41
Feedstock [€/kg]	1.32	1.32	1.46
Fixed O&M [€/kg]	0.53	0.26	0.21
Total [€/kg]	2.57	1.89	2.08

or more), H_2 can be produced at prices close to the U.S. Department of Energy (DOE) targets [179] as seen in Figure 4.13. Increasing the short-term flexibility of hydro power plants to 24 hours (from 6 hours) reduce the wasted energy in the system by 40% and the operating costs for the electrolyzer is reduced by 27%. This enables a low total costs for H_2 production at 2.57 and 1.89 €/kg with current and future CAPEX and fixed O&M respectively as shown in Table 4.2. The estimated electrolytic H_2 costs with current electrolyzer CAPEX are high compared to the current price of H_2 from SMR without CCS which ranges from 0.6-2.0 €/kg [180, 181]. Electrolytic H_2 is on price parity with present fossil based H_2 when using the estimated future electrolysis CAPEX and fixed O&M costs. The estimated prices[3] of electrolytic H_2 from PEMEL in the last months of 2020 was 2.8-3.3 €/kg in California and the Netherlands while it was 4.5-4.9 €/kg in Japan [182], which is higher than the DOE 2020 target.

In Article 4, the impact of flexible H_2 production is limited by its location in the transmission grid (only one fixed location) and the operational limits given by the installed capacities. In a potential extension of the case study, the SRHD-CEP could be used to incorporate investment decisions. This would likely result in more installed storage and electrolysis capacity compared to the deterministic investment results in Article 1. Similar to Article 2, the share of H_2 produced from SMR or electrolysis could be variable. Thus, more H_2 could be produced from SMR with CCS if the costs of electrolytic H_2 production in the electricity system is too large due to lacking hydro power flexibility.

[3] Prices including CAPEX. Assuming a electrolysis plant design of 40 000 kg/day and 95% capacity utilization.

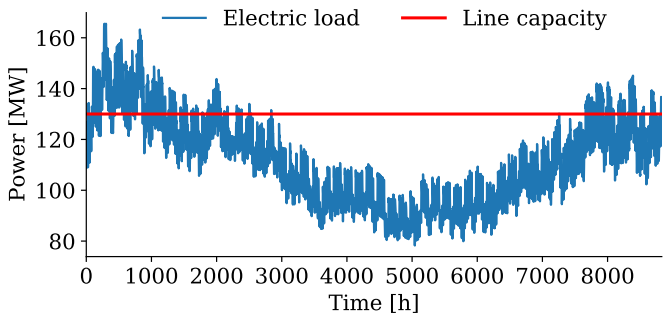

Figure 4.14: Electric load profile and transmission line capacity in the two-bus case study of Article 5.

4.2.2 Effect of Wind Power Uncertainty on Optimal Capacities

Wind power production uncertainty affects the optimal level of investments in the power system as shown in Article 5 (also indirectly in Article 4). The stochastic rolling horizon dispatch capacity expansion problem (SRHD-CEP) developed in Article 5 endogenously consider the impact of short-term uncertainty in wind power production on power system operation and investments. The model also preserves the chronological order of operations to enable short and long-term storage operation. Investment and operation is separated by benders decomposition as shown in 3.1.8. A deterministic model is integrated in the Benders decomposition which is initially used for generating a lower bound for operational costs and afterwards used for the long term storage strategy in the SRHD operational model. The algorithm for for solving the SRHD-CEP is described in Section 3.2.6. Article 5 compares the performance of the deterministic capacity expansion problem (D-CEP) with the SRHD-CEP for two different ways of generating the benders cuts as shown in Figure 4.15. The cut-types investigated is characterized by:

a-cut) Cuts obtained from expected (day-ahead) values of the SRHD

b-cut) Cuts obtained from the average of realized (real-time) and expected (day-ahead) values from the SRHD

The impact of short-term uncertainty on the optimal wind power and storage capacities is analyzed in a two-bus system with limited transmission capacity as illustrated in Figure 3.2. A generic storage model is used (not H_2 specific) as shown in Equation (3.38) to (3.41), which can give a high-level representation most storage technologies with only minor modifications. The electricity demand profile used in the case study compared to the transmission line capacity is shown in Figure 4.14.

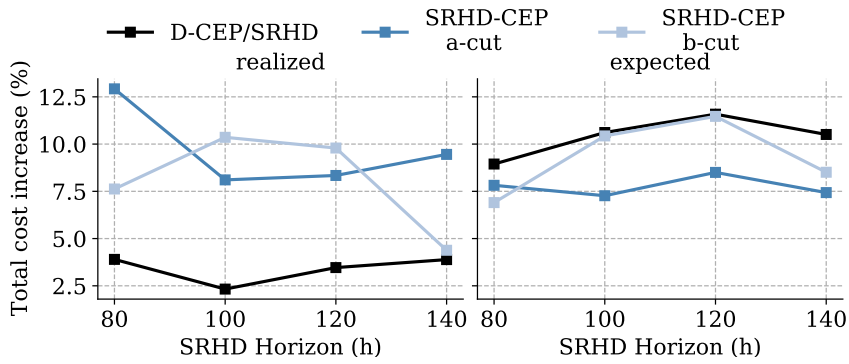

Figure 4.15: Total costs for D-CEP and the two versions of the SRHD-CEP. The D-CEP investments are evaluated with the SRHD operational model (D-CEP/SRHD). Total costs are measured by realized (real-time) and expected (day-ahead)values respectively and reported as a percentage increase from the perfect information solution (D-CEP).

The total costs of investment and operation are evaluated by realized and expected values as a function of different SRHD horizons as shown in Figure 4.15. Values are reported relative to a benchmark defined by the D-CEP with perfect information (lowest possible realized costs). The D-CEP investments are also compared to the SRHD-CEP solutions, to get realistic operational costs operation is simulated by the SRHD. The combined D-CEP/SRHD result in the lowest realized costs for the simulated year, a 2.3-3.9% increase over the same investment with deterministic operation (benchmark). However, the main purpose of a CEP is to find the optimal investments that gives the lowest total cost over several years, thus the most important performance parameter should be the expected cost. By evaluating the performance by expected costs, it is clear that optimal investments from the SRHD-CEP with cuts generated from the day-ahead values (type a cuts) gives the best result with 2.5-3% lower expected costs than the D-CEP investments. The expected total costs are 7.3-8.5% higher than the benchmark. A-cuts give the right investments as they result in investments that gives the lowest expected total costs, this is a result of avoiding the fixed day-ahead schedules that distort the investment signals in the benders algorithm.

The horizon of the two-stage model in the SRHD are originally 80 hours which is given by the weather forecasts. The effect of extending the horizon using persistence forecasts is investigated in Figure 4.15. For example, the horizon can be extended to 100 hours by adding 20 hours of persistence forecasts, this is done by adding the mean value of the last 20 hours of the original forecasts for all hours from 80 to 100. Extending the horizon to 100 hours helps to improve SRHD performance as it gives more realistic storage operation than the end-of-horizon value

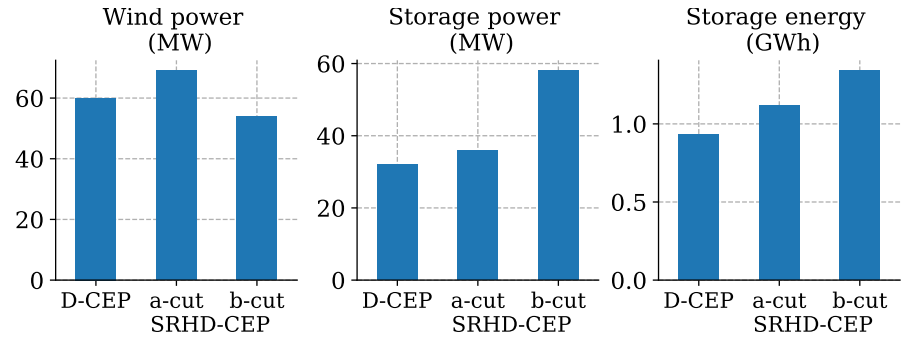

Figure 4.16: Optimal investments for D-CEP and SRHD-CEP models with the two different versions of L2 cuts and 100 hour SRHD horizon.

from the deterministic operation model. Increasing the horizon to more than 100 hours does not result in any cost reductions as the inaccuracy of the persistence forecasts becomes too large.

The SRHD-CEP with a-cuts result in more installed capacities for both wind power and energy storage compared to the D-CEP as shown in Figure 4.16. The SRHD-CEP increase the resulting capacities compared to the deterministic results by around 12.5-20% from 60 to 69 MW for wind power, 32 to 36 MW for storage power and 930 to 1120 MWh for storage energy. For b-cuts, fixed day-ahead schedules result in non optimal investments skewed away from wind power and towards more storage capacity as it can be used for internal balancing which requires no balancing premiums. B-cuts do not account for that more investments in wind power can result in different day-ahead schedules, whereas a-cuts do.

The estimated operational costs from the deterministic (grey) and the SRHD cutting planes (red-blue) are shown in Figure 4.17. The deterministic cutting planes are a tight lower bound to the SRHD costs. Thus, the costs are higher at every point where the algorithm checks the SRHD costs explicitly (black dots) i.e. the solution of each L2 iteration illustrated in Figure 3.11. The lower bound significantly reduce the number of SRHD-CEP iterations needed as it efficiently limits the range of capacities considered. For example, the deterministic cuts provide lower limits (steep operational cost increase) for the capacities of around 400 MWh storage energy and 40 MW wind power as seen in Figure 4.17. The difference between the deterministic and stochastic operational cost estimation (planes) are large at the deterministic solution (red dot) and the intermediate investments searched by the algorithm (black dots) before finding the stochastic solution (green dot). The difference between the deterministic and stochastic cost estimation is less at the optimal SRHD-CEP solution (green dot).

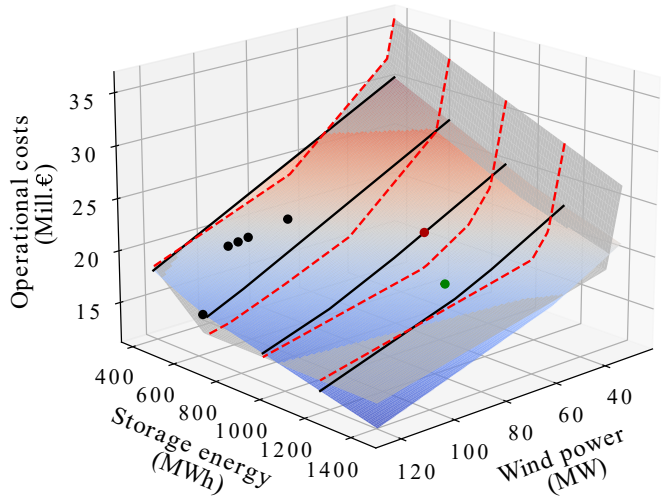

Figure 4.17: Cutting planes show the stochastic (red-blue) and deterministic (grey) operational cost as a function of the storage energy and wind power capacity. The differences between the stochastic (black/solid) and deterministic(red/dotted) planes are highlighted by lines of fixed storage energy capacity. Points indicate the capacities searched by the algorithm in Figure 3.11. The D-CEP and SRHD-CEP optimal solutions are red and green respectively, while intermediate SRHD-CEP solutions are black.

Table 4.3: Computational times and iterations of the A-cut SRHD-CEP algorithm for different SRHD horizons when simulating the two-bus system for a year.

SRHD horizon (h)	80	100	120	140
L1 time (sec/itr)	31	31	32	30
L2 time (min/itr)	42	57	75	94
L2 iterations	7	8	9	11
Total time (hours)	5.1	7.8	11.4	17.5

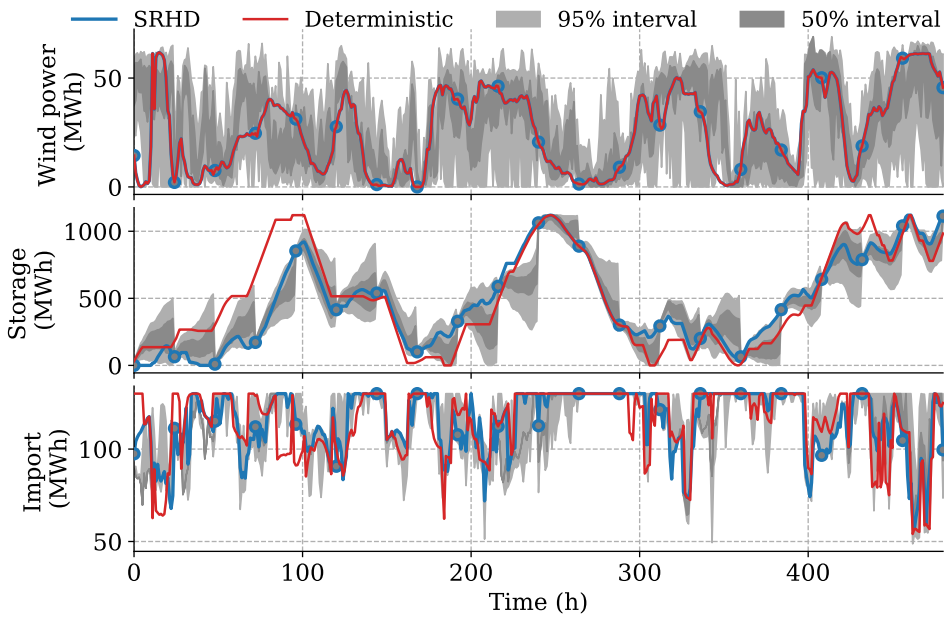

Figure 4.18: Deterministic and SRHD (first-stage) system operation for the first 20 days of the year and SRHD-CEP investments (a-cut and 100 hour horizon), represented by a) wind power, b) storage level and c) import from the market bus. The start of each two-stage model is marked with points, while 50 and 95 % confidence intervals show the day-ahead uncertainty.

The D-CEP iterations (L1) are significantly faster to solve than the SRHD-CEP iterations (L2) where the solution times goes from around 31 seconds to 42-94 minutes (dependent on the SRHD horizon) per iteration as shown in Table 4.3. While longer SRHD horizons are beneficial for simulating realistic operation, it also lead to increased computational times. Not only does the solution times of the SRHD increase with longer SRHD horizons, but it also lead to more SRHD-CEP iterations.

Figure 4.18 shows that there is significant uncertainty from wind power that propagates into the storage operation. The SRHD lead to much more conservative storage handling compared to the deterministic case that are charging and discharging the storage faster and keeps the storage level closer to the maximum storage level. The storage handling is more conservative in the SRHD as including short-term uncertainty accurately represent a significant risk of demand curtailment in periods with constrained transmission capacity. The risk of rationing result in lower charging/discharging power and storage levels which are generally further from the capacity limits. This reduces the flexibility that can be obtained for the storage

compared to deterministic operation and more capacity is needed.

4.2.3 Importance of Representing Wind Power Uncertainty for Electricity System Operation in Investment Models

The SRHD-CEP proposed in Article 5 can be useful for determining optimal and realistic H_2 investments in electricity systems with high renewable shares and energy storage. D-CEP significantly underestimates the optimal capacities required for satisfactory electricity system operation in a more realistic setting. This is also apparent from Article 4, where significant line upgrades (typically 2X original capacity) where required to avoid excessive load rationing in the SRHD when taking into account actual wind power uncertainty. More capacity than shown by deterministic models are required for both generation, transmission and energy storage to handle the short-term uncertainty arising from VRE sources. Increased operational flexibility can also play a crucial role as for hydro power flexibility in Article 4.

The types and timescales of different flexibility resources are important and have to be combined optimally dependent on the mix of available VRE sources. Batteries and transmission expansions alone are not economically viable for obtaining a renewable share of 85-100 % as shown in Article 2, where demand side flexibility from producing H_2 by PEMEL is important for deep decarbonization. H_2 production can efficiently deliver demand-side flexibility to regulate uncertain wind power production on similar scales as hydro power and natural gas turbines, but is dependent on the amount of H_2 produced as shown in Article 4 and Article 2 respectively.

Many capacity expansion models use clustering methods where the temporal dimension of the operational representation is reduced and represented by a number of typical days or periods. Representative days or periods might not be sufficient in a sector coupled system with large-scale H_2 production. As shown in Article 2, the storage duration of such systems could be relatively long with a storage filling/depletion time of up to 36 hours. The time it takes to storage fill/deplete the storage is also expected to increase under stochastic operations along with increased capacities, thus the length of representative periods have to be relatively long to include several storage cycles.

Long storage cycles are also challenging in the SRHD where it can be necessary with longer horizon than what is given by weather forecasts. In the literature, persistence forecasts have proved to be good for forecasting some hours ahead of real-time and works well for extending the SRHD horizon. Extending the SRHD horizon leads to increased computational times, alternatively the deterministic model in the SRHD-CEP loop could be substituted for a operation model with reserves

or robust operation to provide better end-of-horizon storage values.

In the SRHD-CEP, investments can be formulated as integers such that the master problem becomes a MILP. This enables modelling of units in the power system that typically has some degree of "lumpiness" such as transmission lines or larger power plant (e.g. nuclear power plants). Thus, transmission expansion can be modeled by using binary variables to turn "on" or "off" predefined transmission line expansions.

The two-stage problem from the SRHD can also be decomposed by benders decomposition in order to enable modeling of larger systems. Decomposing the two-stage problem allows the scenarios to be solved separately and solved in parallel to reduce computational time. When Benders decomposition is applied to stochastic optimization it is commonly referred to as the L-shaped method [145] which is widely used for stochastic economic dispatch and unit commitment models [183, 184, 185] . However, for further decomposition to be beneficial the size of the problem has to be large enough to justify the increased computational overhead related to parallelization. The two-stage model decomposition can be useful to further increase the operational detail. With the first- and second-stage separated the first-stage can be modeled as a MILP. This enables the SRHD to use a more detailed unit commitment problem formulation of the operational problem instead of the stochastic economic dispatch. However, the second-stage has to stay linear to obtain the dual values and generate cuts for the investment model.

Chapter 5

Conclusion

Hydrogen (H_2) has great potential to contribute to global emissions reduction through end-use applications in transportation and industry. On the production side, market-based H_2 production from renewables can also contribute with valuable demand-side flexibility in the electricity system. In this thesis, the potential impact of large-scale flexible H_2 production by electrolysis on two electricity systems with different characteristics was investigated.

5.1 Main Results

The results shows that flexible H_2 production can give important contributions in the hydro power dominated Norwegian power system by alleviating congestion and increasing security of supply. In the natural gas dominated electricity system of Texas in the US, large-scale H_2 production has the potential to contribute with significant flexibility to enable high shares of VRE, phasing out coal, reducing emissions from natural gas and enabling CCS at a lower cost than offered for electricity generation.

In both systems, H_2 production can be used as a way of transporting energy from remote locations to load centers where it can be used in H_2 specific applications. In Texas, this will result in large amounts of H_2 production in the north-west where wind conditions are good, the H_2 is transported to the load centers further to the east by pipelines. In regions with good renewable energy resources which are located far away from load centers, H_2 can be liquefied and exported over long distances on ships or trucks. This is the case for energy surplus regions such as northern Norway, the good renewable energy resource can be exploited by exporting LH_2 to regions with energy deficits such as Central Europe or Asia.

The price of electrolytic H_2 has to be low in order to compete with fossil based H_2 and make it an attractive option for reducing emissions in end-use applications. The cost of producing H_2 from electrolysis is dominated by the operational costs that are almost entirely from electricity consumption. The operational costs are set to represent an increasing share of the H_2 production cost as the capital costs of electrolyzers is projected to decrease by as much as 50 % within 2040-50. In electricity systems with few zero emission flexibility resources, H_2 can be produced at low cost in periods with surplus electricity from VRE. Dependent on the total H_2 demand in the system, flexible electrolysis operation results in operational costs of 20-60 % compared to the average electricity price accrued under traditional operation with constant production. In systems with large amounts flexibility from for example hydro power, significant VRE can be integrated resulting in low and stable electricity prices, in turn resulting in low cost H_2.

Demand-side flexibility from H_2 production is complementary to flexibility from batteries (2-7 hours) as it is better suited for longer-term balancing (5-36 hours). Thus batteries are well suited to store electricity from solar power plants, while H_2 storage is well suited for both wind and solar power plants. The combination of batteries and flexible H_2 production enables significantly higher shares of VRE compared to a system without H_2 production. In the Texas case study, the level of VRE electricity generation changed from 78 to 87 and 94 % with increasing H_2 demand and a CO_2 price of $60/tonne.

Many electricity systems around the world rely on natural gas power plants to provide the flexibility needed on the one to several days basis which result in CO_2 emissions. The results presented in this thesis show that flexible H_2 production can provide much of the same service on the demand-side, reducing the need for electricity from natural gas. The electricity produced from natural gas is reduced by 5-53 % in the Texas case study dependent on the H_2 demand, and thus reducing a lot of emissions in the electricity sector. As a result of the reduced utilization of gas turbines, gas turbines with CCS that require higher utilization due to additional capital costs become less profitable. Instead, CCS is utilized for H_2 production from SMR. H_2 that is produced from a combination of electrolysis and natural gas has a low carbon footprint, less than 1.2 kg CO_2/kg H_2, if the CO_2 price is sufficient ($\geq$ $90/tonne) to enable CCS with the SMR. As a comparison, SMR w/o CCS has a carbon footprint of 10-16 kg CO_2/kg H_2

Short-term uncertainty can have a significant impact on optimal investments in the power system, but is difficult to take into consideration in combination with energy storage. A stochastic rolling horizon dispatch (SRHD) was developed and integrated within a capacity expansion problem (CEP) using Benders cuts, resulting in a stochastic rolling horizon dispatch capacity expansion problem (SRHD-CEP).

The SRHD-CEP results in investments that consider short-term uncertainty with detailed simulation of sequential storage operation and market structures. The SRHD-CEP is tested on a two-bus case study with a wind power plant, energy storage and a electric load connected to a electricity market through a constrained transmission line. The case study show that the SRHD-CEP result in 12.5-20% more installed capacity for wind power and energy storage, lower expected total costs and more conservative storage handling than the deterministic alternative (D-CEP). The extra generation and storage capacities are especially important in transmission constrained systems in order to avoid rationing of demand. This algorithm has relatively low computational requirements compared to other methods for representing short-term uncertainty and storage together with investment decisions, which can prove valuable for regulators, researchers and other power system stakeholders when designing the low carbon energy systems of the future.

5.1.1 Concluding Remarks

This thesis investigated the benefits and costs of flexible H_2 production in future power systems with high shares of VRE production. Several CEP variants are developed in order to asses the impact of constrained transmission grids, hydro power flexibility, sector-coupling and short-term uncertainty on H_2 production and the development and operation of the power system. The main conclusions from this work can be summarized as follows.

- In systems with low-emission flexibility from hydro power such as Norway, H_2 production can provide demand-side flexibility to increase security of supply in constrained grids in remote areas. However, the cost of H_2 production is dependent on the level of hydro power flexibility wich is needed to balance variations in wind power production.

- In the absence of low-emission flexibility, demand-side flexibility from H_2 production can contribute to phase out natural gas power plants and the related CO_2 emissions. This is shown for a case study of the state of Texas in the US.

- Flexible H_2 production can supplement batteries with flexibility on a longer time-scale. This enables significantly higher maximum shares of electricity generation from VRE than without H_2 production and is obtained at lower CO_2 prices.

- For integrated H_2 and electricity systems with a significant H_2 demand, CCS is more cost-efficient for SMR than natural gas power plants.

- Increasing CO_2 prices favors electrolysis while increasing H_2 demand favors natural gas based H_2 (SMR) with CCS.
- With CO_2 prices of \$90/tonne or more, H_2 production from natural gas and electricity result in low emissions of less than 1.2 kg CO_2/kg H_2 at affordable production costs around 1.35-1.75 \$/kg H_2.
- Analyzing capacities from deterministic capacity expansion problem (CEP) under stochastic operation shows that it is important to consider short-term uncertainty in the CEP, especially in systems that have limited transmission capacity and long duration energy storage.
- A stochastic rolling horizon dispatch capacity expansion problem (SRHD-CEP) was developed that can include detailed operation (short-term uncertainty, storage and markets) when evaluating optimal investments in power systems. A two-bus case study is used to demonstrate how this is a tractable model for considering investments in flexible resources (energy storage) as alternatives to more traditional investments (transmission lines and generators) which is going to be more important as VRE becomes a larger share of total generation in the power system.

5.2 Recommendations for Future Research

In this thesis a certain H_2 demand is assumed based on H_2 export or local utilization in the transportation sector. More studies are needed to identify detailed scenarios (location, quantity and profiles) for future H_2 demand in other sectors such as industry, shipping, natural gas distribution networks and more. Some ongoing work in for example the H_2@Scale project funded by the DOE is showing promising result for this in the US [186, 174] and is a example of what is needed also in other parts of the world. Furthermore, H_2 is taking a more central role in the recent energy scenarios outlined by the European Commission for a carbon neutral Europe by 2050 [187] and the European green new deal [188].

To properly capture the synergies between flexible H_2 production and the electricity system it is crucial with a sector coupled approach such as presented in Article 2. Adding more details to this kind of model can be challenging due to the size arising from modeling several parallel systems (electricity, H2, heat, natural gas etc.). Some particularly interesting extensions on the H_2 side is to model line-packing and H_2 transport by tucks/ships in the liquid or gaseous state. Line-packing would allow gas to be stored in the gas pipelines by increasing the pressure and thus exploit the multi-purpose potential of the H_2 pipelines to give additional flexibility. Whereas line-packing gives flexibility in the temporal dimension,

H_2 transport by trucks might provide flexibility in the spacial dimension by routing trucks to different location dependent on the situation. However, representing vehicle-routing in the sector-coupled model is a challenging task.

A case study for H_2 production in Europe can be carried out with the same model that is used to model Texas in Article 2. Using this model gives a good assessment of the trade-of between electrolytic and natural gas based H_2 pathways which is not typically seen in other studies. An initial study is conducted for the north-sea countries using an early version of the model [15] which provides a good starting-point for a more detailed analysis with the updated model. Extensions can be made to endogenously model CCS under the north-sea and offshore wind, which are prioritized R&D activities for supporting emission-free energy production in the region.

The SRHD-CEP in Article 5 has potential to model large systems by also decomposing the two stage operation model using the L-shaped method and solving the second stage in parallel. Further improvements to the computational time can be gained from dividing the operational year into some few periods by fixing the storage levels at these times with values form the deterministic model and solving these segments of the year in parallel. Unit commitment constraints can be included to represent the limited ramping capability of thermal units if they are linearized[1] such that duals can be obtained for the cuts.

Flexible H_2 production can be integrated into the SRHD-CEP and used to analyze the impact of short-term uncertainty on the optimal investments in the case study of northern Norway from Article 1 and Article 4. In such a study, transmission expansion could be endogenous to the model as investments and operation are decomposed in the SRHD-CEP such that investments are represented by integers. This is different from the original study in Article 1 where transmission capacities were given as input to the model based on predetermined scenarios.

Flexibility from H_2 production and transmission can delay or offer an alternative to transmission grid upgrades as illustrated by Article 2. Including short-term uncertainty is crucial to asses how flexibility can be a realistic alternative to transmission upgrades (as shown in Article 4). The model framework from Article 5 can be combined with e.g. a security-constrained optimal power flow (SCOPF) in order to determine if long-term flexibility contracts (activated by the TSO in order to avoid congestion) with H_2 production or hydro power are cost-efficient and realistic alternatives to transmission upgrades.

[1] Unit commitment constraints only in need to be linear in the second-stage if the two-stage model is decomposed.

Article Article 4 show that flexible H_2 production and wind power uncertainty can have important implications on hydro power storage strategies. Detailed representations of flexible H_2 production and uncertain wind power production in medium- and short-term hydro power scheduling models can be important for optimal utilization of flexibility from hydro power. The impact of including such detailed representations on hydro power strategies should be investigated using state-of-the-art hydro power scheduling models such as ProdRisk and SHOP [189] for future scenarios of electricity systems with high levels of H_2 production, wind power and hydro power.

Bibliography

[1] V. Masson-Delmotte, P. Zhai, H.-O. Pörtner, D. Roberts, J. Skea, P. Shukla, A. Pirani, W. Moufouma-Okia, C. Péan, R. Pidcock, S. Connors, J. Matthews, Y. Chen, X. Zhou, M. Gomis, E. Lonnoy, T. Maycock, M. Tignor, and T. Waterfield, "Summary for Policymakers. In: Global Warming of 1.5°C. An IPCC Special Report on the impacts of global warming of 1.5°C above pre-industrial levels and related global greenhouse gas emission pathways, in the context of strengthening the global response to," IPCC, Tech. Rep. 3, 2018.

[2] International Renewable Energy Agency, *Global Renewables Outlook: Energy transformation 2050*, 2020. [Online]. Available: https://www.irena.org/publications/2020/Apr/Global-Renewables-Outlook-2020

[3] European Comission, "A Hydrogen Strategy for a climate neutral Europe," 2020.

[4] IEA - International Energy Agency, "The Future of Hydrogen - Seizing today's opportunities," Tech. Rep., 2019. [Online]. Available: https://www.iea.org/reports/the-future-of-hydrogen

[5] O. Ulleberg, T. Nakken, and A. Ete, "The wind/hydrogen demonstration system at Utsira in Norway: Evaluation of system performance using operational data and updated hydrogen energy system modeling tools," *International Journal of Hydrogen Energy*, vol. 35, no. 5, pp. 1841–1852, 2010.

[6] H. Landinger, U. Bünger, T. Raksha, W. Weindorf, J. Simón, L. Correas, and F. Crotogino, ""Assessment of the Potential, the Actors and Relevant Business Cases for Large Scale and Long Term Storage of Renewable Electricity

by Hydrogen Underground Storage in Europe": Update of Benchmarking of large scale hydrogen underground storage with competi," no. June, 2014.

[7] M. Korpås, "Distributed energy systems with wind power and energy storage," *183*, pp. 1–80, 2004.

[8] M. Victoria, K. Zhu, T. Brown, G. B. Andresen, and M. Greiner, "The role of storage technologies throughout the decarbonisation of the sector-coupled European energy system," *Energy Conversion and Management*, vol. 201, p. 111977, 12 2019.

[9] B. Lux and B. Pfluger, "A supply curve of electricity-based hydrogen in a decarbonized European energy system in 2050," *Applied Energy*, vol. 269, no. April, p. 115011, 2020.

[10] C. J. Greiner, "Doctoral Thesis: Sizing and Operation of Wind-Hydrogen Energy Systems," Ph.D. dissertation, NTNU, 2010.

[11] F. R. Førsund, B. Singh, T. Jensen, and C. Larsen, "Phasing in wind-power in Norway: Network congestion and crowding-out of hydropower," *Energy Policy*, vol. 36, pp. 3514–3520, 2008.

[12] IRENA, *Innovation landscape for a renewable-powered future: Solutions to integrate variable renewables*, 2019.

[13] Sintef Energy Reseach, "Sintef project: Hyper," 2017. [Online]. Available: http://www.sintef.no/projectweb/hyper/

[14] D. Q. A. Pinel, *Hydrogen Production from Wind and Solar Power in Weak Grids in Norway (Master thesis)*. Norwegian University of Science and Technology, 2017.

[15] M. Moldestad, *Evaluating pathways for hydrogen produced from low-carbon energy sources (Master thesis)*. Norwegian University of Science and Technology, 2020.

[16] W. Tong, "Fundamentals of wind energy," in *WIT Transactions on State of the Art in Science and Engineering*. WIT Press, 6 2010, vol. 44, pp. 3–48.

[17] National Renewable Energy Laboratory (NREL), "2019 Annual Technology Baseline: Electricity," 2019. [Online]. Available: https://atb.nrel.gov/

[18] Energy Initiative Massachusetts Institute of Technology, *The future of solar energy - An interdisciplinary MIT study*. Energy Initiative Massachusetts Institute of Technology, 2015.

[19] G. N. Tiwari, A. Tiwari, and Shyam, *Handbook of Solar Energy*, ser. Energy Systems in Electrical Engineering. Singapore: Springer Singapore, 2016, no. i.

[20] IRENA International Renewable Energy Agency, *Renewable Power Generation Costs in 2018*, 2019th ed., Abu Dhabi, 2019. [Online]. Available: https://www.irena.org/-/media/Files/IRENA/Agency/Publication/2018/Jan/IRENA_2017_Power_Costs_2018.pdf

[21] D. Edward and A. Myhrer, "Teknologianalyser 2018 Kostnadseffektiv vindkraft," no. 3, pp. 1–2, 2021.

[22] NVE, "Nasjonal Ramme For Vindkraft," The Norwegian Water Resources and Energy Directorate, Oslo, Tech. Rep. 12, 2019.

[23] IEA Wind TCP Task 26–Wind Technology, *Cost, and Performance Trends in Denmark, Germany, Ireland, Norway, Sweden, the European Union, and the United States: 2008–2016*, M. M. Hand, Ed. National Renewable Energy Laboratory, Golden, CO (US), 2018, no. NREL/TP-6A20.71844. [Online]. Available: https://www.nrel.gov/docs/fy19osti/71844.pdf.

[24] S. Stoft, *Power System Economics - Designing Markets for Electricity*. IEEE Press & WILEY-INTERSCIENCE, 2002.

[25] O. B. Fosso, A. Gjelsvik, A. Haugstad, B. Mo, and I. Wangensteen, "Generation scheduling in a deregulated system. the norwegian case," *IEEE Transactions on Power Systems*, vol. 14, no. 1, pp. 75–80, 1999.

[26] I. Wangensteen, *Power system economics - the nordic electricity market*. Fagbokforlaget, 2011.

[27] E. Ela, M. Milligan, A. Bloom, J. Cochran, A. Botterud, A. Townsend, and T. Levin, "Overview of wholesale electricity markets," in *Studies in Systems, Decision and Control*. Springer International Publishing, 2018, vol. 144, pp. 3–21. [Online]. Available: https://link.springer.com/chapter/10.1007/978-3-319-74263-2_1

[28] K. Skytte, "The regulating power market on the Nordic power exchange Nord Pool: an econometric analysis," *Energy Economics*, vol. 21, no. 4, pp. 295–308, 8 1999.

[29] M. N. Hjelmeland, "Thesis for the Degree of Philosophiae Doctor Medium-Term Hydropower Scheduling In a Multi-Market Setting," Ph.D. dissertation, 2019.

[30] A. Helseth, M. Fodstad, and B. Mo, "Optimal Medium-Term Hydropower Scheduling Considering Energy and Reserve Capacity Markets," *IEEE Transactions on Sustainable Energy*, vol. 7, no. 3, pp. 934–942, 2016.

[31] T. Gómez, I. Herrero, P. Rodilla, R. Escobar, S. Lanza, I. d. l. Fuente, M. L. Llorens, and P. Junco, "European Union Electricity Markets," no. february, pp. 20–31, 2019. [Online]. Available: https://www.emissions-euets.com/internal-electricity-market-glossary

[32] ENTSOE, "ENTSO-E MARKET REPORT 2019," European Network of Transmission System Operators for Electricity, Tech. Rep., 2019. [Online]. Available: https://eepublicdownloads.entsoe.eu/clean-documents/mc-documents/190814_ENTSO-EMarketReport2019.pdf?Web=1

[33] A. Ehrenmann, P. Henneaux, J. Bruce, L. Schumacher, G. Küpper, and B. Klasman, "The future electricity intraday market design," European Commission, Tech. Rep., 2019. [Online]. Available: https://ec.europa.eu/energy/en/studies/future-electricity-intraday-market-design

[34] H. Farahmand, T. Aigner, G. L. Doorman, M. Korpås, and D. Huertas-Hernando, "Balancing market integration in the northern European continent: A 2030 case study," *IEEE Transactions on Sustainable Energy*, vol. 3, no. 4, pp. 918–930, 2012.

[35] M. Håberg, *Doctoral thesis Optimal Activation and Congestion Management in the European Balancing Energy Market Martin Håberg Optimal Activation and Congestion Management in the European Balancing Energy Market Thesis for the Degree of Philosophiae Doctor*, 2019, vol. 9.

[36] S. Jaehnert and C. Naversen, *Fundamental Multi-Product Price Forecasting in Power Markets*, 2018.

[37] M. Milligan, B. Frew, K. Clark, and A. Bloom, "Marginal Cost Pricing in a World without Perfect Competition: Implications for Electricity Markets with High Shares of Low Marginal Cost Resources," NREL, Tech. Rep. December, 2017.

[38] S. Ø. Ottesen, "Techno-economic models in Smart Grids. Demand side flexibility optimization for bidding and scheduling problems," Ph.D. dissertation, Norwegian University of Science and Technology (NTNU), 2017.

[39] National Renewable Energy Laboratory, "H2A: Hydrogen Analysis Production Case Studies | Hydrogen and Fuel Cells | NREL," 2019. [Online]. Available: https://www.nrel.gov/hydrogen/h2a-production-case-studies.html

[40] D. Sadler, H. S. Anderson, M. Sperrink, A. Cargill, M. Sjøvoll, K. I. Åsen, J. E. Finnesand, T. Melien, R. Thorsen, L. Hagesæther, P. Ringrose, B. Nazarian, and H. H. Kvadsheim, "H21 North of England," Cadent, Equinor and Northern Gas Networks, Tech. Rep., 2018. [Online]. Available: https://www.equinor.com/content/dam/statoil/documents/climate-and-sustainability/Equinor-H21-North-of-England-Report-v1.pdf

[41] B. Parkinson, P. Balcombe, J. F. Speirs, A. D. Hawkes, and K. Hellgardt, "Levelized cost of CO 2 mitigation from hydrogen production routes," *Energy and Environmental Science*, vol. 12, no. 1, pp. 19–40, 1 2019.

[42] Y. Khojasteh Salkuyeh, B. A. Saville, and H. L. MacLean, "Techno-economic analysis and life cycle assessment of hydrogen production from natural gas using current and emerging technologies," *International Journal of Hydrogen Energy*, 2017.

[43] IEA, "Techno - Economic Evaluation of SMR Based Standalone (Merchant) Hydrogen Plant with CCS," IEA, Paris, France, Tech. Rep. February, 2017. [Online]. Available: http://ieaghg.org/exco_docs/2017-02.pdf

[44] T. Grant, D. Morgan, and K. Gerdes, "Quality Guidelines for Energy System Studies: Carbon Dioxide Transport and Storage Costs in NETL Studies," National Energy Technology Laboratory, Tech. Rep. August, 2019.

[45] Gassnova SF, "Potential for reduced costs for carbon capture , transport and storage value chains (CCS)," 2020. [Online]. Available: https://ccsnorway.com/wp-content/uploads/sites/6/2020/10/Potential-for-reduced-cost-for-carbon-capture-2019.pdf

[46] O. Schmidt, A. Gambhir, I. Staffell, A. Hawkes, J. Nelson, and S. Few, "Future cost and performance of water electrolysis: An expert elicitation study," *International Journal of Hydrogen Energy*, vol. 42, no. 52, pp. 30 470–30 492, 2017.

[47] FCH JU, "Eu Energy Commissioner Visit To Refhyne, the World'S Largest Pem Hydrogen Electrolysis Plant Under Construction," 2020. [Online]. Available: https://refhyne.eu/wp-content/uploads/2020/07/REFHYNE-Press-Release-3_EU-Energy-Commissioner-Visits-Site.pdf

[48] A. Ursua, L. Gandia, and P. Sanchis, "Hydrogen Production From Water Electrolysis: Current Status and Future Trends," *Proceedings of the IEEE*, vol. 100, no. 2, pp. 410 –426, 2012.

[49] G. Glenk and S. Reichelstein, "Economics of converting renewable power to hydrogen," *Nature Energy*, vol. 4, no. 3, pp. 216–222, 3 2019.

[50] A. Buttler and H. Spliethoff, "Current status of water electrolysis for energy storage, grid balancing and sector coupling via power-to-gas and power-to-liquids: A review," *Renewable and Sustainable Energy Reviews*, vol. 82, no. February 2017, pp. 2440–2454, 2018.

[51] J. Proost, "State-of-the art CAPEX data for water electrolysers, and their impact on renewable hydrogen price settings," *International Journal of Hydrogen Energy*, vol. 44, no. 9, pp. 4406–4413, 2 2019.

[52] National Renewable Energy Laboratory (NREL), "H2A: Hydrogen Analysis Production Case Studies | Hydrogen and Fuel Cells | NREL." [Online]. Available: https://www.nrel.gov/hydrogen/h2a-production-case-studies.html

[53] D. Peterson, J. Vickers, and D. DeSantis, "Hydrogen Production Cost From PEM Electrolysis - 2019," Department of Energy, Tech. Rep., 2020. [Online]. Available: https://www.hydrogen.energy.gov/pdfs/19009_h2_production_cost_pem_electrolysis_2019.pdf

[54] T. Nguyen, Z. Abdin, T. Holm, and W. Mérida, "Grid-connected hydrogen production via large-scale water electrolysis," *Energy Conversion and Management*, vol. 200, no. October, p. 112108, 2019.

[55] J. Eichman, M. Koleva, O. J. Guerra, B. Mclaughlin, J. Eichman, M. Koleva, and O. J. Guerra, "Optimizing an Integrated Renewable- Electrolysis System," NREL, Tech. Rep. March, 2020.

[56] D. Thomas, D. Mertens, M. Meeus, W. Van der Laak, and I. Francois, "Power-to-gas. Roadmap for Flanders. Final Report," Tech. Rep. October, 2016. [Online]. Available: https://www.waterstofnet.eu/_asset/_public/powertogas/P2G-Roadmap-for-Flanders.pdf

[57] K. Kanellopoulos and H. Blanco, "The potential role of H2 production in a sustainable future power system - An analysis with METIS of a decarbonised system powered by renewables in 2050," European Commission, Tech. Rep., 2019.

[58] F. Alshehri, V. G. Suárez, J. L. Rueda Torres, A. Perilla, and M. A. van der Meijden, "Modelling and evaluation of PEM hydrogen technologies for frequency ancillary services in future multi-energy sustainable power systems," *Heliyon*, vol. 5, no. 4, p. e01396, 4 2019.

[59] J. Eichman, A. Townsend, and M. Melaina, "Economic Assessment of Hydrogen Technologies Participating in California Electricity Markets," *National Renewable Energy Laboratory*, no. February, p. 31, 2016. [Online]. Available: www.nrel.gov/publications.%0Ahttps://www.nrel.gov/docs/fy16osti/65856.pdf

[60] H. Barthelemy, M. Weber, and F. Barbier, "Hydrogen storage: Recent improvements and industrial perspectives," *International Journal of Hydrogen Energy*, vol. 42, no. 11, pp. 7254–7262, 3 2017.

[61] A. Ozarslan, "Large-scale hydrogen energy storage in salt caverns," *International Journal of Hydrogen Energy*, vol. 37, no. 19, pp. 14 265–14 277, 2012.

[62] C. van Leeuwen and A. Zauner, "Report on the costs involved with PtG technologies and their potentials across the EU," University of Groningen, Tech. Rep. Innovative large-scale energy storage technologies and Power-to-Gas concepts after optimisation, 2018. [Online]. Available: https://www.storeandgo.info/publications/deliverables/

[63] D. G. Caglayan, N. Weber, H. U. Heinrichs, J. Linßen, M. Robinius, P. A. Kukla, and D. Stolten, "Technical potential of salt caverns for hydrogen storage in Europe," *International Journal of Hydrogen Energy*, vol. 45, no. 11, pp. 6793–6805, 2020.

[64] C. Hemme and W. van Berk, "Potential risk of H2S generation and release in salt cavern gas storage," *Journal of Natural Gas Science and Engineering*, vol. 47, pp. 114–123, 2017.

[65] K. E. Lamb, M. D. Dolan, and D. F. Kennedy, "Ammonia for hydrogen storage; A review of catalytic ammonia decomposition and hydrogen separation and purification," *International Journal of Hydrogen Energy*, vol. 44, no. 7, pp. 3580–3593, 2019.

[66] S. Carr, G. C. Premier, A. J. Guwy, R. M. Dinsdale, and J. Maddy, "Hydrogen storage and demand to increase wind power onto electricity distribution networks," *International Journal of Hydrogen Energy*, vol. 39, no. 19, pp. 10 195–10 207, 2014.

[67] C. Darras, G. Bastien, M. Muselli, P. Poggi, B. Champel, and P. Serre-Combe, "Techno-economic analysis of PV/H2 systems," *International Journal of Hydrogen Energy*, vol. 40, no. 30, pp. 9049–9060, 2015.

[68] R. Gammon, A. Roy, J. Barton, and M. Little, "HYDROGEN AND RENEWABLES INTEGRATION (HARI)," 2006.

[69] S. Karellas and N. Tzouganatos, "Comparison of the performance of compressed-air and hydrogen energy storage systems: Karpathos island case study," *Renewable and Sustainable Energy Reviews*, vol. 29, pp. 865–882, 2014.

[70] S. P. Katikaneni, F. Al-Muhaish, A. Harale, and T. V. Pham, "On-site hydrogen production from transportation fuels: An overview and techno-economic assessment," *International Journal of Hydrogen Energy*, vol. 39, no. 9, pp. 4331–4350, 2014.

[71] J. Linnemann and R. Steinberger-Wilckens, "Realistic costs of wind-hydrogen vehicle fuel production," *International Journal of Hydrogen Energy*, vol. 32, no. 10-11, pp. 1492–1499, 2007.

[72] M. Ozaki, S. Tomura, R. Ohmura, and Y. H. Mori, "Comparative study of large-scale hydrogen storage technologies: Is hydrate-based storage at advantage over existing technologies?" *International Journal of Hydrogen Energy*, vol. 39, no. 7, pp. 3327–3341, 2014.

[73] A. Pääkkönen, H. Tolvanen, and J. Rintala, "Techno-economic analysis of a power to biogas system operated based on fluctuating electricity price," *Renewable Energy*, vol. 117, pp. 166–174, 2018.

[74] S. Prince-Richard, M. Whale, and N. Djilali, "A techno-economic analysis of decentralized electrolytic hydrogen production for fuel cell vehicles," *International Journal of Hydrogen Energy*, vol. 30, no. 11, pp. 1159–1179, 2005.

[75] J. X. Weinert, "A Near-Term Economic Analysis of Hydrogen Fueling Stations. Institute of Transportation Studies, University of California, Davis." *Research Report UCD-ITS-RR-05-04*, no. 530, 2005.

[76] X. Xu, B. Xu, J. Dong, and X. Liu, "Near-term analysis of a roll-out strategy to introduce fuel cell vehicles and hydrogen stations in Shenzhen China," *Applied Energy*, vol. 196, pp. 229–237, 2017.

[77] E. Zoulias, R. Glockner, N. Lymberopoulos, T. Tsoutsos, I. Vosseler, O. Gavalda, H. Mydske, and P. Taylor, "Integration of hydrogen energy technologies in stand-alone power systems analysis of the current potential for applications," *Renewable and Sustainable Energy Reviews*, vol. 10, no. 5, pp. 432–462, 10 2006.

[78] R. K. Ahluwalia, P. Contact, J.-k. Peng, D. O. E. Manager, and K. Randolph, "System Analysis of Physical and Materials-Based Hydrogen Storage," DOE Hydrogen and Fuel Cells Program, Tech. Rep., 2018. [Online]. Available: https://www.hydrogen.energy.gov/pdfs/progress19/h2f_st001_ahluwalia_2019.pdf

[79] R. K. Ahluwalia, T. Q. Hua, J.-K. Peng, and H. S. Roh, "System Level Analysis of Hydrogen Storage Options. Project ID: ST001," 2019. [Online]. Available: https://www.hydrogen.energy.gov/pdfs/review19/st001_ahluwalia_2019_o.pdf

[80] H. Holttinen, *The impact of large scale wind power production on the Nordic electricity system*, 2004, no. 554.

[81] P. Du, R. Baldick, and A. Tuohy, *Integration of Large-Scale Renewable Energy into Bulk Power Systems - From Planning to Operation*, ser. Power Electronics and Power Systems, P. Du, R. Baldick, and A. Tuohy, Eds. Cham: Springer International Publishing, 2017.

[82] F. Van Hulle, J. O. Tande, K. Uhlen, L. Warland, M. Korpås, P. Meibom, P. Sørensen, P. E. Morthorst, N. Cutululis, G. Giebel, H. Larsen, A. Woyte, G. Dooms, P.-A. Mali, A. Delwart, F. Verheij, C. Kleinschmidt, N. Moldovan, H. Holttinen, B. Lemström, S. Uski-Joutsenvuo, P. Gardner, G. van der Toom, J. McLean, S. Cox, K. Purchala, S. Wagemans, A. Tiedemann, P. Kreutzkamp, C. Srikandam, and J. Völker, "Integrating Wind - Developing Europe's power market for the large-scale integration of wind power," *Wind Energy*, vol. 5, p. 102, 2009. [Online]. Available: http://doi.wiley.com/10.1002/we.57

[83] J. Goop, M. Odenberger, and F. Johnsson, "The effect of high levels of solar generation on congestion in the European electricity transmission grid," 2017.

[84] W. Lasher, "The competitive renewable energy zones process," *Ercot*, 2014.

[85] N. Lee, F. Flores-Espino, and D. Hurlbut, "Renewable energy zones (REZ) transmission planning process: A Guidebook for practitioners," 2017. [Online]. Available: https://www.nrel.gov/docs/fy17osti/69043.pdf

[86] J. Andrade and R. Baldick, "Estimation of Transmission Costs for New Generation," University of Texas at Austin, Tech. Rep., 2017.

[87] Entso-e, "Project 349 - MAREX Organic Power Interconnector." [Online]. Available: https://tyndp.entsoe.eu/tyndp2018/projects/projects/349

[88] California ISO, "Fast facts - What the duck curve tells us about managing a green grid," p. 4, 2016.

[89] P. Denholm, M. O'Connell, G. Brinkman, and J. Jorgenson, "Overgeneration from Solar Energy in California: A Field Guide to the Duck Chart," NREL, Tech. Rep. November, 2015. [Online]. Available: http://www.nrel.gov/docs/fy16osti/65453.pdf

[90] PG&E, "PG&E Poised to Expand Battery Energy Storage Capacity by More Than 420 Megawatts," 2020. [Online]. Available: https://www.pge.com/en/about/newsroom/newsdetails/index.page?title=20200519_pge_poised_to_expand_battery_energy_storage_capacity_by_more_than_420_megawatts

[91] M. Jafari, M. Korpås, and A. Botterud, "Power system decarbonization: Impacts of energy storage duration and interannual renewables variability," *Renewable Energy*, vol. 156, pp. 1171–1185, 2020. [Online]. Available: https://doi.org/10.1016/j.renene.2020.04.144

[92] H. Lund and B. Mathiesen, "Energy system analysis of 100% renewable energy systems—The case of Denmark in years 2030 and 2050," *Energy*, vol. 34, no. 5, pp. 524–531, 5 2009.

[93] P. Hou, P. Enevoldsen, J. Eichman, W. Hu, M. Z. Jacobson, and Z. Chen, "Optimizing investments in coupled offshore wind - electrolytic hydrogen storage systems in Denmark," *Journal of Power Sources*, vol. 359, pp. 186–197, 2017. [Online]. Available: http://dx.doi.org/10.1016/j.jpowsour.2017.05.048

[94] S. Kær, Søren Knudsen; Al Shakhshir, "Power2Hydrogen WP1 Potential of hydrogen in energy systems," pp. 1–66, 2016. [Online]. Available: http://hybalance.eu/wp-content/uploads/2017/01/Power2Hydrogen-WP1-report-Potential-of-hydrogen-in-energy-systems.pdf

[95] Dansk Fjernvarme, "Heat Generation in Denmark," pp. 191–194, 2016. [Online]. Available: https://www.danskfjernvarme.dk/-/media/danskfjernvarme/viden/publikationer/faktaark/faktaark_heat_generation_in_denmark.pdf

[96] J. G. Carton and A. G. Olabi, "Wind/hydrogen hybrid systems: Opportunity for Ireland's wind resource to provide consistent sustainable energy supply," *Energy*, vol. 35, no. 12, pp. 4536–4544, 2010.

[97] P. D. Lund, J. Lindgren, J. Mikkola, and J. Salpakari, "Review of energy system flexibility measures to enable high levels of variable renewable electricity," *Renewable and Sustainable Energy Reviews*, vol. 45, pp. 785–807, 5 2015.

[98] O. Ehret and K. Bonhoff, "Hydrogen as a fuel and energy storage: Success factors for the German Energiewende," *International Journal of Hydrogen Energy*, vol. 40, pp. 5526–5533, 2015. [Online]. Available: http://ac.els-cdn.com/S036031991500275X/1-s2.0-S036031991500275X-main.pdf?_tid=390a112c-9d0d-11e7-ac14-00000aacb35d&acdnat=1505806757_b877b7e651bcf3ade87f4276d589e1c4

[99] Z. Chehade, C. Mansilla, P. Lucchese, S. Hilliard, and J. Proost, "Review and analysis of demonstration projects on power-to-X pathways in the world," *International Journal of Hydrogen Energy*, vol. 44, no. 51, pp. 27 637–27 655, 2019. [Online]. Available: https://doi.org/10.1016/j.ijhydene.2019.08.260

[100] L. Welder, P. Stenzel, N. Ebersbach, P. Markewitz, M. Robinius, B. Emonts, and D. Stolten, "Design and evaluation of hydrogen electricity reconversion pathways in national energy systems using spatially and temporally resolved energy system optimization," *International Journal of Hydrogen Energy*, vol. 44, no. 19, pp. 9594–9607, 4 2019.

[101] L. Welder, D. Ryberg, L. Kotzur, T. Grube, M. Robinius, and D. Stolten, "Spatio-temporal optimization of a future energy system for power-to-hydrogen applications in Germany," *Energy*, vol. 158, pp. 1130–1149, 9 2018.

[102] A. Lahnaoui, C. Wulf, H. Heinrichs, and D. Dalmazzone, "Optimizing hydrogen transportation system for mobility by minimizing the cost of transportation via compressed gas truck in North Rhine-Westphalia," *Applied Energy*, vol. 223, no. March, pp. 317–328, 2018.

[103] M. Moreno-Benito, P. Agnolucci, and L. G. Papageorgiou, "Towards a sustainable hydrogen economy: Optimisation-based framework for hydrogen infrastructure development," *Computers and Chemical Engineering*, 2017.

[104] S. Samsatli, I. Staffell, and N. J. Samsatli, "Optimal design and operation of integrated wind-hydrogen-electricity networks for decarbonising the domestic transport sector in Great Britain," *International Journal of Hydrogen Energy*, vol. 41, no. 1, pp. 447–475, 2016.

[105] J. André, S. Auray, D. De Wolf, M. M. Memmah, and A. Simonnet, "Time development of new hydrogen transmission pipeline networks for France," *International Journal of Hydrogen Energy*, vol. 39, no. 20, pp. 10 323–10 337, 2014.

[106] C. Yang and J. Ogden, "Determining the lowest-cost hydrogen delivery mode," *International Journal of Hydrogen Energy*, vol. 32, no. 2, pp. 268–286, 2 2007.

[107] L. Decker, "Latest Global Trend in Liquid Hydrogen Production," 2019. [Online]. Available: https://www.sintef.no/globalassets/project/hyper/presentations-day-1/day1_1430_decker_latest-global-trend-in-liquid-hydrogen-production_linde.pdf

[108] M. Melaina, O. Antonia, and M. Penev, "Blending Hydrogen into Natural Gas Pipeline Networks: A Review of Key Issues," NationalRenewable Energy Laboratory, Denver, Tech. Rep. March, 2013.

[109] S. Schiebahn, T. Grube, M. Robinius, V. Tietze, B. Kumar, and D. Stolten, "Power to gas: Technological overview, systems analysis and economic assessment for a case study in Germany," pp. 4285–4294, 2015.

[110] S. Schemme, J. L. Breuer, M. Köller, S. Meschede, F. Walman, R. C. Samsun, R. Peters, and D. Stolten, "H2-based synthetic fuels: A techno-economic comparison of alcohol, ether and hydrocarbon production," *International Journal of Hydrogen Energy*, vol. 45, no. 8, pp. 5395–5414, 2020.

[111] P. Colbertaldo, S. B. Agustin, S. Campanari, and J. Brouwer, "Impact of hydrogen energy storage on California electric power system: Towards 100% renewable electricity," *International Journal of Hydrogen Energy*, vol. 44, no. 19, pp. 9558–9576, 4 2019.

[112] T. Brown, D. Schlachtberger, A. Kies, S. Schramm, and M. Greiner, "Synergies of sector coupling and transmission reinforcement in a cost-optimised, highly renewable European energy system," *Energy*, vol. 160, pp. 720–739, 2018. [Online]. Available: https://doi.org/10.1016/j.energy.2018.06.222

[113] IRENA, *Renewable Power Generation Costs in 2017*, Abu Dhabi, 2018.

[114] M. Robinius, J. Linßen, T. Grube, M. Reuß, P. Stenzel, K. Syranidis, P. Kuckertz, and D. Stolten, "Comparative Analysis of Infrastructures: Hydrogen Fueling and Electric Charging of Vehicles," Forschungszentrums Jülich, Tech. Rep. January, 2018.

[115] B. Emonts, M. Reuß, P. Stenzel, L. Welder, F. Knicker, T. Grube, K. Görner, M. Robinius, and D. Stolten, "Flexible sector coupling with hydrogen: A climate-friendly fuel supply for road transport," *International Journal of Hydrogen Energy*, vol. 44, no. 26, pp. 12 918–12 930, 2019.

[116] S. Cloete and L. Hirth, "Flexible power and hydrogen production: Finding synergy between CCS and variable renewables," *Energy*, vol. 192, p. 116671, 2 2020.

[117] D. Berstad, R. Anantharaman, O. Wilhelmsen, V. Skjervold, and P. Neksa, "Large-Scale Hydrogen Production and Liquefaction for Regional and Global Export," pp. 14–15, 2018. [Online]. Available: https://brage.bibsys.no/xmlui/bitstream/handle/11250/2499714/Berstad+H2FC.pdf?sequence=2

[118] D. O. Berstad, J. H. Stang, and P. Nekså, "Comparison criteria for large-scale hydrogen liquefaction processes," *International Journal of Hydrogen Energy*, vol. 34, no. 3, pp. 1560–1568, 2009.

[119] D. Berstad, G. Skaugen, and I. Wilhelmsen, "Dissecting the exergy balance of a hydrogen liquefier: Analysis of a scaled-up claude hydrogen liquefier with mixed refrigerant pre-cooling," *International Journal of Hydrogen Energy*, no. xxxx, 2020.

[120] Ø. Wilhelmsen, D. Berstad, A. Aasen, P. Nekså, and G. Skaugen, "Reducing the exergy destruction in the cryogenic heat exchangers of hydrogen liquefaction processes," *International Journal of Hydrogen Energy*, vol. 43, no. 10, pp. 5033–5047, 3 2018.

[121] R. Hånde and Ø. Wilhelmsen, "Minimum entropy generation in a heat exchanger in the cryogenic part of the hydrogen liquefaction process: On the validity of equipartition and disappearance of the highway," *International Journal of Hydrogen Energy*, vol. 44, no. 29, pp. 15 045–15 055, 2019.

[122] G. Skaugen, D. Berstad, and Ø. Wilhelmsen, "Comparing exergy losses and evaluating the potential of catalyst-filled plate-fin and spiral-wound heat exchangers in a large-scale Claude hydrogen liquefaction process," *International Journal of Hydrogen Energy*, vol. 45, no. 11, pp. 6663–6679, 2020. [Online]. Available: https://doi.org/10.1016/j.ijhydene.2019.12.076

[123] Y. Ishimoto, M. Voldsund, P. Nekså, S. Roussanaly, D. Berstad, and S. O. Gardarsdottir, "Large-scale production and transport of hydrogen from Norway to Europe and Japan: Value chain analysis and comparison of liquid

hydrogen and ammonia as energy carriers," *International Journal of Hydrogen Energy*, vol. 45, no. 58, pp. 32 865–32 883, 2020.

[124] R. S. Go, F. D. Munoz, and J. P. Watson, "Assessing the economic value of co-optimized grid-scale energy storage investments in supporting high renewable portfolio standards," *Applied Energy*, vol. 183, pp. 902–913, 12 2016.

[125] D. S. Mallapragada, N. A. Sepulveda, and J. D. Jenkins, "Long-run system value of battery energy storage in future grids with increasing wind and solar generation," *Applied Energy*, vol. 275, no. February, p. 115390, 2020. [Online]. Available: https://doi.org/10.1016/j.apenergy.2020.115390

[126] S. Nakamura, "A review of electric production simulation and capacity expansion planning programs," *International Journal of Energy Research*, vol. 8, no. 3, pp. 231–240, 1984.

[127] N. Blair, E. Zhou, D. Getman, D. J. Arent, N. Blair, E. Zhou, D. Getman, and D. J. Arent, "Electricity Capacity Expansion Modeling , Analysis , and Visualization : A Summary of Selected High-Renewable Modeling Experiences," no. October, 2015.

[128] N. E. Koltsaklis and A. S. Dagoumas, "State-of-the-art generation expansion planning: A review," *Applied Energy*, vol. 230, pp. 563–589, 11 2018.

[129] H. Faanes, G. Doorman, M. Korp, and M. Hjelmeland, "TET4135 - Energy Systems Planning and Operation," no. January, 2016.

[130] S. Simoes, W. Nijs, P. Ruiz, A. Sgobbi, D. Radu, P. Bolat, C. Thiel, and S. Peteves, *The JRC-EU-TIMES model. Assessing the long-term role of the SET Plan Energy technologies*, 2013, no. EUR 26292 EN.

[131] H. Blanco, W. Nijs, J. Ruf, and A. Faaij, "Potential for hydrogen and Power-to-Liquid in a low-carbon EU energy system using cost optimization," *Applied Energy*, vol. 232, pp. 617–639, 12 2018.

[132] K. Sakellaris, J. Canton, E. Zafeiratou, and L. Fournié, "METIS – An energy modelling tool to support transparent policy making," *Energy Strategy Reviews*, vol. 22, no. April, pp. 127–135, 2018.

[133] C. Skar, G. L. Doorman, G. A. Pérez-Valdés, and A. Tomasgard, *A multi-horizon stochastic programming model for the European power system*, 2016. [Online]. Available: http://www.ntnu.no/documents/7414984/202064323/1_Skar_ferdig.pdf/855f0c3c-81db-440d-9f76-cfd91af0d6f0

[134] H. Marañón-Ledesma and A. Tomasgard, "Analyzing demand response in a dynamic capacity expansion model for the European power market," *Energies*, vol. 12, no. 15, 2019.

[135] S. Backe, M. Korpås, and A. Tomasgard, "Heat and electric vehicle flexibility in the European power system: A case study of Norwegian energy communities," *International Journal of Electrical Power and Energy Systems*, vol. 125, no. September 2020, p. 106479, 2020. [Online]. Available: https://doi.org/10.1016/j.ijepes.2020.106479

[136] B. H. Bakken, H. I. Skjelbred, and O. Wolfgang, "eTransport: Investment planning in energy supply systems with multiple energy carriers," *Energy*, vol. 32, no. 9, pp. 1676–1689, 2007.

[137] J. Jenkins and N. Sepulveda, "Enhanced Decision Support for a Changing Electricity Landscape: the GenX Configurable Electricity Resource Capacity Expansion Model," *MIT Energy Initiative Working Paper*, pp. 1–40, 2017. [Online]. Available: https://energy.mit.edu/wp-content/uploads/2017/10/Enhanced-Decision-Support-for-a-Changing-Electricity-Landscape.pdf

[138] M. Brown, W. Cole, K. Eurek, J. Becker, D. Bielen, I. Chernyakhovskiy, S. Cohen, W. Frazier, P. Gagnon, N. Gates, D. Greer, S. S. Gudladona, J. Ho, P. Jadun, K. Lamb, T. Mai, M. Movers, C. Murphy, A. Rose, A. Schleifer, D. Steinberg, Y. Sun, N. Vincent, E. Zhou, and M. Zwerling, "Regional Energy Deployment System (ReEDS) Model Documentation: Version 2019," *National Renewable Energy Laboratory (NREL)*, no. November, 2019. [Online]. Available: https://www.nrel.gov/docs/fy20osti/74111.pdf

[139] M. E. Henriksen, A. M. Østenby, and S. Skau, "Hva er egentlig potensialet for opprusting og utvidelse av norske vannkraftverk ?" pp. 1–3, 2020. [Online]. Available: https://publikasjoner.nve.no/faktaark/2020/faktaark2020_06.pdf%0Ahttps://www.nve.no/energiforsyning/kraftproduksjon/vannkraft/reinvesteringsbehov-opprusting-og-utvidelse/?ref=mainmenu

[140] B. S. Palmintier and M. D. Webster, "Heterogeneous unit clustering for efficient operational flexibility modeling," *IEEE Transactions on Power Systems*, vol. 29, no. 3, pp. 1089–1098, 2014.

[141] B. S. Palmintier, "Incorporating Operational Flexibility Into Electric Generation Planning - Impacts and Methods for System Design and Policy Analysis," Ph.D. dissertation, Massachusetts Institute of Technology, 2013. [Online]. Available: https://dspace.mit.edu/handle/1721.1/79147

[142] J. F. Benders, "Partitioning Procedures for Solving Mixed-Variable Programming Problems," *Numerische Mathematik*, vol. 4, no. 1, pp. 238–252, 1962.

[143] M. F. Pereira, L. V. G. Pinto, S. F. Cunha, and G. Oliveira, "A Decomposition Approach To Automated Generation/Transmission Expansion Planning," *IEEE Transactions on Power Apparatus and Systems*, vol. PAS-104, no. 11, pp. 3074–3083, 11 1985.

[144] A. M. Geoffrion, "Generalized Benders decomposition," *Journal of Optimization Theory and Applications*, vol. 10, no. 4, pp. 237–260, 10 1972.

[145] R. Rahmaniani, T. G. Crainic, M. Gendreau, and W. Rei, "The Benders decomposition algorithm: A literature review," pp. 801–817, 6 2017.

[146] M. V. F. Pereira and L. M. V. G. Pinto, "Multi-stage stochastic optimization applied to energy planning," *Mathematical Programming*, vol. 52, no. 1-3, pp. 359–375, 1991. [Online]. Available: http://link.springer.com/article/10.1007/BF01582895

[147] A. Ruszczyński, "Decomposition Methods," pp. 141–211, 2003.

[148] A. Gjelsvik, B. Mo, and A. Haugstad, "Long- and medium-term operations planning and stochastic modelling in hydro-dominated power systems based on stochastic dual dynamic programming," in *Hanbook of power systems I, Energy systems*, 2010, no. 1, pp. 33–55.

[149] R. Bellman, "Dynamic programming," *Science*, vol. 153, no. 3731, pp. 34–37, 7 1966. [Online]. Available: https://science.sciencemag.org/content/153/3731/34https://science.sciencemag.org/content/153/3731/34.abstract

[150] S. Stage and Y. Larsson, "Incremental Cost of Water Power," *Transactions of the American Institute of Electrical Engineers. Part III: Power Apparatus and Systems*, vol. 80, no. 3, pp. 361–364, 1961.

[151] P. L. Carpentier, M. Gendreau, and F. Bastin, "Long-term management of a hydroelectric multireservoir system under uncertainty using the progressive hedging algorithm," *Water Resources Research*, vol. 49, no. 5, pp. 2812–2827, 2013.

[152] A. Helseth, "Stochastic network constrained hydro-thermal scheduling using a linearized progressive hedging algorithm," *Energy Systems*, vol. 7, no. 4, pp. 585–600, 11 2015. [Online]. Available: http://link.springer.com/10.1007/s12667-015-0184-2

[153] J. L. Higle, B. Rayco, and S. Sen, "Stochastic scenario decomposition for multistage stochastic programs," *IMA Journal of Management Mathematics*, vol. 21, no. 1, pp. 39–66, 2010.

[154] F. D. Munoz and J.-P. Watson, "A scalable solution framework for stochastic transmission and generation planning problems," *Computational Management Science*, vol. 12, no. 4, pp. 491–518, 10 2015.

[155] F. Munoz, B. Hobbs, and J.-P. Watson, "New bounding and decomposition approaches for MILP investment problems: Multi-area transmission and generation planning under policy constraints," *European Journal of Operational Research*, vol. 248, no. 3, pp. 888–898, 2 2016.

[156] C. Skar, *Doctoral thesis Modeling low emission scenarios for the European power sector Christian Skar Modeling low emission scenarios for the European power sector Thesis for the Degree of Philosophiae Doctor*, 2016, vol. 0.

[157] P. Meibom, R. Barth, B. Hasche, H. Brand, C. Weber, and M. O'Malley, "Stochastic optimization model to study the operational impacts of high wind penetrations in Ireland," *IEEE Transactions on Power Systems*, vol. 26, no. 3, pp. 1367–1379, 2011.

[158] Y. Wang, Z. Zhou, A. Botterud, K. Zhang, and Q. Ding, "Stochastic coordinated operation of wind and battery energy storage system considering battery degradation," *Journal of Modern Power Systems and Clean Energy*, vol. 4, no. 4, pp. 581–592, 2016.

[159] M. Korpås and A. T. Holen, "Operation planning of hydrogen storage connected to wind power operating in a power market," *IEEE Transactions on Energy Conversion*, vol. 21, no. 3, pp. 742–749, 2006.

[160] S. Sethi and G. Sorger, "A Theory of Rolling Horizon Decision Making," *Annals of Operations Research*, vol. 29, pp. 387–416, 1991.

[161] G. Warland and B. Mo, "Stochastic Optimization Model for Detailed Long-term Hydro Thermal Scheduling Using Scenario-tree Simulation," in *Energy Procedia*, vol. 87, 2016, pp. 165–172.

[162] J. B. Bremnes, "A comparison of a few statistical models for making quantile wind power forecasts," *Wind Energy*, vol. 9, no. 1-2, pp. 3–11, 1 2006.

[163] P. Pinson, H. Madsen, and G. Papaefthymiou, "From Probabilistic Forecasts to Statistical Scenarios of Short-term Wind Power Production," *WIND ENERGY Wind Energ*, vol. 12, pp. 51–62, 2009.

[164] D. S. Mallapragada, D. J. Papageorgiou, A. Venkatesh, C. L. Lara, and I. E. Grossmann, "Impact of model resolution on scenario outcomes for electricity sector system expansion," *Energy*, vol. 163, pp. 1231–1244, 11 2018.

[165] I. J. Scott, P. M. Carvalho, A. Botterud, and C. A. Silva, "Clustering representative days for power systems generation expansion planning: Capturing the effects of variable renewables and energy storage," *Applied Energy*, vol. 253, no. August, p. 113603, 2019. [Online]. Available: https://doi.org/10.1016/j.apenergy.2019.113603

[166] H. Park and R. Baldick, "Stochastic generation capacity expansion planning reducing greenhouse gas emissions," *IEEE Transactions on Power Systems*, vol. 30, no. 2, pp. 1026–1034, 3 2015.

[167] S. Ramabhotla, S. Bayne, and M. Giesselmann, "Economic dispatch optimization of microgrid in islanded mode," in *International Energy and Sustainability Conference 2014, IESC 2014*. Institute of Electrical and Electronics Engineers Inc., 3 2014.

[168] K. Dasgupta, J. Hazra, S. Rongali, and M. Padmanaban, "Estimating return on investment for grid scale storage within the economic dispatch framework," in *Proceedings of the 2015 IEEE Innovative Smart Grid Technologies - Asia, ISGT ASIA 2015*. Institute of Electrical and Electronics Engineers Inc., 1 2016.

[169] P. Fortenbacher, A. Ulbig, and G. Andersson, "Optimal Placement and Sizing of Distributed Battery Storage in Low Voltage Grids Using Receding Horizon Control Strategies," *IEEE Transactions on Power Systems*, vol. 33, no. 3, pp. 2383–2394, 5 2018.

[170] J. I. Levene, M. K. Mann, R. M. Margolis, and A. Milbrandt, "An analysis of hydrogen production from renewable electricity sources," *Solar Energy*, vol. 81, no. 6, pp. 773–780, 6 2007.

[171] U.S. Energy Information Administration, "Wind is a growing part of the electricity mix in Texas - Today in Energy - U.S. Energy Information Administration (EIA)." [Online]. Available: https://www.eia.gov/todayinenergy/detail.php?id=45476

[172] M. Melaina, B. Bush, M. Muratori, J. Zuboy, and S. Ellis, "National Hydrogen Scenarios: How Many Stations, Where, and When?" Prepared by the National Renewable Energy Laboratory for the H2 USA Locations Roadmap Working Group, Tech. Rep. October, 2017.

[173] A. Elgowainy, "Hydrogen Demand Analysis for H2 @ Scale," 2019. [Online]. Available: https://www.hydrogen.energy.gov/pdfs/review19/sa172_elgowainy_2019_o.pdf

[174] M. Ruth, "H2 @ Scale : Hydrogen Integrating Energy Systems," 2019. [Online]. Available: https://www.nrel.gov/docs/fy20osti/75422.pdf

[175] M. Majidi-Qadikolai and R. Baldick, "Stochastic Transmission Capacity Expansion Planning with Special Scenario Selection for Integrating $n-1$ Contingency Analysis," *IEEE Transactions on Power Systems*, vol. 31, no. 6, pp. 4901–4912, 2016.

[176] U.S. EIA, "Annual Energy Outlook 2019 with projections to 2050," *Annual Energy Outlook 2019 with projections to 2050*, vol. 44, no. 8, pp. 1–64, 2019.

[177] United States Environmental Protection Agency, "Documentation for National Electric Energy Data System (NEEDS) v.5.13," 2019. [Online]. Available: https://www.epa.gov/airmarkets/documentation-national-electric-energy-data-system-needs-v513

[178] Statnett SF, "Balsfjord-Skaidi | Statnett." [Online]. Available: https://www.statnett.no/en/our-projects/northern-norway/balsfjord-skaidi/

[179] United States Department of Energy, "Hydrogen Production," *Fuel Cell Technologies Office Multi-Year Research, Development and Demonstration Plant*, vol. 11007, pp. 1–44, 2015.

[180] J. Proost, "Critical assessment of the production scale required for fossil parity of green electrolytic hydrogen," *International Journal of Hydrogen Energy*, vol. 2050, no. xxxx, 2020.

[181] Ammonia Energy Association, "The cost of hydrogen: Platts launches Hydrogen Price Assessment - Ammonia Energy Association." [Online]. Available: https://www.ammoniaenergy.org/articles/the-cost-of-hydrogen-platts-launches-hydrogen-price-assessment/

[182] S&P Global Platts, "Hydrogen Price Assessments." [Online]. Available: https://www.spglobal.com/platts/en/our-methodology/price-assessments/natural-gas/hydrogen-price-assessments

[183] Q. Zheng, J. Wang, and A. Liu, "Stochastic Optimization for Unit Commitment — A Review," *IEEE Transactions on Power Systems*, vol. PP, no. 99, pp. 1–12, 2014. [Online]. Available: http://ieeexplore.ieee.org/stamp/stamp.jsp?tp=&arnumber=6912028

[184] Y. Liu and N. K. C. Nair, "A Two-Stage Stochastic Dynamic Economic Dispatch Model Considering Wind Uncertainty," *IEEE Transactions on Sustainable Energy*, vol. 7, no. 2, pp. 819–829, 4 2016.

[185] J. Soares, B. Canizes, M. A. F. Ghazvini, Z. Vale, and G. K. Venayagamoorthy, "Two-Stage Stochastic Model Using Benders' Decomposition for Large-Scale Energy Resource Management in Smart Grids," *IEEE Transactions on Industry Applications*, vol. 53, no. 6, pp. 5905–5914, 11 2017.

[186] M. F. Ruth and P. Jadun, "H2 @ Scale Analysis Overview Timeline and Budget Barriers (Systems Analysis)," 2019.

[187] European Commission, "A Clean Planet for all. A European long-term strategic vision for a prosperous, modern, competitive and climate neutral economy," European Commission, Brussels, Tech. Rep., 2018. [Online]. Available: https://eur-lex.europa.eu/legal-content/EN/TXT/?uri=CELEX:52018DC0773

[188] European Parliament, "The European Green Deal," European Parliament, Strasbourg, Tech. Rep., 2020.

[189] B. Mo and H. O. Hågenvik, "Applying the RrodRisk - SHOP simulator for investment decisions," SINTEF Energy Research, Tech. Rep., 2020. [Online]. Available: https://hdl.handle.net/11250/2716944

Appendix A

Publications

A.1 Regional Effects of Hydrogen Production in Congested Transmission Grids with Wind and Hydro Power

Regional Effects of Hydrogen Production in Congested Transmission Grids with Wind and Hydro Power

Espen Flo Bødal and Magnus Korpås
NTNU Norwegian University of Science and Technology
Department of Electric Power Engineering
Trondheim, Norway
Email: espen.bodal@ntnu.no

***Abstract*—Some of the best wind and natural gas resources in Norway are located in rural areas. Hydrogen can be produced from natural gas in combination with carbon capture and storage to utilize the natural gas resources without significant CO_2-emissions. The hydrogen can be liquefied and transported to regions with energy deficits. This creates a demand for hydrogen produced from electrolysis of water, which facilitates wind power development without requiring large investments in new transmission capacity. A regional optimization model is developed and used to investigate sizing of the electrolyser capacity and hydrogen storage, as well as regional effects of producing hydrogen from electrolysis. In the model, the transmission grid is represented by dc power flow equations and opportunities for wind power investments in the region are included.**

The model is used in a case study which shows that hydrogen storage contributes to significantly increase grid utilization, even with small amounts of storage. Increased regional transmission capacity results in more wind power development compared to increased capacity towards the central grid. Hydrogen storage is only profitable to reduce congestion in this deterministic model, thus using hydrogen storage to reduce the costs in the spot market is not profitable.

NOMENCLATURE

Indices

i, j	Bus
t	Time stage

Parameters

Δ	Price addition for import $[€/MW]$
$\eta^{d/s}$	Conversion factor from power to hydrogen $[MWh/Nm^3]$, directly from electrolyser or from hydrogen storage
γ_i	Conversion factor, effect to energy $[MWh/MW]$
λ_t^s	Spot price $[€/MWh]$
$C^{r/i}$	Cost of rationing $[€/MWh]$ or hydrogen import $[€/Nm^3]$
$C^{v+/v-}$	Cost for violating end reservoir level $[€/MWh]$
$C^{w/e/s}$	Annualized cost of wind power $[€/MW]$, hydro power $[€/MW]$ or electrolysers $[€/Nm^3]$
D_{ti}	Electricity demand $[MWh]$
E_i^{pot}	Potential for electrolyser capacity $[MW]$
H_i^D	Hydrogen demand from electrolysis $[MWh]$
H_i^{pot}	Potential for hydrogen storage capacity $[Nm^3]$
I_{ti}	Inflow to hydro power reservoirs $[MWh]$
P_t^w	Wind power production profile
$Q_{ti}^{min/max}$	Min or max hydro power production $[MW]$
S^{ref}	Reference power for the system $[MW]$
T_{ij}^{max}	Max transmission capacity from bus i to j $[MW]$
$V_i^{0/max}$	Initial volume or max capacity for reservoir $[MWh]$
W_i^{init}	Initially installed wind power $[MW]$
W_i^{pot}	Potential for wind power expansion $[MW]$
X_{ij}	Reactance on line between bus i and j $[p.u.]$

Sets

$\mathcal{B}$	All buses
$\mathcal{C}_i$	Buses connected to bus i by transmission lines
$\mathcal{H}, \mathcal{W}, \mathcal{H}_2$	Buses with hydro power, wind power or hydrogen plants
$\mathcal{N}$	All normal buses (Market bus excluded)
$\mathcal{T}$	Time stages

Variables

δ_{ti}	Voltage phase angle at bus
c_{ti}	Energy curtailment $[MW]$
e_i^{max}	Installed electrolyser capacity $[MW]$
f_{tij}	Power flow from bus i to j $[p.u.]$
h_{ti}^d	Hydrogen supplied to load directly from electrolyser $[Nm^3]$
$h_{t,i}^{imp}$	Hydrogen imported/ not served $[Nm^3]$
h_i^{max}	Installed hydrogen storage capacity $[Nm^3]$
h_{ti}^p	Hydrogen production from electrolysis to storage $[Nm^3]$
h_{ti}^s	Hydrogen supplied to load from storage tanks $[Nm^3]$
h_{ti}	Level of hydrogen in storage tank $[Nm^3]$
$p_{ti}^{imp/exp}$	Power import or export $[MW]$
q_{ti}	Hydro power production $[MW]$
r_{ti}	Rationing of power $[MW]$
s_{ti}	Spillage/ bypass of water $[MWh]$
$v^{+/-}$	Violation of end reservoir level $[MWh]$
v_{ti}	Reservoir level $[MWh]$
$w_i^{exp/max}$	Wind power expansion or installed capacity $[MW]$
w_{ti}	Wind power production $[MW]$

I. INTRODUCTION

In 2015, Norway was the worlds third largest exporter of natural gas exporting 115 billion cubic meter (1219 TWh). In comparison the total hydro power production, which is the backbone of the Norwegian electric power system with 96% of the total production, was 137 TWh as the worlds sixth largest producer [1]. Increased attention to reducing CO_2-emissions as result of their contributions to global warming stresses the importance of finding new ways to utilize the fossil resources without emitting CO_2. One way of utilizing natural gas resources is to produce hydrogen through a process called steam methane reforming (SMR), combining this with carbon capture and storage (CCS) allows the natural gas resources to be utilized without significant CO_2-emissions.

978-1-5090-5499-2/17/$31.00 ©2017 IEEE

Many of the future natural gas resources are located offshore from rural areas which also has good wind power resources. The development of wind power resources in these areas are constrained by weak transmission grids and the cost of constructing new transmission lines makes these wind resources unprofitable [2], [3]. Producing hydrogen from natural gas in areas with good wind resources results in development of more renewable electricity production, as it also establishes a demand for hydrogen produced from electrolysis of water. Liquefaction of hydrogen is energy demanding and results in an additional increase of electricity demand in the region. Energy can thus be transported out of the region in the form of liquid hydrogen for example by ship, reducing the need for costly grid investments. The combination of hydrogen production from natural gas with CCS, wind and hydro power is part of a project at Sintef Energy Research named Hyper [4], as a part of this project the effects of variable hydrogen production from electrolysis in a transmission constrained power system with good wind power resources needs to be studied further to assess the possible benefits.

Wind-hydrogen systems have been analysed for several years, both as isolated and grid connected systems. Significant efforts have been devoted to this topic by many researchers and test facilities are constructed for studying the properties of these systems. Two examples are the test facilities at Utsira in Norway [5] and at the National Renewable Energy Laboratory in the US [6]. Large scale hydrogen production is considered to facilitate wind power integration in Denmark, Ireland and Germany in [7],[8] and [9] respectively. The main focus in these studies is on balancing generation and demand in power systems with high penetration of intermittent renewable energy sources, as wind and solar power, by storing energy as hydrogen and convert it back to electricity using fuel cells.

In [10] a logical simulation model is used to simulate operation of a wind-hydrogen system with and without storage in a constrained transmission grid, the analysis shows promising result for using hydrogen production with storage as a load management method in constrained grids, contributing to increased utilization of the wind power resources. A model for sizing and operation of wind-hydrogen systems in weak distribution grids based on optimization is developed in [11]. Grid simulations are used to create linearized functions for the limits of export and import to the wind-hydrogen bus based on the load in the local distribution grid. The result shows that it's beneficial to use the power grid as backup power for hydrogen production compared to building a larger hydrogen storage. For electricity markets with large variations in the spot price it would be beneficial to install more wind power, electrolyser capacity and hydrogen storage to produce more hydrogen when prices are low and export more power when prices are high. Both these models are used on small scale wind-hydrogen systems and focus more on operation of a local system, not considering regional effects on other producers, wind power in several buses or the regional transmission grid.

In [12] a stochastic optimization model with dc power flow equations is developed for scheduling of hydro-thermal power systems and solved using a method based on stochastic dual dynamic programming. The model is applied in a case study for future scenarios of the Islandic power system with wind and pumped hydro power. Significant computing resources are needed to solve this model as stochasticity is considered both in power price and generation. It's obvious that considering stochasticity when optimizing the size of electrolyser and hydrogen storage in such a system would not be tractable without significant computing resources.

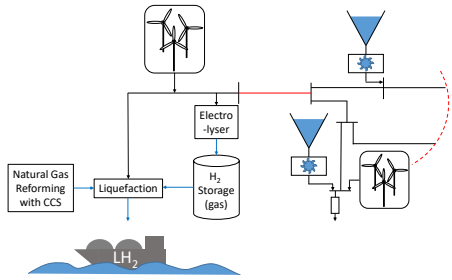

Fig. 1. Illustration of a regional power system with production of hydrogen from wind and hydro power in a constrained transmission grid (red lines).

The scope of this paper is to establish a method for optimizing the size of both the electrolyser and hydrogen storage and to examine the regional effects on the power system due to variable hydrogen production from electric power. A deterministic model for the regional power system is developed and used for this purpose, including dc power flow equations, wind power farms and hydro power plants with reservoirs. Analysis of important economic aspects of the system such as cost of hydrogen production and profits of hydro power producers are also included.

The paper is organized as follows; first the optimization model is described in chapter II, then a case study is presented in chapter III and the results from the case study are presented and discussed in chapter IV. Finally the conclusions are given in chapter V.

II. Methodology

A illustration of a regional power system with hydrogen production is shown in Figure 1, the system comprise hydro power with reservoirs, wind power, firm loads and hydrogen production plants with electrolysers and storage tanks. The system borders is chosen to exclude the detailed liquefaction process which is instead defined as a constant hydrogen and electricity demand. The regional transmission grid is modelled by dc power flow equations thus neglecting power loss in the transmission grid, while the rest of the power system is modelled by a "market bus" with a deterministic power price.

The power system is represented by a linear programming model defined by Equation (1) to (9) with hourly time stages. The objective is to minimize investment cost in wind power,

electrolysers and hydrogen storage while maximizing the profits from energy exchange between the region and the external power market. Export from the regional system is equivalent with import to the market bus, p_{t0}^{imp}, and import to the regional system is equivalent with export from the market bus, p_{t0}^{exp}. A small price difference on the power price is introduced to avoid importing and exporting at the same time, this reflects the real situation in the transmission grid where the marginal loss part of the tariff is opposite for producers and consumers [13]. The objective also includes penalties for rationing, hydrogen import and end reservoir violations.

$$\begin{aligned}\max -\frac{T}{8760}\Big[\sum_{i\in\mathcal{W}} C_i^w w_i^{exp} + \sum_{i\in\mathcal{H}_2} C_i^e e_i^{max} + \sum_{i\in\mathcal{H}_2} C_i^s h_i^{max}\Big] \\ + \sum_{t\in\mathcal{T}}\Big[\lambda^s p_{t0}^{imp} - (\lambda^s+\Delta)p_{t0}^{exp} - \sum_{i\in\mathcal{N}} C^r r_{ti} - \sum_{i\in\mathcal{H}_2} C^i h_{ti}^i\Big] \\ - \sum_{i\in\mathcal{H}}(C^{v+}v_i^+ + C^{v-}v_i^-) \qquad (1)\end{aligned}$$

s.t.

$$w_{ti} + c_{ti} = \gamma_i w_i^{max} P_{ti}^w \qquad \forall i\in\mathcal{W}, \forall t\in\mathcal{T} \qquad (2)$$

$$w_{ti}^{max} = W_i^{init} + w_i^{exp} \qquad \forall i\in\mathcal{W} \qquad (3)$$

$$v_{ti} = v_{(t-1)i} - q_{ti} - s_{ti} + I_{ti} \qquad \forall i\in\mathcal{H}, \forall t\in\mathcal{T} \qquad (4)$$

$$v_{0i} = V_i^0 \qquad \forall i\in\mathcal{H} \qquad (5)$$

$$v_{Ti} - v_i^+ + v_i^- = V_i^0 \qquad \forall i\in\mathcal{H} \qquad (6)$$

$$h_{ti} = h_{(t-1)i} + h_{ti}^p - h_{ti}^s \qquad \forall i\in\mathcal{H}_2, \forall t\in\mathcal{T} \qquad (7)$$

$$h_{ti}^d + h_{ti}^s + h_{ti}^i = H_{ti}^D \qquad \forall i\in\mathcal{H}_2, \forall t\in\mathcal{T} \qquad (8)$$

$$\begin{aligned}w_{ti} + q_{ti} - \eta^d h_{ti}^d - \eta^s h_{ti}^p \\ - p_{ti}^{exp} + p_{ti}^{imp} + r_{ti} = D_{ti} \qquad \forall i\in\mathcal{N}, \forall t\in\mathcal{T} \qquad (9)\end{aligned}$$

$$p_{ti}^{exp} - p_{ti}^{imp} = S^{ref}\sum_{j\in\mathcal{C}_i} f_{tij} \qquad \forall i\in\mathcal{B}, \forall t\in\mathcal{T} \qquad (10)$$

$$f_{tij} = \frac{1}{X_{ij}}(\delta_{ti} - \delta_{tj}) \qquad \forall j\in\mathcal{C}_i, \forall i\in\mathcal{B}, \forall t\in\mathcal{T} \qquad (11)$$

$$w_{ti} \le w_i^{max} \le W_i^{init} + W_i^{pot} \qquad \forall i\in\mathcal{W}, \forall t\in\mathcal{T} \qquad (12)$$

$$v_{ti} \le V_i^{max} \qquad \forall i\in\mathcal{H}, \forall t\in\mathcal{T} \qquad (13)$$

$$Q_{ti}^{min} \le q_{ti} \le Q_i^{max} \qquad \forall i\in\mathcal{H}, \forall t\in\mathcal{T} \qquad (14)$$

$$\eta^d h_{ti}^d + \eta^s h_{ti}^p \le e_i^{max} \le E_i^{pot} \qquad \forall i\in\mathcal{H}_2, \forall t\in\mathcal{T} \qquad (15)$$

$$h_{ti} \le h_i^{max} \le H_i^{pot} \qquad \forall i\in\mathcal{H}_2, \forall t\in\mathcal{T} \qquad (16)$$

$$f_{tij} \le T_{ij}^{max}/S^{ref} \qquad \forall j\in\mathcal{C}_i, \forall i\in\mathcal{B}, \forall t\in\mathcal{T} \qquad (17)$$

The wind power plants can produce, w_{ti}, or curtail, c_{ti}, power dependent on the installed wind power capacity, w_i^{max}, the energy coefficient, γ_i, and wind power profile, P_{ti}^w, as stated in Equation (2). As shown in Equation (3) the installed wind power capacity comprise initial wind power capacity, W_i^{init}, and capacity expansion determined by the model, w_i^{exp}.

Hydro power plants are modelled by a reservoir balance shown in Equation (4) where the reservoir volume, v_{ti}, is dependent on the reservoir volume in the previous hour, hydro power production, q_{ti}, spillage, s_{ti} and inflow, I_{ti}. To ensure comparability between different cases the reservoir volume at the end of the model horizon is forced to be equal to the initial reservoir volume by Equation (6), any violations are penalized in the objective.

The representation of the hydrogen plants include a storage balance as shown in Equation (7) where the hydrogen storage level, h_{ti}, is dependent on level in the previous hour, hydrogen production, h_{ti}^p, and hydrogen demand supplied from storage, h_{ti}^s. The hydrogen demand can be covered by supplying hydrogen directly from the electrolyser, h_{ti}^d, from the storage tanks or by importing hydrogen, h_{ti}^i, from an external source as stated by the hydrogen balance in Equation (8). Importing hydrogen can also be treated as "hydrogen not supplied", where the cost of imported hydrogen is representing a penalty for not serving the hydrogen load. Supplying the hydrogen demand directly from the electrolyser gives a better conversion factor, $\eta^d \le \eta^s$, as compression to storage pressure is avoided.

The energy balance for a bus is shown in Equation (9), where wind power production, hydro power production, rationing and power import are power injections into the bus while power is extracted by producing hydrogen, covering demand or exporting power. Export and import are subject to the flow balance in Equation (10) and dc load flow equations in Equation (11).

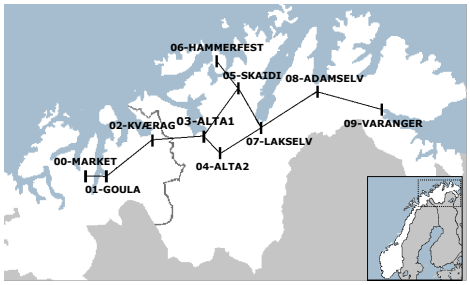

Fig. 2. Illustration of case study system based on Finnmark in Northern Norway.

III. Case Study

The case study illustrated in Figure 2 is created based on a region in Northern Norway with good wind conditions and large amounts of future natural gas resources. The region has a constrained connection to the rest of the Nordic power system which is restricting development of wind power. A facility for natural gas processing and liquefaction to LNG currently exist at Melkøya in Hammerfest (bus 6), this bus is thus chosen as the location for the hydrogen production facility in the case study. The power requirements of the LNG plant is currently fully supplied by on-site gas turbines with a capacity of 225 MW. In this case study, the power requirements for the

TABLE I
BUS DATA FOR THE CASE SYSTEM. POTENTIAL WIND POWER IS BASED ON PERMIT APPLICATIONS [15].

Bus Nr.	Wind [MW]	Wind Pot [MW]	Hydro [MW]	Reservoir [GWh]	Load [GWh/yr]
1	0.0	10.0	80	224.8	225.5
2	0.0	0.0	85	231.9	35.1
3	0.0	0.0	17.7	46.5	374.3
4	0.0	0.0	145.2	56.7	22.7
5	40.5	160.0	4.2	5.0	121.5
6	0.0	10.0	1.1	0.0	188.2
7	0.0	0.0	1.7	1.6	136.6
8	40.0	1550.0	55.1	168.5	80.2
9	95.0	453.0	78.3	16.1	680.3
Sum	175.5	2173.0	468.3	751.1	1864.4

liquefaction and hydrogen plant is considered to be supplied by the power system.

The region is the most promising for wind power in Norway according to a study by the Norwegian Water Resources and Energy Directorate (NVE) [14] with almost twice the wind power potential of any other region. A significant number of wind power development projects have applied for permits, most of them are located in the eastern part of the region at bus 8 and 9, far away from the central grid. Table I gives an overview of the most important bus data for the case study including an estimate of potential wind power capacity based on permit applications. The developed wind power is low compared to the wind power potential, mainly as a result of low transmission capacities in combination with a surplus hydro power production and low power prices recent years.

As the transmission capacity from the region is limited the Norwegian TSO, Statnett, is currently building a new transmission line with a voltage level of 420 kV from the market bus to bus 5 in Figure 2. Further expansions from bus 5 to bus 8 is also under consideration but is dependent on the development of load in the region especially from the petroleum industry as it is not regarded viable from a socioeconomic perspective for the purpose of extracting wind power alone [3]. Based on the current plans for the transmission grid, three grid cases are considered by doubling the capacity on the existing lines:

- Local (L): line 5-6 (included in all alternatives).
- Regional (R): line segment 5-7-8.
- National (N): line segment 0-1-2-3-5.

Based on the detailed study of hydrogen storage in [16] the annualized cost of hydrogen storage is calculated to be approximately 4.16 and 2.63 €/(Nm^3·yr) for storage at 9.5 and 350 bar respectively, assuming 4% discount rate, 24 years lifetime and 0.5% maintenance cost. The investment cost for a large scale (≥50 MW) state-of-the-art alkaline electrolysis plant is around 500 €/kW [17]. By including a reinvestment of 57% of the initial investment cost after 12 years, maintenance cost of 5% and a total lifetime at 24 years the annualized costs are calculated to be 69.47 €/(kW·yr). The

TABLE II
INSTALLED CAPACITIES FOR ELECTROLYSER AND HYDROGEN STORAGE AND RATIONED ENERGY. HYDROGEN STORAGE IS REPRESENTED BY VOLUME AND HOURS OF HYDROGEN DEMAND.

	Local		Regional		National
Capacities	E	ES	E	ES	
Elec [MW]	107.99	128.87	107.99	110.97	107.99
Storage [Nm^3]	-	231003.8	-	101550.8	0.0
Storage [h]	-	9.97	-	4.38	0.0
Rat [MWh]	199.47	0.0	354.63	0.0	0.0

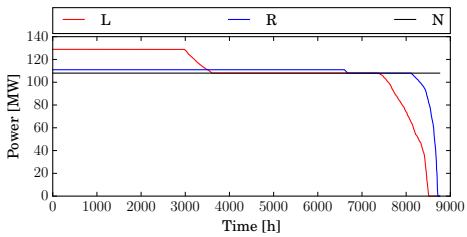

Fig. 3. Duration curve of the electrolyser for hydrogen production with storage.

power requirement for hydrogen production delivered directly from the electrolyser to liquefaction at 20 bar is estimated to be 4.66 kWh/Nm^3, when compression to storage pressure at 350 bar is included the power requirement increase to 4.79 kWh/Nm^3.

Four different load cases are considered in the bus with hydrogen production; a base case (B) with no change from the current system, a load case where the electricity demand for liquefaction is included (D), a case with hydrogen production without storage (E) and a case with hydrogen production and storage (ES). Spot price, wind power production and load are based on historic data for the power system from 2015.

IV. RESULTS AND DISCUSSION

As shown from Table II both the local and the regional grid cases requires hydrogen storage to avoid rationing of energy. In the local case the storage capacity is double the size of the regional case. To be able to utilize the storage capacity efficiently the electrolyser capacity is significantly higher in the local case compared to a case without storage, requiring about ten extra electrolysers, while the electrolyser capacity is only slightly higher for the regional case resulting in only one additional electrolyser. As shown in Figure 3 the utilization of the additional electrolysers decrease with increasing storage capacity. In the national case, when the connection to the central grid is strong, it's not profitable to invest in storage only to reduce operational costs from the spot market.

The local and regional case for constant electrolyser production is subject to the highest investments in new wind power capacity due to rationing. Rationing makes it profitable

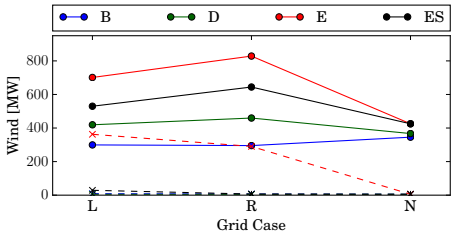

Fig. 4. Total wind power capacity in the region (solid lines) and wind power curtailment (dotted lines) for different cases.

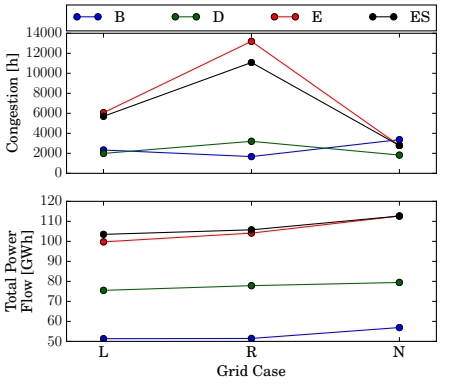

Fig. 5. Total numbers of hours with congestion for all lines (top) and sum of power flow for all lines in the region (bottom).

from a system point-of-view to invest in wind power capacity, considering that grid reinforcements and hydrogen storage are unavailable, even though significant amounts of wind power is curtailed as shown in Figure 4. The largest amount of wind power development, without unacceptable amounts of rationing and curtailment, is for the regional case with hydrogen storage. For the national case the effects of additional loads on wind development is significantly reduced and the differences between the grid cases are small.

Expanding the grid capacity from the local case to the regional case results in increased amounts intermittent energy in the form of wind power in the region for the cases with increased load and thus more congestion as shown in the upper part Figure 5. The congestion is significantly less when a hydrogen storage is included, thus reducing the levels of wind power curtailment and rationing. Even though the hours of congestion is lower when hydrogen storage is included the total power transmitted by the transmission grid is higher as shown in the lower part of Figure 5, resulting in a more efficient use of the transmission grid capacity. The hydrogen

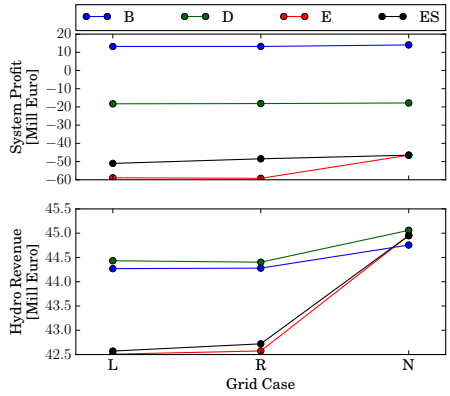

Fig. 6. Total system profit from exchange with the external market, including investment cost for wind power and hydrogen plant and costs from rationing (top). Total revenue for all hydro power plants in the region (bottom).

storage doesn't effect the total power flow as much in the regional case compared to the local case as the optimal hydrogen storage capacity is lower, but it still has a larger effect with respect to reducing the hours of congestion in the regional case as more wind power is developed.

As shown in the upper part of Figure 6 the system revenue is positive in the base case, supplying power requirements of the natural gas processing and hydrogen liquefaction from the regional power system increases the total system load which results in a negative profit. Further increasing the load by producing hydrogen from electrolysis and investing in electrolyser and hydrogen storage reduce the system profit even more. The system profit is lower when hydrogen storage is not included and the grid is constrained due to rationing.

The total revenue for all the hydro power producers in the region is shown in the lower part of Figure 6 which shows that more load in the region is positive for hydro power producers as long as it doesn't result in significant levels of congestion. The revenue is higher for load case D but significantly lower for the cases with hydrogen production from electrolysis as these cases result in high levels of grid congestion. The hydro power producers are forced to move production to less profitable hours when congestion increase due to more wind power, as hydro power with reservoirs can store energy while wind power plants cannot. This effect is reduced when more grid capacity is available with the regional expansion. The case with hydrogen storage results in less congestion for the cases with low levels of grid expansion and thus also higher revenues for the hydro power producers. The best case for the hydro power producers is clearly the national case with a stronger connection to the central grid as it results in less wind power development and less congestion allowing them

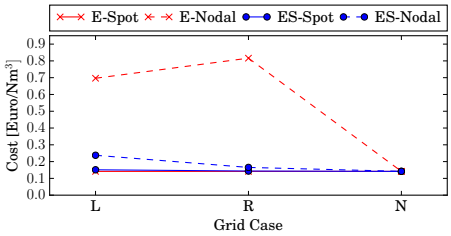

Fig. 7. Hydrogen production cost including investment and operational costs.

to produce at the highest prices.

The cost of hydrogen production is shown in Figure 7 and comprise both investment and operational costs. The operational costs are calculated both from spot and nodal prices, where the nodal prices are obtained from the duals of the energy balance in Equation (9) and is the marginal cost of energy in the given bus. When using the nodal price to calculate the cost of hydrogen production the total cost for the power system is included and the case with hydrogen storage is significantly cheaper than without hydrogen storage. The case without storage results in slightly lower costs when only considering the spot price, thus the main purpose of the storage isn't to reduce the cost of purchasing power from the spot market but to reduce congestion. Grid tariffs would be added to the cost of hydrogen production in addition to the spot price, this tariff is suppose to represent the cost of utilizing the transmission grid [13] and would likely be higher for the case without storage as the nodal price indicates. The differences between the cost of hydrogen production with storage in the regional case and the national case is relatively small, 0.165 and 0.142 €/Nm^3 respectively. The significant uncertainty related to both wind and hydro power would likely increase both optimal hydrogen storage and the cost of hydrogen production.

V. Conclusion

The sizing of electrolyser and hydrogen storage in a transmission constrained system is studied and some effects of hydrogen production on the power system are investigated. A case study in Northern Norway is analysed using a deterministic optimization model which also allows for wind power investments. The case study shows that the hydrogen storage has a high degree of utilization and the numbers of electrolysers increases rapidly with the storage capacity. Hydrogen storage is important to avoid rationing when the transmission grid is constrained and helps to reduce the hours of congestion and utilize the transmission grid more efficiently.

A regional expansion of the grid between the hydrogen production and the wind power facilitate wind power development but also increases the congestion level. Hydro power revenue is reduced due to increased congestion, this effect is smaller when hydrogen storage is included as congestion is reduced. Hydrogen storage is important to the cost of hydrogen production in constrained transmission grids due to the reduced congestion, while it's not profitable when a strong connection to the market is available and it would only be used to reduce the operational costs from the spot market.

Acknowledgment

This publication is based on results from the research project Hyper, performed under the ENERGIX programme. The authors acknowledge the following parties for financial support: Statoil, Shell, Kawasaki Heavy Industries, Linde Kryotechnik, Mitsubishi Corporation, Nel Hydrogen and the Research Council of Norway (255107/E20).

References

[1] IEA - International Energy Agency, "Key world energy statistics," 2016.
[2] F. R. Førsund, B. Singh, T. Jensen, and C. Larsen, "Phasing in wind-power in Norway: Network congestion and crowding-out of hydropower," *Energy Policy*, vol. 36, pp. 3514–3520, 2008.
[3] Statnett, "Kraftsystemet i Finnmark," Tech. Rep., 2016. [Online]. Available: http://www.statnett.no/PageFiles/13394/Dokumenter/Rapporter fra Statnett/Analyserapport Kraftsystemet i Finnmark.pdf
[4] Sintef Energy Reseach, "Sintef project: Hyper," 2017. [Online]. Available: http://www.sintef.no/projectweb/hyper/
[5] Ø. Ulleberg, T. Nakken, and A. Eté, "The wind/hydrogen demonstration system at Utsira in Norway: Evaluation of system performance using operational data and updated hydrogen energy system modeling tools," *International Journal of Hydrogen Energy*, vol. 35, no. 5, pp. 1841–1852, 2010.
[6] K. H. Pi, J. Martin, M. Peters, O. Smith, and D. Terlip, "Overview of an Integrated Research Facility for Advancing Hydrogen Infrastructure Project ID : Timeline," 2016. [Online]. Available: https://www.hydrogen.energy.gov/pdfs/review16/tv038_peters_2016_p.pdf
[7] C. Jørgensen and S. Ropenus, "Production price of hydrogen from grid connected electrolysis in a power market with high wind penetration." *International Journal of Hydrogen Energy*, vol. 33, no. 20, pp. 5335–5344, 2008.
[8] J. Carton and A. Olabi, "Wind/hydrogen hybrid systems: Opportunity for Ireland's wind resource to provide consistent sustainable energy supply," *Energy*, vol. 35, no. 12, pp. 4536–4544, 2010.
[9] M. Ball, M. Wietschel, and O. Rentz, "Integration of a hydrogen economy into the German energy system: an optimising modelling approach," *International Journal of Hydrogen Energy*, vol. 32, no. 10-11, pp. 1355–1368, 2007.
[10] M. Korpås and C. J. Greiner, "Opportunities for hydrogen production in connection with wind power in weak grids," *Renewable Energy*, vol. 33, no. 6, pp. 1199–1208, 2008.
[11] C. J. Greiner, M. Korpas, and T. Gjengedal, "A Model for Techno-Economic Optimization of Wind Power Combined with Hydrogen Production in Weak Grids," *EPE Journal*, no. 2, pp. 52–59, jun 2009.
[12] A. Helseth, A. Gjelsvik, B. Mo, and Ú. Linnet, "A model for optimal scheduling of hydro thermal systems including pumped-storage and wind power," *IET Generation, Transmission & Distribution*, no. 12, pp. 1426–1434, 2013.
[13] Statnett, "Tariffhefte 2017," 2017. [Online]. Available: http://statnett.no/Documents/Kraftsystemet/Tariffer og avtaler/Priser/Tariffhefte 2017.pdf
[14] NVE, "Vindkart for Norge," Tech. Rep., 2009. [Online]. Available: https://www.nve.no/energiforsyning-og-konsesjon/vindkraft/vindressurser/
[15] NVE, "Permit applications," 2016. [Online]. Available: https://www.nve.no/konsesjonssaker/
[16] M. Ozaki, S. Tomura, R. Ohmura, and Y. H. Mori, "Comparative study of large-scale hydrogen storage technologies: Is hydrate-based storage at advantage over existing technologies?" *International Journal of Hydrogen Energy*, vol. 39, no. 7, pp. 3327–3341, 2014.
[17] H. G. Langås and NEL Hydrogen, "Large scale hydrogen production," p. 21, 2015. [Online]. Available: http://www.sintef.no/contentassets/9b9c7b67d0dc4fbf9442143f1c52393c/9-hydrogen-production-in-large-scale-henning-g.-langas-nel-hydrogen.pdf

A.2 Production of Hydrogen from Wind and Hydro Power in Constrained Transmission grids, Considering the Stochasticity of Wind Power

Production of Hydrogen from Wind and Hydro Power in Constrained Transmission grids, Considering the Stochasticity of Wind Power

Espen Flo Bødal, Magnus Korpås

Department of Electric Power Engineering, Norwegian University of Science and Technology NTNU, Trondheim, Norway

E-mail: espen.bodal@ntnu.no

Abstract. Producing hydrogen from renewable energy sources can be used as a way of extracting large quantities of energy from remote regions far from load centers. These regions have weak transmission grids and building new transmission lines are expensive due to large distances. The tight restrictions on the power systems in these regions makes daily operation difficult and unexpected variations in wind power production can have significant negative impacts, such as rationing of power.

A stochastic rolling horizon model is formulated and implemented to consider the importance of including wind power stochasticity when operating flexible hydrogen loads in a congested power system. Wind power scenarios are created using realized wind power production and meteorological weather forecasts. The resulting operation plans of hydrogen storage and hydro power plants, using expected values or wind power scenarios, are tested and compared in a simulator with the realized wind power production.

Results from the case study show that the stochastic model gives a better strategy than the deterministic model which use the expected value of wind production by about 5.6% and there is potential for further cost reductions by improving the forecasting. When including more than 27 wind power scenarios the changes in results are small. The case study also shows that hydrogen storage is important to avoid rationing in certain situations and increase power flow.

1. Introduction

The best wind resources both on- and off-shore are often located in remote areas far from load centers. New transmission lines have to be constructed in order to exploit these excellent resources and export the energy over large distances. This requires large investments which must be considered when calculating the socioeconomic benefit of these wind power projects and often makes them unprofitable[1]. In Norway, this is the case for the northern pars of the county, where there are exceptionally good conditions for wind power production. A wind turbine in this region can produce up to twice as much energy as a wind turbine in southern Norway, comparable with offshore wind turbines but at significantly lower costs. The grid connection between northern and southern Norway, where most of the people and consumption is located, is too weak to support integration of large amounts of wind power in the north [2]. Producing hydrogen and exporting liquefied hydrogen (LH_2) on ships, similar to liquefied natural gas (LNG) can be a good option for utilizing the wind resource.

Nomenclature

Indices

i, j	Bus
s	Second stage node
t	Time stage

Parameters

Δ	Price addition for import [€/MW]
$\eta^{d/s}$	Conversion factor from power to hydrogen [MWh/Nm^3], directly from electrolyser or from hydrogen storage
λ_t^s	Spot price [€/MWh]
ρ_s	Probability of wind power scenario
C_t^d	Cost for changing production from plan [€/MWh]
$C^{r/i}$	Cost of rationing [€/MWh] or hydrogen import [€/Nm^3]
$C^{v+/v-}$	Cost for violating end reservoir level [€/MWh]
D_{ti}	Electricity demand [MWh]
E_i^{max}	Capacity of electrolyser [MW]
H_t^D	Hydrogen demand from electrolysis [MWh]
H_i^{max}	Capacity of hydrogen storage[Nm^3]
I_{ti}	Inflow to hydro power reservoirs [MWh]
$P_{ti}^{min/max}$	Min or max power production [MW]
P_{tis}^w	Wind power production scenario [MWh]
S^{ref}	Reference power for the system [MW]
T_{ij}^{max}	Transmission capacity from bus i to j [MW]
$V_i^{0/max}$	Initial volume or max capacity for reservoir [MWh]
X_{ij}	Reactance on line between bus i and j [$p.u.$]

Sets

$\mathcal{B}$	All buses
$\mathcal{C}_i$	Buses connected to bus i by transmission lines
$\mathcal{H}, \mathcal{W}, \mathcal{P}, \mathcal{H}_2$	Hydro power, wind power, all power plants or hydrogen plants
$\mathcal{N}$	All normal buses (Market bus excluded)
$\mathcal{S}$	Wind Power Scenario
$\mathcal{T}$	Time stages

Variables

δ_{tis}	Voltage phase angle at bus
c_{tis}	Energy curtailment [MW]
$d_{tis}^{H_2-/+}$	Negative/ positive change in hydrogen production [MW]
$d_{tis}^{hydro-/+}$	Negative/ positive change in hydro power production [MW]
f_{tijs}	Power flow from bus i to j [$p.u.$]
h_{tin}^d	Hydrogen supplied to load directly from electrolyser [Nm^3]
h_{tis}^{imp}	Hydrogen imported/ not served [Nm^3]
h_{tin}^p	Hydrogen production from electrolysis to storage [Nm^3]
h_{tin}^s	Hydrogen supplied to load from storage tanks [Nm^3]
h_{tin}	Level of hydrogen in storage tank [Nm^3]
$p_{tis}^{imp/exp}$	Power import or export [MW]
p_{tis}	Production [MW]
r_{tis}	Rationing of power [MW]
s_{tin}	Spillage/ bypass of water [MWh]
$v_n^{+/-}$	Violation of end reservoir level [MWh]
v_{tin}	Reservoir level [MWh]

A project headed by SINTEF Energy Research called HYPER looks at the possibility of producing hydrogen, both from natural gas with carbon capture and storage (CCS) and from hydro and wind power. The locations of natural gas resources are often co-located with good wind resources, both on-shore and off-shore. In the case of northern Norway there are already production of LNG from natural gas.

Several positive effects can be obtained by producing LH_2 instead of LNG and storing the CO_2 in depleted natural gas reservoirs. Firstly, emissions from the use of natural gas as a energy source is greatly reduced by storing the CO_2 at the production site where there are storage capacity in the depleted natural gas reservoirs. Secondly, this creates infrastructure for liquefaction of hydrogen and a supply chain to the to the energy demand, this can be used

to accelerate the development of wind power by producing hydrogen through electrolysis. The costs of electrolysis plants are dropping and are competitive for large plants, the most critical cost element when considering the profitability of such a plant is in fact the cost of energy which in this case is very low. Thirdly, producing hydrogen from wind power in a flexible manner by including hydrogen storage can increase the utilization of existing transmission lines and reduce the amount of new transmission capacity needed to develop wind power. Utilization of transmission lines in regions with large amounts of wind power is low due to the variable nature of wind power and the correlation between wind farms. Closely located wind farms are often producing or idle at the same time creating congestion at one time and no line utilization at another time. This correlation problem is reduced the grater the area that is considered due to the smoothing effect, but can still have a significant impact.

Wind-hydrogen systems is extensively studied in the literature. In [3] a local wind-hydrogen system is studied where they consider wind power by using deterministic forecasts to make a plan for trading power in the spot-market and then simulates imbalances settled in the balancing market using a receding horizon approach. The system consist of one bus with wind generation, electrolyser, hydrogen storage, fuel cell, electrical load, hydrogen load and a connection to the external grid. The case study showed that the fuel cell was only used for cases with large energy price variations and high imbalance costs.

Hydrogen production in weak transmission grids are studied in [4] and [5]. In [4] they use a logistic simulation model to study the effects on wind power integration and sizing of hydrogen storage by including hydrogen loads. While in [5] they use a optimization model and also include fuel cells. The results show there is large benefits using a grid connected setup in terms of electrolyser sizing and operating conditions.

The authors have previously presented a method for optimal sizing of components for large scale hydrogen production in a regional power system with congested transmission lines, wind and hydro power [6]. The results show that the sizing of the hydrogen storage and integration of wind power is highly dependent on the grid configuration, hydrogen storage is very important to avoid rationing if the region is weakly connected to the rest of the system.

Rolling horizon models frequently used when studying integration of wind power in the power system. In [7] they use a stochastic rolling horizon model with wind power scenarios for a system consisting of a wind farm and batteries to study the effects of considering battery degradation when bidding in the real-time electricity market. In a system level study in [8] they use a rolling horizon model to study the effects of large scale wind power integration in Ireland. The model includes a detailed description the power system with unit commitment constraints and representations of the spot and reserves markets. They update the plans every 3 hours and the results show that 34 % of the load inn the Irish power system can be provided by wind power.

The model presented in this paper is a rolling horizon model for studying the storage strategies of flexible hydrogen production and hydro power. The model includes stochastic wind power and is different from the [8] as it includes storage and a linearized representation of the transmission grid, but not unit commitment constraints. The model use scenarios of wind power production such as in [7] with equal probability and find the storage strategy that is best considering all scenarios.

The rest of the paper is organized as follows, in Chapter 2 the three most important parts of the model is presented; the generation of wind power scenarios, the planning model and the simulator model. A case study based on the region of northern Norway is outlined in Chapter 3. The results from the case study are presented in Chapter 4 and the conclusions are given in Chapter 5.

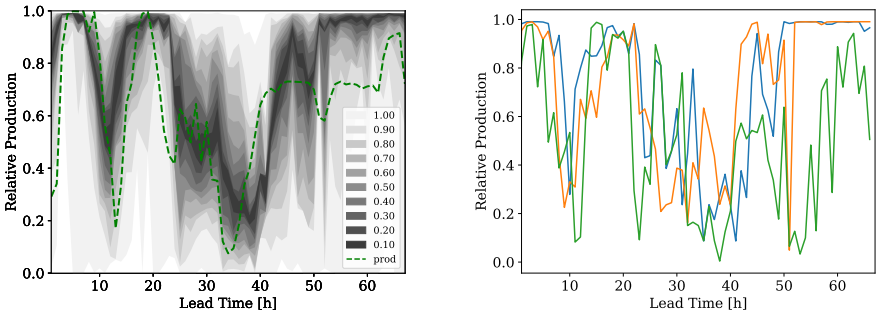

(a) Quantile forecast of relative production for Raggovidda wind farm in northern Norway.

(b) Scenarios of wind power production sampled from the quantile distribution.

Figure 1: Quantile forecats are used to creating wind power scenarios for the stochastic model.

2. Model

The model presented in this paper is a model for a regional power system with flexible hydrogen loads, wind and hydro power. The model consist of three main parts, wind forecasting, strategy calculation and simulation, these parts are explained in detail in this chapter.

2.1. Wind Power Scenarios

The representation of wind power uncertainty is obtained by sampling production scenarios from quantile forecasts as explained in detail in [9]. In short the method consist of random sampling from a multivariate normal distribution using a correlation matrix representing temporal and spatial correlations. The sampled values are matched by their probability in the cumulative distribution function (cdf) of the normal distribution, the wind power production scenario is obtained by matching these probabilities in the cdf of the quantile distribution.

The quantile forecasts are created by using histrorical metrological forecasts from The Norwegian Meteorological Institute and production records from existing wind farms obtained from The Norwegian Water Resources and Energy Directorate. The data is used in a local quantile regression algorithm for generating the quantile forecasts as in [10], a example of an quantile forecast for the wind farm Raggovidda is shown in Figure 1a.

2.2. Planning Model

The planning model optimize the expected cost of operating a region of the power system, all the electrical and hydrogen demand has to be served either by using generation from within the region or by importing power from the external power market. This can be modelled as optimizing profit from selling power to the external market as stated in the first two terms in the objective function in Equation (1). Power is sold to the market node at the spot price or it can be purchased from the market node for the spot price plus tariffs. Penalty terms are added in each time step for rationing of power, import of hydrogen from external sources, deviation from scheduled power consumption for producing hydrogen and deviation from production plans for hydro power. Predefined reservoir handling curves are used to represent the long term hydro power strategy, deviation from these plans at the end of the planning horizon are penalized in the final term of the objective function.

$$\max \sum_{s\in\mathcal{S}} \rho_s \Big[\sum_{t\in\mathcal{T}} \Big[\lambda_t^s p_{t0s}^{imp} - (\lambda_t^s + \Delta) p_{t0s}^{exp} - \sum_{i\in\mathcal{N}} C^r r_{tis} - \sum_{i\in\mathcal{H}_2} C^i h_{tis}^i - \sum_{i\in\mathcal{H}_\in} C_t^d (d_{tis}^{H_2-} + d_{tis}^{H_2+}) - \sum_{i\in\mathcal{H}} C_t^d (d_{tis}^{hydro-} + d_{tis}^{hydro+}) \Big] - \sum_{i\in\mathcal{H}} (C^{v+} v_{is}^+ + C^{v-} v_{is}^-) \Big] \quad (1)$$

s.t.

$$p_{tis} + c_{tis} = P_{tis}^w \qquad \forall i \in \mathcal{W}, \forall t \in \mathcal{T}, \forall s \in \mathcal{S} \quad (2)$$

$$v_{tis} = v_{(t-1)is} - p_{tis} - s_{tis} + I_{ti} \qquad \forall i \in \mathcal{H}, \forall t \in \mathcal{T}, \forall s \in \mathcal{S} \quad (3)$$

$$v_{0is} = V_i^0 \qquad \forall i \in \mathcal{H}, \forall s \in \mathcal{S} \quad (4)$$

$$v_{Tis} - v_{is}^+ + v_{is}^- = V_{T,i}^{curve} \qquad \forall i \in \mathcal{H}, \forall s \in \mathcal{S} \quad (5)$$

$$h_{tis} = h_{(t-1)is} + h_{tis}^p - h_{tis}^s \qquad \forall i \in \mathcal{H}_2, \forall t \in \mathcal{T}, \forall s \in \mathcal{S} \quad (6)$$

$$h_{tis}^d + h_{tis}^s + h_{tis}^i = H_{tis}^D \qquad \forall i \in \mathcal{H}_2, \forall t \in \mathcal{T}, \forall s \in \mathcal{S} \quad (7)$$

$$\sum_{j\in\mathcal{P}_i} p_{tjs} - \eta^d h_{tis}^d - \eta^s h_{tis}^p - p_{tis}^{exp} + p_{tis}^{imp} + r_{tis} = D_{ti} \qquad \forall i \in \mathcal{N}, \forall t \in \mathcal{T}, \forall s \in \mathcal{S} \quad (8)$$

$$d_{tis}^{H_2-} - d_{tis}^{H_2+} = \eta^d (h_{ti}^{d,plan} - h_{tis}^d) + \eta^s (h_{ti}^{p,plan} - h_{tis}^p) \qquad \forall i \in \mathcal{H}_2, \forall t \in \mathcal{T}, \forall s \in \mathcal{S} \quad (9)$$

$$d_{tis}^{hydro-} - d_{tis}^{hydro+} = (p_{ti}^{plan} - p_{tis}) \qquad \forall i \in \mathcal{H}, \forall t \in \mathcal{T}, \forall s \in \mathcal{S} \quad (10)$$

$$p_{ti}^{exp} - p_{ti}^{imp} = S^{ref} \sum_{j\in\mathcal{C}_i} f_{tij} \qquad \forall i \in \mathcal{B}, \forall t \in \mathcal{T}, \forall s \in \mathcal{S} \quad (11)$$

$$f_{tijs} = \frac{1}{X_{ij}} (\delta_{tis} - \delta_{tjs}) \qquad \forall j \in \mathcal{C}_i, \forall t \in \mathcal{T}, \forall i \in \mathcal{B}, \forall s \in \mathcal{S} \quad (12)$$

$$0 \le v_{tis} \le V_i^{max} \qquad \forall i \in \mathcal{H}, \forall t \in \mathcal{T}, \forall s \in \mathcal{S} \quad (13)$$

$$P_{ti}^{min} \le p_{tis} \le P_i^{max} \qquad \forall i \in \mathcal{H}, \forall t \in \mathcal{T}, \forall s \in \mathcal{S} \quad (14)$$

$$0 \le \eta^d h_{tis}^d + \eta^s h_{tis}^p \le E_i^{max} \qquad \forall i \in \mathcal{H}_2, \forall t \in \mathcal{T}, \forall s \in \mathcal{S} \quad (15)$$

$$0 \le h_{tis} \le H_i^{max} \qquad \forall i \in \mathcal{H}_2, \forall t \in \mathcal{T}, \forall s \in \mathcal{S} \quad (16)$$

$$-T_{ij}^{max} \le f_{tijs} S^{ref} \le T_{ij}^{max} \qquad \forall j \in \mathcal{C}_i, \forall i \in \mathcal{B}, \forall t \in \mathcal{T}, \forall s \in \mathcal{S} \quad (17)$$

Potential wind power production has to be used for wind power production or it has to be curtailed as stated in Equation (2), potential wind power is the only time series which is dependent on scenario as shown by the subscript s. Hydro power reservoirs are governed by the reservoir balance in Equation (3), initial reservoir level is stated in Equation (4) and end reservoir has to follow the handling curve in Equation (5). The storage balance for hydrogen is governed by Equation (6), while the hydrogen balance in Equation (7) states that hydrogen demand can be supplied either by hydrogen directly from the electrolyser, from the storage tanks or from imported hydrogen from other sources.

The energy balance in Equation (8) states that production from wind and hydro power and exchange has to supply consumption by the hydrogen production plant and normal electricity demand. Rationing can be used as an option to balance the production and demand but to a significant cost. A common plan for hydro power production and hydrogen plant power

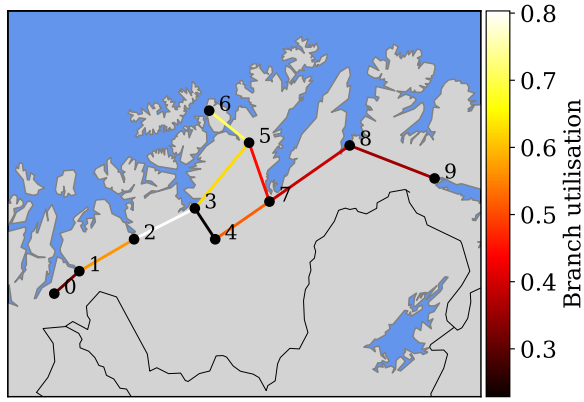

Figure 2: Case study system based on the power system in Finnmark, northern Norway. Lines are colored according to the line utilization in the run with 120 wind power samples. Power is on average flowing from both ends towards node 6.

consumption for all scenarios is the main output from the planning model, the production in each scenario can deviate from these plans as shown in the deviation constraints in Equation (9) and (10), but deviations are penalized in the objective function. This penalization of deviations are necessary as hydro power is modelled by aggregating plants to one plant per bus, if more detailed modelling of hydro power such as start-up cost, ramping constraint, minimum run time, water travel time was included this penalty would have been represented internally by the model.

The nodal balance for power flow is stated in Equation (11), while the line flow is governed by the dc power flow Equation in (12). Finally limits on reservoir volume, production, electrolyser capacity, hydrogen storage capacity and power flow is represented by Equation (13) to (17).

2.3. Simulator

A simulator is used to test the value of the different strategies, the simulator is based on the same formulation as above but for one single scenario. The single wind scenario used in the simulator is the historical realized production and the plan variables are now input parameters. The simulator use the same scheduling horizon as the strategy model, but only the first 24 hours of the simulator results are used as final results. The storage and reservoir levels obtained in the 24th hour of the simulator is sent back to the strategy model for the next iteration of the planning.

3. Case Study

The case study is based on the region of Finnmark in northern Norway, the region has the best wind power potential in Norway and a facility production of LNG at Melkøya. In [6] the same area is studied and different options for grid expansion and wind power development are

Table 1: Bus data for the case system.

Bus Nr.	1	2	3	4	5	6	7	8	9	Sum
Wind [MW]	10.0	0.0	0.0	0.0	200.5	0.0	0.0	40.0	287.1	537.6
Hydro [MW]	80	85	17.7	145.2	4.2	1.1	1.7	55.1	78.3	468.3
Reservoir [GWh]	224.8	231.9	46.5	56.7	5.0	0.0	1.6	168.5	16.1	751.1
Load [GWh/yr]	225.5	35.1	374.3	22.7	121.5	188.2	136.6	80.2	680.3	1864.4

Table 2: Line capacities for the case system.

Line	0, 1	1, 2	2, 3	3, 4	3, 5	4, 7	5, 6	5, 7	7, 8	8, 9
Capacity [MW]	205	179.5	216.5	109.8	216.5	109.8	426.6	261.8	219.6	205.9

analyzed in light of large scale hydrogen production. The system is shown in Figure 2 and consist of a market bus (0) and 9 normal buses (1-9). The most important bus and line data is shown in Table 1 and 2. The hydrogen plant can serve the hydrogen load directly or via storage, the two conversion factors are estimated to 4.66 kWh/Nm^3 and 4.79 kWh/Nm^3 respectively. The hydrogen production plant is located in node 6 and has a electrolyser capacity of 108 MW and a storage capacity of 101 551 Nm^3.

The price in the regulating power market is representative of the flexibility cost of the system, it follow the power price but are about 10% higher for up regulation which is low compared to other systems. Using such a low price results in little difference when considering the uncertainty of wind power as it costs little to change production plans in real time. As the amount of wind power increase and the region is isolated due to grid congestions this regulating price is likely to increase. In the case study the penalty value for deviation for hydrogen production and hydro power plans is set to the same the power price, thus regulating in real time is twice as costly as making the best plan a day ahead.

4. Results

The rolling horizon model is tested with different numbers of wind power scenarios from one, using the expected wind power production, up to 120 scenarios. The preformance of the model is shown in Figure 3. Figure 3a shows the cost of the regional power system, the cost consist of power exchange cost and flexibility penalties. The red line represent the costs obtained when using the expected wind power for planning the operation as in a deterministic model, this typically results in strategies that are close to the limits of the system and perform badly when tested in the simulator for the realized values. The blue line represents the cost when using different amounts of wind power samples, as the number of samples increases the costs decreases due to a better representation of the uncertainty from wind power. The lowest cost that can be obtained is shown by the green line, in this case the realized wind power production is known in the strategy calculation and no changes needs to be made from the original plan resulting in no penalty costs.

The best solution for the stochastic cases are obtained when 90 samples are used. The value of the stochastic solution (VSS), defined as the difference between the expected value solution and the stochastic solution, is in this case 26 893 € or 5.6 % savings in total costs. The expected value of perfect information (EVPI) is the difference between the stochastic solution and the perfect information solution, which is 180 246 € or 37.6 % of cost reduction from the stochastic solution. Better wind power forecasts can reduce the costs for the stochastic solution

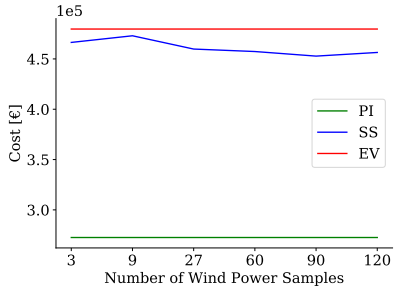

(a) Cost of operating the regional power system using perfect information (PI), stochastic scenarios (SS) or the expected value (EV) in the strategy calculations.

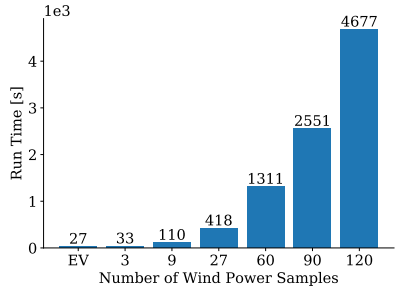

(b) Run time of the strategy calculation, the run time in the simulator is negligible.

Figure 3: Value of the solution and run time for the strategy calculation, showing the performance of the model.

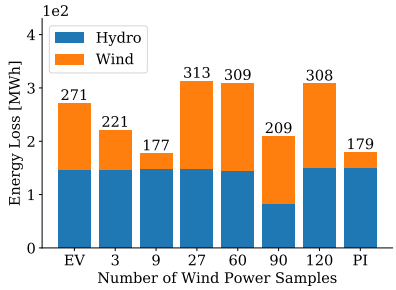

(a) Energy lost from spilling water in hydro power plants or curtailing wind power production.

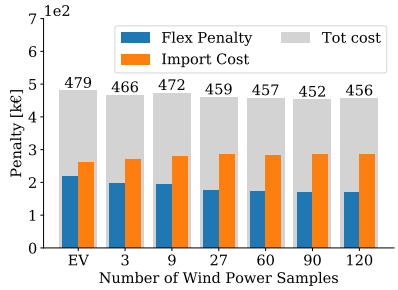

(b) Breakdown of the total costs obtained in the different runs into penalty and import costs.

Figure 4: Energy lost and cost breakdown.

by capturing some of the saving potential from better information, thus increasing the VSS. Both the VSS and EVPI is dependent on the cost of flexibility, reducing the cost of flexibility reduces these values.

Figure 3b show the time used by the strategy calculations for the different number of wind samples. The solution time increases with the number of wind power samples, there is little gain in cost reduction by having more than 27 samples while the solution time increases significantly.

Figure 4a shows the lost energy due to spillage of water or curtailment of wind, the cases with low numbers of wind scenarios have lower wind curtailment compared to the cases where wind power uncertainty is better represented. However, the cases with high wind power curtailment have more reduction in penalty costs than the increase in import costs which results in lower

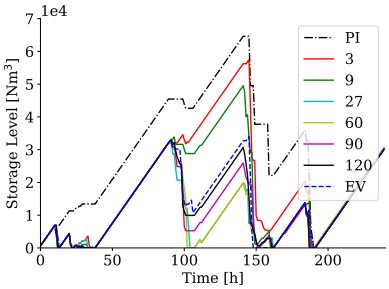

(a) Storage level for hydrogen storage in bus 6.

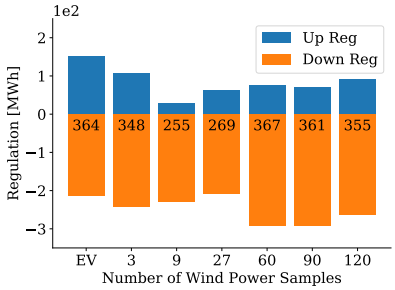

(b) Up and down regulation of the hydrogen load for the different cases. The total up and down regulation is stated inside the bars.

Figure 5: Hydrogen storage level and regulation of the hydrogen plant.

Table 3: Increased flow on lines as a result of hydrogen storage.

Line	0, 1	1, 2	2, 3	3, 4	3, 5	4, 7	5, 6	5, 7	7, 8	8, 9	Mean
EV [%]	-0.32	0.59	0.70	-1.42	1.03	2.22	0.22	-0.60	-0.77	2.12	0.38
120 [%]	1.22	0.83	0.66	1.36	0.65	0.89	0.22	-0.22	-0.05	1.48	0.70
PI [%]	1.43	0.83	0.67	3.16	0.35	-0.17	0.22	0.13	2.60	2.87	1.21

total costs as seen from Figure 4b. Better utilization of the heavily congested line between node 2 and 3 by more accurate scheduling results in higher imports and lower penalty costs.

The storage strategies for solutions with more than 27 samples are quite similar as seen from Figure 5a, in this case the strategy are approaching the expected value strategy as the number of wind power scenarios increase. These strategies are quite different from the perfect information strategy, the low sample strategies 3 and 9 are actually closer. Figure 5b shows how the hydrogen plant energy consumption is regulated from the planned production, it seems like the there isn't any direct relationship between the amount of wind power scenarios and total regulation but the amount of regulation for 60 to 120 scenarios is very similar and is more down regulated than the rest.

The model is also used on the same case study but without hydrogen storage to test the importance of hydrogen storage and how this changes with wind power scenarios. Table 3 shows the increased power flow on the lines when hydrogen storage is included compared to when it is not, the power flow on the lines is on average increased with 0.38 % when using the expected value, 0.7 % when using 120 wind power samples and 1.21 % when using perfect information. These values are small as the system has a lot of flexible hydro power that can be used instead and might be increased by moving the hydrogen production to another node or distributing it over more buses. The most important difference without hydrogen storage is that it results in rationing in hour 100 due to grid congestion on line (2,3) and (4,7), with storage the hydrogen load can be reduced and rationing avoided.

5. Conclusion

A rolling horizon model was developed for assessing the value of including stochastic wind power in a regional power system with hydrogen production. The case study shows that the stochastic model gives solutions that reduce the costs in the system by 5.6 % compared to a deterministic model based on expected values. Using perfect information gives a solution with 37.6 % reduced costs, these results are dependent on the flexibility cost which is set high in this case. This is also the upper limit for how low the costs can become in the stochastic solution, some of these cost reductions can be gained by improving forecasts etc.

Increasing number of scenarios give better solutions, however increasing the number of scenarios to more than 27 gives little reductions in cost compared to the increased run time. Including hydrogen storage gives increased power flow. The increased power flow due to hydrogen storage could be larger in a less flexible system or if the hydrogen load is distributed over several buses. The most important effect of the hydrogen storage is that it helps avoid rationing in specific situations when the transmission grid is constrained.

6. Future Work

In future work the simulator will be integrated into the strategy model such that the first stage simulate the result with the realized wind and the current plan while the second stage makes the plan for the next day. This would result in the model operating more like the markets work in reality, and is similar to the model sequence in [7]. Additionally a feature where deviations in a small range around the reservoir curve is priced based on the water value instead of the deviation penalty will also be considered.

Acknowledgment

This publication is based on results from the research project Hyper, performed under the ENERGIX programme. The authors acknowledge the following parties for financial support: Statoil, Shell, Kawasaki Heavy Industries, Linde Kryotechnik, Mitsubishi Corporation, Nel Hydrogen and the Research Council of Norway (255107/E20).

References

[1] F. R. Førsund, B. Singh, T. Jensen, and C. Larsen, "Phasing in wind-power in Norway: Network congestion and crowding-out of hydropower," *Energy Policy*, vol. 36, pp. 3514–3520, 2008.

[2] NVE, "Vindkart for Norge," 2009. [Online]. Available: https://www.nve.no/energiforsyning-og-konsesjon/vindkraft/vindressurser/

[3] M. Korpås and A. T. Holen, "Operation planning of hydrogen storage connected to wind power operating in a power market," *IEEE Transactions on Energy Conversion*, vol. 21, no. 3, pp. 742–749, 2006.

[4] M. Korpås and C. J. Greiner, "Opportunities for hydrogen production in connection with wind power in weak grids," *Renewable Energy*, vol. 33, no. 6, pp. 1199–1208, 2008.

[5] C. J. Greiner, M. Korpas, and T. Gjengedal, "A Model for Techno-Economic Optimization of Wind Power Combined with Hydrogen Production in Weak Grids," *EPE Journal*, vol. 19, no. 2, pp. 52–59, jun 2009.

[6] E. F. Bødal and M. Korpås, "Regional Effects of Hydrogen Production in Congested Transmission Grids with Wind and Hydro Power," in *14th International Conference on the European Energy Market*, 2017.

[7] Y. Wang, Z. Zhou, A. Botterud, K. Zhang, and Q. Ding, "Stochastic coordinated operation of wind and battery energy storage system considering battery degradation," *Journal of Modern Power Systems and Clean Energy*, vol. 4, no. 4, pp. 581–592, 2016.

[8] P. Meibom, R. Barth, B. Hasche, H. Brand, C. Weber, and M. O'Malley, "Stochastic optimization model to study the operational impacts of high wind penetrations in Ireland," *IEEE Transactions on Power Systems*, vol. 26, no. 3, pp. 1367–1379, 2011.

[9] P. Pinson, H. Madsen, and G. Papaefthymiou, "From Probabilistic Forecasts to Statistical Scenarios of Short-term Wind Power Production," *WIND ENERGY Wind Energ*, vol. 12, pp. 51–62, 2009.

[10] J. B. Bremnes, "A comparison of a few statistical models for making quantile wind power forecasts," *Wind Energy*, vol. 9, no. 1-2, pp. 3–11, jan 2006.

A.3 Value of hydro power flexibility for hydrogen production in constrained transmission grids

INTERNATIONAL JOURNAL OF HYDROGEN ENERGY 45 (2020) 1255–1266

Available online at www.sciencedirect.com

ScienceDirect

journal homepage: www.elsevier.com/locate/he

Value of hydro power flexibility for hydrogen production in constrained transmission grids

Espen Flo Bødal[*], *Magnus Korpås*

Department of Electric Power Engineering Norwegian University of Science and Technology, NTNU O. S. Bragstads Plass 2E, 7034 Trondheim, Norway

ARTICLE INFO

Article history:
Received 15 November 2018
Received in revised form
1 May 2019
Accepted 3 May 2019
Available online 28 May 2019

Keywords:
Power system analysis
Hydro power
Wind power
Large scale hydrogen production
Energy storage

ABSTRACT

The cost of large scale hydrogen production from electrolysis is dominated by the cost of electricity, representing 77–89% of the total costs. The integration of low-cost renewable energy is thus essential to affordable and clean hydrogen production from electrolysis. Flexible operation of electrolysis and hydro power can facilitate integration of remote energy resources by providing the flexibility that is needed in systems with large amounts of variable renewable energy. The flexibility from hydro power is limited by the physical complexities of the river systems and ecological concerns which makes the flexibility not easily quantifiable. In this work we investigate how different levels of flexibility from hydro power affects the cost of hydrogen production.

We develop a two-stage stochastic model in a rolling horizon framework that enables us to consider the uncertainty in wind power production, energy storage and the structure of the energy market when simulating power system operation. This model is used for studying hydrogen production from electrolysis in a future scenario of a remote region in Norway with large wind power potential. A constant demand of hydrogen is assumed and flexibility in the electrolysis operation is enabled by hydrogen storage. Different levels of hydro power flexibility are considered by following a reservoir guiding curve every hour, 6 h or 24 h.

Results from the case study show that hydrogen can be produced at a cost of 1.89 €/kg in the future if hydro power production is flexible within a period of 24 h, fulfilling industry targets. Flexible hydrogen production also contributes to significantly reducing wasted energy from spillage from reservoirs or wind power curtailment by up to 56% for 24 h of flexibility. The results also show that less hydro power flexibility results in increased flexible operation of the electrolysis plant where it delivers 39–46% more regulating power, operates more on higher power levels and stores more hydrogen.

* *Corresponding author.*
E-mail address: espen.bodal@ntnu.no (E.F. Bødal).
https://doi.org/10.1016/j.ijhydene.2019.05.037

1256 INTERNATIONAL JOURNAL OF HYDROGEN ENERGY 45 (2020) 1255–1266

Nomenclature

Indices

i, j	Bus
s	Second stage node
t	Time stage

Parameters

Δ	Price addition for import [€ /MW]
$\eta^{d/s}$	Conversion factor, power to hydrogen [MWh/Nm^3], directly or via storage
λ_t^s	Day-ahead price [€ /MWh]
ρ_s	Probability of wind power scenario
C_t^d	Cost for deviating from schedual [€ /MWh]
$C^{r/i}$	Cost of rationing [€ /MWh] or hydrogen import [€ /Nm^3]
$C^{v+/v-}$	Cost for violating end reservoir level [€ /MWh]
D_{ti}	Electricity demand [MWh]
E_i^{max}	Capacity of electrolysis plant [MW]
H_t^D	Hydrogen demand [MWh]
H_i^{max}	Capacity of hydrogen storage [Nm^3]
I_{ti}	Inflow to hydro power reservoirs [MWh]
$P_{ti}^{min/max}$	Min or max power production [MW]
P_{tis}^w	Wind power scenario [MWh]
S^{ref}	Reference power for the system [MW]
T_{ij}^{max}	Transmission capacity from bus i to j [MW]
$V_i^{0/max}$	Initial volume or max capacity for reservoir [MWh]
X_{ij}	Reactance between bus i and j [p.u.]
$\mathscr{B}$	All buses
$\mathscr{C}_i$	Buses connected to bus i by transmission lines
$\mathscr{H}, \mathscr{W}, \mathscr{P}, \mathscr{H}_2$	Hydro power, wind power, all power plants or hydrogen plants
$\mathscr{M}$	Market Bus
$\mathscr{N}$	Normal buses (excl. market bus)
$\mathscr{S}$	Wind Power Scenario
$\mathscr{T}$	Time stages

Variables

δ_{tis}	Voltage phase angle at bus
c_{tis}	Energy curtailment [MW]
$d_{tis}^{exp/imp-/+}$	Negative/positive change in export/import [MW]
$d_{tis}^{H_2-/+}$	Negative/positive change in hydrogen production [MW]
$d_{tis}^{hydro-/+}$	Negative/positive change in hydro power production [MW]
f_{tijs}	Power flow from bus i to j [p.u.]
h_{tin}^d	Hydrogen directly from electrolysis [Nm^3]
h_{tis}^{imp}	Hydrogen imported/not served [Nm^3]
h_{tin}^p	Hydrogen to storage [Nm^3]
h_{tin}^s	Hydrogen from storage [Nm^3]
h_{tin}	Hydrogen storage level [Nm^3]
$p_{tis}^{imp/exp}$	Power import or export [MW]
p_{tis}	Production [MW]
r_{tis}	Rationing of power [MW]
s_{tin}	Spillage/bypass of water [MWh]
$v_n^{+/-}$	Violation of end reservoir level [MWh]
v_{tin}	Reservoir level [MWh]

Introduction

In 2015, 96% of all hydrogen production was based on fossil energy sources such as natural gas, coal and oil, resulting in a significant carbon footprint [1]. Natural gas is the largest energy source for fossil hydrogen production with 46% of the global market. To reduce the carbon footprint of hydrogen production from natural gas, CO_2 can be captured from the production process using steam-methane reforming (SMR). SMR has a typical capture rate of 90% of the produced CO_2, reducing emissions from 9.26 to 0.93 kg CO_2/kg H_2 according to case studies by the National Renewable Energy Laboratory (NREL) [2]. NREL estimates the current prices of large-scale hydrogen production from natural gas with carbon sequestration at 340 ton/day to be 1.56 $[1]/kg in 2015, for a plant starting up in 2040 the costs increase to 1.72 $/kg H_2 due to higher feed stock costs as a result of higher natural gas prices.

The other commercial option for hydrogen production is to produce hydrogen by electrolysis, using either alkaline, proton exchange membranes (PEM) or solid oxide (SO) electrolysis [3]. Alkaline and PEM electrolysis are mature technologies, while SO is still in the R&D-phase. The carbon footprint of hydrogen produced from electrolysis depends on the emissions of the electricity source, if the electric power used for the electrolysis is renewable, such as solar, wind or hydro power, the hydrogen has a very low carbon footprint.

[1] Monetary values from NREL cases are in 2016 dollars.

The largest electrolysis plant for hydrogen production installed in history was used to produce ammonia for use in fertilizer at Rjukan in Norway with a capacity of 60 ton/day [3], which would amount to about 130 MW of electric load using today's alkaline electrolysers. Currently an electrolysis plant is under planning in connection to Rhineland refinery in Germany and will be the largest electrolysis plant in the world for hydrogen production with a capacity of about 3.6 ton/day [4].

Small scale wind-hydrogen systems are extensively studied in the past and several test facilities are in operation as for example at Utsira in Norway [5] and other countries such as United States, Canada, Germany, Italy, Finland, United Kingdom, Japan, and Spain [6]. Different types of systems exist with different purposes, ranging from pure energy storage systems as at Utsira where hydrogen is stored and used in fuel cells to generate electricity at a later time to systems where hydrogen is produced as a product for use as fuel or in industrial processes known as power-to-gas [7]. Hydrogen storage solutions are increasingly considered as alternative to electric power grid upgrades in rural areas with weak or no grid connections such as the islands communities along the Norwegian Coast, the Faroe Islands and Svalbard [8–11].

For a large-scale electrolysis plant built in 2015 with PEM electrolysers and a production capacity of 50 ton/day the hydrogen production cost estimated by NREL was 5.18 $/kg, while a for a plant built in 2040 it is 4.48 $/kg. The expected reduction in hydrogen production cost is due to a reduction in total capital costs of about 60%, whereof the cost of

electrolysers are assumed to be reduced from 900 to 400 $/kW in line with observations and expert expectations [12]. The share of the total production costs that arise from electricity consumption thus increase from 77.2% to 88.5%, while the electricity price is assumed not to be significantly different in this case. This shows that the price of hydrogen production from electrolysis is going to be even more heavily influenced by the electricity price in the future as the capital cost of electrolysis is reduced [13]. The US Department of Energy (DoE) estimated the cost of alkaline electrolysis to be 4.75 $/kg in 2011 and set targets of 3.47 and 2.32 $/kg in 2015 and 2020 respectively. The DOE cost targets for hydrogen production include a significant reduction in electricity price from to 0.073 $/kWh in 2011 to 0.057 and 0.036 $/kWh for 2015 and 2020 respectively [14].

To lower the cost of electrolytic hydrogen production the electrolysis facility need to be located in an area with low electricity costs. The cost of renewable energy technologies such as wind and solar power has dropped significantly the latest years and are now competitive with producing electricity from coal and other fossil sources [15]. The areas with the best conditions for producing renewable electricity is often located far from consumers and are not developed due to the large costs of constructing transmission lines [16]. This creates areas with low-cost clean electric energy that is "trapped" due to it's location and insufficient transmission infrastructure such as western China [17], the North-Sea region [18] or western Texas [13]. Producing hydrogen in these areas can be a way to utilize these energy sources without building costly transmission lines [19–21]. However, there are still are significant costs associated with transporting hydrogen to consumers, but it can be done in a more flexible way in the form of gaseous hydrogen, liquefied hydrogen or ammonia on ships, trucks or in pipelines.

To produce hydrogen in an area with a lot of intermittent renewable energy we need extra electrolysis capacity and hydrogen storage. Hydrogen storage allows the hydrogen production plant to run flexibly to counteract the variations in electricity produced from renewable sources [22]. This flexibility allows for integration of more renewable energy, has significant value to the electric power system [23] and is a popular topic in electric power system research [24].

Rolling horizon is a framework for optimization models where the same model is solved sequentially with a constant horizon, the parameters are updated and are dependent on the solution of the previous instance of the model. This framework is frequently used when studying integration of renewable energy and the regulating market. The sequential temporal structure of the rolling horizon framework is a realistic way to simulate how energy markets work in practice and gives a good representation of the challenges arising from renewables resulting in more uncertainty in power system operation [25], flexible hydrogen production [26] or energy storage management [27]. Rolling horizon based models are more computationally tractable than more sophisticated scenario-tree based models that often requires parallel computing on high performance computers to allow for detailed modelling of large power systems [28].

The value of flexible hydrogen production is dependent on other sources of flexibility in the power system. In systems dominated by hydro power with reservoirs there are potentially a lot of available flexibility as water can be stored for later. However, it is not obvious to which extent hydro power producers will be able to deliver flexibility due to the complexity of the waterways, variation in inflow and grid constraints. In this paper, we investigate the impact short-term hydro power flexibility has on the value of flexible hydrogen production.

The rolling horizon modelling framework presented in this paper is a further development of previous work [29] and includes the combination of power flow, long-term hydro power storage and short-term hydrogen storage in addition to short-term wind power uncertainty. In this work we focus on shorter term uncertainties, and leave out the long-term uncertainty and some of the modelling details. The long-term uncertainty can have a significant impact on the hydro power strategies, but the problem would be intractable when considering both long and short-term uncertainties in the same optimization model. The market structure of the current electric power system is included, modelled as a two-stage optimization problem with a day-ahead market and a simplified model of the real-time balancing market. The regional power system is modelled with a detailed grid description, including electric loads, hydro power plants, wind power plants, and a facility for large-scale electrolysis and hydrogen liquefaction.

In Section Method we explain the main parts of the model, which can be grouped into three parts; how the wind power scenarios are generated, the two-stage optimization model and the rolling horizon framework. The case study of a remote area in northern Norway is presented in Section Case study. In Section Results the results from the case study are presented and discussed, while the conclusions are given in Section Conclusion.

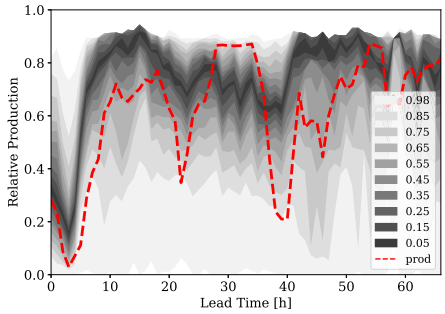

Fig. 1 – Example of a quantile forecast. The different colors represents probability intervals for the wind power production for a given hour ahead in time. The green line represents the actual production that occurred. (For interpretation of the references to colour in this figure legend, the reader is referred to the Web version of this article.)

Method

Wind power forecasting

Numerical weather predictions and historical observations of produced wind power are used to create quantile forecasts as shown in the example in Fig. 1. This is done by using wind speeds and directions from weather forecasts made by The Norwegian Meteorological Institute [30] and recorded production by the Norwegian Water Resources and Energy Directorate [31] in a local quantile regression algorithm as described in detail in Ref. [32]. The local quantile regression is formulated as a linear optimization problem as described in Ref. [33] and solved. One optimization problem has to be solved for each wind power plant, quantile and lead-time resulting in solving a lot of small optimization problems for making one quantile forecast.

From the quantile forecast we can sample wind power scenarios [34], in short we use the historical production records to create a correlation matrix for spatial and temporal correlations and sample scenarios from a multivariate normal distribution which is transformed into wind power scenarios using the culumative gaussian normal distribution and the cumulative distribution function (cdf) of the quantile forecasts.

Rolling horizon framework

For each day in the rolling horizon algorithm a two-stage optimization problem is solved. The two stages are replicating the structure of the Nordic electric power market [35] and are illustrated in Fig. 2. In the first stage, we are following a production schedule that was made the day before, while making the needed adjustments as one would in the regulating power market to balance supply and demand of electricity. The hour-to-hour adjustments to the production schedule comes at a higher cost, representing a premium of readiness related to costs that arise for delivering power on short notice [36].

The production schedule that is followed in the first stage represents the day-ahead market bids, where producers make an optimal dispatch based on the information they have the day before the actual operational day. We assume that the producers are risk-neural, such that the day-ahead generation schedule is the one that gives the lowest expected costs considering a set of scenarios for wind power production.

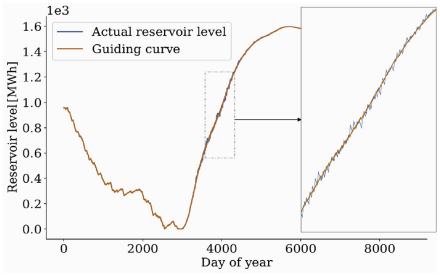

Fig. 3 – Example of the reservoir level following the guiding curve for long-term hydro power management.

The production schedule for the next day is represented by the first 24 h of the second stage. This schedule is sent to the next two-stage problem as the rolling algorithm moves on to the next iteration. The consecutive two-stage problems are connected through these production schedules, the storage levels in the hydrogen storage and reservoirs, which are passed between them in the rolling horizon algorithm. In this way the rolling horizon algorithm rolls though the year, with a separate two-stage problem representing each day where they all are connected by passing on information about generation schedules and storage levels. This gives a realistic representation of how the system is operated as it preserves the chronology of information, such as how much wind power we expect tomorrow at a given instance in time.

Long-term strategy

As hydro power reservoirs can store water for many years the short-term scheduling horizon of the rolling horizon model, which is in the range of several days to a couple of weeks, is too short to determine a good reservoir operation strategy. Thus a long-term strategy needs to be an input to the rolling horizon model, there are several ways to implement this strategy and here we use guiding curves as shown in Fig. 3, meaning an input reservoir level that has to be reached at specified times e.g. the end of the day. This gives the rolling

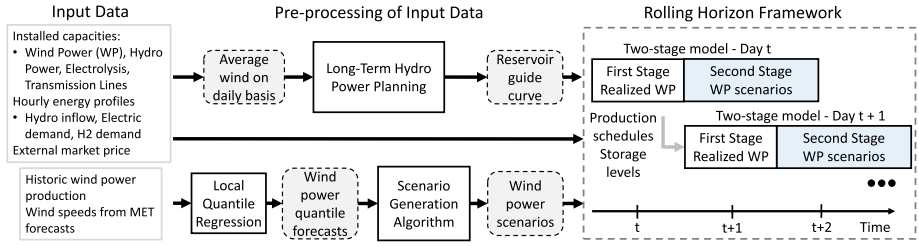

Fig. 2 – Illustration of the input data, modelling steps and rolling horizon framework.

horizon model the opportunity to use hydro power as a source of flexibility in the short-term, while also considering a long-term strategy. The intra-day variations from the guiding curve look small due to the large amount of energy stored in the reservoir, but have a significant impact on the result. A more sophisticated method would be to use a water-value matrix [37,38], setting the marginal value of the water at different times and reservoir levels, but this is more complicated and not the focus of this work.

The combination of modelling short-term stochastic properties of renewables and flexibility from resources with both short and long-term storage in a tractable way separates this work from previous work on integration of renewables or hydrogen production, that usually focus either on short-term dynamics or long-term trends.

Regional power system operation

The mathematical formulation of the two-stage optimization problem is presented in the following equations. The objective is given in Eq. (1) and represents the optimal operation of a region of the power system. The objective is to find a solution that minimize the operational costs of supplying regional electric and hydrogen loads that are given by load-profiles. This is equivalent to maximizing the profit from selling power to the rest of the system, represented by the market bus (i = 0). For simplicity of notation the first stage is included in the set of scenarios or nodes with a probability of one ($\rho_0 = 1$).

$$\max \sum_{s\in\mathscr{S}}\rho_s\left[\sum_{t\in\mathscr{T}}\left[\lambda^s_t p^{imp}_{t0s} - (\lambda^s_t+\Delta)p^{exp}_{t0s} - \sum_{i\in\mathscr{I}} C^r r_{tis} - \sum_{i\in\mathscr{H}_2} C^i h^i_{tis} - \sum_{i\in\mathscr{H}_2} C^d_t\left(d^{H_2-}_{tis} + d^{H_2+}_{tis}\right) - \sum_{i\in\mathscr{H}} C^d_t\left(d^{hydro-}_{tis} + d^{hydro+}_{tis}\right) - \sum_{i\in\mathscr{H}} C^d_t\left(d^{exp-}_{tis} + d^{exp+}_{tis} + d^{imp-}_{tis} + d^{imp+}_{tis}\right)\right] - \sum_{i\in\mathscr{H}}\left(C^{v+}v^+_{is} + C^{v-}v^-_{is}\right)\right] \tag{1}$$

In the two first terms of the objective function we have the power price, λ^s_t, times imports to, p^{imp}_{t0s}, and exports from, p^{exp}_{t0s}, the market bus, meaning income from exports from the system and costs of imports to the system respectively. An additional margin, Δ, is added to the power price for importing power to represent grid tariffs. The electric and hydrogen loads within the region have to be served, in the case the required load cannot be served penalties are included for rationing power, r_{tis}, and rationing/importing hydrogen from other sources, h^i_{tis}, in the third and fourth term. The cost of deviating from the production schedule for the controllable units, hydro power, $d^{hydro-/+}_{tis}$, hydrogen loads, $d^{H_2-/+}_{tis}$, and import or export to the market bus, $d^{exp/imp-/+}_{tis}$, are included in the fifth, sixth and seventh term of the objective function. The final part of the objective function ensures that at the reservoir levels follow the long-term strategy described by the guiding curves for the hydro power reservoirs at specified times, any deviation, $v^{-/+}_{is}$, from the specified reservoir levels results in a penalty in the objective.

$$p_{tis} + c_{tis} = P^w_{tis} \quad \forall i\in\mathscr{W}, \forall t\in\mathscr{T}, \forall s\in\mathscr{S} \tag{2}$$

Wind power, P^w_{tis}, cannot be stored and has to be used for production of electricity, p_{tis}, when available or curtailed, c_{tis}, as stated in Equation (2).

$$v_{tis} = v_{(t-1)is} - p_{tis} - s_{tis} + I_{ti} \quad \forall i\in\mathscr{H}, \forall t\in\mathscr{T}, \forall s\in\mathscr{S} \tag{3}$$

$$v_{0is} = V^0_i \quad \forall i\in\mathscr{H}, \forall s\in\mathscr{S} \tag{4}$$

$$v_{Tis} - v^+_{is} + v^-_{is} = V^{curve}_{T,i} \quad \forall i\in\mathscr{H}, \forall s\in\mathscr{S} \tag{5}$$

Hydro power plants often have reservoirs and can store water to be used later, this is governed by the reservoir balance in Eq. (3), where the reservoir level at the end of a time-step, v_{tis}, is equal to the reservoir level at the end of the previous time-step, $v_{(t-1)is}$, minus production, p_{tis}, and spillage, s_{tis}, plus the inflow to the reservoir, I_{ti}. The initial reservoir level, v_{0is}, is known and set by Eq. (4) while the end reservoir level, v_{Tis}, should follow the long-term strategy given by the guiding curve, $V^{curve}_{T,i}$, as stated in Eq. (5) or penalties will occur in the objective function.

$$h_{tis} = h_{(t-1)is} + h^p_{tis} - h^s_{tis} \quad \forall i\in\mathscr{H}_2, \forall t\in\mathscr{T}, \forall s\in\mathscr{S} \tag{6}$$

$$h^d_{tis} + h^s_{tis} + h^i_{tis} = H^D_{tis} \quad \forall i\in\mathscr{H}_2, \forall t\in\mathscr{T}, \forall s\in\mathscr{S} \tag{7}$$

The hydrogen plant also has a storage which is governed by the hydrogen storage balance in Eq. (6). This is similar to the reservoir balance for hydro power reservoirs, the main difference is that loading of the hydrogen storage is governed by a decision variable for hydrogen production to storage, h^p_{tis}, as compared to the inflow in the reservoir balance which is a parameter and thus not controllable. Eq. (7) is the hydrogen balance and makes sure the required amount of hydrogen is supplied to the hydrogen load, H^D_{tis}, either directly from the electrolyser, h^d_{tis}, from storage, h^s_{tis}, or imported from other sources, h^i_{tis}, at high costs.

$$\sum_{j\in\mathscr{P}_i} p_{tjs} - \eta^d h^d_{tis} - \eta^s h^p_{tis} - p^{exp}_{tis} + p^{imp}_{tis} + r_{tis} = D_{ti} \quad \forall i\in\mathscr{N}, \forall t\in\mathscr{T}, \forall s\in\mathscr{S} \tag{8}$$

The energy balance is shown in Eq. (8) and states that produced energy from all sources connected to a bus plus imported electricity, p^{imp}_{tis}, has to be equal to the electricity needed to cover normal electric demand, D_{ti}, exported electricity, p^{exp}_{tis}, and electricity for hydrogen production, $\eta^s h^p_{tis}$ and $\eta^s h^p_{tis}$. If this is not the case, demand has to be rationed, r_{tis}, which represents a high cost. The energy demand for hydrogen production is divided into two parts, hydrogen produced directly to the hydrogen load, h^d_{tis}, or hydrogen produced to storage, h^p_{tis}, as hydrogen produced to storage demands more energy per unit of hydrogen due to compression to higher pressure.

$$d^{H_2-}_{tis} - d^{H_2+}_{tis} = \eta^d\left(h^{d,plan}_{ti} - h^d_{tis}\right) + \eta^s\left(h^{p,plan}_{ti} - h^p_{tis}\right) \quad \forall i\in\mathscr{H}_2, \forall t\in\mathscr{T}, \forall s\in\mathscr{S} \tag{9}$$

$$d^{hydro-}_{tis} - d^{hydro+}_{tis} = p^{plan}_{ti} - p_{tis} \quad \forall i\in\mathscr{H}, \forall t\in\mathscr{T}, \forall s\in\mathscr{S} \tag{10}$$

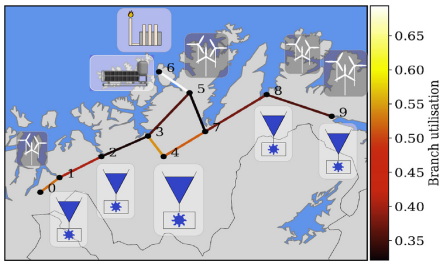

Fig. 4 – Illustration of the case study in Finnmark, northern Norway. Hydrogen production is located in node 6 with electrolysis, SMR and liquefaction. Buses 1, 5, 8 and 9 have wind farms and buses 1, 2, 4, 8 and 9 have hydro power plants. The size of the symbols indicate the installed capacities of each technology. The Transmission lines are colored with the average branch utilization.

$$d_{tis}^{exp-} - d_{tis}^{exp+} = p_{ti}^{exp,plan} - p_{tis}^{exp} \quad \forall i \in \mathcal{M}, \forall t \in \mathcal{T}, \forall s \in \mathcal{S} \tag{11}$$

$$d_{tis}^{imp-} - d_{tis}^{imp+} = p_{ti}^{imp,plan} - p_{tis}^{imp} \quad \forall i \in \mathcal{M}, \forall t \in \mathcal{T}, \forall s \in \mathcal{S} \tag{12}$$

In Eqs. (9) and (10) variables are used to account for positive and negative deviations, $d_{tis}^{hydro-/+}$ or $d_{tis}^{H_2-/+}$, from the production schedules for hydro power production and hydrogen demand, p_{ti}^{plan} or $h_{ti}^{d,plan}$. Similar, Eqs. (11) and (12) accounts for deviations from the schedules for import, d_{tis}^{imp+}, and export, d_{tis}^{exp+}, from or to the market bus. In the first stage the production schedules are a parameter-input from the previous run of the two-stage model, while for the second stage the production schedules are variables that are common for all scenarios (no s in the subscript) and determined by the optimization.

$$p_{ti}^{exp} - p_{ti}^{imp} = S^{ref} \sum_{j \in \mathcal{C}_i} f_{tij} \quad \forall i \in \mathcal{B}, \forall t \in \mathcal{T}, \forall s \in \mathcal{S} \tag{13}$$

Table 1 – Bus data for the case system. The electricity for hydrogen production and liquefaction is included in the bus 6 load. Liquefaction represent a constant load profile amounting to 1436 GWh/yr. The hydrogen production electric load profile is a result of the optimization with a total electricity demand of 946 GWh/yr.

Bus	Wind	Hydro	Reservoir	Inflow	Load
Nr.	[MW]	[MW]	[GWh]	[GWh/yr]	[GWh/yr]
1	10.0	80	224.8	303.6	225.5
2	0.0	85	231.9	363.5	35.1
3	0.0	17.7	46.5	92.3	374.3
4	0.0	145.2	56.7	894.6	22.7
5	200.5	4.2	5.0	16.4	121.5
6	6.7	1.1	0.0	3.0	2570.8
7	0.0	1.7	1.6	16.3	136.6
8	40.0	55.1	168.5	196.6	80.2
9	387.1	78.3	16.1	82.4	680.3
Sum	644.3	468.3	751.1	1968.7	4247.0

$$f_{tijs} = \frac{1}{X_{ij}} (\delta_{tis} - \delta_{tjs}) \quad \forall j \in \mathcal{C}_i, \forall t \in \mathcal{T}, \forall i \in \mathcal{B}, \forall s \in \mathcal{S} \tag{14}$$

The nodal flow balance in Eq. (13) states that the sum of all power flows, f_{tij}, from a bus is equal to net power injected into the grid at that location, ie. the difference between power exported, p_{ti}^{exp}, and power imported, p_{ti}^{imp}. The power flow on each individual transmission line is dependent on the differences in voltage angle, δ_{tis}, between the two buses and the inverse of the line reactance, X_{ij}, as described by the dc power flow equation in Eq. (14). The dc power flow equations are linearized versions of the full ac power flow equations and are widely used to represent power flow in large power system models [39]. Eqs. (15)–(19) states the upper and lower bounds for reservoir level, produced power, electrolyser power, hydrogen storage level and line flow.

$$0 \le v_{tis} \le V_i^{max} \quad \forall i \in \mathcal{H}, \forall t \in \mathcal{T}, \forall s \in \mathcal{S} \tag{15}$$

$$P_{ti}^{min} \le p_{tis} \le P_i^{max} \quad \forall i \in \mathcal{H}, \forall t \in \mathcal{T}, \forall s \in \mathcal{S} \tag{16}$$

$$0 \le \eta^d h_{tis}^d + \eta^s h_{tis}^p \le E_i^{max} \quad \forall i \in \mathcal{H}_2, \forall t \in \mathcal{T}, \forall s \in \mathcal{S} \tag{17}$$

$$0 \le h_{tis} \le H_i^{max} \quad \forall i \in \mathcal{H}_2, \forall t \in \mathcal{T}, \forall s \in \mathcal{S} \tag{18}$$

$$-T_{ij}^{max} \le f_{tijs} S^{ref} \le T_{ij}^{max} \quad \forall j \in \mathcal{C}_i, \forall i \in \mathcal{B}, \forall t \in \mathcal{T}, \forall s \in \mathcal{S} \tag{19}$$

The model is implemented in Python using the PYOMO optimization package and solved with the GUROBI optimization solver. We run the model on a Dell Latitude E7470 laptop and the typical solution time is 6–7 h for the case study.

Case study

The rolling horizon model is used in a case study for large-scale hydrogen production in Finnmark, northern Norway. The Region is illustrated in Fig. 4 and has a constrained grid connection towards the south of Norway where most of the consumption is located. This region is a favorable region in Norway for on-shore wind power, but most of its potential is not developed due to transmission constraints. The installed wind power in this case study is set to be three times the present capacity. The hydrogen production facility is placed in bus 6 where there is currently a facility for production of liquefied natural gas. An overview of power plants, electric loads and transmission capacities are given in Tables 1 and 3 based on data from the Norwegian Natural Resources and Energy Directorate [40] and Statistics Norway [41] (see Table 2).

Table 2 – Parameter input to the model in €/MWh. The electricity price series in market node is represented by the average value.

Mean electricity price	$\overline{\lambda^s}$	20.44
Rationing	C^r	5000
Guiding curve deviation	$C^{v+/v-}$	50
Hydrogen import	C^i	6000
Regulating cost [% of spot price]	C_t^d	0.15/0.30

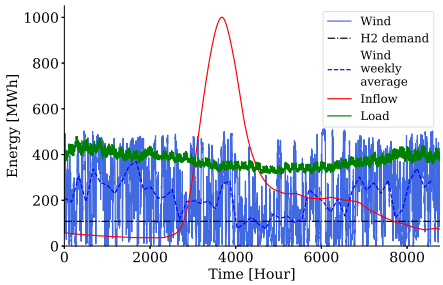

Fig. 5 – Profiles for the total energy available from wind and inflow or consumed by the electrical and hydrogen loads throughout 2015, used as input to the model.

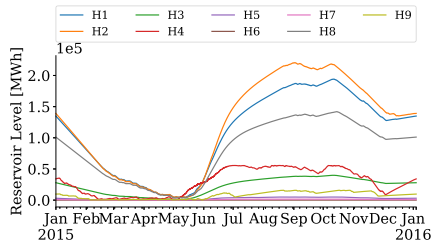

Fig. 6 – Long-term strategies for hydro power reservoirs according to bus number. The strategies are results from a long-term operational model for the system that uses perfect foresight of mean daily wind power.

Electric loads and market prices in the market bus are represented by historical data for 2015 from Nord Pool [42]. The total profiles for all available energy, wind and inflow, and demand, electricity and hydrogen, is shown in Fig. 5. Weekly average wind power and electric load has a clear correlation with lower levels in the summer and higher levels in the winter, while hydro power inflow has a characteristic peak when the snow melts in the spring. The need for both short and long-term storage is apparent to be able to match the fluctuating wind energy and the peak in hydro power inflow with the demand profiles.

The guiding curves for the long-term hydro reservoir strategies are shown in Fig. 6 and obtained from a deterministic operational model using average daily wind power. The electrolysis plant is assumed to serve a hydrogen demand of 50 ton/day, equivalent to an electric load of 108 MW, which would make it the largest electrolysis plant in the world for hydrogen production only comparable to the decommissioned Rjukan plant. The hydrogen demand is constant as it goes to a liquefaction plant that is assumed to be in constant operation.

In this case study we use installed capacities based on results from a deterministic investment model used for sizing of electrolysis capacity, hydrogen storage and installed wind power capacities for a given electric transmission grid scenario [43]. However, as shown in Table 3, the transmission capacities had to be significantly increased from the deterministic model output to avoid rationing as a result of introducing uncertainty from wind power. More electrolysis capacity is added to include more flexibility in the system. In summary the electrolysis capacity is 150 MW (2894 kg/h) and hydrogen storage is 9129 kg. This equals a minimum depletion time of the hydrogen storage of about 4.4 h and a minimum filling time of 11.6 h when considering the constant hydrogen load. The hydrogen plant can either serve the hydrogen load directly at an energy consumption of 51.8 kWh/kg or fill the storage at 53.3 kWh/kg at 350 bar [44]. The electrolysis plant is assumed be co-located with hydrogen production from natural gas, where the natural gas plant produces 450 ton/day based on steam-methane reforming (SMR). The hydrogen is liquefied and transported by ship to a region where energy is needed. The net energy demand for the SMR and liquefaction process is added to the load profile for bus 6 as a constant load at 164 MW, where the SMR process includes steam turbines resulting in a surplus of 14 MW electric power and the liquefaction demand of 178 MW.

Hydro power is allowed to deviate from the guiding curve within a certain interval of hours depending on the flexibility level without receiving any penalties as explained above. Six cases are considered in total by combining three different levels for hydro power flexibility for two different regulating price premiums (RP). The flexibility intervals are set to 0, 6 and 24 h and denoted as low, medium or high hydro power flexibility. The regulating price premium is 15 and 30% of the day-ahead price both for up and down regulation. It should be noted that these numbers are set higher than observed in the market today, which is typically around 10% [36]. This is due to the relatively low amounts of wind power in the Nordic area compared to flexible hydro power, but may change as more variable wind power is integrated into the power system and more flexibility is needed for balancing supply and demand of electricity [35]. The number of wind power samples needed to give a good representation of the uncertainty is investigated in Ref. [45], in this case study we use 30 wind power samples as

Table 3 – Line reactance and capacities for the case system, including an adjustment factor for line capacity compared to a deterministic sizing model.

Line	0, 1	1, 2	2, 3	3, 4	3, 5	4, 7	5, 6	5, 7	7, 8	8, 9
Reactance [p.u]	0.027	0.035	0.046	0.075	0.076	0.147	0.028	0.031	0.048	0.047
Capacity [MW]	307.5	359.0	433.0	109.8	324.8	109.8	426.6	523.6	439.2	411.4
Cap Increase	1.5	2.0	2.0	1.0	1.5	1.0	1.0	2.0	2.0	2.0

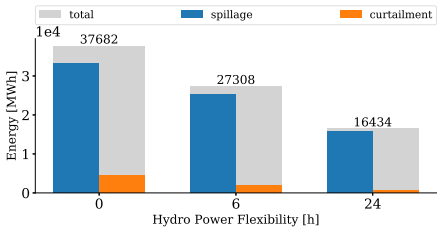

Fig. 7 – Energy wasted by spilling water from hydro power or curtailing wind power over the year for the low regulating price. Energy wasted in a model with perfect foresight of wind power production is subtracted from these numbers.

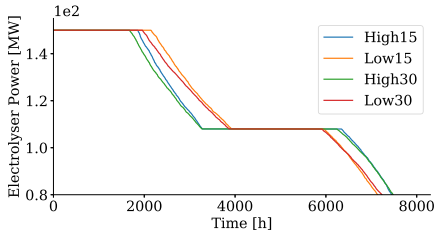

Fig. 9 – Duration curves for the electrolysis power for high and low hydro power flexibility and regulating prices of 15 and 30% of the day-ahead price.

more samples increase the solution time without significant improvements of the solution.

Results

The regional power system is almost in net balance with respect to the annual energy use versus production, thus the total costs are mainly determined by the regulating costs. As regulating penalties occur when using any resource to react to deviations from expected wind power production, which are the same for all cases, there are only small differences of 1.7–3.4% in the total costs of the system for the different levels of hydro power flexibility. These differences are mainly due to the fact that more energy is wasted when hydro power is less flexible and can't react to unforeseen wind power, which leads to more spillage and curtailment as seen in Fig. 7 for the low regulating price. For increasing hydro power flexibility the total amount of wasted energy is substantially decreased, compared to the worst case with no hydro power flexibility the energy waste is reduced by 28% and 56% when increasing the flexibility to 6 and 24 h. The increase in wasted energy due to higher regulation prices is smaller and range from 2 to 9%.

The total amount of regulating power needed to balance the system is the same in all the cases, the main difference are how the regulating power is distributed between the different hydro power plants and the electrolysis. In the low hydro power flexibility case, hydro power is still used for regulation, but at higher costs as the reservoir levels are deviating from the reservoir guide curve resulting in penalties. A significant shift of regulating power from the hydro power plants to the electrolysis is observed when the hydro power flexibility is reduced as shown in Fig. 8. The increase in regulating power from the electrolysis as a result of less hydro power flexibility is 39–46%. Increasing the regulating price results in a reduced amount of regulating power delivered by the electrolysis plant of 7–11%.

Figs. 9 and 10 shows duration curves for electrolysis power and storage level, in duration curves the values are sorted from highest to lowest, this gives an indication on how the components are operating. The two most common operational states of the electrolysis plant is either to operate at maximum capacity or to supply the hydrogen load directly by producing the exact amount of hydrogen required, as illustrated by the flat parts of the duration curve in Fig. 9. The electrolysis produce more hydrogen directly to the hydrogen load when hydro power can deliver flexibility as this is more efficient by avoiding compression to higher pressures.

The operation on high power levels increase when hydro power is less flexible and the electrolysis has to deliver a higher share of the regulating power. More hydrogen is

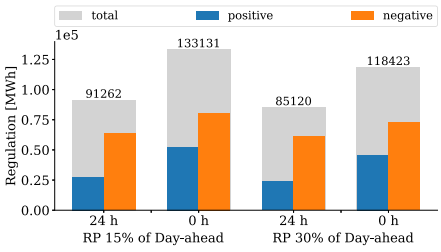

Fig. 8 – Regulation by the hydrogen plant for different levels of hydro power flexibility and regulation price.

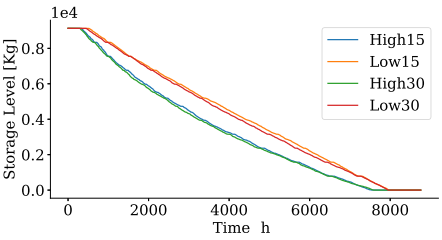

Fig. 10 – Duration curves for the hydrogen storage for high and low hydro power flexibility and regulating prices of 15 and 30% of the day-ahead price.

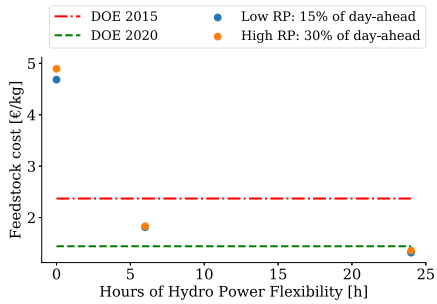

Fig. 11 – Cost of producing hydrogen compared to the DOE targets for 2015 and 2020, the targets are converted from 2007 to 2015 values to adjust for inflation [46].

produced to the hydrogen storage to be able to react to unforeseen wind power production, or lack thereof. The higher storage utilization can be observed in Fig. 10, where the area under the duration curve is larger. The storage is more utilized at all levels, but especially on intermediate levels to allow for both up and down regulation. From Fig. 9, we see that when the regulating price is high then the electrolysis produce less the top the power levels as it is expensive to regulate and energy is rather curtailed or spilled. As a result the utilization of the hydrogen storage is also slightly reduced for increasing regulating prices.

In Fig. 11 we compare the feedstock costs, i.e. cost of electricity for hydrogen production, from the cases with the DOE targets for large scale hydrogen production in 2015 and 2020. In recent NREL cases for hydrogen production, feedstock in PEM electrolysisis currently estimated to represent around 77% of the cost of hydrogen production at about 3.60 €/kg. In areas with large amount of renewables the feedstock costs can be significantly lower, specially if there is hydro power for

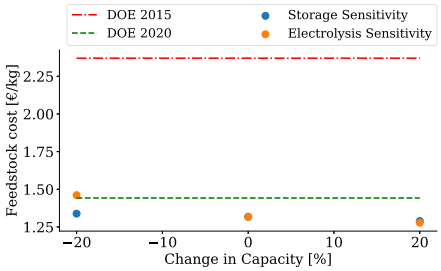

Fig. 12 – Sensitivities of the feedstock cost for hydrogen production from changing the storage and electrolysis capacity respectively. Based on the case with 24 h of hydro power flexibility that gives the cheapest electrolysis feedstock costs.

balancing the natural variability in renewable power output. Flexible hydro power production contributes to significantly lowering the feedstock costs, going from 0 to 6 h of flexibility results is a large drop in production costs while going from 6 to 24 h gives a smaller but still very significant cost reductions of about 27%. The lowest cost is about 1.32 €/kg for the low regulating price, which is lower than the 2020 DOE targets at 1.46 €/kg (adjusted for inflation to 2015 values [46]). The feedstock cost is calculated by using the dual value of the hydrogen balance in Equation (7), this value represent the marginal cost of producing one more unit of hydrogen to the power system at the location of the electrolysis plant in bus 6. From the dual value of Eq. (8), we get a corresponding average electricity price of 25.6 €/MWh in bus 6, as a point of reference the historical average of the energy price in this area was 30.82 €/MWh from 2013 to 2019. The increase in feedstock costs for higher regulating prices are about 1–5%.

It should be noted that in all cases the reservoir levels have some deviations from the reservoir guiding curves at the fixed points, which affects the cost of hydrogen production. The reservoir deviation penalty is set by trial and error to be 50 €/MWh and is a signal designed to affect the hydro power strategy without any direct physical meaning. However, it can also be interpreted as high regulation cost for the hydro power plants when they deliver additional regulation compared to what the flexibility in each case allow.

Increasing the installed capacities of wind power, transmission lines, hydro power generators, reservoirs, electrolysis or hydrogen storage can further reduce the feedstock costs but this has to be investigated using an investment model that considers the capital costs of the different technologies against the operational benefits. The sensitivity of the feedstock cost to changes in electrolysis capacity and hydrogen storage is shown in Fig. 12 for the case with the lowest hydrogen feedstock costs. The differences in feedstock costs when changing the hydrogen storage with ± 20% is about 2% in either direction. Reducing the electrolysis capacity by 20% have a more significant effect with an 11% increase in the feedstock costs, while 20% more capacity only gives a 3% reduction in feedstock costs.

If we use the excel tool from the NREL analysis [2] and oversize the electrolysis plant to fit our case study with a capacity of (150 MW/51.84 kWh/kg) · 24 h/day = 70 ton/day, we get the capital costs and fixed O&M costs shown in Table 4. In the capital cost we also include an additional 0.02 €/kg for the hydrogen storage [29]. The costs are calculated for two cases, where the main difference is the electrolysis stack cost of 810 and 360 €/kWh for the current and future case respectively. Using the feedstock

Table 4 – Cost of hydrogen production for the case with high levels of hydro power flexibility, using current and future estimates of capital and fixed O&M costs.

	Current	Future	DOE - 2020
Capital [€/kg]	0.72	0.31	0.41
Feedstock [€/kg]	1.32	1.32	1.46
Fixed O&M [€/kg]	0.53	0.26	0.21
Total [€/kg]	2.57	1.89	2.08

cost from this analysis we get a total cost of hydrogen production of 2.57 and 1.89 €/kg for the present or future case respectively. As seen from the results, using the current investment cost results in total cost higher than the DOE target while future costs results in total costs below the DOE target. This is still higher than reported cost estimates for hydrogen produced from natural gas with carbon sequestration at 1.56 $/kg or 1.41 €/kg, which doesn't include the cost of carbon storage. This shows that with high levels of wind penetration electrolysis can get close to the costs of hydrogen production from natural gas in the future. There is however, several factors that has to be considered further by performing an investment analysis, such as the cost of carbon storage and how much wind power it is economical to integrate before lower electricity prices makes it unprofitable.

Conclusion

In this work we present a model for optimizing the operation of a region in the power system with high wind power penetration and large scale hydrogen production. The model takes into consideration power flow, energy storage and short-term uncertainty from wind power. The model is based on a rolling horizon framework, use scenarios to represent wind power uncertainty and guiding curves for long-term energy storage strategies.

The value of flexible hydro power on the cost of hydrogen production from electrolysis is investigated in a case study of a future scenario of the power system in the Finnmark region in northern Norway. The flexibility from hydro power is quantified by allowing the reservoir level to deviate from the guiding curve within a time range of 0, 6 or 24 h. The case study shows how the system is affected by the presence of flexibility from hydro power and how the electrolysis plant increasingly delivers flexibility when the hydro power has a tight operating range.

Increasing levels of hydro power flexibility reduces the lost energy in the system by up to 56% with 24 h of flexibility compared to no flexibility. Low hydro power flexibility in the 0 h case causes the amount of regulation delivered by the electrolysis to increase by up to 39–46% compared to when hydro power has high flexibility in the 24 h case.

The case study shows that flexibility from hydro power is important for the cost of hydrogen production in power systems with high levels of wind power penetration. Increasing the time range in which the reservoir level can deviate from the guiding curve from 6 to 24 h results in a reduction in cost from electricity consumption for the electrolysis of 27%, from 1.83 to 1.32 €/kg. The lowest total costs at 1.89 €/kg are fulfilling the US Department of Energy targets for large scale hydrogen production in 2020, and is close to competing with hydrogen production from natural gas with carbon sequestration which is estimated at 1.41 €/kg. It should be noted that our results are obtained using regulating power price premiums of 15 and 30% of the day-ahead price which is higher than observed in the market today.

Significant modifications to the installed capacities found by a deterministic investment model had to be made to make the stochastic case study feasible. This shows that short therm uncertainty should be taken into account when making investments in systems with high amount of wind power. In future work the model presented here will be expanded to an investment model. Additionally the effect of penalties from the guiding curve deviations will be studied more in detail and other methods for representing the hydro power flexibility that has lower or more economically correct impact on the objective and dual values will be tested.

Acknowledgements

This publication is based on results from the research project Hyper, performed under the ENERGIX programme. The authors acknowledge the following parties for financial support: Equinor, Shell, Kawasaki Heavy Industries, Linde Kryotechnik, Mitsubishi Corporation, Nel Hydrogen and the Research Council of Norway (255107/E20). The authors would also like to thank Prof. Øivind Wilhelmsen at SINTEF and NTNU for feedback on this manuscript.

REFERENCES

[1] Iea. Technology roadmap hydrogen and fuel cells. Tech. rep 2015. https://www.google.com/url?sa=t&rct=j&q=&esrc=s&source=web&cd=1&cad=rja&uact=8&ved=2ahUKEwiOkur3orHiAhXBtYsKHQq5AQcQFjAAegQIAhAB&url=https%3A%2F%2Fwww.iea.org%2Fpublications%2Ffreepublications%2Fpublication%2FTechnologyRoadmapHydrogenandFuelCells.pdf&usg=AOvVaw1oUrtvuRFv9p-oodIc4pQC.

[2] National Renewable Energy Laboratory, H2A: Hydrogen analysis production case studies | hydrogen and fuel cells | NREL. URL https://www.nrel.gov/hydrogen/h2a-production-case-studies.html.

[3] Ursua A, Gandia L, Sanchis P. Hydrogen production from water electrolysis: current status and future trends. Proc IEEE 2012;100(2):410–26. https://doi.org/10.1109/JPROC.2011.2156750.

[4] REFHYNE clean refinery hydrogen for europe. URL https://refhyne.eu/.

[5] Ulleberg O, Nakken T, Ete A. The wind/hydrogen demonstration system at Utsira in Norway: evaluation of system performance using operational data and updated hydrogen energy system modeling tools. Int J Hydrogen Energy 2010;35(5):1841–52. https://doi.org/10.1016/j.ijhydene.2009.10.077.

[6] Argumosa M d P, Simonsen B, Schoenung S. Evaluations of hydrogen demonstration projects. Int Energy Agency 2010:1–35.

[7] Lyseng B, Niet T, English J, Keller V, Palmer-Wilson K, Robertson B, Rowe A, Wild P. System-level power-to-gas energy storage for high penetrations of variable renewables. Int J Hydrogen Energy 2018;43(4):1966–79. https://doi.org/10.1016/J.IJHYDENE.2017.11.162.

[8] Greiner CJ, KorpÅs M, Holen AT. A Norwegian case study on the production of hydrogen from wind power. Int J Hydrogen Energy 2007;32(10):1500–7. https://doi.org/10.1016/j.ijhydene.2006.10.030.

[9] Korpås M, Greiner CJ. Opportunities for hydrogen production in connection with wind power in weak grids. Renew Energy 2008;33(6):1199–208. https://doi.org/10.1016/j.renene.2007.06.010.

[10] Greiner CJ, Korpas M, Gjengedal T. A model for techno-economic optimization of wind power combined with hydrogen production in weak grids. EPE Journal 2009;19(2):52–9. https://doi.org/10.1080/09398368.2009.11463717.

[11] Statkraft, Energy solution: renewable proposal for svalbard | explained. URL https://explained.statkraft.com/articles/2018/energy-solution-renewable-proposal-for-svalbard/.

[12] Saba SM, Müller M, Robinius M, Stolten D. The investment costs of electrolysis A comparison of cost studies from the past 30 years. Int J Hydrogen Energy 2018;43(3):1209–23. https://doi.org/10.1016/J.IJHYDENE.2017.11.115.

[13] Levene JI, Mann MK, Margolis RM, Milbrandt A. An analysis of hydrogen production from renewable electricity sources. Sol Energy 2007;81(6):773–80. https://doi.org/10.1016/J.SOLENER.2006.10.005.

[14] United States Department of Energy. Hydrogen production, fuel cell technologies office multi-year research. Development and Demonstration Plant 2015;11007:1–44. https://doi.org/10.2172/1219578.

[15] IRENA. Renewable power generation costs in 2017. 2018. Abu Dhabi.

[16] Førsund FR, Singh B, Jensen T, Larsen C. Phasing in wind-power in Norway: network congestion and crowding-out of hydropower. Energy Policy 2008;36:3514–20. https://doi.org/10.1016/j.enpol.2008.06.005.

[17] Lu X, McElroy MB, Peng W, Liu S, Nielsen CP, Wang H. Challenges faced by China compared with the US in developing wind power. Nature Energy 2016;1(6):16061. https://doi.org/10.1038/nenergy.2016.61.

[18] Welder L, Stenzel P, Ebersbach N, Markewitz P, Robinius M, Emonts B, Stolten D. Design and evaluation of hydrogen electricity reconversion pathways in national energy systems using spatially and temporally resolved energy system optimization. Int J Hydrogen Energy 2019;44(19):9594–607. https://doi.org/10.1016/J.IJHYDENE.2018.11.194.

[19] Jiang Y, Wen B, Wang Y. Optimizing unit capacities for a wind-hydrogen power system of clustered wind farms. Int Trans Electrical Energy Systems 2019;29(2):e2707. https://doi.org/10.1002/etep.2707.

[20] Grube T, Doré L, Hoffrichter A, Hombach LE, Raths S, Robinius M, Nobis M, Schiebahn S, Tietze V, Schnettler A, Walther G, Stolten D. An option for stranded renewables: electrolytic-hydrogen in future energy systems. Sustainable Energy Fuels 2018;2(7):1500–15. https://doi.org/10.1039/C8SE00008E.

[21] B. Olateju, A techno-economic assessment of sustainable large scale hydrogen production from renewable and non-renewable sources doi:10.7939/R33F4KW3X.

[22] Zhang G, Wan X. A wind-hydrogen energy storage system model for massive wind energy curtailment. Int J Hydrogen Energy 2014;39(3):1243–52. https://doi.org/10.1016/J.IJHYDENE.2013.11.003.

[23] Nastasi B, Lo Basso G. Hydrogen to link heat and electricity in the transition towards future Smart Energy Systems. Energy 2016;110:5–22. https://doi.org/10.1016/J.ENERGY.2016.03.097.

[24] Lund PD, Lindgren J, Mikkola J, Salpakari J. Review of energy system flexibility measures to enable high levels of variable renewable electricity. Renew Sustain Energy Rev 2015;45:785–807. https://doi.org/10.1016/J.RSER.2015.01.057.

[25] Meibom P, Barth R, Hasche B, Brand H, Weber C, O'Malley M. Stochastic optimization model to study the operational impacts of high wind penetrations in Ireland. IEEE Trans Power Syst 2011;26(3):1367–79. https://doi.org/10.1109/TPWRS.2010.2070848.

[26] Korpås M, Holen AT. Operation planning of hydrogen storage connected to wind power operating in a power market. IEEE Trans Energy Convers 2006;21(3):742–9. https://doi.org/10.1109/TEC.2006.878245.

[27] Wang Y, Zhou Z, Botterud A, Zhang K, Ding Q. Stochastic coordinated operation of wind and battery energy storage system considering battery degradation. Journal of Modern Power Systems and Clean Energy 2016;4(4):581–92. https://doi.org/10.1007/s40565-016-0238-z.

[28] Helseth A, Gjelsvik A, Mo B, Linnet l. A model for optimal scheduling of hydro thermal systems including pumped-storage and wind power, IET Generation. Transm Distrib 2013;7(12):1426–34. https://doi.org/10.1049/iet-gtd.2012.0639.

[29] Bødal EF, Korpås M. Production of hydrogen from wind and hydro power in constrained transmission grids, considering the stochasticity of wind power. J Phys Conf Ser 2018;1104(1):012027. https://doi.org/10.1088/1742-6596/1104/1/012027.

[30] Norwegian Meteorological Institute, TdsStaticCatalog http://thredds.met.no/thredds/metno.html. URL http://thredds.met.no/thredds/metno.html.

[31] The Norwegian water resources and energy directorate, wind power. URL https://www.nve.no/energiforsyning-og-konsesjon/vindkraft/?ref=mainmenu.

[32] Bremnes JB. A comparison of a few statistical models for making quantile wind power forecasts. Wind Energy 2006;9(1–2):3–11. https://doi.org/10.1002/we.182.

[33] Koenker R. Fundamentals of quantile regression. In: Quantile regression. Cambridge University Press; 2005 [Ch. Fundamenta].

[34] Pinson P, Madsen H, Papaefthymiou G. From probabilistic forecasts to statistical scenarios of short-term wind power production. Wind Energ 2009;12:51–62. https://doi.org/10.1002/we.284.

[35] Skytte K, Grohnheit PE. Market prices in a power market with more than 50% wind power. Cham: Springer; 2018. p. 81–94. https://doi.org/10.1007/978-3-319-74263-2{_}4.

[36] Skytte K. The regulating power market on the Nordic power exchange Nord Pool: an econometric analysis. Energy Econ 1999;21(4):295–308. https://doi.org/10.1016/S0140-9883(99)00016-X.

[37] Stage S, Larsson Y. Incremental cost of water power. Trans Am Inst Electr Eng Part III: Power Apparatus Systems 1961;80(3):361–4. https://doi.org/10.1109/AIEEPAS.1961.4501045.

[38] Lindqvist J. Operation of a hydrothermal electric system: a multistage decision process, power apparatus and systems, Part III. Trans Am Inst Electr Eng 1962;81(April):1–6.

[39] Stott B, Jardim J, Alsac O. DC power flow revisited. IEEE Trans Power Syst 2009;24(3):1290–300. https://doi.org/10.1109/TPWRS.2009.2021235.

[40] The Norwegian water resources and energy directorate, Norwegian power system. URL https://www.nve.no/map-services/?ref=mainmenu.

[41] Statistics Norway, Net consumption of electricity, by consumer group (GWh) (M) 2010 - 2017. Statbank Norway. URL https://www.ssb.no/en/statbank/table/10314/.

[42] Nordpool. Historical market data. URL, https://www.nordpoolgroup.com/historical-market-data/.

[43] Bødal EF, Korpås M. Regional effects of hydrogen production in congested transmission grids with wind and hydro power. In: 14th international conference on the european energy market - EEM. IEEE; 2017. p. 1–6. https://doi.org/10.1109/EEM.2017.7982013.

[44] Ozaki M, Tomura S, Ohmura R, Mori YH. Comparative study of large-scale hydrogen storage technologies: is hydrate-based storage at advantage over existing technologies? Int J Hydrogen Energy 2014;39(7):3327–41. https://doi.org/10.1016/j.ijhydene.2013.12.080.

[45] Bødal EF, Korpås M. Production of hydrogen from wind and hydro power in constrained transmission grids, considering the stochasticity of wind power. J Phys Conf Ser Oct. 2018;1104(1):012027.

[46] U.S. Bureau of Labor Statistics, CPI inflation calculator. URL https://www.bls.gov/data/inflation_calculator.htm.

A.4 Decarbonization synergies from joint planning of power and hydrogen production: A Texas case study

INTERNATIONAL JOURNAL OF HYDROGEN ENERGY 45 (2020) 32899–32915

Available online at www.sciencedirect.com

ScienceDirect

journal homepage: www.elsevier.com/locate/he

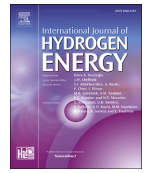

Decarbonization synergies from joint planning of electricity and hydrogen production: A Texas case study

Espen Flo Bødal [a,*], *Dharik Mallapragada* [b], *Audun Botterud* [c], *Magnus Korpås* [a]

[a] *Norwegian University of Science and Technology, Trondheim, Norway*
[b] *MIT Energy Initiative, Massachusetts Institute of Technology, Cambridge, MA, USA*
[c] *Laboratory for Information and Decision Systems, Massachusetts Institute of Technology, Cambridge, MA, USA*

HIGHLIGHTS

- Flexibility from electrolytic H_2 production enables more renewable integration.
- Carbon capture occurs at lower CO_2 prices for production of H_2 than electricity.
- Electrolytic H_2 production is dominant for CO_2 prices of $30–60/tonne or more.
- Increased H_2 demand favors natural gas based H_2.
- Emissions are less than 1.2 kg CO_2/kg H_2 for CO_2 prices of $90/tonne or more.

ARTICLE INFO

Article history:
Received 20 July 2020
Received in revised form
8 September 2020
Accepted 16 September 2020
Available online 13 October 2020

Keywords:
Hydrogen
Electrolysis
Power system analysis
Renewable energy

ABSTRACT

Hydrogen (H_2) shows promise as an energy carrier in contributing to emissions reductions from sectors which have been difficult to decarbonize, like industry and transportation. At the same time, flexible H_2 production via electrolysis can also support cost-effective integration of high shares of variable renewable energy (VRE) in the power system. In this work, we develop a least-cost investment planning model to co-optimize investments in electricity and H_2 infrastructure to serve electricity and H_2 demands under various low-carbon scenarios. Applying the model to a case study of Texas in 2050, we find that H_2 is produced in approximately equal amounts from electricity and natural gas under the least-cost expansion plan with a CO_2 price of $30–60/tonne. An increasing CO_2 price favors electrolysis, while increasing H_2 demand favors H_2 production from Steam Methane Reforming (SMR) of natural gas. H_2 production is found to be a cost effective solution to reduce emissions in the electric power system as it provides flexibility otherwise provided by natural gas power plants and enables high shares of VRE with less battery storage. Additionally, the availability of flexible electricity demand via electrolysis makes carbon capture and storage (CCS) deployment for SMR cost-effective at lower CO_2 prices ($90/tonne CO_2) than for power generation ($180/tonne CO_2). The total emissions attributable to H_2 production is found to be dependent on the H_2 demand. The marginal emissions from H_2 production increase with the H_2 demand for CO_2 prices less than $90/tonne CO_2, due to shift in supply from electrolysis to SMR. For a CO_2 price of $60/tonne we estimate the production weighted-average H_2 price to be between $1.30–1.66/kg across three H_2 demand

* *Corresponding author.*
E-mail address: espen.bodal@ntnu.no (E.F. Bødal).
https://doi.org/10.1016/j.ijhydene.2020.09.127

32900 INTERNATIONAL JOURNAL OF HYDROGEN ENERGY 45 (2020) 32899–32915

scenarios. These findings indicate the importance of joint planning of electricity and H_2 infrastructure for cost-effective energy system decarbonization.

Nomenclature

Indices

i	Plant type
n, m	Nodes
t	Time step

Costs

C_i^{energy}	Storage energy cost [$/MWh] or [$/kg]
C^e	Emission cost [$/kg]
C_i^{fix}	Fixed cost [$/plant]
C_i^{inv}	Investment cost [$/plant]
C_i^{power}	Storage power cost [$/MW] or [$/(kg/h)]
C_i^{rat}	Rationing cost [$/MWh] or [$/kg]
C_i^{ret}	Retirement cost [$/plant]
C_i^{var}	Variable cost [$/MWh] or [$/kg]

Parameters

η_i	Charge/discharge efficiency for storage type i
γ_i	Emission rate [kg CO_2/MWh] or [kg CO_2/kg H_2]
A_i	Auxillary electricity [MWh/kg]
D_{tn}	Electricity or H_2 demand [MWh] or [kg]
E_i	Cost of CO_2-emissions [$/kg]
F_i	Conversion rate [MWh/kg H_2] or [kg H_2/MWh]
P_i	Max or min plant capacity [MW] or [kg/h]
P_{tin}	Power profile [MWh]
R_i	Maximum ramping [MW] or [kg/h]
$T_{nm}^{init/max}$	Initial or maximum transmission capacity from node n to m [MW] or [kg/h]
$X_{in}^{init/max}$	Initial or maximum number of power plants

Sets

$\mathcal{L}$	Transmission lines and pipelines
$\mathcal{N}$	All nodes
$\mathcal{P}$	Plants types for electricity or H_2 production
$\mathcal{R}$	VRE power plants types
$\mathcal{S}$	Storage types
$\mathcal{T}$	Time steps

Indexed Sets

$\mathcal{A}_n$	Plants types requiring auxiliary power at node n
$\mathcal{B}_n$	Nodes connected to node n by transmission
$\mathcal{C}_n$	Nodes connected to node n by conversion plants
$\mathcal{F}_n$	Conversion plant types at node n
$\mathcal{P}_n$	Plants types at node n
$\mathcal{S}_n$	Storage types at node n

Investment Variables

e_n^{cap}	Storage charge/discharge capacity [MW] or [kg/h]
s_{in}^{cap}	Storage level capacity [MWh] or [kg]
x_{in}^{trans}	New lines or pipes
x_{in}	New plants

Operation Variables

c_{tin}	Energy curtailment of VRE [MWh]
$e_{tin}^{in/out}$	Storage charge/discharge [MW] or [kg/h]
f_{tnm}	Flow on lines or pipelines [MW] or [kg/h]
$p_{tn}^{exp/imp}$	Import/export [MW]
p_{tin}	Production [MW] or [kg/h]
r_{tn}	Load curtailment [MW] or [kg]
s_{tn}	Storage level [MWh] or [kg]
u_{tin}	Number of committed plants

Introduction

Policymakers across the world are looking for cost-effective ways to reduce CO_2 emissions by mid-century throughout all sectors of the economy to address climate change. Electrification of various end-uses is gaining traction as a cost-effective strategy for reducing CO_2 emissions in various sectors, most notably, light duty vehicle transportation [1]. Electrification not only improves end-use energy efficiency in many cases, but also concentrates emissions sources upstream, in the power sector, where decarbonization efforts are accelerating with the adoption of variable renewable energy (VRE) generation capacity. While direct electrification is appealing, it may be impractical in several end-uses such as industrial applications using fossil-fuel as feedstocks and heavy-duty transportation [2–4], where volumetric and gravimetric energy density are key performance requirements. In this context, use of alternative energy carriers like hydrogen (H_2) produced from electricity or other low-carbon sources remains an appealing prospect. Furthermore, H_2 can be used to produce ammonia and synthetic fuels that are well suited for directly replacing fossil based fuels, for example in shipping and aviation, without major modifications to existing machines or fueling systems [5–7].

The production of H_2 in the world today is almost entirely based on fossil energy sources, of which 76% is from natural gas and 23% from coal, with electrolysis accounting for less than 0.1% of supply [8]. To date, the relatively high cost of electrolytic H_2, estimated to be $4.8/kg using US costs, compared to fossil-fuel routes using natural gas ($1.2/kg) has limited its adoption [9]. Moreover, the cost of electrolytic H_2 production is dominated by the cost of electricity (~77% of

total costs) when the electrolyzer is operated continuously [9]. Three factors are anticipated to change this picture. First, the investment costs of proton exchange membrane electrolysis (PEMEL) is projected to reduce substantially over the coming decades, with one estimate suggesting declines from $900/kW in 2018 to $400/kW by 2040 [10]. The future capital cost reduction for electrolytic H_2 will mainly arise from economies of scale and increased automation in the production of electrolyzers [11], but also larger electrolyzer stacks and multi-stack electrolysis plants [12]. Second, increasing penetration of VRE generation in the electric grid is anticipated to lead to more hours of zero wholesale electricity prices. Operating electrolyzers in a flexible manner can exploit these hours of low electricity prices for H_2 production while also providing demand-side flexibility to support greater levels of VRE integration in the electric grid [13–18]. Third, increasing policy emphasis on CO_2 emissions reduction is likely to favor H_2 produced from VRE electricity sources rather than fossil-fuel intensive H_2 production processes. Collectively, these factors raise the prospect of H_2 produced from electricity becoming competitive with natural gas based H_2 within the coming decades [12,19,20].

Unlocking cost-effective electrolytic H_2 production at scale could accelerate decarbonization of energy uses which are difficult to electrify, but can also provide large amounts of flexibility to the power grid when operated as a flexible load. Over-sizing the electrolyzer compared to the H_2 demand and installing H_2 storage enables the H_2 production to be flexible and produce more H_2 when there is a surplus of electricity (indicated by low prices) in the system and less when there is a deficit (indicated by high prices) [21–23]. In power systems with large shares of VRE generation, the variations in electricity price is expected to be higher than in current grids, implying that flexible H_2 production can significantly lower the electricity related H_2 production costs and increase plant profitability [24] compared to producing H_2 at a constant rate [20,22,25–27]. Furthermore, flexible electrolytic H_2 production is well suited to provide ancillary services to the electricity system, which can be an additional potential source of income for electrolyzers and contribute to reducing H_2 costs [28–31].

To accurately capture the value of flexibility from H_2 production by electrolysis, and thus the cost of H_2, it is necessary to model the operation of the electrolysis plant in conjunction with the electric power system directly. Furthermore, for a holistic estimate of the benefits provided by energy storage, either as H_2 or other storage types, it is important to consider an investment planning framework, as most of the benefits of energy storage or demand flexibility generally arise from deferring investments in new generation and transmission capacity [32,33].

Prior studies on the interactions between electricity and H_2 infrastructure, including production, storage and transport can be grouped according to the resolution used in the representation of various stages of the H_2 supply chain. Traditional electricity focused capacity expansion models include H_2 in the form of energy storage only, where a storage system is designed by combining electrolyzer, H_2 storage tanks and re-conversion by fuel cell or H_2 turbines [34,35]. This use of H_2 for electricity storage suffer from low round-trip efficiency, typically 30–50% [16], and is mostly used as a long-term storage option to complement other short-duration storage technologies.

Studies which focus on the H_2 supply chain, such as storage and transport in the form of pipes, compressed H_2 or liquefied H_2 trucks tend to have a simplified representation of the interactions with the electricity system such as residual loads or only VRE electricity supply [36–39].

Recently, a few studies have evaluated the flexibility provided by sector-coupling through coordinated expansion of electricity and H_2 infrastructure [40]. Some of these studies consider the use of H_2 for electricity storage [41] or as a complete system with H_2 demand. In general, the models with comprehensive H_2 system models often have restriction in term of spacial or temporal resolution [42,43] or are split into soft-linked investment and operation models [44], all of which impacts the results especially in VRE dominated systems. Models that include detailed electricity and H_2 system models usually only consider H_2 production by electrolysis and do not include H_2 produced from the dominant natural gas pathways [45]. Models that include H_2 production from natural gas tend to have a low spatial resolution [46] or low modeling detail of conventional electricity generation [47,48].

In this work, we develop a capacity expansion model to evaluate the cost-optimal electricity and H_2 infrastructure needed to serve future electricity and H_2 demand across a range of policy and technology scenarios. The modeling framework optimizes for investment subject to a number of operational and policy constraints. These include investment limitations on physical installations according to resource potential as well as operational limitations on generation and transport. Ramping constraints enforce the rate of change in electricity and H_2 production for the different technologies. Balance constraints keeps track of the balance between production and consumption, storage level and flow of H_2 and electricity between locations. The operational constraints are enforced while modeling hourly resolution of system operation throughout the entire year. We model electricity and H_2 transmission by overhead lines and pipelines respectively, as the best VRE sources often are located far away from major energy demand centers. H_2 is produced from PEMEL or natural gas with or without carbon capture and storage (CCS) and can be converted to electricity by a proton exchange membrane fuel cell (PEMFC) or H_2 compatible gas turbines. We model H_2 production from natural gas via steam-methane reforming (SMR). The model is applied for a case study of Texas in 2050 under a range of H_2 demand and carbon price scenarios. We summarize the new contributions to the literature arising from this work as follows:

a) We develop a coordinated electricity and H_2 system capacity expansion model with high temporal and spatial resolution that considers the dynamics between electricity and H_2 in terms of major technological options for production, storage and transport.
b) We conduct a comprehensive case study of electricity and H_2 production for the U.S. state of Texas with realistic assumptions, considering the impact of different CO_2 prices and H_2 demands.
c) The results show that flexible H_2 supply from PEMEL enables more integration of VRE and reduces battery storage

requirements in the grid. Moreover, increasing H_2 demand makes PEMEL more expensive, thereby shifting H_2 production towards SMR. Due to the synergies between VRE generation and PEMEL loads, we find that CCS adoption is attractive for SMR at lower CO_2 prices compared to CCS adoption for electricity generation in the power sector.

The rest of the paper has the following structure. In Section Method we describe the optimization model used for studying the interaction between H_2 and electricity infrastructure. Section Case study and input assumptions presents the electricity and H_2 system in Texas, as well as the baseline technical and economic assumptions to characterize electricity and H_2 demand, production, transport and storage technologies. Section Results discusses the model results under various CO_2 prices, technology costs and demand scenarios. Section Discussion and conclusion discusses the major findings of the work and identifies areas for future analysis.

Method

The joint electric and H_2 capacity expansion model finds the least-cost portfolio to meet future electricity and H_2 demand in a region. The model is formulated as a linear programming (LP) problem, as stated in Eqs (1)–(13). The electricity and H_2 parts of the system are separated by dedicating nodes to each respective energy carrier. The electric nodes are connected to electricity generating technologies, battery storage, transmission lines and electric loads. The formulation at H_2 nodes are equivalent to the electricity nodes, H_2 is produced from SMR with or without (w/wo) CCS to meet H_2 demand, stored in storage tanks or transported on H_2 pipelines as illustrated in Fig. 1. A set of technologies that consist of PEMEL, fuel cells (PEMFC) and H_2 turbines are connecting the two types of nodes by representing generation on one side and loads on the other side. The technical features of electricity and H_2 technologies are described by the same set of constraints, which consist of operational limits on production and ramping determined by the commitment status and balances for energy, storage and transmission.

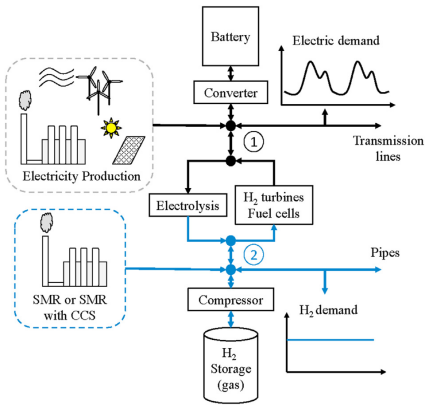

Fig. 1 – Schematic illustration of the energy balances in electric nodes (1) and a H_2 nodes (2). The system consist of several such node pairs connected by overhead lines and H_2 pipelines.

The objective function in Eq. (1) minimizes the investment, retirement, fixed and variable operational costs. The total investment cost is represented by the sum of all individual investments in electricity generating power plants, PEMEL, SMR w/wo CCS, power converters, pumps, batteries, H_2 tanks and transmission capacity in the form of overhead lines and pipelines. The investments in storage capacities are represented by separate power and energy capacities. Variable operational costs arise from fuel costs and variable O&M costs, in addition we consider a technology dependent emission rate and a uniform CO_2-emission cost. At a given time period, unserved electricity or H_2 demand is associated with a penalty.

$$\min \sum_{n\in\mathcal{N}} \Big[\sum_{i\in\mathcal{P}}(C_i^{inv}x_{in} + C_i^{ret}x_{in}^{ret} + C_i^{fix}(X_{in}^{init} + x_{in} - x_{in}^{ret})) + \sum_{i\in\mathcal{S}}(C_i^{power}e_{in}^{cap} + C_i^{energy}s_{in}^{cap}) + \sum_{n,m\in\mathcal{L}} C_{nm}^{Trans}x_{nm}^{trans} + \sum_{t\in\mathcal{T}}\Big[\sum_{i\in\mathcal{P}}(C_i^{var} + \gamma_i C^{e})p_{tin} + \sum_{n\in\mathcal{N}} + C^{rat}r_{tn}\Big]\Big] \quad (1)$$

Power plants and H_2 production facilities are grouped by technology and location. This allows us to model commitment and expansion decisions as integers instead of binaries, an approach that is shown to drastically reduce the computational time with low approximation errors [49]. We also relax the integer commitment and investment decision to be continuous in order to further reduce the computational time, which has been shown to be a reasonable approximation [50, p. 162–174] especially when the optimal integer variable is much greater than 1. Investments in new capacity is bounded by an upper limit that typically represents the resource potential at a given location, as stated in Eq. (2).

$$x_{in} \le X_{in}^{max} \quad \forall i\in\mathcal{P}, \forall n\in\mathcal{N} \quad (2)$$

The operation of the system is governed by Eqs 3–14 for all times, $\forall t\in\mathcal{T}$, and all nodes, $\forall n\in\mathcal{N}$. The plants that can be committed for operation is restricted by the investment decisions as stated in Eq. (3). The plants have both minimal and maximum production limits as shown in Eq. (4). They also have ramping constraints that limit how fast they can increase or decrease their production from one period to another as shown in Eq. (5). The relaxation of the commitment decisions allows power plants to ramp faster than what is technically possible. However, the combination of ramping and minimum production constraints gives a reasonable level of detail in the representation of power plant operations for this type of investment model.

$$u_{tin} \le X_{in}^{init} + x_{in} - x_{in}^{ret} \quad \forall i\in\mathcal{P} \quad (3)$$

$$P_i^{min}u_{tin} \le p_{tin} \le P_i^{max}u_{tin} \quad \forall i\in\mathcal{P} \quad (4)$$

INTERNATIONAL JOURNAL OF HYDROGEN ENERGY 45 (2020) 32899–32915

$$-R_i u_{tin} \le p_{tin} - p_{(t-1)in} \le R_i u_{tin} \forall i \in \mathcal{P} \quad (5)$$

Available VRE production is used for producing electricity unless it is curtailed as stated in Eq. (6).

$$p_{tin} + c_{ti} = P_{tin}(X_{in}^{init} + x_i) \quad \forall i \in \mathcal{R} \quad (6)$$

The energy balances for electricity and H_2 are represented by the same constraint as stated in Eq. (7). Electricity or H_2 is produced or imported to serve the demand or export. Indexed sets determines the generation, storage and conversion technologies at each specific node. $\mathcal{P}_n$ represents the different generating technologies, i.e. power plants at the electric nodes or PEMEL and SMR at the H_2 nodes. H_2 and electricity can be shifted in time by using storage to add or withdraw from the energy balances. Unserved demand is penalized in the objective function. The set of conversion technologies, $\mathcal{F}_n$, are defined at the node they are producing. Conversion technologies used to produce H_2 or electricity at node n represents a load at a node of the opposite type specified by $\mathcal{C}_n$. Similarly, auxiliary electricity for H_2 compression is represented as an additional load. An illustrative example of the energy balance is given in Appendix A.

$$\sum_{i \in \mathcal{P}_n} p_{tin} - p_{tn}^{exp} + p_{tn}^{imp} + \sum_{i \in \mathcal{S}_n} (e_{tin}^{out} - e_{tin}^{in}) + r_{tn}$$

$$= D_{tn} + \sum_{m \in \mathcal{C}_n} \left(\sum_{i \in \mathcal{F}_m} F_i p_{tim} + \sum_{i \in \mathcal{A}_m} A_i e_{tim}^{in} \right) \quad (7)$$

The storage balance for the two different storage types batteries and H_2 storage, specified by index i, is shown in Eq. (8). The storage balance states that the electricity or H_2 stored is given by the energy stored in the previous time-stage plus the net energy input into the storage. The maximum storage level is restricted by the storage level capacity in Eq. (9). The rate in which the storage can be loaded or unloaded is given by in Eqs (10) and (11), which corresponds to the installed converter or compressor capacity.

$$s_{tin} = s_{(t-1)in} + \eta^{in} e_{tin}^{in} - (1/\eta^{out}) e_{tin}^{out} \quad \forall i \in \mathcal{S} \quad (8)$$

$$s_{tin} \le s_{in}^{cap} \quad \forall i \in \mathcal{S} \quad (9)$$

$$e_{tin}^{out} \le e_{in}^{cap} \quad \forall i \in \mathcal{S} \quad (10)$$

$$e_{tin}^{in} \le e_{in}^{cap} \quad \forall i \in \mathcal{S} \quad (11)$$

Power exchange between electric nodes or H_2 flow between H_2 nodes are governed by Eq. (12). The exchange balance states that the net electricity or H_2 exchanged with the rest of the system is equal to the flows in all the pipelines or overhead lines which are connected to the node. The maximum flow in the individual pipelines or overhead lines are bound by their respective capacity in Eqs (13) and (14). We simplify the physical electricity and H_2 flow and use a transport model as the individual lines and pipes are aggregated into transmission corridors. Thus, electric transmission losses and hydrogen compression for pipeline transport are not taken into account. Line-packing for the hydrogen pipelines represents a potential way of storing hydrogen in the pipelines, but is not considered in this model.

$$p_{tn}^{exp} - p_{tn}^{imp} = \sum_{m \in B_n} f_{tnm} \quad \forall n \in \mathcal{N} \quad (12)$$

$$f_{tnm} \le T_{nm}^{init} + T_{nm}^{max} x_{nm}^{trans} \quad \forall n, m \in \mathcal{L} \quad (13)$$

$$f_{tnm} \ge -(T_{nm}^{init} + T_{nm}^{max} x_{nm}^{trans}) \quad \forall n, m \in \mathcal{L} \quad (14)$$

The model is implemented in the Python programming language, using the Pyomo modeling framework for optimization models [51,52] and solved by the Gurobi solver.

Case study and input assumptions

We assess the configuration of a joint H_2 and electricity system to supply future electricity and H_2 demand for the state of Texas in 2050. Texas represents an interesting case study, since: a) it is a region with high quality VRE resources, which has been noted as the state with the highest H_2 production potential from wind and solar power in the US [13], b) cheap availability of natural gas based on close proximity of natural gas resources, and c) significant existing H_2 demand from various petrochemical operations.

The electricity system in Texas, regulated by the Electric Reliability Council of Texas (ERCOT), is currently dominated by fossil energy sources, i.e. mainly natural gas but also coal. However, the north-western and western parts of Texas have excellent wind and solar resources. Although these are located far away from the major load centers in the east and south-east it is one of the fastest growing renewable regions in the world [53]. H_2 can be produced at the energy source and then transported to the consumers via pipelines. Alternatively the energy can be transported by electric transmission lines and used for H_2 production close to the point of consumption. We use a 13-node model of the Texas power system as shown in Fig. 2 [54], which indicate the spatial distribution of nodes where production and consumption of electricity and H_2 is located and possible pathways for new overhead lines and pipelines. We initialize the model with existing generation

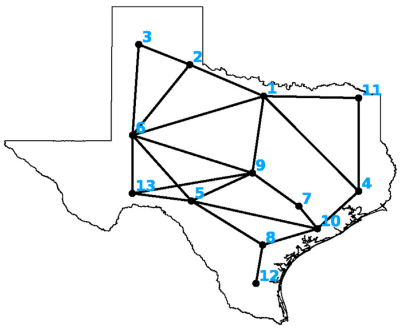

Fig. 2 – The spacial representation and distribution of nodes and the pathways considered for the overhead lines/ pipelines in the Texas case study.

capacity at each node as of 2018 sourced from the NEEDS database [55] (see Table B 2).

Electricity and H_2 demand

The baseline electricity demand for 2050 is calculated based on an average yearly growth of 1% [56] from 2015. The annual electric load from the region is increased from 347 TW h in 2015 to 492 TW h in 2050, a relative increase of 42%. The load profile is obtained by using the actual loads in 2015 from the eight different weather zones defined by ERCOT [57]. The load profiles are transformed to node level by distributing the loads from zone to county level based on population distribution across counties and then aggregating the county-level load to the closest node.

As compared to electricity demand, there is substantial uncertainty in the demand for H_2 in 2050 given its relatively narrow use in industrial processes today. For this study, we defined a baseline scenario of H_2 demand based on a projection from NREL regarding potential H_2 use in the transportation sector by 2050 [58]. While this demand estimate is based on the transport sector, from the model perspective, the demand could also be viewed to represent H_2 consumption in other sectors as well. For simplicity, we have assumed a constant temporal profile for H_2 consumption throughout every hour of the year, with daily consumption estimates reported in the Appendix (Table B.6). Furthermore, we exclude the existing H_2 demand from industrial operations in Texas, since many of those facilities are served by on-site H_2 supply.

The annual baseline H_2 demand in this analysis is 0.68 million metric tonnes (mmt)/year. For reference, this is around 17% of the potential H_2 demand in the Texas "triangle" region at 3.9 mm t/year based on 2015 gasoline consumption [59]. Currently, the total US H_2 demand is around 10 mm t/year [60] and preliminary analysis in the H_2@Scale project estimates potential hydrogen demand in 2050 to be more than 9 times current levels (~ 100 mm t/year) [61]. Although a detailed analysis of potential H_2 demand is outside the scope of this work, we do consider the impact of scaling the baseline H_2 demand by a factor of 10 and 50.

H_2 production

Today, large scale H_2 production is mainly based on SMR and is associated with life cycle greenhouse gas (GHG) emissions of 10–16 kg CO_2eq/kg H_2 [62–64], of which process emissions account for approximately 9 kg CO_2/kg H_2 [62]. The cost of H_2 production is dominated by fuel costs, with the cost of natural gas accounting for 72% of the levelized cost in the U.S. ($1.15–1.32/kg H_2 [9]). 90% of the operational CO_2-emissions from the SMR-process can be captured by including CCS, with an estimated cost of to be $47–110/tonne CO_2 captured (levelized cost of $0.3–2.1/kg H_2) [64]. For this study, we assume that CCS lowers the plant GHG emissions associated with H_2 production from natural gas down to 0.93 CO_2/kg H_2 at a cost of $83/tonne CO_2.

The plant design, capacity costs, variable costs, fixed costs and emissions used in this analysis is based on the techno-economic evaluation of merchant SMR H_2 plants by the IEA [64]. They give a detailed breakdown of costs for SMR with or without CCS for a plant with a capacity of 216 tonnes H_2/day. Natural gas prices and the cost for carbon transportation and storage are streamlined for both H_2 and electricity producing technologies and set to be $5.24/MMBtu [65] and $11/tonne CO_2 [66] respectively.

We model the cost and performance for PEMEL plants based on the H2A production studies available from NREL [9]. The plant cost and performance is based on 60 tonnes H_2/day, with an installed capital costs of ~ $530/kW, which is in line with the long-term cost projections for multi-MW electrolysis plants in the literature [8,10,20,67,68]. The energy requirement for H_2 compression to 100 bar for storage is modeled to be 1.3 kW h/kg [69], and related capital costs are estimated to be $1200/kW [67]. The electrolysis plant has a state-of-the-art efficiency of 65% based on LHV. Further details on costs and characteristics for the H_2 producing technologies are found in Table B 4.

H_2 storage in pressure vessels (100 bar) buried underground at 100 bar is estimated to cost $516/kg [70,71]. Geological H_2 storage in salt caverns are the most cost-effective method for storing large quantities of H_2 [72] and currently widely used for natural gas and H_2 storage in Texas [67,73]. However, availability of salt caverns storage capacity is uncertain and therefore is not included in this analysis.

Electricity generation and storage

Investment, fixed and variable operating & maintenance costs in 2050 for electricity generation technologies were sourced from the mid scenario of the NREL Annual Technology Baseline 2019 edition [65]. This includes the cost of battery storage, where we separately define the cost of power and energy and allow the model to figure out the optimal energy to power ratio (i.e. duration) to be deployed at each location. The cost for H_2 re-conversion technologies are obtained from Refs. [37], and includes H_2 compatible gas turbines and PEMFC. Further details are available in Table B 3.

Energy transport

The cost of overhead line transmission expansion is modeled using a cost per mile estimate of $3000/(miles·MW) for the first 5 GW and $4000/(miles·MW) for the next 5 GW of each transmission corridor. This estimate is based on the costs of the CREZ transmission expansion in Texas at $2500/(miles·MW) and set higher to account for lines in more urban areas and decreasing future land availability [74]. The system is updated to include the CREZ expansion of ~ 11.5 GW [75,76] and investments in new transmission capacity is limited on each segment to 15 GW. H_2 pipelines are set to have a investment cost of $210/(m·GW) and $560/m [36].

Computation

The computation time for the model ranges from 1 to 2 h for each set of parameters. The parameters are changed in an automatic loop to do sensitivity analysis on the CO_2 price, resulting in 10 iterations and a total of 16–18 h of computational time. The computations are performed on a shared server typically using 28 threads for the optimization and up

INTERNATIONAL JOURNAL OF HYDROGEN ENERGY 45 (2020) 32899–32915

to 50–60 GB of memory. The processor is an Intel Xeon E5-2690 v4 with a clock frequency of 2.6 GHz (28 cores and 56 logical processors).

Results

Implications of CO_2 price

To investigate the effects of a CO_2 price, we run the model for different CO_2 prices in increments of $30/tonne from 0 to 270 $/tonne. This range spans the range of social cost of carbon estimated for 2050 by the US Environmental Protection Agency (EPA), which results show CO_2 prices from $69/tonne to $212/tonne [77].

Fig. 4.1 shows that introducing a CO_2 price of $30/tonnes leads to a significant growth in VRE electricity from 58 to 78 GW for wind power and 39–53 GW for solar power. In fact, this CO_2 price is on par with the European CO_2 quota prices in most of 2019 and 2020 at $30–35/tonne. The initial growth in VRE is followed by a more gradual growth when the CO_2 price is increased further. The deployment of VRE is followed by a large deployment of battery storage from 3 to 23 GW

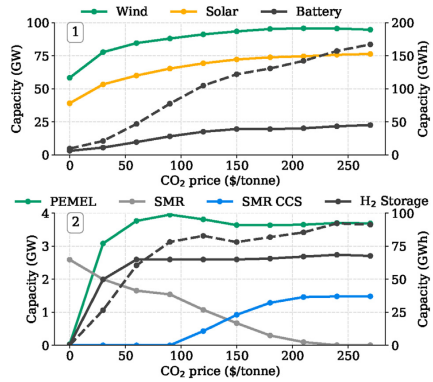

Fig. 4 – 1) VRE and battery capacity and 2) H_2 production and storage capacity as a function of the CO_2 price. H_2 capacities are converted to power by the lower heating value of H_2. Storage energy capacity is represented by the dotted lines and secondary y-axis (right).

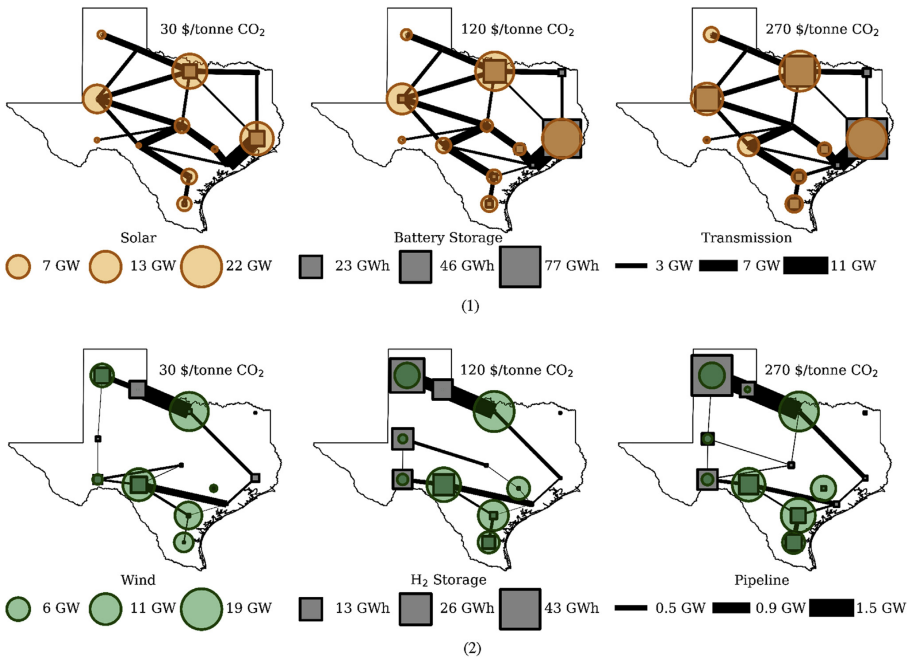

Fig. 3 – Development in 1) solar power, battery energy and overhead transmission line capacity and 2) wind power, H_2 storage and pipeline capacity. Overhead lines and pipelines with capacity under 1 GW and 1 tonne/h are excluded.

(10–167 GW h), where the storage duration (energy capacity divided by power capacity) increases linearly from 2 to 7 h.

H_2 is entirely produced from SMR in the absence of a price for CO_2 emissions as shown in Fig. 4.2. However, the H_2 share from SMR is gradually reduced with increasing CO_2 prices as SMR leads to significant emissions. Significant shares of the H_2 production is initially taken over by PEMEL with storage that can produce H_2 from electricity in surplus periods, followed by SMR with CCS for a CO_2 price higher than \$90/tonne. H_2 capacities are converted to power by the lower heating value of H_2 (LHV_{H_2} = 33.3 kW h/kg), placing the largest amount of H_2 storage capacity at 12% and 54% of the maximum battery storage capacity for power and energy respectively, not accounting for efficiency of converting H_2 back to power. The duration of the H_2 storage increase from 13 to 36 h of H_2 supply when PEMEL capacity is built out (CO_2 prices of \$30/tonne or more).

The spatial deployment of VRE generation, storage and transmission capacity is shown in Fig. 3 at CO_2 prices of 30, 120 and 270 \$/tonne. At low CO_2 prices, solar power is primarily developed close to the main load centers in the east/north and in the west where solar irradiation is high, and is co-located with significant battery capacity as shown in Fig. 3.1. With increasing CO_2 prices and thus VRE deployment, more solar capacity is constructed in the south and west. The transmission capacity from west to east is also upgraded in the southern part of the state. Significant amounts of battery capacity is constructed in the nodes where solar power plants are located. Batteries appear to be preferred over new transmission capacity due to the intermittent VRE electricity production, and the limited geographical smoothing of solar PV output.

Wind power is initially developed in the south/south-west and north/north-west as shown in Fig. 3.2. H_2 storage supports the integration of wind and solar in western Texas and two main H_2 pipeline corridors are constructed going from west to east. For higher CO_2 prices more wind power is developed in the north-west, also called the Texas panhandle, and in the south. H_2 pipeline infrastructure connecting these two regions to the major demand regions in the west are reinforced. Most of the H_2 storage capacity is deployed at a CO_2 price of \$120/tonne in contrast to the development in battery storage capacity that continues for higher CO_2 prices.

Solar power generation and battery storage charging has a correlation coefficient that is increasing with the CO_2 price, from around 0.28 to 0.45, which is higher than wind-battery and VRE-PEMEL correlations of 0.2–0.3. VRE-PEMEL correlation increase to the level of solar-battery correlation for higher H_2 demands, while wind-battery correlation stay low. This shows that batteries are synergistic with solar power development while flexible H_2 production is supporting the integration of both solar and wind power as shown in previous studies on H_2 production in the electricity system [35,41]. This is also supported by the resulting optimal duration of battery (2–7 h) and H_2 storage (5–36 h), and the locations for the different storage types observed in Fig. 3.

Effect of increasing the H_2 demand

The baseline H_2 demand assumed here is only a small fraction of the total electricity demand. To understand the implications of higher H_2 demand, we analyzed two additional scenarios for H_2 demand corresponding to 10X (scenario b) and 50X (scenario c) the baseline demand (scenario a). The additional H_2 demand can be interpreted to represent H_2 demand for industry, heavy-duty transportation or export of H_2 to other states or countries. For context, the H_2 demand in case a, b and c is equivalent to 4.6, 46 and 230% of the total electric demand in the system, respectively, if converted to energy by the LHV_{H_2} (assuming no losses).

The maximum VRE share is significantly increased from (a) 86.4% to (b) 90.9% and (c) 95.8% as shown in Fig. 5.1. In the scenarios with higher H_2 demand, (b) and (c), the capacity of battery storage required to integrate VRE generation is actually reduced as shown in Fig. 5.2. This is because the flexibility from producing large amounts of H_2 enables the integration of more VRE energy without requiring massive amounts of batteries or natural gas power plants. In (c), we get a VRE share as high as 94% at a CO_2 price of \$60/tonne and 1.3 GW of battery storage, while the same CO_2 price gives a VRE share of 78% in scenario (a) and 87% in scenario (b) requiring 9.7 and 5.9 GW of battery storage respectively.

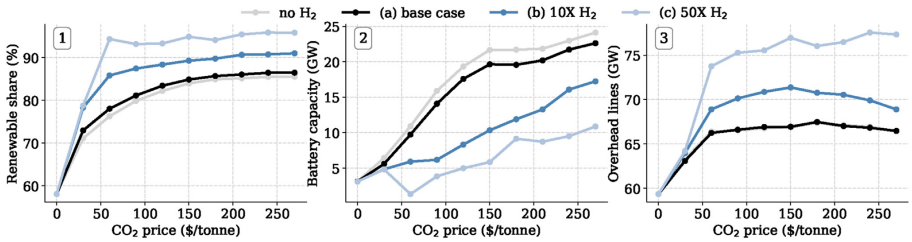

Fig. 5 – 1) VRE share of total electricity production, 2) battery storage capacity (power) and 3) transmission line capacity, by CO_2 price for the different H_2 demand scenarios.

INTERNATIONAL JOURNAL OF HYDROGEN ENERGY 45 (2020) 32899–32915

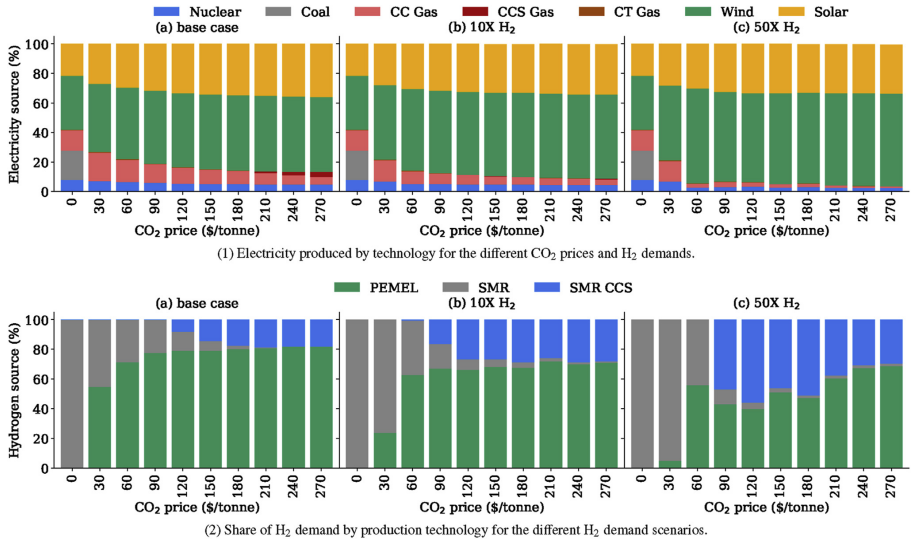

Fig. 6 – Share of electricity and H_2 produced by the different technologies for different CO_2 prices and H_2 demand scenarios.

Integrating VRE requires significant transmission expansion as shown in Fig. 5.3, most of which is realized at a CO_2 price of $60/tonne. The availability of demand flexibility from sources such as electrolytic H_2 production also increases the impact of battery storage and transmission investments with increasing VRE penetration, as highlighted by the increase in VRE penetration with increasing H_2 demand seen in Fig. 5.1. Higher H_2 demand also contributes to reducing the levels of VRE curtailment (defined as percent of available VRE generation), which changes from (a) 6–13% to (b) 5–10% and (c) 4–20% for a CO_2 price above $30/tonne. Scenario (c) with high CO_2 prices results in a large amount of H_2 production from VRE and more than 500 GW of renewable capacity with a curtailment level of almost 20%. However, for a CO_2 price of $60/tonne the installed renewable capacity is 425 GW with significantly lower levels of curtailment at 13%.

The electric energy generation mix for different CO_2 prices and H_2 demands are shown in Fig. 6.1. The electricity produced from coal is reduced to zero at a CO_2 price of $30/tonne. Some of this energy is replaced by natural gas with lower emission intensity and higher operational flexibility than coal. Natural gas is gradually replaced by more VRE generation as demand side flexibility is provided by H_2 produced from PEMEL. Electricity generation from natural gas is reduced by up to (a) 5%, (b) 27% and (c) 53% for CO_2 prices of $30/tonne or higher compared to a reference case with no H_2 production.

Moreover, for CO_2 prices of $180/tonne and above we observe some of the natural gas being replaced by natural gas with CCS. The break-even CO_2 price for CCS adoption in the power sector is higher than those noted by other studies in the literature, primarily [78], because of the synergy between flexible demand from electrolytic H_2 and VRE generation. Gas based electricity generation has lower levelized cost of energy (LCOE) when CCS is included for CO_2 prices of $70/tonne or higher assuming a unity capacity factor (based on the input parameters). This threshold for CCS deployment increases to 100, 150 and 200 $/tonne CO_2 for lower capacity utilization of 0.5, 0.3 and 0.2 as lower utilization favors generation with lower capital expenses (without CCS). Fig. 6.1 shows that the break-even cost of natural gas with CCS is moved to higher CO_2 prices as the H_2 demand increase and more flexibility is available from the H_2 system. In general, the need for flexibility from natural gas based electricity generation is reduced with increasing H_2 demands, which leads to lower utilization of the gas power plants and less incentives to adopt the more capital intensive CCS options. H_2 for electricity generation requires CO_2 prices of more than $210/tonne for scenarios a and b, and $180/tonne for scenario c. Moreover, the share of H_2 to power generation in those cases is less than 0.5% of total generation (not visible in Fig. 6.1).

We compare the shares of the total H_2 demand obtained from the different H_2 plant types, PEMEL, SMR and SMR with CCS, in Fig. 6.2. H_2 is exclusively produced from SMR if no CO_2 pricing is in place. Increasing CO_2 prices favor H_2 production from PEMEL as compared to SMR. The lowest CO_2 price of $30/tonne results in a drastic increase in the H_2 produced from PEMEL to 55% of the total H_2 production in the base case. However, PEMEL becomes less competitive with SMR when

producing larger quantities of H_2 as the electricity demand for PEMEL increases and there is a limited number of hours with VRE surplus and very low electricity prices. As a result, an increasing H_2 demand favors SMR and the PEMEL share at a CO_2 price of $30/tonne is reduced to 24% and only 5% of the H_2 produced in case (b) and (c) respectively.

A CO_2 price of $120/tonne is required to introduce CCS with SMR in the base case, as seen from Fig. 6.2. This is higher than the cost of CO_2 capture for SMR ($83/tonne) because of electrolyzer flexibility and synergy with VRE generation and less than 100% utilization of the SMR plant. Beyond $120/tonne, there is less incentive to shift to electrolytic H_2 supply because of the reduced marginal emissions penalty associated with natural gas based H_2 production with CCS. SMR with CCS is introduced for a lower CO_2 price ($90/tonne) in (b) and (c) as H_2 from PEMEL becomes less competitive with higher hydrogen demand and SMR capacity utilization increases. However, at the highest hydrogen demand in scenario (c) and high CO_2 prices (≥$180/tonne) hydrogen production shifts from SMR with CCS to PEMEL as the former represents a significant share of the total emissions. Here, the maximum electrolyzer capacities for Texas are (a) 6, (b) 47 and (c) 218 GW. As a point of comparison, the newly stated targets by the European Commission are at least 6 and 40 GW of electrolyzer capacity to be installed by 2024 and 2030 respectively [79].

Total and relative CO_2 emissions

Fig. 7 shows the total emissions from joint electricity and H_2 production for a range of CO_2 prices. For comparison between the scenarios, we define the base demand scenario without a CO_2 price as a reference, with emissions set to be 100%. In the base demand scenario, implementing a CO_2 price of $30/tonne results in a large reduction of 66% of the total CO_2 emissions as coal is phased out. Further emissions reduction happens more gradually as the CO_2 price increase until 91% of the initial emissions are mitigated. The H_2 production in (b) is more reliant on SMR which results in a 16–55% increase in total emissions for CO_2 price less than $60/tonne. However, for CO_2 prices of $120/tonne or higher, H_2 is mostly produced from PEMEL (~80%) or SMR with CCS (~20%) resulting in a emissions increase of only 2% compared to (a).

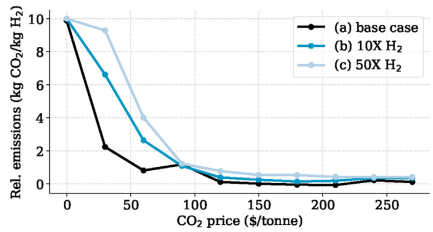

Fig. 8 – Relative CO_2 emissions from producing H_2.

Emissions increase to four times the base case at no CO_2 price for the highest H_2 demand in scenario (c). Producing these amounts of H_2 in Texas will result in significant increases in CO_2 emissions from the base case as it relies heavily on natural gas based H_2 production. For a CO_2 price of more than $90/tonne the emissions are reduced by a order of magnitude as CCS is implemented, and the emissions range between 22 and 58% of the reference value (100% mark) which is about twice the base case emissions for the same CO_2 prices.

We run the model for a scenario without H_2 production in order to quantify the emissions directly attributable to H_2 production. The emissions in the scenario with no H_2 production is subtracted from the total emissions in scenario (a)-(c) and divided by the total amount of H_2 produced in order to calculate the relative emissions (Fig. 8). For CO_2 prices of $0–90/tonne the relative emissions are reduced from 10 to 1.2 kg CO_2/kg H_2 as a large share of the H_2 production from CO_2 intensive SMR (10 kg CO_2/kg H_2) are phased out. H_2 production for CO_2 prices of $120/tonne or more is mostly based on PEMEL and SMR with CCS with a resulting carbon footprint ranging from (a) 0.11 to −0.07, (b) 0.14 to 0.39 and (c) 0.77 to 0.40 kg CO_2/kg H_2.

The relative CO_2 emissions for the base case is negligible or even negative for CO_2 prices ranging from $150–210/tonne. This is because flexible production of electrolytic H_2 displaces the need for flexible generation from CO_2-intensive natural

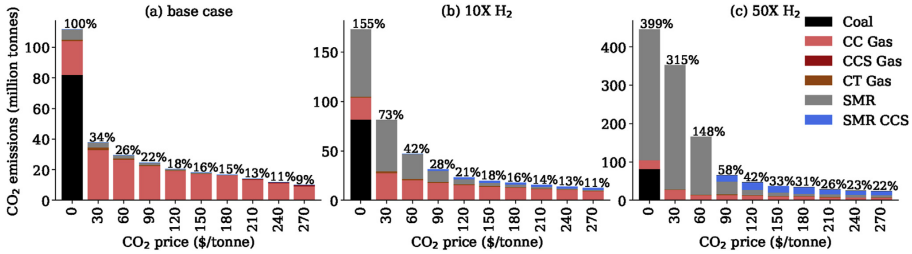

Fig. 7 – Total CO_2 emissions broken down by plant type. Base case with zero CO_2 price is set as reference at 100% for comparisons between the cases as the figures are of different scales.

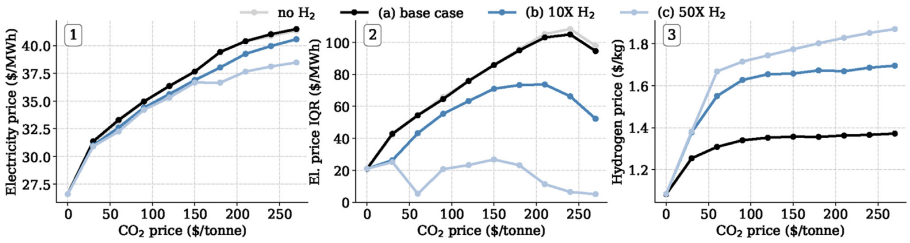

Fig. 9 – 1) average price cost of electricity production, 2) interquartile range (IQR) of the electricity price and 3) price of H_2 production, as a function of CO_2 price and H_2 demand. The IQR is the difference between the 25th and 75th quantile of the electricity price. The prices are weighted by the share of total electricity or H_2 produced at the different locations.

gas power plants, thus contributing to lower electricity sector emissions. The reduction in electricity sector emission is larger than the emissions caused by the H_2 production itself, resulting in lower total emissions for producing H_2. This is possible as most of the H_2 from natural gas include CCS for a CO_2 price of \$150/tonne CO_2 and above, resulting in a low carbon footprint, while CCS for natural gas based electricity production does not emerge until \$210/tonne.

Finally, note that the emissions impacts discussed here are only the emissions related to the production of H_2. Using this H_2 in an application such as H_2 vehicles would lead to further emission reductions from displacing petroleum-based fuels [80]. Using a fuel displacement of 2.46 gallons/kg H_2 [59] and 8.89 kg CO_2/gallon from the US Energy Information Administration (EIA), H_2 can displace around 21.9 kg CO_2/kg H_2 in light duty vehicles (not considering emissions from H_2 production). H_2 can also lead to significant emission reductions in the industrial sector, where replacing coke/coal in manufacturing of steel [81] is one of many applications.

Price of electricity and H_2 production

The marginal cost of electricity and H_2 production can be obtained from the optimization output as the dual values of the energy balances in H_2 and electricity nodes respectively, stated in Eq. (7). Below, we will refer to the systems marginal cost as the price, thus assuming perfect markets based on short-term marginal cost pricing which in theory minimize the average total cost of generation in the long run. In practice, these prices will deviate from real wholesale market prices as additional mechanisms (capacity markets, capacity payments, scarcity pricing etc.) are needed to address reliability and revenue sufficiency due to inherent wholesale market failures [82]. However, more realistic prices could be obtained by fixing the investments before obtaining the duals such that prices to only reflect short-term costs and not capital costs.

The average electricity price for the different scenarios of H_2 production is shown Fig. 9.1. The electricity price is similar for all the scenarios at low CO_2 prices as H_2 is mostly produced from SMR. The electricity price is lower for higher H_2 demands as the CO_2 price surpasses \$30/tonne. The lower electricity price for higher H_2 demands can be explained by the mitigation of large amounts of battery and transmission capacity that otherwise would have been needed to integrate significant amounts of VRE electricity generation at high CO_2 prices. In addition, the flexible H_2 production enables phasing out of natural gas with less CCS and H_2 electricity generation that otherwise would increase the marginal cost of electricity production as seen for a CO_2 price of \$180/tonne or higher.

Producing H_2 from electricity using flexible PEMEL has a smoothing effect on the electricity price as seen in Fig. 9.2, that shows the interquartile range (IQR) of the electricity price, i.e. the difference between the 25th and 75th quantile. The IQR of the electricity price increases with the CO_2 price and VRE deployment, this is balanced by investments in battery capacity that contains the spread in electricity prices. It is high in the base case but decreases significantly when more H_2 is produced in scenarios (b) and (c) due to the flexibility from hydrogen storage.

Similarly to the electricity price in Fig. 9.1, the H_2 price is shown in Fig. 9.3. These prices are in line with prices for H_2 production from wind power in Texas found by recent studies [59]. At zero CO_2 price the marginal H_2 production cost is similar for all the demand cases as H_2 production is exclusively from SMR. For a CO_2 price of \$30/tonne the H_2 price is increased more for scenarios (b) and (c) as compared to the base case (a). Lower prices in (a) are achieved by producing higher amounts of H_2 from PEMEL at only 20% of the average electricity price, whereas (b) and (c) are more reliant on natural gas based H_2 with larger emissions and faces higher electricity prices for PEMEL. From a CO_2 price of \$120/tonne the H_2 prices in case (a) and (b) are not significantly affected by the CO_2 price as 70–80% of the H_2 is produced from PEMEL and the rest is mostly produced from SMR with CCS at a low emission rate. For H_2 demand scenario (c) the H_2 price is increasing as up to 55% of the H_2 produced is based on SMR

with CCS, which have some emissions that drives the marginal cost with increasing CO_2 prices.

Discussion and conclusion

H_2 has the potential to be an important energy carrier that enables CO_2 emissions reductions, particularly in sectors and applications where direct electrification is too expensive or not feasible. Here, we implement a least-cost capacity expansion model with high temporal resolution for coordinated electricity and H_2 infrastructure planning that considers multiple technologies associated with generation and storage of both energy vectors. We specifically investigate the synergies between integration of VRE electricity production and flexible H_2 production by electrolysis (PEMEL) compared against H_2 production from SMR with or without CCS.

For a case study of Texas with pre-defined H_2 demand scenarios in 2050, we find that flexibility from producing H_2 enables larger shares of VRE to be integrated into the power system with less battery storage, as compared to the case with no H_2 demand. The simulated H_2 production by PEMEL correlate with wind power production and can help facilitate development of wind resources in the Texas pan handle (north-west) and southern part of the state. H_2 pipeline corridors are required across the demand scenarios to transport energy from west to east. The infrastructure outcomes are found to be sensitive to both the scale of H_2 demand (baseline, 10X, 50X) and CO_2 prices ($30–270/tonne). A share of VRE electricity generation of 94% is attainable with 1.3 GW of batteries and at a CO_2 of $60/tonne in the highest H_2 demand scenario while the same CO_2 price results in 78% VRE and 9.7 GW batteries in the lowest H_2 demand scenario. The maximum VRE share increase with the H_2 demand to a maximum of 86.4, 90.9 and 95.8% across the H_2 demand scenarios.

In the absence of CO_2 prices, SMR without CCS is the most cost-effective option for H_2 supply even with PEMEL capital costs that are roughly 50% lower than their costs in 2020. However, H_2 produced from electricity is strongly favored by increasing CO_2 prices and represents around half of the H_2 production at a relatively low CO_2 price of $30–60/tonne across the demand scenarios investigated here.

Flexible PEMEL operation complements VRE integration and displaces not only battery storage but also electricity production from natural gas and related emissions, by up to 5% in the lowest H_2 demand scenario and up to 53% in the highest demand scenario. Emissions attributable to serving H_2 demand generally increase with increasing H_2 demand for low CO_2 prices ($30–60/tonne), but are relatively small (less than 1.2 kg CO_2/kg H_2) beyond CO_2 prices of $90/tonne. Notably, for the baseline H_2 demand, the emissions attributable to H_2 demand are negative for CO_2 prices of $150–210/tonne. This suggests that H_2 production from electrolysis is a cost-effective solution to reduce carbon emissions, not only on the consumption side in for example fuel-cell vehicles, but also on the production side in the electric power system, as it enables higher levels of VRE in the system with less electricity from natural gas.

The integrated planning of H_2 and electricity infrastructure also reveals that deployment of CCS for H_2 production occurs at lower CO_2 prices ($90/tonne CO_2) than deployment of CCS for electricity generation ($180/tonne CO_2). Moreover, our estimate of CO_2 prices needed to make CCS-based power generation cost-effective are higher than those estimated by other studies [78], because we account for the impact of flexibility associated with new electricity demands (e.g. PEMEL operation) which reduce utilization of gas turbines. As a result, flexible H_2 production contributes to lowering and stabilizing the electricity price especially at CO_2 prices of $180/tonne or more as electricity generation from natural gas with CCS is reduced.

The marginal price of H_2 production does not see large changes for CO_2 prices above $90/tonne due to the synergies between flexible electrolysis and electricity generation from VRE. However, if the H_2 demand is very high, more of the H_2 will be produced by SMR with CCS for high CO_2 prices and the H_2 price is therefore somewhat sensitive to the CO_2 price.

The above framework can be adapted to study a broad range of technologies and sector-coupling issues. One area of future work would consider the role for other energy storage technologies such as compressed-air storage, electrochemical flow batteries or pumped hydro, which could compete with the flexible demand from the H_2 system. Another area of future work involves sector coupling with sectors needing heating and cooling end-use services where thermal storage could potentially be important. Incorporating temporal variability in H_2 demand can further increase the flexibility requirements provided by energy storage.

In our analysis, we only see small levels of re-conversion from H_2 to electricity at high CO_2 prices as it is expensive compared to CCS and the round-trip efficiency is low. Further sensitivity analysis on parameters such as carbon transport and storage cost, electrolyzer capital cost and natural gas prices could shed light on break-even points between cost of electricity generation from H_2 and natural gas with CCS.

Model improvements to be considered in future work include use of integer investment decisions for technologies with large plant sizes such as thermal power plants, transmission lines and SMR facilities. Representation of energy transport constraints for electricity and hydrogen can be enhanced by: a) employing DC power flow equations, b) model pipeline's ability to provide H_2 storage through line-packing and c) evaluating trade-off between truck and pipeline transport for H_2. These extensions will enable more accurate modeling of integrated H_2 and electricity infrastructure roll out.

To conclude, we point out that supporting adoption of H_2 in end-use applications and supplying that via electrolysis serves to benefit decarbonization and VRE integration in the power sector. This is contingent on electrolyzers to be able to effectively participate in electricity markets as we have envisioned here and regulators have a role in order create the right policies to make that happen.

INTERNATIONAL JOURNAL OF HYDROGEN ENERGY 45 (2020) 32899–32915 32911

Declaration of competing interest

The authors declare that they have no known competing financial interests or personal relationships that could have appeared to influence the work reported in this paper.

Acknowledgements

This publication is based on results from the research project Hyper, performed under the ENERGIX programme. The authors acknowledge the following parties for financial support: Equinor, Shell, Kawasaki Heavy Industries, Linde Kryotechnik, Mitsubishi Corporation, Nel Hydrogen and the Research Council of Norway (255107/E20) . D.S.M. contributed to this study while being supported by the Low-Carbon Energy Center on Electric Power Systems at the MIT Energy Initiative.

Appendix A. Illustrative example of Energy Balance

Here we give a illustrative example of the notation and energy balance used in the model. Consider the two nodes from Fig. 1, one electric and one H_2, which are connected by PEMEL and PEMFC. At the electric node, electricity is produced from wind and solar power, while H_2 is produced by SMR at the H_2 node.

The set of nodes is given by Eq. (A.1).

$$\mathcal{N} = \{1, 2\} \tag{A.1}$$

Node 1 is the electric node while node 2 is the H_2 node, thus the sets of production technologies at the nodes are shown in Eq. (A.2) and (A.3) respectively.

$$\mathcal{P}_1 = \{\text{Wind}, \text{Solar}, \text{PEMFC}\} \tag{A.2}$$

$$\mathcal{P}_2 = \{\text{SRM}, \text{PEMEL}\} \tag{A.3}$$

Similarly, we define the sets of storage technologies in Eq. (A.4) and (A.5).

$$\mathcal{S}_1 = \{\text{Battery}\} \tag{A.4}$$

$$\mathcal{S}_2 = \{H_2 \text{ Storage}\} \tag{A.5}$$

The conversion technologies producing at node n represents loads at another node given by the connectivity in set C_n. For our example, PEMFC producing electricity at node 1 consumes H_2 at node 2 as shown by Eq. (A.6). PEMEL producing H_2 at node 2 consumes electricity at node 1, shown by Eq. (A.7).

$$\mathcal{C}_1 = \{2\} \tag{A.6}$$

$$\mathcal{C}_2 = \{1\} \tag{A.7}$$

The conversion technology types representing the loads in C_n are given by the sets in Eq. (A.8) and (A.9).

$$\mathcal{F}_1 = \{\text{PEMEL}\} \tag{A.8}$$

$$\mathcal{F}_2 = \{\text{PEMFC}\} \tag{A.9}$$

The H_2 storage requires compression to 100 bar, this is represented as an auxiliary electric load at C_n by the set in Eq. (A.10).

$$\mathcal{A}_1 = \{H_2 \text{ Storage}\} \tag{A.10}$$

$$\mathcal{A}_2 = \{\} \tag{A.11}$$

From the sets we have defined and the generalized formulation of the energy balance in Eq. (7) the resulting energy balance for the electric node for time step t, is shown in (A.12).

$$\begin{aligned} &p_{t,\text{Wind},1} + p_{t,\text{Solar},1} + p_{t,\text{PEMFC},1} - p^{exp}_{t,1} + p^{imp}_{t,1} \\ &+ (e^{out}_{t,\text{Battery},1} - e^{in}_{t,\text{Battery},1}) + r_{t,1} \\ &= D_{t,1} + F_{\text{PEMEL}} p_{t,\text{PEMEL},2} + A_{\text{H2S}} e^{in}_{t,\text{H2S},2} \end{aligned} \tag{A.12}$$

Similarly, the energy balance at the H_2 node in kg of H_2 is shown in Eq. (A.13).

$$\begin{aligned} &p_{t,\text{SMR},2} + p_{t,\text{PEMEL},2} - p^{exp}_{t,2} + p^{imp}_{t,2} \\ &+ (e^{out}_{t,\text{H2S},2} - e^{in}_{t,\text{H2S},2}) + r_{t,2} \\ &= D_{t,2} + F_{\text{PEMFC}} p_{t,\text{PEMFC},1} \end{aligned} \tag{A.13}$$

Appendix B. Input Parameters

Table B.1 – Parameters used in the case study

Parameter	Value
Discount rate	6.6%
Retirement cost	10% of inv. cost
Natural gas price	$5.24/mmBtu
Rationing cost	$10 000/MWh
	$10 000/kg H$_2$
Carbon storage and transport cost	$11/tonne

Table B.2 – Installed capacity in 2019 adopted from the NEEDS model [55].

Bus	CC Gas [MW]	CT Gas [MW]	Nuclear [MW]	Wind [MW]	Solar [MW]	Coal [MW]	Biomass [MW]
1	6598	5621	2400	2168	24		
2				3999	340		
3		1540		5842		2085	
4	9729	8191					146
5				1051	141		
6	2850	3190		7913	873		
7	1943	1008			5	5744	
8	3098	2064		543	96	2371	
9	4072	1843		1680	52	940	
	4118	2490	2560			2507	
11	4854	1726				4187	5
12	2949	618		4849			18
13				998	905		
Sum	40,211	28,291	4,960	29,043	2,436	17,834	169

Table B.3 – Technology costs for 2050 from NREL ATB technology baseline [65]. Fuel units (f.u.) are mmBtu for natural gas and kg for hydrogen.

Type	Inv. cost ($/kW)	Fixed cost ($/kW-year)	Var. cost ($/MWh)	Fuel (f.u./MWh)	Emission (kg/MWh)	CCS rate (kg/MWh)	Size (MW)	Min. Gen. (MW)	Ramp Rate (%/h)	Lifetime (years)
Wind	1011	33	0	0	0	0	100	0	1	30
Solar	683	8	0	0	0	0	150	0	1	30
CT Gas	800	12	7	9.08	481.6	0	240	0	1	55
CC Gas	800	11	3	6.28	333	0	1100	0	0.252	55
CCS Gas	1730	34	7	7.49	39.8	358.2	340	0	0.252	55
Coal	3640	33	24.1	0	834.7	0	650	260	0.1584	75
CCS Coal	5240	80	30.2	0	88.4	795.6	650	325	0.1584	75
Nuclear	5530	101	9.6	0	0	0	2200	2200	0.156	60
Biomass	3490	112	46.9	0	0	0	85	34	0.32	45
CC H2	900	13	2.8	5.69	0	0	1100	0	0.252	25
CT H2	600	6	8.8	8.54	0	0	240	0	1	25
PEMFC	1090	0	8.9	6.7	0	0	50	0	1	10

Table B.4 – Technology costs in 2040 are obtained from the NREL centralized H_2 production case studies for electrolysis [9] and from a IEA GHG technical report on SMR with CCS [64]. Electricity for the SMR and CO_2 capture processes are generated by on-site gas turbines [64].

Type	Inv. cost ($/(kg/h))	Fixed cost ($/(kg/h))	Var. cost ($/kg)	Fuel (mmBtu/kg)	Electricity (MWh/kg)	Emission (kg CO_2/kg H_2)	CCS rate (kg CO_2/kg H_2)	Size (kg/h)	Min. Gen. (kg/h)	Ramp Rate (%/h)	Lifetime (years)
SMR	33800	0	0	0.146	0	10	0	9170	8250	0.1	25
SMR CCS	73480	0	0	0.16	0	0.99	9.01	9170	8250	0.1	25
PEMEL	27310	1915	0	0	51.3	0	0	2000	0	1	40

Table B.5 – Technology costs for storage technologies [9,67,70,71]. Units for the different storage technologies are specified by p.u. and e.u. for power and energy respectively.

Type	p.u.	e.u.	Inv. power ($/pu)	Inv. energy ($/eu)	Fix power ($/pu-yr)	Fix energy ($/eu-yr)	Ramp (%/h)	Eff. In/Out	Aux power (kWh/eu)	Life (years)
Battery storage	kW	kWh	273	84	15.19	0	1	0.92	0	15
Hydrogen storage	kg/h	Kg	1540	516	46	2	1	1	1.284	40

Table B.6 – H_2 demand per node based on high case for adoption of fuel cell vehicles [kg/day] [58].

Bus	1	2	3	4	5	6	7	8	9	10	11	13
H2 demand	764 200	300	3210	334 920	1550	13 240	2390	200 570	190 450	333 950	4250	20 350

REFERENCES

[1] International Energy Agency. World energy outlook 2018. Tech. Rep.. 2018. https://doi.org/10.1787/weo-2018-2-en. 0

[2] Ruhnau O, Bannik S, Otten S, Praktiknjo A, Robinius M. Direct or indirect electrification? A review of heat generation and road transport decarbonisation scenarios for Germany 2050. Energy 2019;166:989–99. https://doi.org/10.1016/j.energy.2018.10.114.

[3] Robinius M, Linßen J, Grube T, Reuß M, Stenzel P, Syranidis K, Kuckertz P, Stolten D. Comparative analysis of infrastructures: hydrogen fueling and electric charging of vehicles. Tech. Rep. January. Forschungszentrums Jülich; 2018.

[4] Tlili O, Mansilla C, Frimat D, Perez Y. Hydrogen market penetration feasibility assessment: mobility and natural gas markets in the US, Europe, China and Japan. Int J Hydrogen Energy 2019;44(31):16048–68. https://doi.org/10.1016/j.ijhydene.2019.04.226.

[5] Horvath S, Fasihi M, Breyer C. Techno-economic analysis of a decarbonized shipping sector: technology suggestions for a fleet in 2030 and 2040. Energy Convers Manag 2018;164(November 2017):230–41. https://doi.org/10.1016/j.enconman.2018.02.098.

[6] García-Olivares A, Solé J, Osychenko O. Transportation in a 100% renewable energy system. Energy Convers Manag 2018;158(August 2017):266–85. https://doi.org/10.1016/j.enconman.2017.12.053.

[7] Schemme S, Breuer JL, Köller M, Meschede S, Walman F, Samsun RC, Peters R, Stolten D. H2-based synthetic fuels: a techno-economic comparison of alcohol, ether and hydrocarbon production. Int J Hydrogen Energy 2020;45(8):5395–414. https://doi.org/10.1016/j.ijhydene.2019.05.028.

[8] IEA - International Energy Agency. The Future of Hydrogen – seizing today's opportunities. Tech. rep. 2019;2019:1–203. URL, https://www.iea.org/reports/the-future-of-hydrogen.

[9] National Renewable Energy Laboratory. H2A: hydrogen analysis production case studies — hydrogen and fuel cells. NREL; 2019. URL, https://www.nrel.gov/hydrogen/h2a-production-case-studies.html.

[10] Saba SM, Müller M, Robinius M, Stolten D. The investment costs of electrolysis – a comparison of cost studies from the past 30 years. Int J Hydrogen Energy 2018;43(3):1209–23. https://doi.org/10.1016/J.IJHYDENE.2017.11.115.

[11] Schmidt O, Gambhir A, Staffell I, Hawkes A, Nelson J, Few S. Future cost and performance of water electrolysis: an expert elicitation study. Int J Hydrogen Energy 2017;42(52):30470–92. https://doi.org/10.1016/j.ijhydene.2017.10.045.

[12] Proost J. Critical assessment of the production scale required for fossil parity of green electrolytic hydrogen. Int J Hydrogen Energy 2020;2050. https://doi.org/10.1016/j.ijhydene.2020.04.259 (xxxx).

[13] Levene JI, Mann MK, Margolis RM, Milbrandt A. An analysis of hydrogen production from renewable electricity sources. Sol Energy 2007;81(6):773–80. https://doi.org/10.1016/J.SOLENER.2006.10.005.

[14] Korpås M, Greiner CJ. Opportunities for hydrogen production in connection with wind power in weak grids. Renew Energy 2008;33(6):1199–208. https://doi.org/10.1016/j.renene.2007.06.010.

[15] Beccali M, Brunone S, Finocchiaro P, Galletto JM. Method for size optimisation of large wind-hydrogen systems with high penetration on power grids. Appl Energy 2013;102:534–44. https://doi.org/10.1016/j.apenergy.2012.08.037.

[16] Lund PD, Lindgren J, Mikkola J, Salpakari J. Review of energy system flexibility measures to enable high levels of variable renewable electricity. Renew Sustain Energy Rev 2015;45:785–807. https://doi.org/10.1016/J.RSER.2015.01.057.

[17] Lyseng B, Niet T, English J, Keller V, Palmer-Wilson K, Robertson B, Rowe A, Wild P. System-level power-to-gas energy storage for high penetrations of variable renewables. Int J Hydrogen Energy 2018;43(4):1966–79. https://doi.org/10.1016/J.IJHYDENE.2017.11.162.

[18] McPherson M, Johnson N, Strubegger M. The role of electricity storage and hydrogen technologies in enabling global low-carbon energy transitions. Appl Energy 2018;216:649–61. https://doi.org/10.1016/j.apenergy.2018.02.110.

[19] Glenk G, Reichelstein S. Economics of converting renewable power to hydrogen. Nature Energy 2019;4(3):216–22. https://doi.org/10.1038/s41560-019-0326-1.

[20] Proost J. State-of-the art CAPEX data for water electrolysers, and their impact on renewable hydrogen price settings. Int J Hydrogen Energy 2019;44(9):4406–13. https://doi.org/10.1016/j.ijhydene.2018.07.164.

[21] Wang D, Muratori M, Eichman J, Wei M, Saxena S, Zhang C. Quantifying the flexibility of hydrogen production systems to support large-scale renewable energy integration. J Power Sources 2018;399(August):383–91. https://doi.org/10.1016/j.jpowsour.2018.07.101.

[22] Bødal EF, Korpås M. Regional effects of hydrogen production in congested transmission grids with wind and hydro power. In: 14th International Conference on the European Energy Market - EEM. IEEE; 2017. p. 1–6. https://doi.org/10.1109/EEM.2017.7982013.

[23] Greiner CJ. Doctoral thesis: sizing and operation of wind-hydrogen energy systems. Ph.D. thesis. NTNU; 2010.

[24] Botterud A, Yildiz B, Conzelmann G, Petri MC. Nuclear hydrogen: an assessment of product flexibility and market viability. Energy Pol 2008;36(10):3961–73. https://doi.org/10.1016/j.enpol.2008.07.007.

[25] Greiner CJ, Korpas M, Gjengedal T. Dimensioning and operating wind-hydrogen plants in power markets. In: 12th WSEAS International Conference on CIRCUITS; 2008. p. 405–14.

[26] Greiner CJ, Korpas M, Gjengedal T. A model for techno-economic optimization of wind power combined with hydrogen production in weak grids. EPE Journal 2009;19(2):52–9. https://doi.org/10.1080/09398368.2009.11463717.

[27] Peterson D, Vickers J, DeSantis D. Hydrogen production cost from PEM electrolysis - 2019. Tech. rep. Department of Energy; 2020. URL, https://www.hydrogen.energy.gov/pdfs/19009_h2_production_cost_pem_electrolysis_2019.pdf.

[28] Korpås M. Distributed energy systems with wind power and energy storage, vol. 183; 2004. p. 1–80.

[29] Kopp M, Coleman D, Stiller C, Scheffer K, Aichinger J, Scheppat B. Energiepark Mainz: technical and economic analysis of the worldwide largest Power-to-Gas plant with

PEM electrolysis. Int J Hydrogen Energy 2017;42(19). https://doi.org/10.1016/j.ijhydene.2016.12.145.
[30] Bødal EF, Korpås M. Value of hydro power flexibility for hydrogen production in constrained transmission grids. Int J Hydrogen Energy 2020;45(2):1255–66. https://doi.org/10.1016/j.ijhydene.2019.05.037.
[31] Alshehri F, Suárez VG, Rueda Torres JL, Perilla A, van der Meijden MA. Modelling and evaluation of PEM hydrogen technologies for frequency ancillary services in future multi-energy sustainable power systems. Heliyon 2019;5(4). https://doi.org/10.1016/j.heliyon.2019.e01396. e01396.
[32] Go RS, Munoz FD, Watson J-P. Assessing the economic value of co-optimized grid-scale energy storage investments in supporting high renewable portfolio standards. Appl Energy 2016;183:902–13. https://doi.org/10.1016/J.APENERGY.2016.08.134.
[33] Mallapragada DS, Sepulveda NA, Jenkins JD. Long-run system value of battery energy storage in future grids with increasing wind and solar generation. Appl Energy 2020;275(February):115390. https://doi.org/10.1016/j.apenergy.2020.115390.
[34] Colbertaldo P, Agustin SB, Campanari S, Brouwer J. Impact of hydrogen energy storage on California electric power system: towards 100% renewable electricity. Int J Hydrogen Energy 2019;44(19):9558–76. https://doi.org/10.1016/J.IJHYDENE.2018.11.062.
[35] Liu H, Brown T, Andresen GB, Schlachtberger DP, Greiner M. The role of hydro power, storage and transmission in the decarbonization of the Chinese power system. Appl Energy 2019;239(November 2018):1308–21. https://doi.org/10.1016/j.apenergy.2019.02.009.
[36] Welder L, Ryberg D, Kotzur L, Grube T, Robinius M, Stolten D. Spatio-temporal optimization of a future energy system for power-to-hydrogen applications in Germany. Energy 2018;158:1130–49. https://doi.org/10.1016/j.energy.2018.05.059.
[37] Welder L, Stenzel P, Ebersbach N, Markewitz P, Robinius M, Emonts B, Stolten D. Design and evaluation of hydrogen electricity reconversion pathways in national energy systems using spatially and temporally resolved energy system optimization. Int J Hydrogen Energy 2019;44(19):9594–607. https://doi.org/10.1016/J.IJHYDENE.2018.11.194.
[38] Emonts B, Reuß M, Stenzel P, Welder L, Knicker F, Grube T, Görner K, Robinius M, Stolten D. Flexible sector coupling with hydrogen: a climate-friendly fuel supply for road transport. Int J Hydrogen Energy 2019;44(26):12918–30. https://doi.org/10.1016/j.ijhydene.2019.03.183.
[39] Samsatli S, Staffell I, Samsatli NJ. Optimal design and operation of integrated wind-hydrogen-electricity networks for decarbonising the domestic transport sector in Great Britain. Int J Hydrogen Energy 2016;41(1):447–75. https://doi.org/10.1016/j.ijhydene.2015.10.032.
[40] Koltsaklis NE, Dagoumas AS. State-of-the-art generation expansion planning: a review. Appl Energy 2018;230:563–89. https://doi.org/10.1016/J.APENERGY.2018.08.087.
[41] Victoria M, Zhu K, Brown T, Andresen GB, Greiner M. The role of storage technologies throughout the decarbonisation of the sector-coupled European energy system. Energy Convers Manag 2019;201:111977. https://doi.org/10.1016/j.enconman.2019.111977.
[42] Blanco H, Nijs W, Ruf J, Faaij A. Potential for hydrogen and Power-to-Liquid in a low-carbon EU energy system using cost optimization. Appl Energy 2018;232:617–39. https://doi.org/10.1016/j.apenergy.2018.09.216.
[43] Pan G, Gu W, Qiu H, Lu Y, Zhou S, Wu Z. Bi-level mixed-integer planning for electricity-hydrogen integrated energy system considering levelized cost of hydrogen. Appl Energy 2020;270(May):115176. https://doi.org/10.1016/j.apenergy.2020.115176.
[44] Kanellopoulos K, Blanco H. The potential role of H2 production in a sustainable future power system - an analysis with METIS of a decarbonised system powered by renewables in 2050. Tech. rep. European Commission; 2019. https://doi.org/10.2760/540707.
[45] Lux B, Pfluger B. A supply curve of electricity-based hydrogen in a decarbonized European energy system in 2050. Appl Energy 2020;269(April):115011. https://doi.org/10.1016/j.apenergy.2020.115011.
[46] Cloete S, Hirth L. Flexible power and hydrogen production: finding synergy between CCS and variable renewables. Energy 2020;192:116671. https://doi.org/10.1016/j.energy.2019.116671.
[47] Lim JY, How BS, Rhee G, Hwangbo S, Yoo CK. Transitioning of localized renewable energy system towards sustainable hydrogen development planning: P-graph approach. Appl Energy 2020;263(November 2019):114635. https://doi.org/10.1016/j.apenergy.2020.114635.
[48] You C, Kwon H, Kim J. Economic, environmental, and social impacts of the hydrogen supply system combining wind power and natural gas. Int J Hydrogen Energy 2020. https://doi.org/10.1016/j.ijhydene.2020.06.095.
[49] Palmintier BS, Webster MD. Heterogeneous unit clustering for efficient operational flexibility modeling. IEEE Trans Power Syst 2014;29(3):1089–98. https://doi.org/10.1109/TPWRS.2013.2293127.
[50] Palmintier BS. Incorporating operational flexibility into electric generation planning - impacts and methods for system design and policy analysis. Ph.D. thesis. Massachusetts Institute of Technology; 2013. URL, https://dspace.mit.edu/handle/1721.1/79147.
[51] Hart WE, Watson JP, Woodruff DL. Pyomo: modeling and solving mathematical programs in Python. Mathematical Programming Computation 2011;3(3):219–60. https://doi.org/10.1007/s12532-011-0026-8.
[52] Hart WE, Laird CD, Watson J-P, Woodruff DL, Hackebeil GA, Nicholson BL, Siirola JD. Optimization modeling in Python - springer optimization and its applications, vol. 67. Springer Nature; 2017. https://doi.org/10.1007/978-3-319-58821-6.
[53] Du P, Baldick R, Tuohy A. Integration of large-scale renewable energy into bulk power systems - from planning to operation, power electronics and power systems. Cham: Springer International Publishing; 2017. https://doi.org/10.1007/978-3-319-55581-2.
[54] Majidi-Qadikolai M, Baldick R. Stochastic transmission capacity expansion planning with special scenario selection for integrating $n-1$ contingency analysis. IEEE Trans Power Syst 2016;31(6):4901–12. https://doi.org/10.1109/TPWRS.2016.2523998.
[55] United States Environmental Protection Agency. Documentation for national electric energy data system (NEEDS) v.5.13. URL, https://www.epa.gov/airmarkets/documentation-national-electric-energy-data-system-needs-v513; 2019.
[56] U.S. EIA. Annual energy outlook 2019 with projections to 2050, annual energy outlook 2019 with projections to 2050, vol. 44; 2019. p. 1–64 (8) DOE/EIA-0383(2012) U.S.
[57] Mann N, Tsai C-H, Gürcan G, Schneider E, Cuevas P, Dyer J, Butler J, Zhang T, Baldick R, Deetjen T, Morneau R. The full cost of electricity (FCe-) capacity expansion and dispatch modeling: model documentation and results for ERCOT scenarios. Tech. rep. University of Texas at Austin; 2017.
[58] Melaina M, Bush B, Muratori M, Zuboy J, Ellis S. National hydrogen scenarios: how many stations, where, and when?. Tech. Rep. October, Prepared by the National Renewable

Energy Laboratory for the H2 USA Locations Roadmap Working Group; 2017.
[59] Nagasawa K, Davidson FT, Lloyd AC, Webber ME. Impacts of renewable hydrogen production from wind energy in electricity markets on potential hydrogen demand for light-duty vehicles. Appl Energy 2019;235(June 2018):1001–16. https://doi.org/10.1016/j.apenergy.2018.10.067.
[60] Elgowainy A. Hydrogen demand analysis for H2 @ scale. URL, https://www.hydrogen.energy.gov/pdfs/review19/sa172_elgowainy_2019_o.pdf; 2019.
[61] Ruth M. H2 @ scale: hydrogen integrating energy systems. URL, https://www.nrel.gov/docs/fy20osti/75422.pdf; 2019.
[62] Parkinson B, Balcombe P, Speirs JF, Hawkes AD, Hellgardt K. Levelized cost of CO 2 mitigation from hydrogen production routes. Energy Environ Sci 2019;12(1):19–40. https://doi.org/10.1039/c8ee02079e.
[63] Khojasteh Salkuyeh Y, Saville BA, MacLean HL. Techno-economic analysis and life cycle assessment of hydrogen production from natural gas using current and emerging technologies. Int J Hydrogen Energy 2017. https://doi.org/10.1016/j.ijhydene.2017.05.219.
[64] IEA. Techno - economic evaluation of SMR based standalone (merchant) hydrogen plant with CCS. Tech. Rep. February. Paris, France: IEA; 2017. URL, http://ieaghg.org/exco_docs/2017-02.pdf.
[65] National Renewable Energy Laboratory (NREL). Annual technology baseline: electricity (2019). 2019. URL, https://atb.nrel.gov/.
[66] Grant T, Morgan D, Gerdes K. Quality guidelines for energy system studies: carbon dioxide transport and storage costs in NETL studies. Tech. Rep. August. National Energy Technology Laboratory; 2019.
[67] van Leeuwen C, Zauner A. Innovative large-scale energy storage technologies and Power-to-Gas concepts after optimisation. Report on the costs involved with PtG technologies and their potentials across the EU, Tech. Rep. University of Groningen; 2018. URL, https://www.storeandgo.info/publications/deliverables/.
[68] Cooley G, Allen A. Interim results presentation 2019. 2019. URL, https://www.itm-power.com/images/Investors/PresentationsAndResearch/Interim-Results-presentation_18.pdf.
[69] André J, Auray S, De Wolf D, Memmah MM, Simonnet A. Time development of new hydrogen transmission pipeline networks for France. Int J Hydrogen Energy 2014;39(20):10323–37. https://doi.org/10.1016/j.ijhydene.2014.04.190.
[70] Ahluwalia RK, Contact P, Peng J-k, Manager DOE, Randolph K. System Analysis of physical and materials-based hydrogen storage. Tech. rep. DOE Hydrogen and Fuel Cells Program; 2018. URL, https://www.hydrogen.energy.gov/pdfs/progress19/h2f_st001_ahluwalia_2019.pdf.
[71] Ahluwalia RK, Hua TQ, Peng J-K, Roh HS. System level analysis of hydrogen storage options. Project ID: ST001. 2019. URL, https://www.hydrogen.energy.gov/pdfs/review19/st001_ahluwalia_2019_o.pdf.
[72] Caglayan DG, Weber N, Heinrichs HU, Linßen J, Robinius M, Kukla PA, Stolten D. Technical potential of salt caverns for hydrogen storage in Europe. Int J Hydrogen Energy 2020;45(11):6793–805. https://doi.org/10.1016/j.ijhydene.2019.12.161.
[73] Tarkowski R. Underground hydrogen storage: characteristics and prospects. 2019. https://doi.org/10.1016/j.rser.2019.01.051. 5.
[74] Andrade J, Baldick R. Estimation of transmission costs for new generation. Tech. rep. University of Texas at Austin; 2017.
[75] Lee N, Flores-Espino F, Hurlbut D. Renewable energy zones (REZ) transmission planning process: a Guidebook for practitioners. 2017. URL, https://www.nrel.gov/docs/fy17osti/69043.pdf.
[76] Lasher W. The competitive renewable energy zones process. Ercot; 2014.
[77] United States Environmental Protection Agency (EPA). Social cost of carbon. Tech. Rep. December. US EPA; 2016. URL, https://www.epa.gov/sites/production/files/2016-12/documents/social_cost_of_carbon_fact_sheet.pdf.
[78] Mathieu P. The IPCC special report on carbon dioxide capture and storage. 2006.
[79] European Comission. A hydrogen strategy for a climate neutral europe. 2020.
[80] Andress D, Nguyen TD, Das S. Reducing GHG emissions in the United States' transportation sector. 2011. https://doi.org/10.1016/j.esd.2011.03.002.
[81] Vogl V, Åhman M, Nilsson LJ. Assessment of hydrogen direct reduction for fossil-free steelmaking. J Clean Prod 2018;203:736–45. https://doi.org/10.1016/j.jclepro.2018.08.279.
[82] Milligan M, Frew B, Clark K, Bloom A. Marginal cost pricing in a world without perfect competition: implications for electricity markets with high shares of low marginal cost resources. Tech. Rep. December. NREL; 2017.

Acronyms

CCS: carbon capture and storage
EIA: US Energy Information Administration
EPA: US Environmental Protection Agency
ERCOT: Electric Reliability Council of Texas
GHG: greenhouse gas
LCOE: levelized cost of energy
LHV: lower heating value
LP: linear programming
NREL: National Renewable Energy Laboratory
PEMEL: proton exchange membrane electrolysis
PEMFC: proton exchange membrane fuel cell
SMR: steam-methane reforming
VRE: variable renewable energy

A.5 Capacity Expansion Planning with Stochastic Rolling Horizon Dispatch

Capacity Expansion Planning with Stochastic Rolling Horizon Dispatch

Espen Flo Bødal[a], Audun Botterud[b], Magnus Korpås[a]

[a]Department of Electric Power Engineering, Norwegian University of Science and Technology, Trondheim, Norway
[b]Laboratory for Information and Decision Systems, Massachusetts Institute of Technology, Cambridge, USA

Abstract

Variable renewable energy sources introduce significant amounts of short-term uncertainty that should be considered when making investment decisions. In this work, we present a method for representing stochastic power system operation in day-ahead and real-time electricity markets within a capacity expansion model. We use Benders cuts and a stochastic rolling horizon dispatch to represent operational costs in the capacity expansion problem (CEP) and investigate different formulations for the cuts. We test the model on a two-bus case study with wind power, energy storage and a constrained transmission line. The case study shows that cuts created from the day-ahead problem gives the lowest expected total cost for the stochastic CEP. The stochastic CEP results in 3% lower expected total cost compared to the deterministic CEP capacities evaluated under uncertain operation. The number of required stochastic iterations is efficiently reduced by introducing a deterministic lower bound, while extending the horizon of the operational problem by persistence forecasting leads to reduced operational costs.

Keywords: Capacity Expansion, Rolling Horizon Model, Short-term uncertainty, Power System Analysis

1. Introduction

The increasing penetration of variable renewable energy (VRE) sources are introducing new challenges in modern power systems. Central to these challenges is the increased level of short-term uncertainty and the need for more flexibility in operation [1]. To balance supply and demand for electricity in the power system, we need a certain share of flexible resources that can reliably change their energy output in a few seconds or minutes to counteract variations in VRE electricity production [2]. The level of VRE that can be integrated into an power system in a cost-effective manner is directly dependent on the level of flexibility in the system [3].

The need for more flexibility, changes in market structures and operational rules have been evident in countries which are integrating large amounts of VRE such as Denmark, China, Ireland and Spain [4, 5]. As power systems are aspiring to increase the share of clean energy sources towards 100 %, even more and cleaner flexible sources are needed.

Traditionally, the long-term power system capacity expansion problem (CEP) focuses on long-term uncertainties in investment costs, yearly electricity demand, and policy decisions, but neglect short-term uncertainties [6]. This can lead to inaccurate results as using a deterministic representation of operations in investment models overvalues fluctuating VRE [7] and undervalue flexible resources, and can also lead to insufficient investments for both thermal generation [8] and transmission capacities [9]. In these type of models, short-term uncertainties from VRE are often implicitly accounted for by using deterministic reserve constraints based on forecast errors [10, 11]. Representing the short-term uncertainty explicitly in the model as a stochastic parameter is expected to give significantly better results compared to using reserve constraints [12], but there are few long-term models for the CEP that do this as it is much more computationally demanding.

The computational complexity of stochastic CEPs can be reduced by either reducing the number of scenarios [11, 13, 14] or reducing the time dimension by using representative operational periods [15]. Reducing the time dimension from a full year to some representative periods of one to several days is a common approach and allows for more detailed operational models that include uncertainty in wind and solar power [7, 16]. However, studies show that the temporal resolution and chronology is especially important in CEPs with large shares of VRE [17] where simple operational representations might lead to over-investments in solar and under-investments in wind and natural gas. Furthermore, the chronology will become more important as energy storage becomes more relevant as a flexible asset due to reduced storage costs and increasing VRE integration. Evidently, insufficient representation of short-term uncertainty, temporal resolution and chronology can be significant factors in undervaluing flexibility and overestimating the optimal VRE levels in power systems.

In power system applications, rolling-horizon frameworks are extensively used in operational models and case studies that focus on short-term VRE uncertainty and flexibility, for example to study VRE integration [18], for large scale battery operation [19] and for local energy storage in proximity to VRE electricity production [20]. Models using this framework are suitable for representing short-term uncertainty in an accurate and realistic way, and can therefore capture the need for flexibility during operation. The METIS model is developed by the Directorate-General for Energy of the European Comission, which use a rolling-horizon approach for detailed simulation of the power system in the context of electricity markets, VRE in-

tegration and sector-coupling [21]. The METIS model is used in integration with the TIMES model to study the future development of the European power system [22], which call attention to the need for more detailed modeling of system operation in future capacity expansion studies.

Stochastic rolling-horizon dispatch (SRHD) models is formulated by a series of two-stage economic dispatch problems integrated in a rolling-horizon framework [23], thereby accounting for operational details such as market products, time stages, and uncertain VRE power production. SRHD within the CEP is previously used for assessing the effect of VRE on different CO_2-emission policies [24]. It has also been used for assessing VRE and storage investments in micro-grids, using various heuristic methods [25, 26]. To the knowledge of the authors, the work of Forthenbacher et al. (2018) is the only study where a SRHD has been integrated in the CEP using Benders cuts [27]. In [27], Benders cuts connect the operational model to the investment model, which is used to determine placing and sizing of batteries in a distribution grid.

In this work we formulate a model for the CEP with SRHD, focusing on the representation of the operational decisions in both the day-ahead and real-time markets. The market representation is an important difference compared to [27], as we model that generators commit to a schedule in the day-ahead market that can be adjusted in the real-time market. This market representation resembles the market representation used in Pineda et al. (2016), who use forecast errors and duration curves to study the impact of short-term uncertainty on the CEP [28]. We improve on the dispatch strategy in [27] by including a long-term storage scheduling model in the algorithm that gives end-of-horizon storage value. The deterministic long-term storage scheduling model is used to accelerate the decomposition algorithm by providing a lower bound to the operational costs. The main contributions of this paper are:

a) We show how to use Benders cuts to extract operational values from the SRHD for a CEP in the context of day-ahead and real-time electricity markets.

a) We propose an algorithm for representing two-stage stochastic rolling horizon dispatch in CEP using Benders cuts. In the algorithm, we integrate a deterministic long-term storage scheduling model to improve storage strategies and give a lower bound which enables faster computation.

c) We show the impact of short-term uncertainty and forecast horizon for operations on optimal investments in a realistic case study.

The operational model in this paper is based on previous work by the authors in [29, 30].

The rest of the paper is organized as follows, in Section 2 we describe the investment model with rolling-horizon operation. Section 3 presents a case study with energy storage and wind. We present the case study results in Section 4 and finally the conclusion in Section 5.

2. Methods

The extensive form formulation of the CEP with energy storage is shown in Equation (1) - (10). Investment and operational cost are minimized as formulated in the objective function in Equation (1). Operational costs consist of fuel, load shedding and exchange costs for power traded with market nodes (system boundary). Investments in power plants and storage are limited by an upper threshold in Equation (2) and (3). The sum of electricity production and curtailment is equal to the production capacity for each power plant as stated in Equation (4). Equation (5) keeps track of the energy level in the storage, accounting for losses. The storage level is limited by the installed storage energy capacity in Equation (6). Storage change or discharge is limited by the storage power capacity in Equation (7). The energy balance in Equation (8) accounts for the balance between energy injected and extracted from the bus. Curtailment of demand may occur during shortages, but at a significant cost.

$$\min \sum_{i\in\mathcal{R}} C_i^w w_i^{max} + \sum_{i\in\mathcal{E}} (C_i^s s_i^{max} + C_i^e e_i^{max}) + \sum_{t\in\mathcal{T}} \Big[\sum_{i\in\mathcal{P}} O_i^f p_{ti} + \sum_{n\in\mathcal{B}} O^s r_{tn} + \sum_{n\in\mathcal{M}} O_{tn}^{ex} p_{tn}^{ex} \Big] \tag{1}$$

$$w_i^{max} \le W_i^{Pot} \qquad \forall i \in \mathcal{R} \tag{2}$$

$$s_i^{max} \le S_i^{Pot}, e_i^{max} \le E_i^{Pot} \qquad \forall i \in \mathcal{S} \tag{3}$$

$$p_{ti} + c_{ti} = P_{ti} w_i^{max} \qquad \forall t \in \mathcal{T}, \forall i \in \mathcal{P} \tag{4}$$

$$s_{ti} = s_{(t-1)i} + \eta^{in} e_{ti}^i - \eta^{out} e_{ti}^o \qquad \forall t \in \mathcal{T}, \forall i \in \mathcal{E} \tag{5}$$

$$s_{ti} \le s_i^{max} \qquad \forall t \in \mathcal{T}, \forall i \in \mathcal{E} \tag{6}$$

$$e_{ti}^i + e_{ti}^o \le e_i^{max} \qquad \forall t \in \mathcal{T}, \forall i \in \mathcal{E} \tag{7}$$

$$\sum_{j\in\mathcal{P}_n} p_{tj} - p_{tns}^{ex} + r_{ti} + \sum_{j\in\mathcal{E}_n} (e_{tj}^o - e_{tj}^i) = D_{tn} \qquad \forall t \in \mathcal{T}, \forall n \in \mathcal{N} \tag{8}$$

$$p_{tns}^{ex} = \sum_{m\in\mathcal{C}_n} B_{nm}(\delta_n - \delta_m) \qquad \forall t \in \mathcal{T}, \forall n \in \mathcal{B} \tag{9}$$

$$-T_{nm} \le B_{nm}(\delta_n - \delta_m) \le T_{nm} \qquad \forall t \in \mathcal{T}, \forall n \in \mathcal{B}, \forall m \in \mathcal{C}_n \tag{10}$$

Equation (9) states the nodal balance, where the net exchange with other buses equal to the flow on all the lines connected to the bus. The line flow is represented by the linearized power flow equation and is equal to the difference in the voltage angle between the busses and proportional to the susceptance of the transmission line. The power flow on the transmission lines are constrained by the transmission capacity as shown in Equation (10).

2.1. Benders decomposition for the capacity expansion problem

A common method for solving the CEP is to decompose investments and operation into two different parts [31], a master problem and a sub-problem, which is solved by iterating between them until the upper and lower bounds of the problem converge. We formulate the master problem as shown in Equation (11), (12), (2) and (3).

$$\min \sum_{i\in\mathcal{R}} C_i^w w_i^{max} + \sum_{i\in\mathcal{E}} (C_i^s s_i^{max} + C_i^e e_i^{max}) + \alpha \tag{11}$$

$$\alpha \geq \alpha^k + \sum_{i\in\mathcal{P}} \pi_i^k P_i (w_i^{max} - W_i^k) + \sum_{i\in\mathcal{E}} \beta_i^k (s_i^{max} - S_i^k) + \gamma_i^k (e_i^{max} - E_i^k) \qquad \forall k \in \mathcal{K} \tag{12}$$

s.t. Equations (2) and (3)

In the master problem the operational costs are estimated by α, which is constrained by Benders cuts in Equation (12) [32]. For a given solution of the investments in the master problem, the sub-problem becomes as stated in Equation (13) to (16), in addition to Equations (5), (8)-(10). Here, the capacities are no longer variables but fixed parameters, W_i^k, S_i^k and E_i^k.

$$\min \sum_{t\in\mathcal{T}} \Big[\sum_{i\in\mathcal{P}} O_i^f p_{ti} + \sum_{n\in\mathcal{B}} O^s r_{tn} + \sum_{n\in\mathcal{M}} O_{tn}^{ex} p_{tn}^{ex} \Big] \tag{13}$$

$$p_{ti} + c_{ti} = P_{ti} W_i^k \qquad \pi_{ti} \qquad \forall t \in \mathcal{T}, \forall i \in \mathcal{P} \tag{14}$$

$$s_{ti} \leq S_i^k \qquad \beta_{ti} \qquad \forall t \in \mathcal{T}, \forall i \in \mathcal{E} \tag{15}$$

$$e_{ti}^i + e_{ti}^o \leq E_i^k \qquad \gamma_{ti} \qquad \forall t \in \mathcal{T}, \forall i \in \mathcal{E} \tag{16}$$

s.t. Equations (5), (8)-(10)

The cuts in the master problem consist of the optimal objective value of the sub-problem, the installed capacities used in the operational model for the current iteration and the dual of the capacity constraints in Equation (14), (15) and (16) summed over all times, e.g. $\pi_i = \sum_{\forall t\in\mathcal{T}} \pi_{ti}$. The upper bound is the objective of the best solution found so far calculated by summing up the values from the master and sub-problem according to the original objective function in Equation (1). The lower bound is the best solution that can be found and is the same as the objective of the master problem in Equation (11).

2.2. Stochastic rolling-horizon dispatch

To include the short-term VRE uncertainty, we substitute the deterministic operational sub-problem with a stochastic rolling-horizon dispatch (SRHD). The basic element of the SRHD is a two-stage problem which is implemented in a rolling horizon framework as illustrated in Figure 1, where parameters are updated as new information becomes available.

In the rolling-horizon framework we introduce day-ahead schedules for energy production and storage. In the first-stage, a fixed day-ahead schedule has to be followed. In the second-stage, a schedule is created (day-ahead) for real-time operation in the following two-stage model. One day-ahead schedule is made considering a range of scenarios for VRE production and passed on to the first-stage of the next instance of the two-stage model, typically the next day, in the rolling-horizon framework. Deviations from the day-ahead schedules have a cost which is representing a "premium-of-readiness" for changing production close to real-time [33]. This is analogous to how the electricity markets are currently organized, illustrated in Figure 1, where a day-ahead schedule is made the day before in the day-ahead market (second-stage of the first two-stage model) and deviations from this plan is accounted for continuously in the real-time market (first-stage of the second two-stage model).

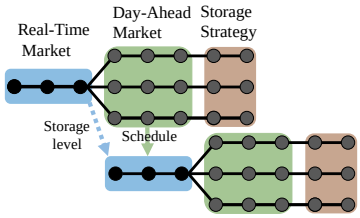

Figure 1: Illustration of the two-stage stochastic operation sub-problem of the SRHD.

The two-stage operation sub-problem is formulated in Equation (17) to (27). The new features compared to the deterministic model in Equation (13) to (16) is the day-ahead schedules enforced by Equation (19) and (20), where positive and negative deviations incur equal costs in the objective. Additionally, we have the scenario index, s, defining the two-stage structure where $\mathcal{S}_1$ is the realized first-stage "scenario" and $\mathcal{S}_2$ is the set of future scenarios for the second-stage. In the objective function described by Equation (17), we add the value of the remaining energy in the storage at the end of two-stage model horizon (calculated externally by the deterministic model).

2.3. Rolling horizon dispatch in capacity expansion with Benders decomposition

Benders decomposition has slow convergence if initialized with an inaccurate description of the operational costs in the master problem [34]. A good lower bound on operational costs can greatly improve the solution time of the algorithm by reducing the number of iterations. This is especially important if solving the operational problem is time consuming such as for the SRHD. The algorithm for solving the investment problem with SRHD operation is illustrated by the flow chart in Figure 2 and consist of two loops solved in sequence, first L1 and then L2. The deterministic operations problem with perfect foresight can be considered a relaxation of the SRHD, as the problems are identical except for the constraints in (19) and (20) and the short-term uncertainty. Thus, solving the decomposed deterministic CEP (D-CEP) first in L1, creates cuts for the investment problem that are a good lower bound for the operational

$$\min \sum_{s\in\mathcal{S}}\sum_{t\in\mathcal{T}_s}\Big[\sum_{i\in\mathcal{P}} O_i^f p_{tis} + \sum_{n\in\mathcal{B}} O^s r_{tns} + \sum_{n\in\mathcal{M}} O_{tn}^{ex} p_{tns}^{ex} + \sum_{i\in\mathcal{P},\mathcal{E}} O_{ti}^r (d_{tis}^n + d_{tis}^p)\Big] - \sum_{i\in\mathcal{E}} V_T s_{Tis} \quad (17)$$

$$p_{tis} + c_{tis} = P_{tis} W_i^* \qquad \forall t\in\mathcal{T}_s, \forall i\in\mathcal{P}, \forall s\in\mathcal{S} \quad (18)$$

$$p_{tis} - d_{tis}^n + d_{tis}^p = P_{ti}^{sch} \qquad \forall t\in\mathcal{T}_s, \forall i\in\mathcal{P}, \forall s\in\mathcal{S}_1 \quad (19)$$

$$p_{tis} - d_{tis}^n + d_{tis}^p = p_{ti}^{sch} \qquad \forall t\in\mathcal{T}_s, \forall i\in\mathcal{P}, \forall s\in\mathcal{S}_2 \quad (20)$$

$$s_{0is} = S^{prev} \qquad \forall i\in\mathcal{E}, \forall s\in\mathcal{S} \quad (21)$$

$$s_{tis} \le S_i^* \qquad \forall t\in\mathcal{T}_s, \forall i\in\mathcal{E}, \forall s\in\mathcal{S} \quad (22)$$

$$s_{tis} = s_{(t-1)is} + e_{tis}^i - e_{tis}^o \qquad \forall t\in\mathcal{T}_s, \forall i\in\mathcal{E}, \forall s\in\mathcal{S} \quad (23)$$

$$e_{tis}^i + e_{tis}^o \le E_i^* \qquad \forall t\in\mathcal{T}_s, \forall i\in\mathcal{E}, \forall s\in\mathcal{S} \quad (24)$$

$$\sum_{i\in\mathcal{P}_n} p_{tis} - p_{tns}^{ex} + r_{tns} + \sum_{i\in\mathcal{E}_n}(e_{tis}^o - e_{tis}^i) = D_{tn} \qquad \forall t\in\mathcal{T}_s, \forall n\in\mathcal{N}, \forall s\in\mathcal{S} \quad (25)$$

$$p_{tns}^{ex} = \sum_{m\in\mathcal{C}_n} B_{nm}(\delta_{tns} - \delta_{tms}) \qquad \forall t\in\mathcal{T}_s, \forall n\in\mathcal{B}, \forall s\in\mathcal{S} \quad (26)$$

$$-T_{nm} \le B_{nm}(\delta_{tns} - \delta_{tms}) \le T_{nm} \qquad \forall t\in\mathcal{T}_s, \forall n\in\mathcal{B}, \forall m\in\mathcal{C}_n, \forall s\in\mathcal{S} \quad (27)$$

costs in the SRHD (L2). This significantly reduces the computational time for the algorithm as it requires fewer iterations of L2.

In L2, the deterministic operations problem from L1 is included to reduce the impact of the limited horizon of the two-stage problem by providing end-of-horizon storage values obtained from the duals of the storage balance in Equation (5). This enables the SRHD to operate storage with dynamics beyond the horizon of the VRE forecasts. The impact of the end-of-horizon storage values on real-time and day-ahead operations is low if the two-stage model horizon is sufficiently long compared to the storage types considered.

The SRHD-CEP introduce three main challenges: 1) cut-generation in the context of short-term commitments and overlapping time-stages, 2) end-of-horizon effects in the two-stage model and 3) accurate representation of expected wind power production by forecasts over time. We investigate the impact of these challenges (especially 1 and 2) on the performance of the SRHD-CEP and the effect of short-term wind power uncertainty on investments in a two-bus case study.

3. Case Study

We use the SRHD-CEP to find the optimal capacity expansion in a two-bus case study where local electricity demand is served by a combination of wind power, energy storage and a transmission line. The transmission line has limited capacity and is connected to the electricity market, represented by a price series as illustrated in Figure 3a. A combination of energy storage and wind power is needed to supply the electric load as the transmission capacity of 130 MW is not large enough to supply all the electricity (1000 GWh/year) needed for the load in the winter as shown in Figure 3b.

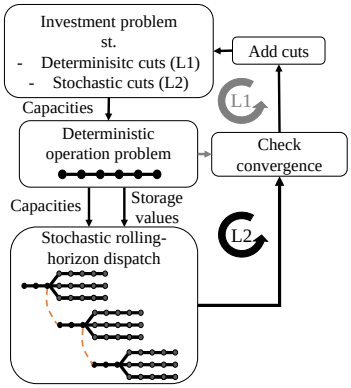

Figure 2: Flow chart of the algorithm for solving the investment problem with stochastic rolling horizon dispatch. First, L1 is solved to convergence followed by L2. An initial lower limit is used for operational costs ($\alpha \ge -1E64$).

Table 1: Wind power and storage costs [35] and unit size.

	Inv. cost (€/kW)	O&M cost (€/kW· yr)	Size (MW/unit)
Wind Power	930	30	3
Storage Power	250	6	1
Storage Energy	80	2	10

We use a technology cost scenario for 2050 for new investments, as shown in Table 1. In this scenario, we assume that the transmission line capacity cannot be expanded and energy storage costs are sufficiently low to make storage an interesting alternative to transmission line upgrades. Other important parameters include losses of 5 % for both charging and discharging, and a value of lost load (VOLL) of 10 000 $/MWh.

Data series for wind and load are obtained from northern Norway where wind power is well suited to supply the electric load as the wind-load seasonal correlation is high. However, the wind power plant has significant short-term variation and uncertainty in power output. Storage can be valuable to alleviate these issues by balancing and improving security of supply. We assume that load, wind power and energy storage are balancing their power collectively as one unit, which results in one aggregate day-ahead schedule for exchange with the market bus. Thus, the storage can be used for internal balancing that might be less costly than purchasing balancing power from the market. We assume a real-time balancing premium at 30% of the spot price for the power exchanged over the transmission line, which is higher than the current market prices but in line with

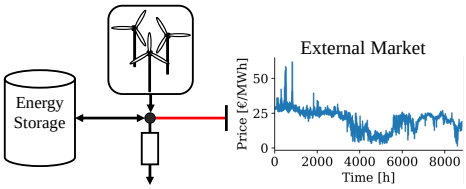

(a) Electricity system with load, energy storage and wind power connected to an electricity market through a constrained transmission line.

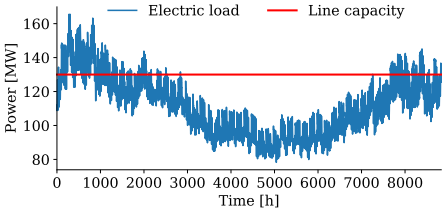

(b) Electric load profile and capacity limit of the transmission line to the power system.

Figure 3: Case study of a region with a limited connection to the rest of the electricity system, where a combination of wind power and storage is needed to supply an electricity demand.

expectations for future systems with high VRE shares [36].

Forecasts of the future wind power production is essential for efficient dispatch to ensure that sufficient storage levels are maintained ahead of time to avoid load shedding in deficit situations and wind power curtailment in surplus situations. Wind power scenarios are created by using historical weather forecasts and historical wind power production to create quantile forecasts for each day [37]. From the quantile forecasts we sample 90 scenarios for each day [38], which is reduced to 30 scenarios using SCENRED2 [39].

We use this case study to investigate how to best calculate the parameters for the Benders cuts, by selecting dual and operational costs from the different stages of the SRHD, resulting in two different cut-types:

a) Cuts obtained from expected (day-ahead) values
b) Cuts obtained from the average of realized (real-time) and expected values (day-ahead).

Cut type b is similar to the cuts used in [27], where they generate cuts from the weighted values of the cut parameters from all the time-stages. However, the market commitments used in our model will effect the dual values in the first-stage. Thus, type a cuts are introduced to investigate the significance of these commitments on the optimal investments.

The models are implemented in python using the PYOMO modelling framework [40] and the Gurobi solver. The simulations are performed on a shared server with 28 cores and 56 logical processors of the type Intel Xeon E5-2690 v4 at 2.6 GHz.

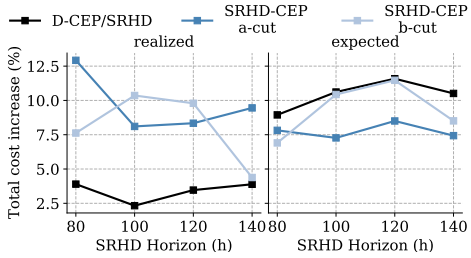

Figure 4: Total costs for D-CEP and the two versions of the SRHD-CEP. The D-CEP investments are evaluated with the SRHD operational model (D-CEP/SRHD). Total costs are measured by a) realized (first-stage) and b) expected (second-stage) values respectively and reported as a percentage increase from the perfect information solution (D-CEP).

4. Results

4.1. Impact of uncertainty and SRHD horizon on investments

We find the realistic D-CEP operating costs by running the SRHD model with the optimal capacities from the D-CEP. The resulting total cost of the D-CEP/SRHD is compared against the SRHD-CEP solutions for the two cut types and different SRHD horizons. The pure D-CEP solution (with deterministic operation) is used as a benchmark as it has perfect information of the future and is a lower limit for the total realized costs. The total costs are shown in Figure 4 as the percentage increase from the benchmark. The operational costs are calculated by two different metrics from the SRHD, on the left by realized costs (first-stage) and on the right by expected costs (expected value of the second-stage scenarios).

It is not surprising that the D-CEP/SRHD result in the lowest total realized costs, 2.3-3.9% more than the benchmark, as the D-CEP investments are optimized with perfect information. In contrast, the two SRHD-CEP solutions result in realized total costs of 4.4-13% higher than the benchmark. However, the better metric for the operational costs in a CEP is the expected value, as the operational costs will be close to the expectation across the 30 scenarios over time. The D-CEP/SRHD gives significantly higher expected total costs, 9-11.6% above the benchmark, because the D-CEP expansion plan results in operations close to the capacity limits and have a higher risk of load shedding. The expected cost is clearly lowest for the SRHD-CEP with a-cuts with total costs of 7.3-8.5% relative to the benchmark. The SRHD-CEP expansion plans result in similar realized and expected costs as the capacities are higher which is better for robust operation under realistic conditions.

A sufficiently long SRHD horizon is important for the storage strategy and gives a more realistic storage value in the presence of significant wind power uncertainty than the end-of-horizon value given by the deterministic model. In Figure 4, we evaluate the impact of the SRHD horizon by adding persistence forecasts[1], in increments of 20 hours, at the end of the

[1]Persistence forecast extend each of the scenarios for the next x hours with the average of the last x hours of the original scenario.

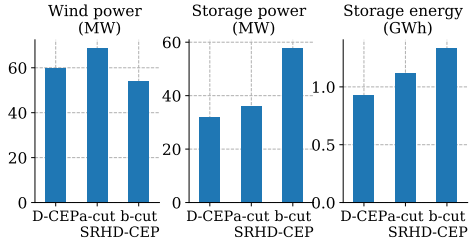

Figure 5: Optimal investments for D-CEP and SRHD-CEP models with the two different versions of L2 cuts and 100 hour SRHD horizon.

80 hours given by the weather forecasts. Extending the horizon to 100 hours is beneficial for the D-CEP/SRHD and the SRHD-CEP with a-cuts as it result in a better storage strategy an lower realized costs. For the SRHD-CEP with a-cuts, better storage handling in the first-stage result in lower expected costs. Longer horizons than 100 hours are less beneficial as the persistence forecasts are not accurate and it is better to use the end-of-horizon storage value.

The optimal capacities from the D-CEP and the two versions of the SRHD-CEP with a horizon of 100 hours are shown in Figure 5. The wind power capacity in the D-CEP is 60 MW, while the capacities are dependent on the cut-type in the SRHD-CEP at a-cut) 69 MW and b-cut) 54 MW. The SRHD-CEP results in more storage capacity than the D-CEP due to the higher risk of load shedding when uncertainty is accounted for in the operation. The storage power capacity is increased from 32 MW in the D-CEP to a-cut) 36 and b-cut) 58 MW in the SRHD-CEP, whereas the energy capacity increase from 930 MWh to a-cut) 1120 and b-cut) 1340 MWh.

The type of cuts used in the SRHD-CEP makes a significant difference for the investments, where a-cuts gives more wind power capacity and b-cuts gives more storage energy capacity (see Figure 5). For b-cuts, fixed day-ahead schedules lead the first-stage to give the wrong investment signal which skews investments from wind power to storage as it can be used for internal balancing (no regulation penalty). The a-cuts represent the operational costs without taking into account the first-stage, instead it obtains the dual values only from the second-stage where day-ahead schedules are variable. In general, a-cuts are superior to b-cuts because 1) fixed day-ahead schedules will not distort investments and 2) capacities should be built to minimize the expected operational cost. In this case, where the transmission grid is constrained without an option to expand the transmission capacity, the D-CEP also under-invests in wind power contrary to less constrained case studies in the literature.

4.2. Representation of stochastic operation

The cutting planes used to represent operational costs in the investment model are shown for the the wind-storage energy dimension in Figure 6, where the storage power is fixed at the D-CEP solution of 32 MW. The operational costs estimated by the D-CEP are shown in grey (L1 in Figure 2) while the estimation

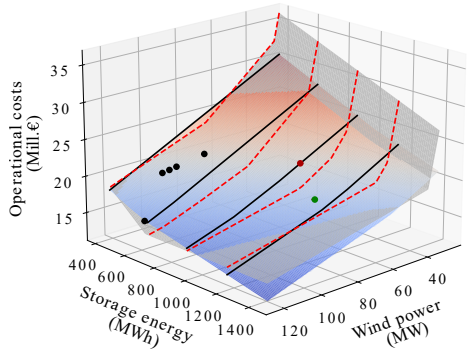

Figure 6: Cutting planes show the difference between stochastic (red-blue) and deterministic (grey) operational cost as a function for the storage energy and wind power capacity. The differences between the stochastic (black/solid) and deterministic (red/dotted) planes are highlighted by lines of fixed storage energy capacity. Points indicate the capacities searched by the SRHD-CEP, where the D-CEP (red) and SRHD-CEP (green) solutions are highlighted.

from the SRHD a-cuts (L2) are shown in a red-blue color gradient. Points in the red-blue plane indicate where operational costs are calculated by the SRHD-CEP.

Figure 6 shows that the operational costs are underrepresented by the cuts from the D-CEP compared to SRHD-CEP. The differences between the two planes are especially large around the optimal D-CEP solution (red point), where the wind power capacity is relatively low and the storage energy capacity is high. This leads the SRHD-CEP to search for alternative solutions with more wind power and less energy storage capacity that potentially gives lower operational costs (black points). However, these solutions proves to be more costly and the SRHD-CEP solution (green point) is found closer to the D-CEP solution but with higher wind power and storage energy capacity.

Initializing the algorithm with a lower bound from the deterministic cuts helps to significantly reduce the area that is searched when using SRHD for cut generation, resulting in only 7 additional iterations to find the SRHD-CEP solution, thereby saving significant computational time. The operational costs are higher at every point where the operational costs are calculated by the SRHD compared to deterministic operation, which supports the use of the deterministic operational model as a lower bound.

In Figure 7 we show a comparison between deterministic operation and SRHD for the first 20 days of the year using the capacities from the SRHD-CEP solution (a-cut and 100 hour horizon). The SRHD is represented by the realized values (start of each two-stage problem is marked with a point) and day-ahead scenarios are illustrated by the 50 and 95 % confidence intervals. Wind power uncertainty is significant, while realized production is the same for both deterministic operation and SRHD. On the other hand, storage operation is much more restricted in the SRHD than under deterministic operation, where the SRHD

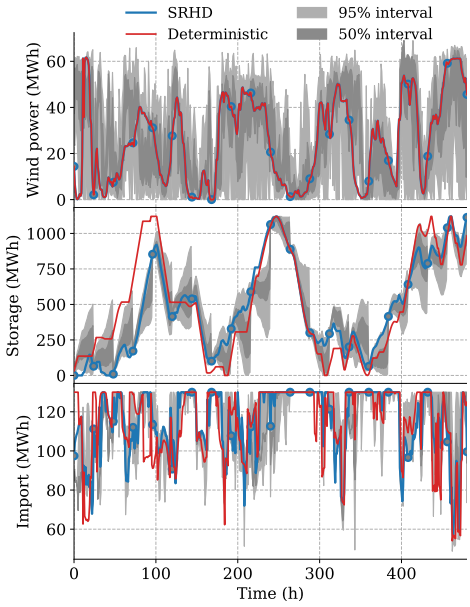

Figure 7: Deterministic and SRHD (first-stage) system operation for the first 20 days of the year and SRHD-CEP investments (a-cut and 100 hour horizon), represented by a) wind power, b) storage level and c) import from the market bus. The start of each two-stage model is marked with points, while 50 and 95 % confidence intervals show the day-ahead uncertainty.

leads to slower storage charge/discharge and generally does not operate as close to the capacity limits due to the higher risk of load shedding arising from uncertain wind power production. System operation between hours 250 and 300 is defining for the system capacities as wind power production is low while demand is high, leading to constraints on the transmission line (Figure 7 c) and maximum discharge from the storage. In the SRHD, an extension of the horizon from 80 to 100 hours is critical for obtaining a sufficient storage level and avoiding load curtailment. Using the deterministic model to set an end-of-horizon storage value in the SRHD with a 80 hour horizon does not give the sufficient storage strategy as indicated by the realized costs in Figure 4.

4.3. Algorithmic performance

The convergence of the proposed algorithm is shown in Figure 8. The deterministic solution in L1 is found after 22 iterations, while an additional 7 iterations are needed to obtain the stochastic solution in iteration 30 (iteration 23 and 31 are redundant and only used to confirm convergence). The computational time for each deterministic iterations is around 31 seconds as shown in Table 2, this is much less than the time required for the stochastic iterations which ranges from 42 to 94 minutes depending on the SRHD horizon. A longer SRHD horizon also leads to more iterations, thus resulting in larger increase in SRHD-CEP computational times than the increased SRHD times indicate.

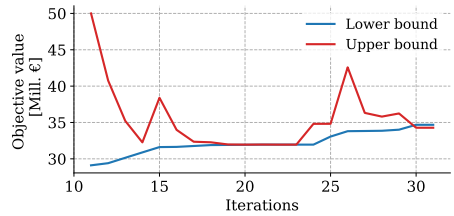

Figure 8: Convergence of the algorithm illustrated in Figure 2, the deterministic solution is obtained after 21 iterations and the stochastic solution at 29 iterations.

Table 2: Computational times and iterations of the algorithm for different SRHD horizons.

SRHD horizon (h)	80	100	120	140
L1 time (sec/itr)	31	31	32	30
L2 time (min/itr)	42	57	75	94
L2 iterations	7	8	9	11
Total time (hours)	5.1	7.8	11.4	17.5

5. Conclusion

In this work, we proposed to include SRHD with a representation of the real-time and day-ahead electricity markets in CEP, in order to include the impact of short-term VRE uncertainty on optimal capacity expansion. In a two bus case study, we showed how to link the operational model to the investment model in the presence of short-term market commitments by using Benders cuts derived from the day-ahead values. The expected total costs are reduced by 2.5-3 % compared to a deterministic investment model without stochastic representation of operation. The resulting capacities of wind power, storage power and storage energy from the SRHD-CEP are 12.5-20 % higher than in the deterministic case. The model is initialized by a lower bound generated from a deterministic operational model, which reduce the number of iterations with the more time-consuming SRHD.

In future work, the capacity expansion with stochastic operations should be tested on a larger system with more sources of uncertainty to see if the effects of including short-term uncertainty results in larger differences from the deterministic solution in a more complex setting. For larger systems it could be beneficial to also decompose the two-stage operational model in order to avoid prohibitive increases in computational times.

Acknowledgment

This publication is based on results from the research project Hyper, performed under the ENERGIX programme. The authors acknowledge the following parties for financial support:

Equinor, Shell, Kawasaki Heavy Industries, Linde Kryotechnik, Mitsubishi Corporation, Nel Hydrogen, Gassco and the Research Council of Norway (255107/E20).

References

[1] N. E. Koltsaklis, A. S. Dagoumas, State-of-the-art generation expansion planning: A review, Applied Energy 230 (2018) 563–589. doi:10.1016/J.APENERGY.2018.08.087.

[2] E. Lannoye, D. Flynn, M. O'Malley, Evaluation of Power System Flexibility, IEEE Transactions on Power Systems 27 (2) (2012) 922–931. doi:10.1109/TPWRS.2011.2177280.

[3] M. Huber, D. Dimkova, T. Hamacher, Integration of wind and solar power in Europe: Assessment of flexibility requirements, Energy 69 (2014) 236–246. doi:10.1016/J.ENERGY.2014.02.109.

[4] H. Lund, B. Mathiesen, Energy system analysis of 100% renewable energy systems—The case of Denmark in years 2030 and 2050, Energy 34 (5) (2009) 524–531. doi:10.1016/J.ENERGY.2008.04.003.

[5] L. Bird, D. Lew, M. Milligan, E. M. Carlini, A. Estanqueiro, D. Flynn, E. Gomez-Lazaro, H. Holttinen, N. Menemenlis, A. Orths, P. Børre Eriksen, J. C. Smith, L. Soder, P. Sorensen, A. Altiparmakis, Y. Yasuda, J. Miller, Wind and solar energy curtailment: A review of international experience, Renewable and Sustainable Energy Reviews (2016). doi:10.1016/j.rser.2016.06.082.

[6] S. Collins, J. P. Deane, K. Poncelet, E. Panos, R. C. Pietzcker, E. Delarue, B. P. Ó Gallachóir, Integrating short term variations of the power system into integrated energy system models: A methodological review, Renewable and Sustainable Energy Reviews 76 (2017) 839–856. doi:10.1016/J.RSER.2017.03.090.

[7] S. Nagl, M. Fürsch, D. Lindenberger, The Costs of Electricity Systems with a High Share of Fluctuating Renewables : A Stochastic Investment and Dispatch Optimization Model for Europe, The Energy Journal 34 (4) (2017) 151–179.

[8] Ninghong Sun, I. Ellersdorfer, D. J. Swider, Model-based long-term electricity generation system planning under uncertainty, in: 2008 Third International Conference on Electric Utility Deregulation and Restructuring and Power Technologies, IEEE, 2008, pp. 1298–1304. doi:10.1109/DRPT.2008.4523607.

[9] S. Spiecker, P. Vogel, C. Weber, Evaluating interconnector investments in the north European electricity system considering fluctuating wind power penetration, Energy Economics 37 (2013) 114–127. doi:10.1016/J.ENECO.2013.01.012.

[10] T. Qiu, B. Xu, Y. Wang, Y. Dvorkin, D. S. Kirschen, Stochastic Multistage Coplanning of Transmission Expansion and Energy Storage, IEEE Transactions on Power Systems 32 (1) (2017) 643–651. doi:10.1109/TPWRS.2016.2553678.

[11] S. Jin, A. Botterud, S. M. Ryan, Temporal Versus Stochastic Granularity in Thermal Generation Capacity Planning With Wind Power, IEEE Transactions on Power Systems 29 (5) (2014) 2033–2041. doi:10.1109/TPWRS.2014.2299760.

[12] P. Seljom, A. Tomasgard, Short-term uncertainty in long-term energy system models — A case study of wind power in Denmark, Energy Economics 49 (2015) 157–167. doi:10.1016/J.ENECO.2015.02.004.

[13] F. D. Munoz, J.-P. Watson, A scalable solution framework for stochastic transmission and generation planning problems, Computational Management Science 12 (4) (2015) 491–518. doi:10.1007/s10287-015-0229-y.

[14] F. Munoz, B. Hobbs, J.-P. Watson, New bounding and decomposition approaches for MILP investment problems: Multi-area transmission and generation planning under policy constraints, European Journal of Operational Research 248 (3) (2016) 888–898. doi:10.1016/J.EJOR.2015.07.057.

[15] K. Poncelet, H. Hoschle, E. Delarue, A. Virag, W. Drhaeseleer, Selecting Representative Days for Capturing the Implications of Integrating Intermittent Renewables in Generation Expansion Planning Problems, IEEE Transactions on Power Systems 32 (3) (2017) 1936–1948. doi:10.1109/TPWRS.2016.2596803.

[16] K. Poncelet, E. Delarue, D. Six, J. Duerinck, W. D'haeseleer, Impact of the level of temporal and operational detail in energy-system planning models, Applied Energy 162 (2016) 631–643. doi:10.1016/j.apenergy.2015.10.100.

[17] D. S. Mallapragada, D. J. Papageorgiou, A. Venkatesh, C. L. Lara, I. E. Grossmann, Impact of model resolution on scenario outcomes for electricity sector system expansion, Energy 163 (2018) 1231–1244. doi:10.1016/J.ENERGY.2018.08.015.

[18] P. Meibom, R. Barth, B. Hasche, H. Brand, C. Weber, M. O'Malley, Stochastic optimization model to study the operational impacts of high wind penetrations in Ireland, IEEE Transactions on Power Systems 26 (3) (2011) 1367–1379. doi:10.1109/TPWRS.2010.2070848.

[19] Y. Wang, Z. Zhou, A. Botterud, K. Zhang, Q. Ding, Stochastic coordinated operation of wind and battery energy storage system considering battery degradation, Journal of Modern Power Systems and Clean Energy 4 (4) (2016) 581–592. doi:10.1007/s40565-016-0238-z.

[20] M. Korpås, A. T. Holen, Operation planning of hydrogen storage connected to wind power operating in a power market, IEEE Transactions on Energy Conversion 21 (3) (2006) 742–749. doi:10.1109/TEC.2006.878245.

[21] K. Sakellaris, J. Canton, E. Zafeiratou, L. Fournié, METIS – An energy modelling tool to support transparent policy making, Energy Strategy Reviews 22 (April) (2018) 127–135. doi:10.1016/j.esr.2018.08.013.

[22] K. Kanellopoulos, H. Blanco, The potential role of H2 production in a sustainable future power system - An analysis with METIS of a decarbonised system powered by renewables in 2050, Tech. rep., European Commission (2019). doi:10.2760/540707.

[23] J. Dillon, M. O'malley, Impact of Uncertainty on Wind Power Curtailment Estimation, 2017.

[24] H. Park, R. Baldick, Stochastic generation capacity expansion planning reducing greenhouse gas emissions, IEEE Transactions on Power Systems 30 (2) (2015) 1026–1034. doi:10.1109/TPWRS.2014.2386872.

[25] S. Ramabhotla, S. Bayne, M. Giesselmann, Economic dispatch optimization of microgrid in islanded mode, in: International Energy and Sustainability Conference 2014, IESC 2014, Institute of Electrical and Electronics Engineers Inc., 2014. doi:10.1109/IESC.2014.7061838.

[26] K. Dasgupta, J. Hazra, S. Rongali, M. Padmanaban, Estimating return on investment for grid scale storage within the economic dispatch framework, in: Proceedings of the 2015 IEEE Innovative Smart Grid Technologies - Asia, ISGT ASIA 2015, Institute of Electrical and Electronics Engineers Inc., 2016. doi:10.1109/ISGT-Asia.2015.7387088.

[27] P. Fortenbacher, A. Ulbig, G. Andersson, Optimal Placement and Sizing of Distributed Battery Storage in Low Voltage Grids Using Receding Horizon Control Strategies, IEEE Transactions on Power Systems 33 (3) (2018) 2383–2394. doi:10.1109/TPWRS.2017.2746261.

[28] S. Pineda, J. M. Morales, Capacity expansion of stochastic power generation under two-stage electricity markets, Computers & Operations Research 70 (2016) 101–114. doi:10.1016/J.COR.2015.12.007.

[29] E. F. Bødal, M. Korpås, Production of Hydrogen from Wind and Hydro Power in Constrained Transmission grids, Considering the Stochasticity of Wind Power, Journal of Physics: Conference Series 1104 (1) (2018) 012027. doi:10.1088/1742-6596/1104/1/012027.

[30] E. F. Bødal, M. Korpås, Value of hydro power flexibility for hydrogen production in constrained transmission grids, International Journal of Hydrogen Energy 45 (2) (2020) 1255–1266. doi:10.1016/j.ijhydene.2019.05.037.

[31] M. F. Pereira, L. V. G. Pinto, S. F. Cunha, G. Oliveira, A Decomposition Approach To Automated Generation/Transmission Expansion Planning, IEEE Transactions on Power Apparatus and Systems PAS-104 (11) (1985) 3074–3083. doi:10.1109/TPAS.1985.318815.

[32] J. F. Benders, Partitioning Procedures for Solving Mixed-Variable Programming Problems, Numerische Mathematik 4 (1) (1962) 238–252.

[33] K. Skytte, The regulating power market on the Nordic power exchange Nord Pool: an econometric analysis, Energy Economics 21 (4) (1999) 295–308. doi:10.1016/S0140-9883(99)00016-X.

[34] R. Rahmaniani, T. G. Crainic, M. Gendreau, W. Rei, The Benders decomposition algorithm: A literature review (6 2017). doi:10.1016/j.ejor.2016.12.005.

[35] National Renewable Energy Laboratory (NREL), 2019 Annual Technology Baseline: Electricity (2019).
URL https://atb.nrel.gov/

[36] A. Moser, A. Maaz, C. Baumann, A. Schäfer, Value of large-scale balancing and storing from Norwegian hydropower for the German power

system and generation portfolios (2016).
[37] J. B. Bremnes, A comparison of a few statistical models for making quantile wind power forecasts, Wind Energy 9 (1-2) (2006) 3–11. doi:10.1002/we.182.
[38] P. Pinson, H. Madsen, G. Papaefthymiou, From Probabilistic Forecasts to Statistical Scenarios of Short-term Wind Power Production, WIND ENERGY Wind Energ 12 (2009) 51–62. doi:10.1002/we.284.
[39] H. Heitsch, W. Römisch, A note on scenario reduction for two-stage stochastic programs, Operations Research Letters 35 (6) (2007) 731–738. doi:10.1016/j.orl.2006.12.008.
[40] W. E. Hart, J. P. Watson, D. L. Woodruff, Pyomo: Modeling and solving mathematical programs in Python, Mathematical Programming Computation 3 (3) (2011) 219–260. doi:10.1007/s12532-011-0026-8.

ISBN 978-82-326-5488-8 (printed ver.)
ISBN 978-82-326-5648-6 (electronic ver.)
ISSN 1503-8181 (printed ver.)
ISSN 2703-8084 (online ver.)